UBIQUITIN-MODIFYING ENZYMES AS DRUG TARGETS AND BIOMARKERS IN CANCER

EDITED BY: Jessica Lilian Bell, Jean Borges Bertoldo, Matthew K. Summers, Alena Malyukova and Yi Sun

PUBLISHED IN: Frontiers in Oncology

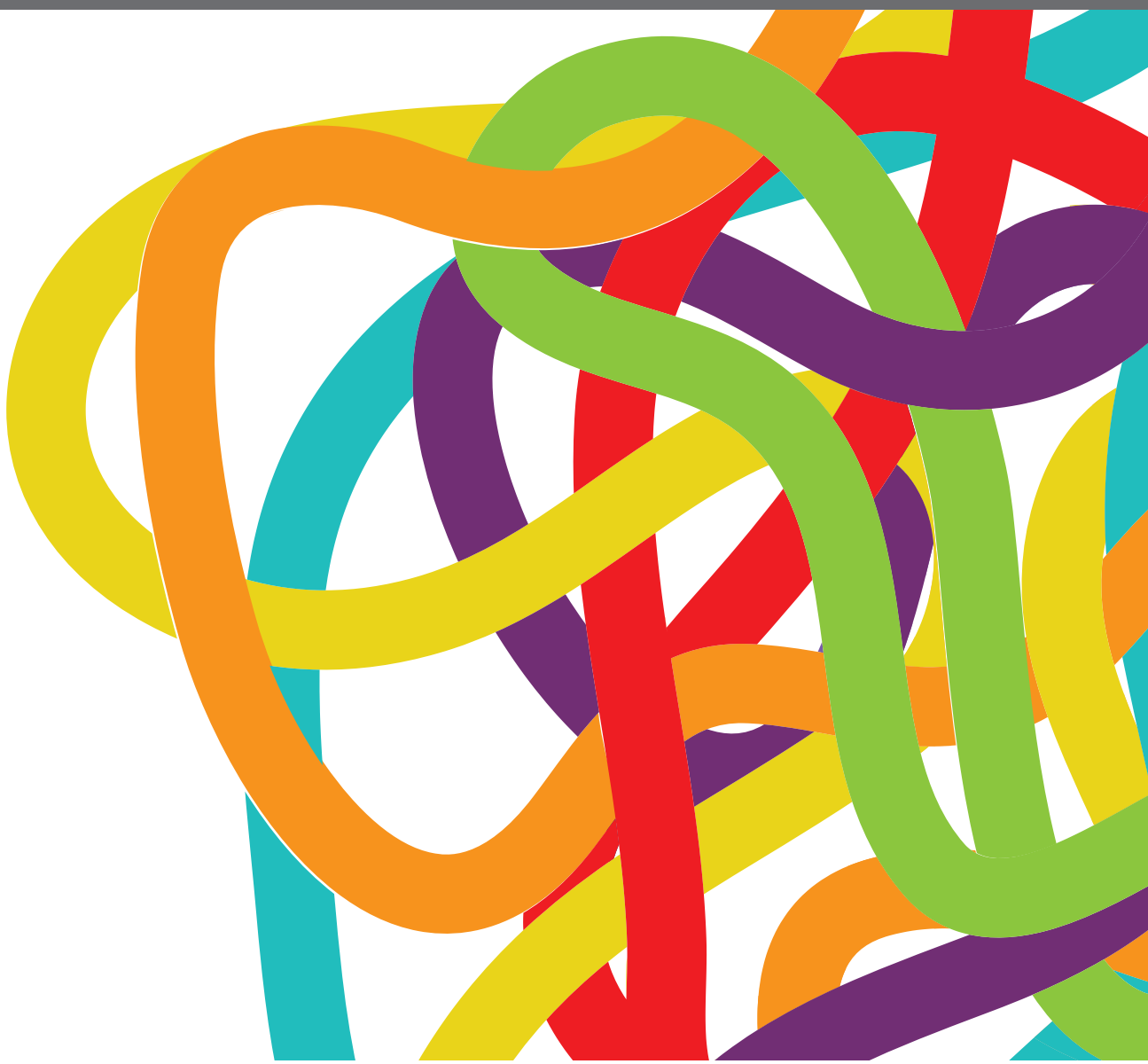

frontiers Research Topics

frontiers

ISSN 1664-8714
ISBN 978-2-88971-587-9
DOI 10.3389/978-2-88971-587-9

About Frontiers

Frontiers is more than just an open-access publisher of scholarly articles: it is a pioneering approach to the world of academia, radically improving the way scholarly research is managed. The grand vision of Frontiers is a world where all people have an equal opportunity to seek, share and generate knowledge. Frontiers provides immediate and permanent online open access to all its publications, but this alone is not enough to realize our grand goals.

Frontiers Journal Series

The Frontiers Journal Series is a multi-tier and interdisciplinary set of open-access, online journals, promising a paradigm shift from the current review, selection and dissemination processes in academic publishing. All Frontiers journals are driven by researchers for researchers; therefore, they constitute a service to the scholarly community. At the same time, the Frontiers Journal Series operates on a revolutionary invention, the tiered publishing system, initially addressing specific communities of scholars, and gradually climbing up to broader public understanding, thus serving the interests of the lay society, too.

Dedication to Quality

Each Frontiers article is a landmark of the highest quality, thanks to genuinely collaborative interactions between authors and review editors, who include some of the world's best academicians. Research must be certified by peers before entering a stream of knowledge that may eventually reach the public - and shape society; therefore, Frontiers only applies the most rigorous and unbiased reviews.
Frontiers revolutionizes research publishing by freely delivering the most outstanding research, evaluated with no bias from both the academic and social point of view. By applying the most advanced information technologies, Frontiers is catapulting scholarly publishing into a new generation.

What are Frontiers Research Topics?

Frontiers Research Topics are very popular trademarks of the Frontiers Journals Series: they are collections of at least ten articles, all centered on a particular subject. With their unique mix of varied contributions from Original Research to Review Articles, Frontiers Research Topics unify the most influential researchers, the latest key findings and historical advances in a hot research area! Find out more on how to host your own Frontiers Research Topic or contribute to one as an author by contacting the Frontiers Editorial Office: frontiersin.org/about/contact

UBIQUITIN-MODIFYING ENZYMES AS DRUG TARGETS AND BIOMARKERS IN CANCER

Topic Editors:
Jessica Lilian Bell, Children's Cancer Institute Australia, Australia
Jean Borges Bertoldo, Martin Luther University of Halle-Wittenberg, Germany
Matthew K. Summers, The Ohio State University, United States
Alena Malyukova, Karolinska Institutet (KI), Sweden
Yi Sun, Zhejiang University, China

Citation: Bell, J. L., Bertoldo, J. B., Summers, M. K., Malyukova, A., Sun, Y., eds. (2021). Ubiquitin-modifying Enzymes as Drug Targets and Biomarkers in Cancer. Lausanne: Frontiers Media SA. doi: 10.3389/978-2-88971-587-9

Table of Contents

frontiers in Oncology

EDITORIAL
published: 15 September 2021
doi: 10.3389/fonc.2021.758983

Editorial: Ubiquitin-Modifying Enzymes as Drug Targets and Biomarkers in Cancer

Jessica L. Bell[1], Alena Malyukova[2], Jean B. Bertoldo[3], Matthew K. Summers[4] and Yi Sun[5]*

[1] Children's Cancer Institute, School of Women's and Children's Health, Lowy Cancer Centre, University of New South Wales (UNSW), Sydney, NSW, Australia, [2] Department of Cell and Molecular Biology, Karolinska Institute, Stockholm, Sweden, [3] Institute of Molecular Medicine, Faculty of Medicine, Martin-Luther University of Halle-Wittenberg, Halle, Germany, [4] Department of Radiation Oncology, Arthur G James Comprehensive Cancer Center and Richard L. Solove Research Institute, The Ohio State University, Columbus, OH, United States, [5] Cancer Institute, The Second Affiliated Hospital, and Institute of Translational Medicine, Zhejiang University School of Medicine, Hangzhou, China

Keywords: ubiquitin, E3 ligase, cancer, proteasome, DUB

Editorial on the Research Topic

Ubiquitin-Modifying Enzymes as Drug Targets and Biomarkers in Cancer

E3 ubiquitin ligases are critical to the regulatory control of a vast array of substrates and binding partners. The E3 ligases comprise the HECT, RING-finger, U-box, and PHD-finger protein families. The RING-finger family has the most members and contain ligases such as the anaphase-promoting complex (APC) and the SCF complex (Skp1-Cullin-F-box protein complex), as well as many TRIM proteins. These proteins are key regulators of cell fate in both non-malignant cells and cancer cells by adding ubiquitin to proteins and are increasingly targets for pharmaceutical modulation. They are opposed to another class of enzymes referred to as deubiquitinating enzymes (or DUBs) from protein families such as USP, UCH, OTU, JAMM, MCPIP, which also have become drug targets. The objective of this special issue was to discuss and advance the current knowledge regarding the roles and targetability of the ubiquitination machinery, in cancer. Review and research papers were accepted focusing on cancer related ubiquitin-modifying enzymes as; biomarkers, therapeutic targets, as an interacting partner of a clinically significant protein in cancer/cancer models and cancer cell phenotypes. In this Research Topic, we eventually accepted nine articles for publication (four research reviews and five research articles), which discuss the roles of ubiquitination enzymes and provide novel insights into how they impact cancer progression.

Ubiquitination plays a critical role in protein stability, MYC and p53 are probably the most reported proteins concerning their stability, being two transcription factors that are highly dynamic in expression and relatively unstable at the protein level. Although their transcriptional regulation is important, post-translational regulators of these proteins have been put forward as drug targets in cancer because direct targeting of the MYC protein or direct activation of p53 has been historically difficult. MYC, an oncoprotein, is often overexpressed and activated in tumours, and contributes to tumour aggressiveness and poor patient outcomes. Deregulation of the ubiquitination/deubiquitination balance in cancers enables MYC stabilization. In addition, SUMOylation crosstalks with the ubiquitination pathway and also controls MYC protein stability and activity. Sun et al. provided a mini-review discussing post-translation regulation of MYC which includes perspectives about MYC regulators as potential therapeutic targets in cancer. The majority of therapeutic strategies discussed by Sun et al. exploit the idea of targeting E3 ligases that promote

OPEN ACCESS

Edited and reviewed by:
Giuseppe Giaccone, Cornell University, United States

****Correspondence:***
Jessica L. Bell
jbell@ccia.org.au

Specialty section:
This article was submitted to Cancer Molecular Targets and Therapeutics, a section of the journal Frontiers in Oncology

Received: *15 August 2021*
Accepted: *25 August 2021*
Published: *15 September 2021*

Citation:
Bell JL, Malyukova A, Bertoldo JB, Summers MK and Sun Y (2021) Editorial: Ubiquitin-Modifying Enzymes as Drug Targets and Biomarkers in Cancer. Front. Oncol. 11:758983. doi: 10.3389/fonc.2021.758983

MYC function, such as SKP2 and HUWE1 or inhibiting DUBs that antagonize MYC ubiquitination. Another promising idea presented in the review is to utilize synthetic lethality in MYC-high cancers by targeting Fbxw7 or UBR5.

p53 is a tumor suppressor protein with roles in most cancer types. It can undergo more than 300 posttranslational modifications and is principally involved in DNA damage response, apoptosis and DNA repair. Mathieu et al. present a review for this special issue on p53 and focus on the molecular mechanisms and interactions that occur between p53 and ubiquitin regulating enzymes, including irregular HECT-p53 interactions which can induce tumorigenesis. Interestingly, inhibitors developed to inhibit this interaction did not show efficacy indicating more research is needed to understand the role of HECT-p53 binding.

In this special issue there are three original research papers investigating the hepatocellular carcinoma context. One of the articles is by Li et al. and shows a new role for CISD2 in sorafenib resistance. Sorafenib is a multi-kinase inhibitor that is a standard treatment for advanced hepatocellular carcinoma, and it has previously been shown to influence protein ubiquitination. CISD2 expression is related to the progression and poor prognosis of hepatocellular carcinoma. Another aspect of hepatocellular carcinoma is initiation of the disease by viruses such as hepatitis B. Wan et al. investigated NEDD4 function in hepatitis B-induced liver cancer. They confirmed that NEDD4 induced the degradation of HBV X protein in a ubiquitin/proteasome-dependent manner *via* K48-linked ubiquitination and provided other results that together suggest NEDD4 acts as a tumor-suppressor in HBV-associated hepatocellular carcinoma. Another manuscript in the special issue investigates ubiquitin-specific proteases (USPs), which are a sub-family of DUBs. Expression of USPs are correlated with various malignancies. Ni et al. systematically investigated USPs expression in hepatocellular carcinoma. Notably, USP39 was correlated with poor prognosis in liver tumour cohorts.

DUBs are of increasing interest in cancer research and Rong et al. reviewed this class of protein, specifically the Ubiquitin C-terminal hydrolases (UCHs), a subfamily of deubiquitinating enzymes (DUBs). Their cancer context of interest is head and neck cancer, a heterogeneous disease where the long-term survival rates remain low and new drug targets are needed. They provide potential mechanisms of the UCH protein family in head and neck cancer pathogenesis and potential drug targets.

Siah2 is an E3 ubiquitin ligase that targets the androgen receptor and plays an important role in prostate cancer. Yan et al. found that the androgen receptor itself stabilizes Siah2 protein by attenuating its self-ubiquitination, likely by blocking its E3 ubiquitin ligase activity. They performed *in vivo* studies showing androgen deprivation therapy in combination with vitamin K3 delayed the development of castration-resistant prostate cancer.

Another research group made use of TCGA datasets to analyze the prognostic value of KLK8 a protein that acts as serine protease. Hua et al. showed that this protease has prognostic value in pancreatic cancer and also exerts pro-proliferation and anti-apoptotic functions in pancreatic cancer cells *via* PI3K/Akt/mTOR pathway.

Recently, a novel strategy named proteolysis-targeting chimeras (PROTACs) has been developed as a designed and targeted method of protein degradation exploiting the cancer cell's own ubiquitin-proteasome system. This provides an additional method of drug discovery. Zhang et al. discuss and summarize the exciting advances in this field.

In summary, the collection of papers within this Research Topic offers insights into the current and emerging knowledge of the multifaceted importance of enzymes of the ubiquitin system in the context of cancer, including their biological functions and potential utility in patient care as prognostic markers, drug targets, and therapeutic tools.

AUTHOR CONTRIBUTIONS

All authors listed have made a substantial, direct and intellectual contribution to the work and approved it for publication.

FUNDING

Funding to JLB and JBB was provided by the Wilhelm-Roux Programme (intramural funding programme of the Medical Faculty, Martin Luther University Halle-Wittenberg, Halle (Saale), Germany). Funding to MS was provided by The Ohio State University Comprehensive Cancer Center/Department of Radiation Oncology. Funding to AM was provided by Cancerföreningen i Stockholm.

ACKNOWLEDGMENTS

All the authors would like to thank all contributing authors and reviewers for their support to the Research Topic.

Conflict of Interest: The authors declare that the research was conducted in the absence of any commercial or financial relationships that could be construed as a potential conflict of interest.

Publisher's Note: All claims expressed in this article are solely those of the authors and do not necessarily represent those of their affiliated organizations, or those of the publisher, the editors and the reviewers. Any product that may be evaluated in this article, or claim that may be made by its manufacturer, is not guaranteed or endorsed by the publisher.

frontiers in Oncology

REVIEW
published: 29 January 2021
doi: 10.3389/fonc.2020.592501

Ubiquitin Carboxyl-Terminal Hydrolases and Human Malignancies: The Novel Prognostic and Therapeutic Implications for Head and Neck Cancer

Chao Rong[1,2†], Ran Zhou[3†], Shan Wan[1], Dan Su[3], Shou-Li Wang[1] and Jochen Hess[2,4]*

[1] Department of Pathology, School of Biology & Basic Medical Sciences, Soochow University, Suzhou, China, [2] Section Experimental and Translational Head and Neck Oncology, Department of Otolaryngology, Head and Neck Surgery, University Hospital Heidelberg, Heidelberg, Germany, [3] Department of Pharmacy, The First Affiliated Hospital of University of Science and Technology of China (USTC), Division of Life Sciences and Medicine, University of Science and Technology of China, Hefei, China, [4] Research Group Molecular Mechanisms of Head and Neck Tumors, Deutsches Krebsforschungszentrum (DKFZ), Heidelberg, Germany

Ubiquitin C-terminal hydrolases (UCHs), a subfamily of deubiquitinating enzymes (DUBs), have been found in a variety of tumor entities and play distinct roles in the pathogenesis and development of various cancers including head and neck cancer (HNC). HNC is a heterogeneous disease arising from the mucosal epithelia of the upper aerodigestive tract, including different anatomic sites, distinct histopathologic types, as well as human papillomavirus (HPV)-positive and negative subgroups. Despite advances in multi-disciplinary treatment for HNC, the long-term survival rate of patients with HNC remains low. Emerging evidence has revealed the members of UCHs are associated with the pathogenesis and clinical prognosis of HNC, which highlights the prognostic and therapeutic implications of UCHs for patients with HNC. In this review, we summarize the physiological and pathological functions of the UCHs family, which provides enlightenment of potential mechanisms of UCHs family in HNC pathogenesis and highlights the potential consideration of UCHs as attractive drug targets.

Keywords: head and neck cancer, ubiquitin C-terminal hydrolases, deubiquitinating enzymes, genomic alteration, clinical relevance

OPEN ACCESS

Edited by:
Jessica Lilian Bell, Children's Cancer Institute Australia, Australia

Reviewed by:
Katerina Strati, University of Cyprus, Cyprus
Tuula Kallunki, Danish Cancer Society Research Center (DCRC), Denmark

****Correspondence:***
Shou-Li Wang
wangshouli@suda.edu.cn

[†]These authors have contributed equally to this work

Specialty section:
This article was submitted to Cancer Molecular Targets and Therapeutics, a section of the journal Frontiers in Oncology

Received: *02 September 2020*
Accepted: *07 December 2020*
Published: *29 January 2021*

Citation:
Rong C, Zhou R, Wan S, Su D, Wang S-L and Hess J (2021) Ubiquitin Carboxyl-Terminal Hydrolases and Human Malignancies: The Novel Prognostic and Therapeutic Implications for Head and Neck Cancer. Front. Oncol. 10:592501. doi: 10.3389/fonc.2020.592501

Abbreviations: MDM2, murine double minute 2; NOX4, NADPH oxidase 4; EGFR, Epidermal growth factor receptor; HIF-1, Hypoxia-inducible factor 1; PHLPP1, PH Domain and Leucine Rich Repeat Protein Phosphatase 1; MITF, Melanocyte Inducing Transcription Factor; CTTN, Cortactin; mTORC1, mTOR complex 1; eIF4F, Eukaryotic initiation factor 4F; TRAF2, TNF Receptor Associated Factor 2; PRDX1, Peroxiredoxin 1; SNRPF, Small Nuclear Ribonucleoprotein Polypeptide F; Smad2, SMAD Family Member 2; GRP78, 78-kDa glucose-regulated protein; E2F1, E2F Transcription Factor 1; HCF-1, Host cell factor C1; ASXL1/2, ASXL Transcriptional Regulator 1/2; MCRS1, Microspherule Protein 1; IP3R3, type-3 inositol-1,4,5-trisphosphate-receptor; ATF3, Activating Transcription Factor 3; 14-3-3 protein; SLC7A11, Solute Carrier Family 7 Member 11.

INTRODUCTION

Head and neck cancer (HNC) represents the seventh most prevalent human malignancies with an annual incidence of 890,000 new cases worldwide, including 76,000 cases in China and 18,260 cases in Germany (1, 2). Anatomically, HNC occurs at distinct sites including lip, oral cavity, nasal cavity, sinonasal cavity, nasopharynx, oropharynx, hypopharynx, larynx, and salivary glands, and etiologic risk factors, epidemiology, treatment strategies as well as clinical outcome differ among individual subsites (3). Over 90% of cases are diagnosed as head and neck squamous cell carcinoma (HNSCC), which arises from the mucosal epithelia of the upper aerodigestive tract. High incidence areas for oral cavity cancer include Middle and South Asia, Western and Southern Europe as well as South Africa. The incidence of oropharyngeal SCC (OPSCC) is elevated in Europe and North America. Nasopharyngeal cancer (NPC) is most common in East and Southeast Asia, especially in South China (4). Tobacco smoking and heavy alcohol consumption have been identified as the most important risk factors in developed countries (5). In developing countries, risk factors also include EpsteinBarr virus (EBV) infection for NPC, areca nut chewing, consumption of preserved foods, and oral hygiene (6–8). During the past two decades, the overall incidence of HNSCC has gradually decreased in western developed countries. However, a subgroup of HNSCC, particularly OPSCC, has been becoming more prevalent in young adults, which is attributed to high-risk human papillomavirus (HPV) infection, predominantly HPV16 (9). High-risk HPV types comprise two oncogenes, E6 and E7, which inactivate the tumor suppressors p53 and retinoblastoma (RB), respectively. As a result, cell cycle progression and cell death in infected cells are disrupted, as initial steps for HPV-related carcinogenesis (10–13). Besides the viral oncogenes E6/E7, HPV E2, E4, and E5 have been shown to facilitate the synergistic effects of viral oncogenesis, which represents an alternative manner to HPV-induced carcinogenesis (14). It has been well-established that HPV-positive and HPV-negative OPSCC have distinct differences in gene expression profiles, genomic alterations, immune landscape, as well as clinical outcomes (15–18). Due to the more favorable prognosis of HPV-positive OPSCC, clinical trials have been launched to investigate HPV-stratified de-escalation treatment based on currently established protocols. However, final results and definitive conclusions are pending, which might improve the post-treatment quality of HPV-related OPSCC patients (19–22).

Despite advances in multi-disciplinary treatment for HNSCC, including surgical approaches, radiotherapy, chemotherapy, molecular-targeted therapy, and immunotherapy, the overall survival of advanced HNSCC has only improved slightly, and appropriate therapy remains a major challenge. Over the past decade, large-scale genomic profiling and proteomic studies, including The Cancer Genome Atlas (TCGA) projects, have highlighted a comprehensive molecular landscape of changes in DNA copy number, somatic mutations, promoter methylation, and protein and gene expression, indicating the critical components and signal pathway in HNSCC pathogenesis (23–25). A better understanding of these molecular underpinnings may inspire novel drug targets as well as molecular biomarkers for personalized treatment.

The proteome is exceedingly complex and has been regarded as the major driver or actuator of fundamental cellular processes. Protein ubiquitination is a post-translational modification process that plays critical roles in numerous biological processes, including cell growth and differentiation, signal transduction, DNA repair, and oncogenesis (26). The conjugation of ubiquitin (Ub) to target proteins is catalyzed by a cascade of ubiquitinating enzymes, including Ub-activating enzymes (E1s), Ub-conjugating enzymes (E2s), and Ub ligases (E3s). Conjugation of Ub to a substrate lysine, its lysines or its N-terminus, results in the generation of different substrate ubiquitin structures, which can be either a mono- or poly-ubiquitylation process and allows targeted proteins to fulfill a diverse range of functions. However, protein ubiquitination is highly reversible. Deubiquitinases or deubiquitinating enzymes (DUBs) catalyze the removal of ubiquitin from target proteins to generate free monomeric Ub (27). The human genome encodes approximately 100 DUBs categorized into six subfamilies: the ubiquitin C-terminal hydrolases (UCHs), the ubiquitin-specific proteases (USPs), the ovarian tumor proteases (OTUs), the Josephin or Machado-Joseph disease protein domain proteases (MJDs), the Jab1/MPN domain-associated metalloisopeptidase (JAMM), and the monocyte chemotactic protein-induced protein family (MCPIP) (27). Among these families, UBPs are mostly described to date, with 60 proteases in humans, which have been well-reviewed by a range of publications (28–31). Recent studies have revealed the emerging functions of UCHs in the pathogenesis and progression of human malignancies. However, few studies on UCHs in HNC are available. One member of UCHs family, BRCA1-associated protein-1 (BAP1), was identified to be associated with poor outcome following radiation in HPV-negative HNSCC clinical sample by proteomic and transcriptomic analysis (32). Moreover, another member of UCHs family, UCHL1 was demonstrated as a tumor suppressor gene in nasopharyngeal carcinoma (NPC) (33). In this review, we systematically summarize the physiological and pathological functions of the UCHs family in human malignancies, providing enlightenment on potential mechanisms of UCHs family in HNC pathogenesis and the potential consideration of UCHs as novel promising drug targets.

STRUCTURES AND FUNCTIONS OF UCHS

Among DUBs family, molecular structures of UCHs were the first to be characterized. Four UCHs in humans have been identified: UCHL1/PGP9.5 (protein gene product 9.5), UCHL3, UCHL5/UCH37, and BAP1. All UCHs share a core catalytic domain with 230 amino acids and close homology among family members. They comprise a confined loop that cleaves short ubiquitylated peptides (up to 20–30 amino acids) from the C-terminal glycine residue (**Figure 1**).

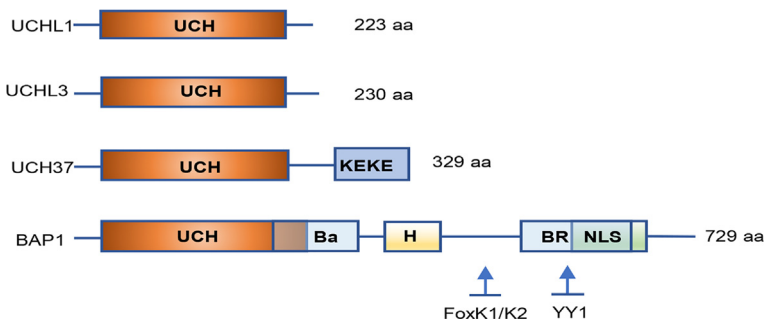

FIGURE 1 | Simplified structure of the UCH family proteins. All UCH members share close homology in their catalytic domains and have a core catalytic domain with 230 amino acids. UCHL3 contains a KEKE motif in the C-terminal tail. BAP1 consists of a long C-terminal extension illustrating numerous functional domains and binding sites for interacting proteins. UCH, ubiquitin C-terminal hydrolase; Ba, BARD1 binding domain; H, HCF-binding motif; BR, BRCA1 binding domain; NLS, nuclear localization signal; YY1, Ying Yang 1 binding region. Inspired by (26).

UCHL1

First identified as a member of UCHs family in the 1980s, UCHL1 is an abundant neuronal protein containing only one UCH domain with very short N- and C- terminal extensions. It possesses one of the most complicated protein knotted structure, which is regarded to protect UCHs from degradation in the proteasome as well as to maintain proper proteasomal function. Besides its DUB function in the recycling of free Ub, UCHL1 is also known to have a ubiquitin ligase activity as a mono-Ub stabilizer by preventing its degradation (34). It was reported that the generation rate of monomeric Ub by UCHL1 *in vitro* is enhanced by the catalytic residues C90 and H161 (35). Analysis of the crystal structure suggests that UCHL1 preferentially binds monomeric or small adducts of Ub, but does not act on large polymers of Ub (36). Therefore, UCHL1 has the potential for numerous ubiquitination-dependent biological processes.

UCHL1 is predominantly expressed in the brain, where it comprises up to 5% of total neuronal proteins. Although the precise function of UCHL1 is not fully clarified in many pathological processes, better understandings of functional UCHL1 has been largely reported in neuronal dysfunction and neurodegenerative disorders (34, 37–39). For instance, the specific distribution and activity of UCHL1 in human tissues has the potential clinical significance for Parkinson's disease (PD) and Alzheimer's disease (AD), might be a major target of reactive oxygen species (ROS) damage (40). Although most cases of PD are sporadic, a small subgroup of PD has been linked to specific genomic mutations (41). Interestingly, The I93M point mutation in UCHL1 has been reported to be associated with PD susceptibility by decreasing hydrolytic activity (42). By contrast, an S18Y variation in UCHL1 shows a protective enzyme with a reduced risk of PD by a reduction of α-synuclein (43). A study has shown that modification of the UCHL1 C152 site decreases injury to gray and white matter, resulting in the recovery of motor function after middle cerebral artery occlusion (44). Another potential feature of UCHL1 is an ATP-independent E3 ligase activity, which promotes Lys63 (K63) polyubiquitination of α-synuclein (34). Moreover, UCHL1 was demonstrated as a novel interactor and substrate of PD linked E3 ubiquitin-protein ligase parkin by the autophagy-lysosome pathway (45).

It has also been reported at much lower levels in kidney, breast epithelium, and reproductive tissues (46, 47), and to be expressed context-dependent in individual cells, such as human fibroblasts during wound healing (48). Uniform cytoplasmic staining of UCHL1 was observed in neurons, but UCHL1 can translocate into the nucleus and regulate microtubule dynamics (49). Although it is absent in most other normal tissues, UCHL1 appears to be aberrantly expressed in many non-neuronal tumors, including breast, prostate, colorectal, gastric, head and neck, and pancreatic ductal carcinomas (33, 50–55). The functions and potential mechanisms of UCHL1 in tumorigenesis have been reviewed by several excellent publications (56, 57). The interactive proteins with UCHL1 as well as other UCH family members in human malignancies are summarized in **Table 1**. In addition, altered expression levels of UCHs in various cancers have also been reviewed in **Table 2**.

Recent findings have revealed significant functions for UCHL1 in immune response and regulation. UCHL1 was found in mouse kidney, spleen, and bone marrow-derived dendritic cells, and its expression and activity were strongly regulated by the immune stimuli LPS and IFN-γ (113). UCHL1 modulates antigen processing by affecting the colocalization of intracellular MHC I with late endosomal/lysosomal compartments necessary for cross priming of CD8 T cells (113). Interestingly, an induced UCHL1 expression was also demonstrated in multipotent mesenchymal stromal cells (MSCs) upon stimulation with proinflammatory cytokines IFN-γ plus TNF-α, and negatively regulated the immunosuppressive capacity and survival of MSC. This discovery may provide potential MSC-based immunotherapy for inflammatory diseases by modulation of UCHL1 (114).

UCHL3

UCHL3 and UCHL1 have significant structural similarity. However, the biological characteristics of UCHL3 are quite distinct concerning expression patterns and ligase activity. Unlike

TABLE 1 | Overview of interacting proteins with UCHs family in various human malignancies.

UCHs family	Interacting protein	Human malignancies	References
UCHL1	P53	Breast cancer, metastatic colon adenocarcinoma, nasopharyngeal carcinoma, hepatocellular carcinoma	(33, 58–60)
	MDM2	Colorectal cancer, prostate cancer, nasopharyngeal carcinoma	(33, 61)
	β-catenin	Colorectal cancer, pediatric high-grade glioma	(62, 63)
	NOX4	Cervical cancer	(64)
	EGFR	Breast cancer	(65)
	HIF-1	Breast, lung cancer	(66, 67)
	cyclin B1	Uterine serous cancer	(68)
	PHLPP1	Lymphoma, lung tumor	(69)
	MITF	Melanoma	(70)
	SMAD2	Breast cancer	(53)
	TGFβ type I receptor	Breast cancer	(53)
	CTTN	Nasopharyngeal carcinoma	(71)
	mTORC1	B-cell lymphoma	(72)
	eIF4F	B-cell lymphoma	(73)
UCHL3	TRAF2	Ovarian cancer	(74)
	BRCA2	Breast cancer	(75)
	RAD51	Breast cancer	(75)
UCH37/UCHL5	PRP19	Hepatocellular carcinoma	(76)
	PRDX1	Hepatocellular carcinoma	(77)
	SNRPF	Glioma	(78)
	Smad2	Ovarian cancer	(79)
	GRP78	Hepatocellular carcinoma	(80)
	E2F1	Liver cancer	(81)
	Rpn13	Cervical cancer	(82)
BAP1	BRCA1/BARD1	Breast cancer, chronic myeloid leukemia, meningioma	(83–85)
	HCF-1	Breast cancer, renal cell carcinoma	(86, 87)
	Ino80	Mesothelioma	(88)
	Gamma-tubulin	Breast cancer	(89)
	ASXL1/2	Mesothelioma	(90)
	MCRS1	Renal cell carcinoma	(91)
	Histone H2A	Head and neck cancer	(32)
	IP3R3	Prostate cancer	(92)
	ATF3	Multiple carcinomas	(93)
	14-3-3 protein	Neuroblastoma	(94)
	SLC7A11	Multiple carcinomas	(95, 96)

UCHL1, which is mainly restricted to neuronal and neurosecretory tissues, UCHL3 is more widely expressed throughout mammalian tissues. Interestingly, UCHL3 hardly exhibits ligase activity, while its hydrolytic activity is two-hundred-fold higher than UCHL1 toward a fluorogenic ubiquitin C-terminal amide (34). It was reported that UCHL3 enables to cleave the C-terminus of NEDD8, which is a ubiquitin-like protein that exerts the function of Ub to be conjugated to a lysine residue of the substrate (115). Next, UCHL3 has also been demonstrated to alleviate cryptorchid-induced germ cell apoptosis in *gad* mice. UCHL3 appears to have dual affinities for ubiquitin and Nedd8, and function as a deNEDDylating enzyme *in vivo*, suggesting that UCHL3 plays a critical role in germ cell apoptosis (116). Several studies using similar UCHL3 knockout mouse models revealed the significant functions in photoreceptor cell degeneration, neurodegeneration, fertilization and embryogenesis, stress responses in skeletal muscle, diet-induced obesity, and osteoblast differentiation (117–122). It is worth mentioning that level of UCHL3 protein in several neurodegenerative diseases is unchanged, while it hydrolyzes the C-terminal extension of a mutant ubiquitin (UBB^{+1}), contributing to the role in neurodegenerative disorders (123).

An increasing number of studies have demonstrated vital functions of UCHL3 on tumorigenesis, including breast, prostate, ovarian, and non-small cell lung cancer (**Table 2**) (50, 74, 101, 102). Luo et al. found that UCHL3 deubiquitinates RAD51 and subsequently facilitates RAD51-BRCA2 interaction, which is critical for homologous recombination (HR) and contributes to therapeutic resistance in breast cancer (75). By contrast, UCHL3 is reduced in metastatic prostate cancer cell lines, and knockdown of UCHL3 promotes epithelial-to-mesenchymal transition (EMT), contributing to cancer cell invasion and metastasis (102). In contrast, high UCHL3 expression was reported in ovarian cancer and predicted a worse clinical outcome. The elevated UCHL3 facilitates carcinogenesis and enhances inflammation by deubiquitinating and stabilizing TNF Receptor Associated Factor 2 (TRAF2) (74). Taken together, the UCHL3 function in cancer remains controversial, suggesting the roles of UCHL3 is complicated and context-dependent in individual tumor types.

UCH37

UCH37 (also known as UCHL5) was identified first as a 19S-associated deubiquitinating enzyme in the 1990s, which comprises a C-terminal extension (residues 227-329) in addition to an N-terminal UCH domain (residues 1–226) (124). It is specific for the distal subunit of Lys48-linked poly-Ub chains. Isolated full-length UCH37 displays weak catalytic activity due to autonomic

TABLE 2 | Expression regulation of UCHs family in human malignancies.

UCHs family	Human malignances	Possible variations (References)
UCHL1	Breast cancer	Down-regulation (58)
	Hepatocellular carcinoma	Down-regulation (59)
	Invasive and metastatic breast cancer	Up-regulation (53, 97)
	Metastatic colon adenocarcinoma	Up-regulation (62)
	Nasopharyngeal carcinoma	Down-regulation (33, 71)
	Prostate cancer	Down-regulation (61)
	Pediatric high-grade glioma	Up-regulation (63)
	Ovarian cancer	Down-regulation (98)
	Non-small cell lung cancer	Up-regulation (99)
	Uterine serous cancer	Up-regulation (68)
	B-cell lymphoma	Up-regulation (100)
UCHL3	Breast cancer	Up-regulation (50)
	Ovarian cancer	Up-regulation (74)
	Non-small cell lung cancer	Up-regulation (101)
	Metastatic prostate cancer	Down-regulation (102)
	Cervical cancer	Up-regulation (103)
UCH37/UCHL5	Hepatocellular carcinoma	Up-regulation (76)
	Glioma	Down-regulation (78)
	Cervical cancer	Up-regulation (103)
	Esophageal squamous cell carcinoma	Up-regulation (104, 105)
BAP1	Breast cancer	Down-regulation (83, 89)
	Chronic myeloid leukemia	Down-regulation (84)
	Mesothelioma	Down-regulation (85, 106, 107)
	Non-small cell lung cancer	Down-regulation (83)
	Renal cell carcinoma	Down-regulation (87, 108)
	Uveal melanoma	Down-regulation (109, 110)
	Basal cell carcinomas	Down-regulation (111)
	Neuroblastoma	Down-regulation (94)
	Esophageal squamous cell carcinoma	Down-regulation (112)

inhibition by the C-terminal extension (125). The proteolytic activity requires a Ub receptor called ADRM1 (named hRpn13 in humans) binding to UCH37 *via* its C-terminal 46 residues (also called the KEKE motif) (125). In addition, hRpn13 was found to directly enhance the de-ubiquitination activity of UCH37 *in vitro* (125–127). The hRpn13-UCH37 complex hydrolyzes large Ub conjugates with incorporation into the 19S complex. By contrast, UCH37 is inhibited by the chromatin remodeling complex component INO80G mediated by the N-terminal domain of NFRKB (nuclear factor related to κB, NFRKB) (128). Rpn13 and INO80G share a conserved deubiquitinase adaptor (DEUBAD) domain that interacts with the C-terminal of UCH37, revealing conformational plasticity to regulate deubiquitinating activity on or off, respectively (128). Functionally, UCH37 is reported to perform a crucial role in certain protein-protein interactions involving several physiological and pathological processes, including development, cell proliferation, and apoptosis, hippocampal synaptic plasticity, Alzheimer's disease, pulmonary fibrosis, as well as human malignancies (26, 129–133).

Wicks and colleagues reported UCH37 interacts with Smad7 to control TGF-β/Smad signaling activity, suggesting that UCH37-mediated deubiquitination might contribute to tumorigenesis (134). The first direct evidence of UCH37 in cancer study was described by a chemistry-based functional proteomics approach in cervical carcinoma. Activity profiling showed UCH37 is induced in the majority of carcinoma tissues and HPV E6/E7 immortalized human keratinocytes, indicating a significant role of UCH37 in tumor transformation (103). Subsequently, an increasing number of studies reported the potential functions in tumor cell proliferation, apoptosis, migration, and invasion, as well as clinical implications (**Table 2**) (76–78, 135–138).

BAP1

The BAP1 protein consists of 729 amino acids that are encoded by the *BAP1* gene located on human chromosome 3p21.1. BAP1 protein was identified as a nuclear-localized DUB. In addition to the N-terminal UCH domain, BAP1 comprises a long C-terminal extension (**Figure 1**). BAP1 was originally found to interact with the RING finger domain of BRCA1 and to perform the cell growth-suppressive function. BAP1 is also involved in chromatin modification and transcription by deubiquitinating lysine residues in HCF1 and YY1. Both recruit histone-modifying complexes and regulate expression of numerous genes involved in multiple physiological processes (139). Moreover, BAP1 interacts with the transcription factor FOXK1/K2 in a phosphorylation-dependent manner, which represses FOXK2-target genes forming a ternary protein complex in which BAP1 bridges FoxK2 and HCF-1. Loss of BAP1 causes the increase of FoxK2 target genes, which is dependent on the Ring1B-Bmi1 complex (140).

Polycomb group proteins exert critical roles in transcriptional regulation, which contributes to a variety of physiological processes, including embryonic development, differentiation, and self-renewal. Polycomb repressive complexes (PRCs) are responsible for histone ubiquitination and methylation (139). BAP1 interacts with additional sex combs like 1 (ASXL1),

forming a polycomb group repressive deubiquitinase complex (PR-DUB). The transcriptional function is regulated through histones modification *via* ubiquitination by PRCs and deubiquitination by PR-DUB. Thus BAP1 deficiency significantly alters ubiquitination level of histone 2A, leading to the dysregulation of cell cycle and cellular senescence (141). A recent study found cytoplasm BAP1 localizes at the ER, where it regulates type 3 inositol-1,4,5-trisphosphate receptor (IP3R3), modulating calcium (Ca^{2+}) release from the endoplasmic reticulum into the cytosol and mitochondria, promoting apoptosis, which plays a critical role in cellular transformation (92). Another study has identified cystine transporter SLC7A11 as a critical BAP1 target gene in human malignancies, which was repressed by BAP1, causing increasing lipid peroxidation and ferroptosis (95).

BAP1 functions as a tumor suppressor through chromatin modulation, transcriptional regulation, cell cycle control, cellular differentiation, and DNA damage repair (142). Loss or mutation of *BAP1* gene is a common event in cancer and serves as a potential pathogenetic mechanism in various human malignancies, including uveal melanoma, mesothelioma, small cell and non-small cell lung carcinomas, renal cell carcinoma (RCC), breast cancer, and hepatocellular carcinoma (**Table 2**) (107, 143–148). Tumors associated with BAP1 somatic mutations have already been discussed in recent reviews (139, 149). Other alterations in the BAP1 gene have been reported, such as large deletions of exons causing premature protein termination, frameshift mutation, splice site mutations, and base substitutions-induced nonsense and missense mutations (143, 149). BAP1 acts as a tumor suppressor depending on both deubiquitination activity interfered by missense mutations and loss of nuclear localization signal by truncating mutations. Furthermore, several studies showed that BAP1 loss or modification is associated with different tumor phenotypes and clinical outcomes (108, 110, 150–152). For example, BAP1-mutated mesothelioma is significantly correlated with female predominance, younger age at onset, epithelioid differentiation, and better prognosis (153). At the same time, BAP1 mutation is strongly associated with a more aggressive, metastatic phenotype in uveal melanomas (143). BAP1 is frequently mutated in sporadic clear cell RCC with an incidence rate of 6–17%, which is associated with high tumor grade, rhabdoid/sarcomatoid transformation, and poor clinical outcome (154, 155). From a therapeutic standpoint in renal cell carcinoma, inactivation of BAP1 sensitizes tumor cells to irradiation and PARP-inhibitors, which might be due to the impaired ability of double-stranded DNA breaks (87).

UCHS MEMBERS IN HNC

Although UCHs members have been well investigated in a variety of human malignancies, the exact function of these enzymes in HNSCC pathogenesis and progression remain elusive. Each member of the UCHs family exerts distinct roles depending on the various tumor types. For example, UCHL1 has been controversially considered as a tumor suppressor or tumor promoter in specific tumor types. It was reported that UCHL1 is silenced by promoter CpG hypermethylation in a large panel of primary tumors including HNSCC cell lines and primary tumors, suggesting a tumor-suppressive function (33, 156). The methylation of the CpG locus associated with the UCHL1 gene is dependent on the anatomic site of HNSCC primary tumors, with most hypermethylation of UCHL1 specifically in oral cavity SCC (157). Restored UCHL1 expression significantly suppressed tumor cell proliferation and induced cellular apoptosis through activation of the p14ARF-p53 signaling pathway (33). A more recent study in nasopharyngeal carcinoma revealed a similar conclusion that UCHL1 promoter hypermethylation was validated in nasopharyngeal carcinoma tissues. In addition, restoration of UCHL1 inhibits tumor invasion and metastasis *in vitro* and *in vivo*. UCHL1 exerts tumor suppressor function by inducing K48-linked ubiquitination of CTTN (71). Currently, it is widely accepted that high-risk HPV infection is a risk factor for HNSCC, particularly in the oropharynx. High-risk HPV infects the oropharyngeal epithelium causing host immune suppression and evasion (11). UCHL1 does not assist HPV genome replication and viral propagation, but suppresses keratinocyte-mediated production of inflammatory cytokines and chemokines, thereby contributing to immune evasion and HPV persistent infection (158). UCHL1 interacts with tumor necrosis factor receptor-associated factor 3 (TRAF3), which acts as a negative regulator of the alternative NF-κB pathway and antiviral type I IFN activation. TRAF3 has been shown as a tumor suppressor that regulates the malignant phenotype of HPV-positive HNSCC (158).

As a tumor suppressor, BAP1 is critical for promoting DNA repair and cellular recovery from DSB *via* modulation of H2A ubiquitination (159). BAP1 was found to mediate radioresistance in an *in vivo* xenograft model and HNSCC cell lines *via* the deubiquitination of H2A and modulation of HR. Moreover, up-regulation of BAP1 was associated with worse clinical outcome in HNSCC, which indicates BAP1 might serve as a potential therapeutic target in HNSCC (32). In summary, it seems that loss of BAP1 foster genomic instability in tumor pathogenesis, however, the activity of BAP1 promotes tumor cell survival and contributes to therapeutic resistance during irradiation.

Induced activity of UCHL1 and UCHL3 were observed in E6/E7 immortalized primary keratinocytes, indicating the potential function of UCHL1 and UCHL3 in HPV-related HNSCC (103). However, few direct evidences concerning the function of UCHL3 and UCH37 in HNSCC have been reported.

Recently, comprehensive epigenetic and genomic profiling studies have highlighted the most frequently altered genes and signaling pathways in HNSCC. The genomic characterization of 279 HNSCCs including HPV-positive and HPV-negative tumors, has been published (23). Moreover, the molecular profiling data from over 500 HNSCC patients are available at the cBioPortal for Cancer Genomics, which provides interactive exploration and analysis of genetic alterations (160, 161). In addition, the GTEx project provides RNA sequencing data from more than 8,000 normal tissues. Currently, several web-based

tools deliver interface-friendly and personalized functions based on TCGA and GTEx data (161, 162). cBioPortal provides visualization for the genomic alteration data. Clinical and genomic analysis of multicohort HNSCC has demonstrated that HPV-positive and HPV-negative tumors present heterogeneity in anatomical regions, mutation profiles, molecular characteristics, immune landscapes, and clinical prognosis. Many evidence revealed the diversity and heterogeneity of HNSCC clinicopathology and therapeutic responses depending on HPV status (163). To better understand the UCHs family mutational landscape in HNSCC, the cBioPortal tool was used to display the types of mutations and their positions in the domain structure of proteins (**Figures 2A, B**). UCHs member genes are altered in 22 (8%) of queried patients. Of these, 20 cases are HPV-negative, and 2 cases are HPV-positive.

UCHL1 alterations accounted for 0.4% in HPV-negative subgroup and no genetic alteration in HPV-positive patients, *UCHL3* for 3.3% in HPV-negative and 2.7% in HPV-positive, *UCHL5* for 2% in HPV-negative and 2.7% in HPV-positive, and *BAP1* for 2.4% in HPV-negative and 0 in HPV-positive. Interestingly, there is no samples overlapped. Concerning the mutation type, one missense mutation in UCH-domain of *UCHL3*, two missense mutations in *UCHL5*, two missense mutations and one truncating mutation in *BAP1*. A web-based tool GEPIA (164) analysis revealed *UCHL1* gene expression in HNSCC tissues is significantly elevated as compared to normal tissues, which is different from the previous studies in nasopharyngeal carcinoma (71) (**Figure 3A**). Survival analyses based on gene expression levels was also applied to evaluate the clinical relevance of UCHs family genes (**Figures 3B, C**). The quartile cut-off method was determined depending on the optimization and visualization of the online web tool. However, numerous problems remain unsolved. We were not able to divide the cohort into two subtypes due to the incompleteness of the HPV status information. More specific subgroups of HNSCC patients for certain phenotypes need to be discovered depending on the protein expression patterns of UCHs family, which may contribute to illuminate the clinical relevance of UCHs family for HNSCC patients. Moreover, the gene networks regulated by UCHs family genes should be identified by analyzing the RNA-sequencing profiling data. Novel signaling pathways and biological processes related to UCHs family in HNSCC are urgent to be clarified. Functional proteomics represents a useful approach to investigate the UCHs family activity-related biological processes in different subtypes of HNSCC. Only BAP1 protein expression data by reverse-phase protein arrays (RPPAs) are available in the TCPA dataset, where BAP1 serves as a strong prognostic predictor for female-related cancer cohorts including samples of invasive breast carcinoma, Ovarian serous cystadenocarcinoma, Uterine Corpus Endometrial Carcinoma (25). More large-scale proteomic profiling data on the other UCHs members are urgent to be produced.

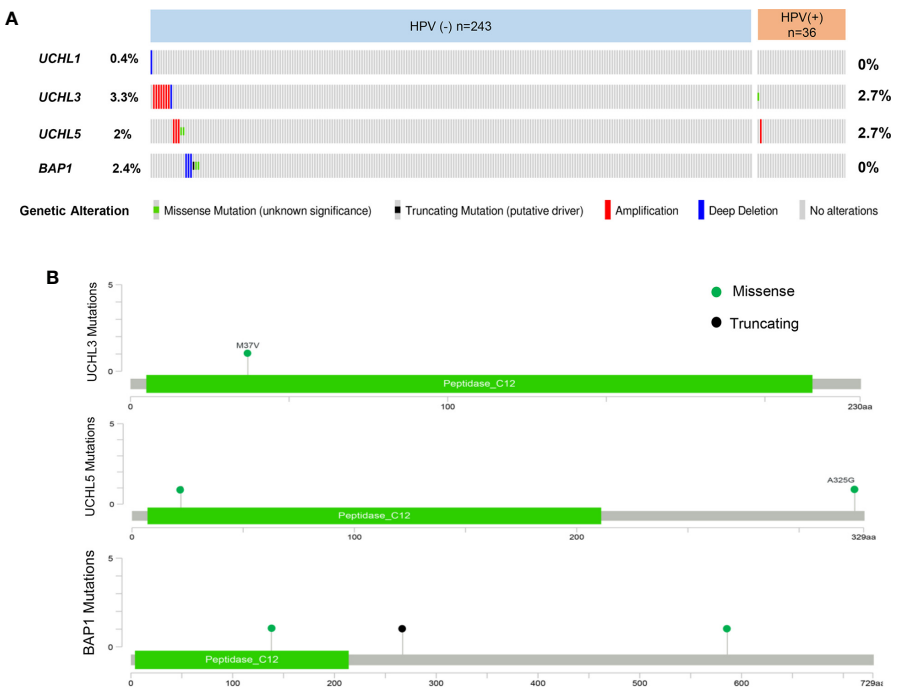

FIGURE 2 | Overview of genetic changes of UCHs family in TCGA HNSCC patients. **(A)** Oncoprint shows altered UCHs family genes. The colors are associated with one class of variants, and the percentage (%) of patients affected is shown on the graph. **(B)** cBioPortal predicted mutation maps showing the positions of mutations on the functional domains of UCHL3, UCHL5, and BAP1 proteins.

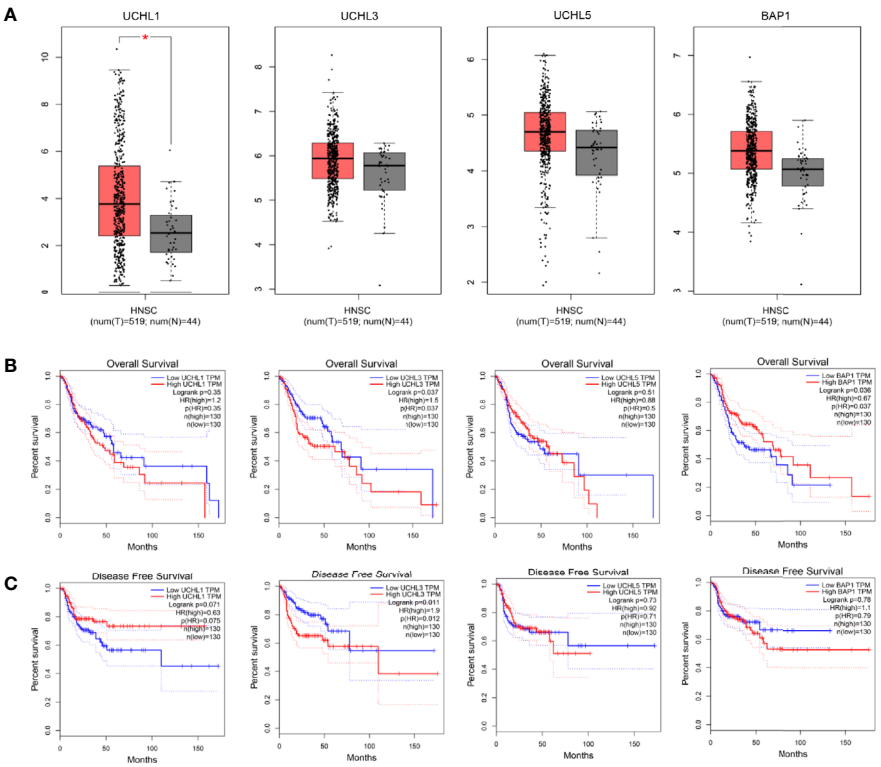

FIGURE 3 | Differential expression analysis of UCH family genes between tumor tissues and normal tissues in the TCGA-HNSC cohort **(A)**. Kaplan-Meier plots analyses show overall **(B)** and disease-free **(C)** survival compared by log-rank test. The Cox proportional hazard ratio (HR) is shown in the survival plots.

Therapeutic Implications for HNC Targeting UCHs members

Research on targeting UCHs members in HNSCC therapy is still in the initial period. To our knowledge, there are no studies focusing on UCHs family molecular inhibitors or drugs for clinical trials, which reflects the lack of theoretical and preclinical research. Encouragingly, UCHs family has been shown to predict therapeutic sensitivity and clinical outcomes for various tumors. For example, UCHL1 strengthens tumor cells chemosensitivity in melanoma and colorectal cancer by stabilizing NOXA (165). BAP1 was also reported to modulate cancer cell sensitivity to radiotherapy and the molecular inhibitors including PARP (olaparib) or histone deacetylase inhibitors (panobinostat), which may become potential therapeutic strategies (87, 166). The small molecule b-AP15 as a previously unidentified class of proteasome inhibitor abrogates the activity of two 19S regulatory-particle-associated deubiquitinases, UCH37/UCHL5, and USP14 (167). *In vivo* b-AP15 prevents tumor progression in four different solid tumor models, including HNSCC, indicating deubiquitinating activity of UCH37/UCHL5 represents a novel therapeutic target for cancer (167).

Over the last decade, the high-risk HPV infection in HNC plays a critical role in staging and prognosis, which promotes personalized therapy and the de-intensification of currently established treatment protocols based on HPV status (168). The underlying mechanisms of UCHs family in HPV-related carcinogenesis remains an enigma. It is worth mentioning that UCHL1 was specifically up-regulated by high-risk HPV in primary keratinocytes to escape innate immunity. Therefore, the precious functions of UCHL1 and other UCHs family members in HPV-related HNSCC need to be disclosed. One of the current therapeutic challenges is to find more suitable biomarkers or surrogate markers for the identity and selection of subpopulation, which would benefit from personalized and therapy. Response rates of HNSCC patients to cetuximab, the only FDA-approved molecularly target-EGFR monoclonal antibody, are only 10% (169). UCHs members have been described to interact with EGFR (170), suggesting the potential of combination therapy with UCHs members for cetuximab treatment in HNSCC.

HNSCC, like other human malignancies, is an immunosuppressive disease. Therefore, immunomodulatory treatment to overcome immune suppressive phenotypes in HNSCC patients has emerged as novel and effective strategies, which include cancer vaccines (e.g., HPV vaccines, tumor peptide antigens), cytokines (e.g., IL2, IFNγ, TNFα), specific monoclonal antibodies (e.g., anti-PD1/PD-L1, CTLA-4 antibodies) (171). Over the past 10 years, the most remarkable therapeutic advances have been achieved in immune checkpoint blockade in HNSCC. FDA approved several target immune checkpoint agents for the treatment of patients with HNSCC.

However, the patients revealed different responses to these agents, with only less than 20% of the responder (172, 173). There are many challenges for the immunotherapy of HNC in the future, such as the selection of responding patients, integration into the spectrum of conventional treatment, reduction of immunosuppression in non-responding patients (174). The DUBs are involved in the regulation of innate and adaptive immune response, which sheds light on the immunoregulatory of UCHs family for combination immunotherapy in HNSCC (114, 175). In addition, a variety of patented compounds targeting UCHs members have been developed, which would prepare a path toward the outstanding achievement of genuinely personalized medicine for the treatment of cancers (176–179).

CONCLUSION AND PERSPECTIVE

In summary, an increasing number of studies suggest that members of UCHs family exert distinct functions in a variety of human malignancies. However, available studies on UCHs in head and neck cancer are limited. It is an exciting time for HNSCC research based on the comprehensive genomic data, as the molecular landscape and altered signaling pathways has been synthetically described. But there are no genetic and proteomic screening tests routinely incorporated into the HNSCC clinically. Emerging evidence has revealed the members of UCHs are associated with the pathogenesis and clinical prognosis of HNSCC, which highlights the prognostic and therapeutic implications of UCHs for patients with HNC. Based on the available data, we have launched a joint project on the expression and function of UCHs in HNSCC, which aims to provide more evidence that UCHs might be the novel prognostic marker and therapeutic target. There are some emerging unresolved issues in HNSCC, such as: what are the precise substrates and regulators of the UCHs family? What are genetic or epigenetic events, and signaling pathways relevant to the UCHs family? Are UCHs family members able to serve as biomarkers for identifying a subset of patients to receive the optimal treatment? Can the agents targeting UCHs family become one of the novel treatment regimens? Optimization of combination regimens of immune checkpoint inhibitors and the agents targeting UCHs family may be a remarkable challenge for immunotherapy of HNSCC. Finally, whether and how the UCHs family members can be translated into the clinical management of HNC remains a formidable mission for the future.

AUTHOR CONTRIBUTIONS

Conception and design: CR, RZ, and JH. Writing—original draft preparation: CR and RZ. Review of the literature: CR, RZ, and SW. Project supervision: DS and S-LW. Critical revision of the manuscript: JH. Revise and resubmit: CR. All authors contributed to the article and approved the submitted version.

FUNDING

CR and SW are supported by the Natural Science Foundation of the Jiangsu Higher Education Institutions of China (No. 20KJB310014, No. 18KJB320017), Natural Science Foundation of Jiangsu Province (No. BK20200878). RZ and DS are supported by Wu Jieping Medical Foundation Research Fund Project of Chinese Medical Association (No. 320.6750.19090-19). S-LW is supported by National Key R&D Program of China (Grant No. 2016YFC1303800). This study was also supported by the Priority Academic Program Development of Jiangsu Higher Education Institutions (PAPD).

ACKNOWLEDGMENTS

We would like to acknowledge cBioPortal and GEPIA that provide the web-based tools for exploring, visualizing, and analyzing cancer genomic data. We apologize to colleagues whose work was not cited in this review due to space constraints.

REFERENCES

1. Bray F, Ferlay J, Soerjomataram I, Siegel RL, Torre LA, Jemal A. Global cancer statistics 2018: GLOBOCAN estimates of incidence and mortality worldwide for 36 cancers in 185 countries. *CA: Cancer J Clin* (2018) 68 (6):394–424. doi: 10.3322/caac.21492
2. Ferlay J, Colombet M, Soerjomataram I, Dyba T, Randi G, Bettio M, et al. Cancer incidence and mortality patterns in Europe: Estimates for 40 countries and 25 major cancers in 2018. *Eur J Cancer (Oxford Engl 1990)* (2018) 103:356–87. doi: 10.1016/j.ejca.2018.07.005
3. Leemans CR, Braakhuis BJ, Brakenhoff RH. The molecular biology of head and neck cancer. *Nat Rev Cancer* (2011) 11(1):9–22. doi: 10.1038/nrc2982
4. Shield KD, Ferlay J, Jemal A, Sankaranarayanan R, Chaturvedi AK, Bray F, et al. The global incidence of lip, oral cavity, and pharyngeal cancers by subsite in 2012. *CA: Cancer J Clin* (2017) 67(1):51–64. doi: 10.3322/caac.21384
5. Argiris A, Karamouzis MV, Raben D, Ferris RL. Head and neck cancer. *Lancet* (2008) 371(9625):1695–709. doi: 10.1016/S0140-6736(08)60728-X
6. Guo X, Johnson RC, Deng H, Liao J, Guan L, Nelson GW, et al. Evaluation of nonviral risk factors for nasopharyngeal carcinoma in a high-risk population of Southern China. *Int J Cancer* (2009) 124(12):2942–7. doi: 10.1002/ijc.24293
7. Tsao SW, Yip YL, Tsang CM, Pang PS, Lau VMY, Zhang G, et al. Etiological factors of nasopharyngeal carcinoma. *Oral Oncol* (2014) 50(5):330–8. doi: 10.1016/j.oraloncology.2014.02.006
8. Chua MLK, Wee JTS, Hui EP, Chan ATC. Nasopharyngeal carcinoma. *Lancet (London England)* (2016) 387(10022):1012–24. doi: 10.1016/S0140-6736(15)00055-0
9. Rietbergen MM, van Bokhoven A, Lissenberg-Witte BI, Heideman DAM, Leemans CR, Brakenhoff RH, et al. Epidemiologic associations of HPV-positive oropharyngeal cancer and (pre)cancerous cervical lesions. *Int J Cancer J Int Du Cancer* (2018) 143(2):283–8. doi: 10.1002/ijc.31315
10. Gillison ML, Koch WM, Capone RB, Spafford M, Westra WH, Wu L, et al. Evidence for a causal association between human papillomavirus and a subset of head and neck cancers. *J Natl Cancer Institute* (2000) 92(9):709–20. doi: 10.1093/jnci/92.9.709

11. Sabatini ME, Chiocca S. Human papillomavirus as a driver of head and neck cancers. *Br J Cancer* (2020) 122(3):306–14. doi: 10.1038/s41416-019-0602-7
12. Syrjanen S. Human papillomavirus (HPV) in head and neck cancer. *J Clin Virol* (2005) 32 Suppl 1:S59–66. doi: 10.1016/j.jcv.2004.11.017
13. Marur S, D'Souza G, Westra WH, Forastiere AA. HPV-associated head and neck cancer: a virus-related cancer epidemic. *Lancet Oncol* (2010) 11(8):781–9. doi: 10.1016/S1470-2045(10)70017-6
14. Ren S, Gaykalova DA, Guo T, Favorov AV, Fertig EJ, Tamayo P, et al. HPV E2, E4, E5 drive alternative carcinogenic pathways in HPV positive cancers. *Oncogene* (2020) 39(40):6327–39. doi: 10.1038/s41388-020-01431-8
15. Braakhuis BJ, Snijders PJ, Keune WJ, Meijer CJ, Ruijter-Schippers HJ, Leemans CR, et al. Genetic patterns in head and neck cancers that contain or lack transcriptionally active human papillomavirus. *J Natl Cancer Institute* (2004) 96(13):998–1006. doi: 10.1093/jnci/djh183
16. Slebos RJ, Yi Y, Ely K, Carter J, Evjen A, Zhang X, et al. Gene expression differences associated with human papillomavirus status in head and neck squamous cell carcinoma. *Clin Cancer Res An* (2006) 12(3 Pt 1):701–9. doi: 10.1158/1078-0432.CCR-05-2017
17. Ang KK, Harris J, Wheeler R, Weber R, Rosenthal DI, Nguyen-Tan PF, et al. Human papillomavirus and survival of patients with oropharyngeal cancer. *New Engl J Med* (2010) 363(1):24–35. doi: 10.1056/NEJMoa0912217
18. Spence T, Bruce J, Yip KW, Liu FF. HPV Associated Head and Neck Cancer. *Cancers (Basel)* (2016) 8(8). doi: 10.3390/cancers8080075
19. Chera BS, Amdur RJ, Tepper J, Qaqish B, Green R, Aumer SL, et al. Phase 2 Trial of De-intensified Chemoradiation Therapy for Favorable-Risk Human Papillomavirus-Associated Oropharyngeal Squamous Cell Carcinoma. *Int J Radiat Oncol Biol Phys* (2015) 93(5):976–85. doi: 10.1016/j.ijrobp.2015.08.033
20. Mirghani H, Amen F, Blanchard P, Moreau F, Guigay J, Hartl DM, et al. Treatment de-escalation in HPV-positive oropharyngeal carcinoma: ongoing trials, critical issues and perspectives. *Int J Cancer J Int Du Cancer* (2015) 136(7):1494–503. doi: 10.1002/ijc.28847
21. Paclitaxel, cisplatin, and cetuximab followed by cetuximab and intensity-modulated radiation therapy in treating patients with HPV-associated stage III or stage IV cancer of the oropharynx that can be removed by surgery; NCT01084083. Available at: http://www.clinicaltrials.gov/.
22. Bigelow EO, Seiwert TY, Fakhry C. Deintensification of treatment for human papillomavirus-related oropharyngeal cancer: Current state and future directions. *Oral Oncol* (2020) 105:104652. doi: 10.1016/j.oraloncology.2020.104652
23. Cancer Genome Atlas N. Comprehensive genomic characterization of head and neck squamous cell carcinomas. *Nature* (2015) 517(7536):576–82. doi: 10.1038/nature14129
24. Akbani R, Ng PK, Werner HM, Shahmoradgoli M, Zhang F, Ju Z, et al. A pan-cancer proteomic perspective on The Cancer Genome Atlas. *Nat Commun* (2014) 5:3887. doi: 10.1038/ncomms4887
25. Li J, Lu Y, Akbani R, Ju Z, Roebuck PL, Liu W, et al. TCPA: a resource for cancer functional proteomics data. *Nat Methods* (2013) 10(11):1046–7. doi: 10.1038/nmeth.2650
26. Fang Y, Shen X. Ubiquitin carboxyl-terminal hydrolases: involvement in cancer progression and clinical implications. *Cancer Metastasis Rev* (2017) 36(4):669–82. doi: 10.1007/s10555-017-9702-0
27. Nijman SM, Luna-Vargas MP, Velds A, Brummelkamp TR, Dirac AM, Sixma TK, et al. A genomic and functional inventory of deubiquitinating enzymes. *Cell* (2005) 123(5):773–86. doi: 10.1016/j.cell.2005.11.007
28. Pfoh R, Lacdao IK, Saridakis V. Deubiquitinases and the new therapeutic opportunities offered to cancer. *Endocr Relat Cancer* (2015) 22(1):T35–54. doi: 10.1530/ERC-14-0516
29. Pal A, Young MA, Donato NJ. Emerging potential of therapeutic targeting of ubiquitin-specific proteases in the treatment of cancer. *Cancer Res* (2014) 74(18):4955–66. doi: 10.1158/0008-5472.CAN-14-1211
30. Reyes-Turcu FE, Ventii KH, Wilkinson KD. Regulation and cellular roles of ubiquitin-specific deubiquitinating enzymes. *Annu Rev Biochem* (2009) 78:363–97. doi: 10.1146/annurev.biochem.78.082307.091526
31. Young MJ, Hsu KC, Lin TE, Chang WC, Hung JJ. The role of ubiquitin-specific peptidases in cancer progression. *J BioMed Sci* (2019) 26(1):42. doi: 10.1186/s12929-019-0522-0
32. Liu X, Kumar M, Yang L, Molkentine DP, Valdecanas D, Yu S, et al. BAP1 Is a Novel Target in HPV-Negative Head and Neck Cancer. *Clin Cancer Res* (2018) 24(3):600–7. doi: 10.1158/1078-0432.CCR-17-1573
33. Li L, Tao Q, Jin H, van Hasselt A, Poon FF, Wang X, et al. The tumor suppressor UCHL1 forms a complex with p53/MDM2/ARF to promote p53 signaling and is frequently silenced in nasopharyngeal carcinoma. *Clin Cancer Res* (2010) 16(11):2949–58. doi: 10.1158/1078-0432.CCR-09-3178
34. Liu Y, Fallon L, Lashuel HA, Liu Z, Lansbury PT Jr. The UCH-L1 gene encodes two opposing enzymatic activities that affect alpha-synuclein degradation and Parkinson's disease susceptibility. *Cell* (2002) 111(2):209–18. doi: 10.1016/s0092-8674(02)01012-7
35. Larsen CN, Price JS, Wilkinson KD. Substrate binding and catalysis by ubiquitin C-terminal hydrolases: identification of two active site residues. *Biochemistry* (1996) 35(21):6735–44. doi: 10.1021/bi960099f
36. Larsen CN, Krantz BA, Wilkinson KD. Substrate specificity of deubiquitinating enzymes: ubiquitin C-terminal hydrolases. *Biochemistry* (1998) 37(10):3358–68. doi: 10.1021/bi972274d
37. Sakurai M, Sekiguchi M, Zushida K, Yamada K, Nagamine S, Kabuta T, et al. Reduction in memory in passive avoidance learning, exploratory behaviour and synaptic plasticity in mice with a spontaneous deletion in the ubiquitin C-terminal hydrolase L1 gene. *Eur J Neurosci* (2008) 27(3):691–701. doi: 10.1111/j.1460-9568.2008.06047.x
38. Day IN, Thompson RJ. UCHL1 (PGP 9.5): neuronal biomarker and ubiquitin system protein. *Prog Neurobiol* (2010) 90(3):327–62. doi: 10.1016/j.pneurobio.2009.10.020
39. Setsuie R, Wada K. The functions of UCH-L1 and its relation to neurodegenerative diseases. *Neurochem Int* (2007) 51(2-4):105–11. doi: 10.1016/j.neuint.2007.05.007
40. Choi J, Levey AI, Weintraub ST, Rees HD, Gearing M, Chin LS, et al. Oxidative modifications and down-regulation of ubiquitin carboxyl-terminal hydrolase L1 associated with idiopathic Parkinson's and Alzheimer's diseases. *J Biol Chem* (2004) 279(13):13256–64. doi: 10.1074/jbc.M314124200
41. Chai C, Lim KL. Genetic insights into sporadic Parkinson's disease pathogenesis. *Curr Genomics* (2013) 14(8):486–501. doi: 10.2174/1389202914666131210195808
42. Leroy E, Boyer R, Auburger G, Leube B, Ulm G, Mezey E, et al. The ubiquitin pathway in Parkinson's disease. *Nature* (1998) 395(6701):451–2. doi: 10.1038/26652
43. Maraganore DM, Farrer MJ, Hardy JA, Lincoln SJ, McDonnell SK, Rocca WA. Case-control study of the ubiquitin carboxy-terminal hydrolase L1 gene in Parkinson's disease. *Neurology* (1999) 53(8):1858–60. doi: 10.1212/wnl.53.8.1858
44. Liu H, Povysheva N, Rose ME, Mi Z, Banton JS, Li W, et al. Role of UCHL1 in axonal injury and functional recovery after cerebral ischemia. *Proc Natl Acad Sci U S A* (2019) 116(10):4643–50. doi: 10.1073/pnas.1821282116
45. McKeon JE, Sha D, Li L, Chin LS. Parkin-mediated K63-polyubiquitination targets ubiquitin C-terminal hydrolase L1 for degradation by the autophagy-lysosome system. *Cell Mol Life Sci* (2015) 72(9):1811–24. doi: 10.1007/s00018-014-1781-2
46. Bradbury JM, Thompson RJ. Immunoassay of the neuronal and neuroendocrine marker PGP 9.5 in human tissues. *J Neurochem* (1985) 44(2):651–3. doi: 10.1111/j.1471-4159.1985.tb05461.x
47. Schumacher U, Mitchell BS, Kaiserling E. The neuronal marker protein gene product 9.5 (PGP 9.5) is phenotypically expressed in human breast epithelium, in milk, and in benign and malignant breast tumors. *DNA Cell Biol* (1994) 13(8):839–43. doi: 10.1089/dna.1994.13.839
48. Olerud JE, Chiu DS, Usui ML, Gibran NS, Ansel JC. Protein gene product 9.5 is expressed by fibroblasts in human cutaneous wounds. *J Invest Dermatol* (1998) 111(4):565–72. doi: 10.1046/j.1523-1747.1998.00330.x
49. Bheda A, Gullapalli A, Caplow M, Pagano JS, Shackelford J. Ubiquitin editing enzyme UCH L1 and microtubule dynamics: implication in mitosis. *Cell Cycle* (2010) 9(5):980–94. doi: 10.4161/cc.9.5.10934
50. Miyoshi Y, Nakayama S, Torikoshi Y, Tanaka S, Ishihara H, Taguchi T, et al. High expression of ubiquitin carboxy-terminal hydrolase-L1 and -L3 mRNA predicts early recurrence in patients with invasive breast cancer. *Cancer Sci* (2006) 97(6):523–9. doi: 10.1111/j.1349-7006.2006.00202.x

51. Ummanni R, Mundt F, Pospisil H, Venz S, Scharf C, Barett C, et al. Identification of clinically relevant protein targets in prostate cancer with 2D-DIGE coupled mass spectrometry and systems biology network platform. *PloS One* (2011) 6(2):e16833. doi: 10.1371/journal.pone.0016833
52. Fukutomi S, Seki N, Koda K, Miyazaki M. Identification of methylation-silenced genes in colorectal cancer cell lines: genomic screening using oligonucleotide arrays. *Scand J Gastroenterol* (2007) 42(12):1486–94. doi: 10.1080/00365520701491173
53. Liu S, Gonzalez-Prieto R, Zhang M, Geurink PP, Kooij R, Iyengar PV, et al. Deubiquitinase Activity Profiling Identifies UCHL1 as a Candidate Oncoprotein That Promotes TGFbeta-Induced Breast Cancer Metastasis. *Clin Cancer Res* (2019). doi: 10.1158/1078-0432.CCR-19-1373
54. Yamashita K, Park HL, Kim MS, Osada M, Tokumaru Y, Inoue H, et al. PGP9.5 methylation in diffuse-type gastric cancer. *Cancer Res* (2006) 66 (7):3921–7. doi: 10.1158/0008-5472.CAN-05-1511
55. Tezel E, Hibi K, Nagasaka T, Nakao A. PGP9.5 as a Prognostic Factor in Pancreatic Cancer. *Clin Cancer Res* (2000) 6:4764–7. doi: 10.1038/bjc.2014.417
56. Hurst-Kennedy J, Chin LS, Li L. Ubiquitin C-terminal hydrolase l1 in tumorigenesis. *Biochem Res Int* (2012) 2012:123706. doi: 10.1155/2012/123706
57. Jara JH, Frank DD, Ozdinler PH. Could dysregulation of UPS be a common underlying mechanism for cancer and neurodegeneration? Lessons from UCHL1. *Cell Biochem Biophys* (2013) 67(1):45–53. doi: 10.1007/s12013-013-9631-7
58. Xiang T, Li L, Yin X, Yuan C, Tan C, Su X, et al. The ubiquitin peptidase UCHL1 induces G0/G1 cell cycle arrest and apoptosis through stabilizing p53 and is frequently silenced in breast cancer. *PloS One* (2012) 7(1):e29783. doi: 10.1371/journal.pone.0029783
59. Yu J, Tao Q, Cheung KF, Jin H, Poon FF, Wang X, et al. Epigenetic identification of ubiquitin carboxyl-terminal hydrolase L1 as a functional tumor suppressor and biomarker for hepatocellular carcinoma and other digestive tumors. *Hepatology* (2008) 48(2):508–18. doi: 10.1002/hep.22343
60. Abdelmaksoud-Dammak R, Saadallah-Kallel A, Miladi-Abdennadher I, Ayedi L, Khabir A, Sallemi-Boudawara T, et al. CpG methylation of ubiquitin carboxyl-terminal hydrolase 1 (UCHL1) and P53 mutation pattern in sporadic colorectal cancer. *Tumour Biol* (2016) 37(2):1707–14. doi: 10.1007/s13277-015-3902-4
61. Ummanni R, Jost E, Braig M, Lohmann F, Mundt F, Barett C, et al. Ubiquitin carboxyl-terminal hydrolase 1 (UCHL1) is a potential tumour suppressor in prostate cancer and is frequently silenced by promoter methylation. *Mol Cancer* (2011) 10:129. doi: 10.1186/1476-4598-10-129
62. Zhong J, Zhao M, Ma Y, Luo Q, Liu J, Wang J, et al. UCHL1 acts as a colorectal cancer oncogene via activation of the beta-catenin/TCF pathway through its deubiquitinating activity. *Int J Mol Med* (2012) 30(2):430–6. doi: 10.3892/ijmm.2012.1012
63. Sanchez-Diaz PC, Chang JC, Moses ES, Dao T, Chen Y, Hung JY. Ubiquitin carboxyl-terminal esterase L1 (UCHL1) is associated with stem-like cancer cell functions in pediatric high-grade glioma. *PloS One* (2017) 12(5): e0176879. doi: 10.1371/journal.pone.0176879
64. Kim HJ, Magesh V, Lee JJ, Kim S, Knaus UG, Lee KJ. Ubiquitin C-terminal hydrolase-L1 increases cancer cell invasion by modulating hydrogen peroxide generated via NADPH oxidase 4. *Oncotarget* (2015) 6 (18):16287–303. doi: 10.18632/oncotarget.3843
65. Jin Y, Zhang W, Xu J, Wang H, Zhang Z, Chu C, et al. UCH-L1 involved in regulating the degradation of EGFR and promoting malignant properties in drug-resistant breast cancer. *Int J Clin Exp Pathol* (2015) 8(10):12500–8.
66. Goto Y, Zeng L, Yeom CJ, Zhu Y, Morinibu A, Shinomiya K, et al. UCHL1 provides diagnostic and antimetastatic strategies due to its deubiquitinating effect on HIF-1alpha. *Nat Commun* (2015) 6:6153. doi: 10.1038/ncomms7153
67. Li X, Hattori A, Takahashi S, Goto Y, Harada H, Kakeya H. Ubiquitin carboxyl-terminal hydrolase L1 promotes hypoxia-inducible factor 1-dependent tumor cell malignancy in spheroid models. *Cancer Sci* (2019). doi: 10.1111/cas.14236
68. Kwan SY, Au-Yeung CL, Yeung TL, Rynne-Vidal A, Wong KK, Risinger JI, et al. Ubiquitin Carboxyl-Terminal Hydrolase L1 (UCHL1) Promotes Uterine Serous Cancer Cell Proliferation and Cell Cycle Progression. *Cancers (Basel)* (2020) 12(1). doi: 10.3390/cancers12010118
69. Hussain S, Foreman O, Perkins SL, Witzig TE, Miles RR, van Deursen J, et al. The de-ubiquitinase UCH-L1 is an oncogene that drives the development of lymphoma in vivo by deregulating PHLPP1 and Akt signaling. *Leukemia* (2010) 24(9):1641–55. doi: 10.1038/leu.2010.138
70. Seo EY, Jin SP, Sohn KC, Park CH, Lee DH, Chung JH. UCHL1 Regulates Melanogenesis through Controlling MITF Stability in Human Melanocytes. *J Invest Dermatol* (2017) 137(8):1757–65. doi: 10.1016/j.jid.2017.03.024
71. Zhao Y, Lei Y, He SW, Li YQ, Wang YQ, Hong XH, et al. Hypermethylation of UCHL1 Promotes Metastasis of Nasopharyngeal Carcinoma by Suppressing Degradation of Cortactin (CTTN). *Cells* (2020) 9(3). doi: 10.3390/cells9030559
72. Hussain S, Bedekovics T, Liu Q, Hu W, Jeon H, Johnson SH, et al. UCH-L1 bypasses mTOR to promote protein biosynthesis and is required for MYC-driven lymphomagenesis in mice. *Blood* (2018) 132(24):2564–74. doi: 10.1182/blood-2018-05-848515
73. Hussain S, Bedekovics T, Ali A, Zaid O, May DG, Roux KJ, et al. A cysteine near the C-terminus of UCH-L1 is dispensable for catalytic activity but is required to promote AKT phosphorylation, eIF4F assembly, and malignant B-cell survival. *Cell Death Discov* (2019) 5:152. doi: 10.1038/s41420-019-0231-1
74. Zhang MH, Zhang HH, Du XH, Gao J, Li C, Shi HR, et al. UCHL3 promotes ovarian cancer progression by stabilizing TRAF2 to activate the NF-kappaB pathway. *Oncogene* (2020) 39(2):322–33. doi: 10.1038/s41388-019-0987-z
75. Luo K, Li L, Li Y, Wu C, Yin Y, Chen Y, et al. A phosphorylation-deubiquitination cascade regulates the BRCA2-RAD51 axis in homologous recombination. *Genes Dev* (2016) 30(23):2581–95. doi: 10.1101/gad.289439.116
76. Fang Y, Fu D, Tang W, Cai Y, Ma D, Wang H, et al. Ubiquitin C-terminal Hydrolase 37, a novel predictor for hepatocellular carcinoma recurrence, promotes cell migration and invasion via interacting and deubiquitinating PRP19. *Biochim Biophys Acta* (2013) 1833(3):559–72. doi: 10.1016/j.bbamcr.2012.11.020
77. Fang Y, He J, Janssen HLA, Wu J, Dong L, Shen XZ. Peroxiredoxin 1, restraining cell migration and invasion, is involved in hepatocellular carcinoma recurrence. *J Dig Dis* (2018) 19(3):155–69. doi: 10.1111/1751-2980.12580
78. Ge J, Hu W, Zhou H, Yu J, Sun C, Chen W. Ubiquitin carboxyl-terminal hydrolase isozyme L5 inhibits human glioma cell migration and invasion via downregulating SNRPF. *Oncotarget* (2017) 8(69):113635–49. doi: 10.18632/oncotarget.23071
79. Fukui S, Nagasaka K, Miyagawa Y, Kikuchi-Koike R, Kawata Y, Kanda R, et al. The proteasome deubiquitinase inhibitor bAP15 downregulates TGF-beta/Smad signaling and induces apoptosis via UCHL5 inhibition in ovarian cancer. *Oncotarget* (2019) 10(57):5932–48. doi: 10.18632/oncotarget.27219
80. Fang Y, Mu J, Ma Y, Ma D, Fu D, Shen X. The interaction between ubiquitin C-terminal hydrolase 37 and glucose-regulated protein 78 in hepatocellular carcinoma. *Mol Cell Biochem* (2012) 359(1-2):59–66. doi: 10.1007/s11010-011-0999-7
81. Han W, Lee H, Han JK. Ubiquitin C-terminal hydrolase37 regulates Tcf7 DNA binding for the activation of Wnt signalling. *Sci Rep* (2017) 7:42590. doi: 10.1038/srep42590
82. Randles L, Anchoori RK, Roden RB, Walters KJ. The Proteasome Ubiquitin Receptor hRpn13 and Its Interacting Deubiquitinating Enzyme Uch37 Are Required for Proper Cell Cycle Progression. *J Biol Chem* (2016) 291 (16):8773–83. doi: 10.1074/jbc.M115.694588
83. Jensen DE, Proctor M, Marquis ST, Gardner HP, Ha SI, Chodosh LA, et al. BAP1: a novel ubiquitin hydrolase which binds to the BRCA1 RING finger and enhances BRCA1-mediated cell growth suppression. *Oncogene* (1998) 16(9):1097–112. doi: 10.1038/sj.onc.1201861
84. Dkhissi F, Aggoune D, Pontis J, Sorel N, Piccirilli N, LeCorf A, et al. The downregulation of BAP1 expression by BCR-ABL reduces the stability of BRCA1 in chronic myeloid leukemia. *Exp Hematol* (2015) 43(9):775–80. doi: 10.1016/j.exphem.2015.04.013
85. Shankar GM, Santagata S. BAP1 mutations in high-grade meningioma: implications for patient care. *Neuro Oncol* (2017) 19(11):1447–56. doi: 10.1093/neuonc/nox094

86. Machida YJ, Machida Y, Vashisht AA, Wohlschlegel JA, Dutta A. The deubiquitinating enzyme BAP1 regulates cell growth via interaction with HCF-1. *J Biol Chem* (2009) 284(49):34179–88. doi: 10.1074/jbc.M109.046755
87. Pena-Llopis S, Vega-Rubin-de-Celis S, Liao A, Leng N, Pavia-Jimenez A, Wang S, et al. BAP1 loss defines a new class of renal cell carcinoma. *Nat Genet* (2012) 44(7):751–9. doi: 10.1038/ng.2323
88. Lee HS, Lee SA, Hur SK, Seo JW, Kwon J. Stabilization and targeting of INO80 to replication forks by BAP1 during normal DNA synthesis. *Nat Commun* (2014) 5:5128. doi: 10.1038/ncomms6128
89. Zarrizi R, Menard JA, Belting M, Massoumi R. Deubiquitination of gamma-tubulin by BAP1 prevents chromosome instability in breast cancer cells. *Cancer Res* (2014) 74(22):6499–508. doi: 10.1158/0008-5472.CAN-14-0221
90. Daou S, Barbour H, Ahmed O, Masclef L, Baril C, Sen Nkwe N, et al. Monoubiquitination of ASXLs controls the deubiquitinase activity of the tumor suppressor BAP1. *Nat Commun* (2018) 9(1):4385. doi: 10.1038/s41467-018-06854-2
91. Peng J, Ma J, Li W, Mo R, Zhang P, Gao K, et al. Stabilization of MCRS1 by BAP1 prevents chromosome instability in renal cell carcinoma. *Cancer Lett* (2015) 369(1):167–74. doi: 10.1016/j.canlet.2015.08.013
92. Bononi A, Giorgi C, Patergnani S, Larson D, Verbruggen K, Tanji M, et al. BAP1 regulates IP3R3-mediated Ca(2+) flux to mitochondria suppressing cell transformation. *Nature* (7659) 2017) 546:549–53. doi: 10.1038/nature22798
93. Dai F, Lee H, Zhang Y, Zhuang L, Yao H, Xi Y, et al. BAP1 inhibits the ER stress gene regulatory network and modulates metabolic stress response. *Proc Natl Acad Sci U S A* (2017) 114(12):3192–7. doi: 10.1073/pnas.1619588114
94. Sime W, Niu Q, Abassi Y, Masoumi KC, Zarrizi R, Kohler JB, et al. BAP1 induces cell death via interaction with 14-3-3 in neuroblastoma. *Cell Death Dis* (2018) 9(5):458. doi: 10.1038/s41419-018-0500-6
95. Zhang Y, Shi J, Liu X, Feng L, Gong Z, Koppula P, et al. BAP1 links metabolic regulation of ferroptosis to tumour suppression. *Nat Cell Biol* (2018) 20(10):1181–92. doi: 10.1038/s41556-018-0178-0
96. Zhang Y, Zhuang L, Gan B. BAP1 suppresses tumor development by inducing ferroptosis upon SLC7A11 repression. *Mol Cell Oncol* (2019) 6(1):1536845. doi: 10.1080/23723556.2018.1536845
97. Luo Y, He J, Yang C, Orange M, Ren X, Blair N, et al. UCH-L1 promotes invasion of breast cancer cells through activating Akt signaling pathway. *J Cell Biochem* (2018) 119(1):691–700. doi: 10.1002/jcb.26232
98. Okochi-Takada E, Nakazawa K, Wakabayashi M, Mori A, Ichimura S, Yasugi T, et al. Silencing of the UCHL1 gene in human colorectal and ovarian cancers. *Int J Cancer J Int Du Cancer* (2006) 119(6):1338–44. doi: 10.1002/ijc.22025
99. Ding X, Gu Y, Jin M, Guo X, Xue S, Tan C, et al. The deubiquitinating enzyme UCHL1 promotes resistance to pemetrexed in non-small cell lung cancer by upregulating thymidylate synthase. *Theranostics* (2020) 10(13):6048–60. doi: 10.7150/thno.42096
100. Bedekovics T, Hussain S, Feldman AL, Galardy PJ. UCH-L1 is induced in germinal center B cells and identifies patients with aggressive germinal center diffuse large B-cell lymphoma. *Blood* (2016) 127(12):1564–74. doi: 10.1182/blood-2015-07-656678
101. Li G, Jin X, Zheng J, Jiang N, Shi W. UCH-L3 promotes non-small cell lung cancer proliferation via accelerating cell cycle and inhibiting cell apoptosis. *Biotechnol Appl Biochem* (2020). doi: 10.1002/bab.1909
102. Song HM, Lee JE, Kim JH. Ubiquitin C-terminal hydrolase-L3 regulates EMT process and cancer metastasis in prostate cell lines. *Biochem Biophys Res Commun* (2014) 452(3):722–7. doi: 10.1016/j.bbrc.2014.08.144
103. Rolen U, Kobzeva V, Gasparjan N, Ovaa H, Winberg G, Kisseljov F, et al. Activity profiling of deubiquitinating enzymes in cervical carcinoma biopsies and cell lines. *Mol Carcinog* (2006) 45(4):260–9. doi: 10.1002/mc.20177
104. Chen Y, Fu D, Xi J, Ji Z, Liu T, Ma Y, et al. Expression and clinical significance of UCH37 in human esophageal squamous cell carcinoma. *Dig Dis Sci* (2012) 57(9):2310–7. doi: 10.1007/s10620-012-2181-9
105. Sha B, Chen X, Wu H, Li M, Shi J, Wang L, et al. Deubiquitylatinase inhibitor b-AP15 induces c-Myc-Noxa-mediated apoptosis in esophageal squamous cell carcinoma. *Apoptosis An Int J Programmed Cell Death* (2019) 24(9-10):826–36. doi: 10.1007/s10495-019-01561-9
106. Leblay N, Lepretre F, Le Stang N, Gautier-Stein A, Villeneuve L, Isaac S, et al. BAP1 Is Altered by Copy Number Loss, Mutation, and/or Loss of Protein Expression in More Than 70% of Malignant Peritoneal Mesotheliomas. *J Thoracic Oncol Off Publ Int Assoc Study Lung Cancer* (2017) 12(4):724–33. doi: 10.1016/j.jtho.2016.12.019
107. Yoshikawa Y, Sato A, Tsujimura T, Emi M, Morinaga T, Fukuoka K, et al. Frequent inactivation of the BAP1 gene in epithelioid-type malignant mesothelioma. *Cancer Sci* (2012) 103(5):868–74. doi: 10.1111/j.1349-7006.2012.02223.x
108. Joseph RW, Kapur P, Serie DJ, Eckel-Passow JE, Parasramka M, Ho T, et al. Loss of BAP1 protein expression is an independent marker of poor prognosis in patients with low-risk clear cell renal cell carcinoma. *Cancer* (2014) 120(7):1059–67. doi: 10.1002/cncr.28521
109. See TR, Stalhammar G, Phillips S, Grossniklaus HE. BAP1 Immunoreactivity Correlates with Gene Expression Class in Uveal Melanoma. *Ocul Oncol Pathol* (2020) 6(2):129–37. doi: 10.1159/000502550
110. Kalirai H, Dodson A, Faqir S, Damato BE, Coupland SE. Lack of BAP1 protein expression in uveal melanoma is associated with increased metastatic risk and has utility in routine prognostic testing. *Br J Cancer* (2014) 111(7):1373–80. doi: 10.1038/bjc.2014.417
111. Mochel MC, Piris A, Nose V, Hoang MP. Loss of BAP1 Expression in Basal Cell Carcinomas in Patients With Germline BAP1 Mutations. *Am J Clin Pathol* (2015) 143(6):901–4. doi: 10.1309/AJCPG8LFJC0DHDQT
112. Mori T, Sumii M, Fujishima F, Ueno K, Emi M, Nagasaki M, et al. Somatic alteration and depleted nuclear expression of BAP1 in human esophageal squamous cell carcinoma. *Cancer Sci* (2015) 106(9):1118–29. doi: 10.1111/cas.12722
113. Reinicke AT, Raczkowski F, Muhlig M, Schmucker P, Lischke T, Reichelt J, et al. Deubiquitinating Enzyme UCH-L1 Promotes Dendritic Cell Antigen Cross-Presentation by Favoring Recycling of MHC Class I Molecules. *J Immunol* (2019) 203(7):1730–42. doi: 10.4049/jimmunol.1801133
114. Gu Y, Ding X, Huang J, Xue M, Zhang J, Wang Q, et al. The deubiquitinating enzyme UCHL1 negatively regulates the immunosuppressive capacity and survival of multipotent mesenchymal stromal cells. *Cell Death Dis* (2018) 9(5):459. doi: 10.1038/s41419-018-0532-y
115. Wada H, Kito K, Caskey LS, Yeh ET, Kamitani T. Cleavage of the C-terminus of NEDD8 by UCH-L3. *Biochem Biophys Res Commun* (1998) 251(3):688–92. doi: 10.1006/bbrc.1998.9532
116. Kwon J, Wang YL, Setsuie R, Sekiguchi S, Sato Y, Sakurai M, et al. Two closely related ubiquitin C-terminal hydrolase isozymes function as reciprocal modulators of germ cell apoptosis in cryptorchid testis. *Am J Pathol* (2004) 165(4):1367–74. doi: 10.1016/S0002-9440(10)63394-9
117. Sano Y, Furuta A, Setsuie R, Kikuchi H, Wang YL, Sakurai M, et al. Photoreceptor cell apoptosis in the retinal degeneration of Uchl3-deficient mice. *Am J Pathol* (2006) 169(1):132–41. doi: 10.2353/ajpath.2006.060085
118. Kurihara LJ, Kikuchi T, Wada K, Tilghman SM. Loss of Uch-L1 and Uch-L3 leads to neurodegeneration, posterior paralysis and dysphagia. *Hum Mol Genet* (2001) 10(18):1963–70. doi: 10.1093/hmg/10.18.1963
119. Setsuie R, Suzuki M, Tsuchiya Y, Wada K. Skeletal muscles of Uchl3 knockout mice show polyubiquitinated protein accumulation and stress responses. *Neurochem Int* (2010) 56(8):911–8. doi: 10.1016/j.neuint.2010.03.021
120. Setsuie R, Suzuki M, Kabuta T, Fujita H, Miura S, Ichihara N, et al. Ubiquitin C-terminal hydrolase-L3-knockout mice are resistant to diet-induced obesity and show increased activation of AMP-activated protein kinase in skeletal muscle. *FASEB J* (2009) 23(12):4148–57. doi: 10.1096/fj.09-132217
121. Suzuki M, Setsuie R, Wada K. Ubiquitin carboxyl-terminal hydrolase l3 promotes insulin signaling and adipogenesis. *Endocrinology* (2009) 150(12):5230–9. doi: 10.1210/en.2009-0332
122. Kim JY, Lee JM, Cho JY. Ubiquitin C-terminal hydrolase-L3 regulates Smad1 ubiquitination and osteoblast differentiation. *FEBS Lett* (2011) 585(8):1121–6. doi: 10.1016/j.febslet.2011.03.053
123. Dennissen FJ, Kholod N, Hermes DJ, Kemmerling N, Steinbusch HW, Dantuma NP, et al. Mutant ubiquitin (UBB+1) associated with neurodegenerative disorders is hydrolyzed by ubiquitin C-terminal hydrolase L3 (UCH-L3). *FEBS Lett* (2011) 585(16):2568–74. doi: 10.1016/j.febslet.2011.06.037

124. Lam YA, DeMartino GN, Pickart CM, Cohen RE. Specificity of the ubiquitin isopeptidase in the PA700 regulatory complex of 26 S proteasomes. *J Biol Chem* (1997) 272(45):28438–46. doi: 10.1074/jbc.272.45.28438
125. Yao T, Song L, Xu W, DeMartino GN, Florens L, Swanson SK, et al. Proteasome recruitment and activation of the Uch37 deubiquitinating enzyme by Adrm1. *Nat Cell Biol* (2006) 8(9):994–1002. doi: 10.1038/ncb1460
126. Hamazaki J, Iemura S, Natsume T, Yashiroda H, Tanaka K, Murata S. A novel proteasome interacting protein recruits the deubiquitinating enzyme UCH37 to 26S proteasomes. *EMBO J* (2006) 25(19):4524–36. doi: 10.1038/sj.emboj.7601338
127. Qiu XB, Ouyang SY, Li CJ, Miao S, Wang L, Goldberg AL. hRpn13/ADRM1/GP110 is a novel proteasome subunit that binds the deubiquitinating enzyme, UCH37. *EMBO J* (2006) 25(24):5742–53. doi: 10.1038/sj.emboj.7601450
128. Sahtoe DD, van Dijk WJ, El Oualid F, Ekkebus R, Ovaa H, Sixma TK. Mechanism of UCH-L5 activation and inhibition by DEUBAD domains in RPN13 and INO80G. *Mol Cell* (2015) 57(5):887–900. doi: 10.1016/j.molcel.2014.12.039
129. Al-Shami A, Jhaver KG, Vogel P, Wilkins C, Humphries J, Davis JJ, et al. Regulators of the proteasome pathway, Uch37 and Rpn13, play distinct roles in mouse development. *PloS One* (2010) 5(10):e13654. doi: 10.1371/journal.pone.0013654
130. Yun D, Zhuang Y, Kreutz MR, Behnisch T. The role of 19S proteasome associated deubiquitinases in activity-dependent hippocampal synaptic plasticity. *Neuropharmacology* (2018) 133:354–65. doi: 10.1016/j.neuropharm.2018.01.043
131. Kikuchi M, Ogishima S, Miyamoto T, Miyashita A, Kuwano R, Nakaya J, et al. Identification of unstable network modules reveals disease modules associated with the progression of Alzheimer's disease. *PloS One* (2013) 8(11):e76162. doi: 10.1371/journal.pone.0076162
132. Mahanic CS, Budhavarapu V, Graves JD, Li G, Lin WC. Regulation of E2 promoter binding factor 1 (E2F1) transcriptional activity through a deubiquitinating enzyme, UCH37. *J Biol Chem* (2015) 290(44):26508–22. doi: 10.1074/jbc.M115.659425
133. Nan L, Jacko AM, Tan J, Wang D, Zhao J, Kass DJ, et al. Ubiquitin carboxyl-terminal hydrolase-L5 promotes TGFbeta-1 signaling by de-ubiquitinating and stabilizing Smad2/Smad3 in pulmonary fibrosis. *Sci Rep* (2016) 6:33116. doi: 10.1038/srep33116
134. Wicks SJ, Haros K, Maillard M, Song L, Cohen RE, Dijke PT, et al. The deubiquitinating enzyme UCH37 interacts with Smads and regulates TGF-beta signalling. *Oncogene* (2005) 24(54):8080–4. doi: 10.1038/sj.onc.1208944
135. Chen Z, Niu X, Li Z, Yu Y, Ye X, Lu S, et al. Effect of ubiquitin carboxy-terminal hydrolase 37 on apoptotic in A549 cells. *Cell Biochem Funct* (2011) 29(2):142–8. doi: 10.1002/cbf.1734
136. Arpalahti L, Laitinen A, Hagstrom J, Mustonen H, Kokkola A, Bockelman C, et al. Positive cytoplasmic UCHL5 tumor expression in gastric cancer is linked to improved prognosis. *PloS One* (2018) 13(2):e0193125. doi: 10.1371/journal.pone.0193125
137. Arpalahti L, Hagstrom J, Mustonen H, Lundin M, Haglund C, Holmberg CI. UCHL5 expression associates with improved survival in lymph-node-positive rectal cancer. *Tumour Biol* (2017) 39(7):1010428317716078. doi: 10.1177/1010428317716078
138. Arpalahti L, Saukkonen K, Hagstrom J, Mustonen H, Seppanen H, Haglund C, et al. Nuclear ubiquitin C-terminal hydrolase L5 expression associates with increased patient survival in pancreatic ductal adenocarcinoma. *Tumour Biol* (2017) 39(6):1010428317710411. doi: 10.1177/1010428317710411
139. Wang A, Papneja A, Hyrcza M, Al-Habeeb A, Ghazarian D. Gene of the month: BAP1. *J Clin Pathol* (2016) 69(9):750–3. doi: 10.1136/jclinpath-2016-203866
140. Okino Y, Machida Y, Frankland-Searby S, Machida YJ. BRCA1-associated protein 1 (BAP1) deubiquitinase antagonizes the ubiquitin-mediated activation of FoxK2 target genes. *J Biol Chem* (2015) 290(3):1580–91. doi: 10.1074/jbc.M114.609834
141. Daou S, Hammond-Martel I, Mashtalir N, Barbour H, Gagnon J, Iannantuono NV, et al. The BAP1/ASXL2 Histone H2A Deubiquitinase Complex Regulates Cell Proliferation and Is Disrupted in Cancer. *J Biol Chem* (2015) 290(48):28643–63. doi: 10.1074/jbc.M115.661553
142. Di Nunno V, Frega G, Santoni M, Gatto L, Fiorentino M, Montironi R, et al. BAP1 in solid tumors. *Future Oncol* (2019) 15(18):2151–62. doi: 10.2217/fon-2018-0915
143. Harbour JW, Onken MD, Roberson ED, Duan S, Cao L, Worley LA, et al. Frequent mutation of BAP1 in metastasizing uveal melanomas. *Science* (2010) 330(6009):1410–3. doi: 10.1126/science.1194472
144. Testa JR, Cheung M, Pei J, Below JE, Tan Y, Sementino E, et al. Germline BAP1 mutations predispose to malignant mesothelioma. *Nat Genet* (2011) 43(10):1022–5. doi: 10.1038/ng.912
145. Fan LH, Tang LN, Yue L, Yang Y, Gao ZL, Shen Z. BAP1 is a good prognostic factor in advanced non-small cell lung cancer. *Clin Invest Med* (2012) 35(4):E182–9. doi: 10.25011/cim.v35i4.17146
146. Njauw CN, Kim I, Piris A, Gabree M, Taylor M, Lane AM, et al. Germline BAP1 inactivation is preferentially associated with metastatic ocular melanoma and cutaneous-ocular melanoma families. *PloS One* (2012) 7(4):e35295. doi: 10.1371/journal.pone.0035295
147. Farley MN, Schmidt LS, Mester JL, Pena-Llopis S, Pavia-Jimenez A, Christie A, et al. A novel germline mutation in BAP1 predisposes to familial clear-cell renal cell carcinoma. *Mol Cancer Res MCR* (2013) 11(9):1061–71. doi: 10.1158/1541-7786.MCR-13-0111
148. Hirsch TZ, Negulescu A, Gupta B, Caruso S, Noblet B, Couchy G, et al. BAP1 mutations define a homogeneous subgroup of hepatocellular carcinoma with fibrolamellar-like features and activated PKA. *J Hepatol* (2019). doi: 10.1016/j.jhep.2019.12.006
149. Murali R, Wiesner T, Scolyer RA. Tumours associated with BAP1 mutations. *Pathology* (2013) 45(2):116–26. doi: 10.1097/PAT.0b013e32835d0efb
150. Baumann F, Flores E, Napolitano A, Kanodia S, Taioli E, Pass H, et al. Mesothelioma patients with germline BAP1 mutations have 7-fold improved long-term survival. *Carcinogenesis* (2015) 36(1):76–81. doi: 10.1093/carcin/bgu227
151. Wang K, McDermott JD, Schrock AB, Elvin JA, Gay L, Karam SD, et al. Comprehensive genomic profiling of salivary mucoepidermoid carcinomas reveals frequent BAP1, PIK3CA, and other actionable genomic alterations. *Ann Oncol* (2017) 28(4):748–53. doi: 10.1093/annonc/mdw689
152. Durante MA, Walter SD, Paez-Escamilla M, Tokarev J, Decatur CL, Dubovy SR, et al. Intraocular Metastasis in Unilateral Multifocal Uveal Melanoma Without Melanocytosis or Germline BAP1 Mutations. *JAMA Ophthalmol* (2019). doi: 10.1001/jamaophthalmol.2019.3941
153. Farzin M, Toon CW, Clarkson A, Sioson L, Watson N, Andrici J, et al. Loss of expression of BAP1 predicts longer survival in mesothelioma. *Pathology* (2015) 47(4):302–7. doi: 10.1097/PAT.0000000000000250
154. Wang SS, Gu YF, Wolff N, Stefanius K, Christie A, Dey A, et al. Bap1 is essential for kidney function and cooperates with Vhl in renal tumorigenesis. *Proc Natl Acad Sci U S A* (2014) 111(46):16538–43. doi: 10.1073/pnas.1414789111
155. Bi M, Zhao S, Said JW, Merino MJ, Adeniran AJ, Xie Z, et al. Genomic characterization of sarcomatoid transformation in clear cell renal cell carcinoma. *Proc Natl Acad Sci U S A* (2016) 113(8):2170–5. doi: 10.1073/pnas.1525735113
156. Tokumaru Y, Yamashita K, Kim MS, Park HL, Osada M, Mori M, et al. The role of PGP9.5 as a tumor suppressor gene in human cancer. *Int J Cancer J Int Du Cancer* (2008) 123(4):753–9. doi: 10.1002/ijc.23354
157. Lleras RA, Smith RV, Adrien LR, Schlecht NF, Burk RD, Harris TM, et al. Unique DNA methylation loci distinguish anatomic site and HPV status in head and neck squamous cell carcinoma. *Clin Cancer Res* (2013) 19(19):5444–55. doi: 10.1158/1078-0432.CCR-12-3280
158. Zhang J, Chen T, Yang X, Cheng H, Spath SS, Clavijo PE, et al. Attenuated TRAF3 Fosters Activation of Alternative NF-kappaB and Reduced Expression of Antiviral Interferon, TP53, and RB to Promote HPV-Positive Head and Neck Cancers. *Cancer Res* (2018) 78(16):4613–26. doi: 10.1158/0008-5472.CAN-17-0642
159. Yu H, Pak H, Hammond-Martel I, Ghram M, Rodrigue A, Daou S, et al. Tumor suppressor and deubiquitinase BAP1 promotes DNA double-strand break repair. *Proc Natl Acad Sci U S A* (2014) 111(1):285–90. doi: 10.1073/pnas.1309085110

160. Gao J, Aksoy BA, Dogrusoz U, Dresdner G, Gross B, Sumer SO, et al. Integrative analysis of complex cancer genomics and clinical profiles using the cBioPortal. *Sci Signal* (2013) 6(269):p11. doi: 10.1126/scisignal.2004088
161. Cerami E, Gao J, Dogrusoz U, Gross BE, Sumer SO, Aksoy BA, et al. The cBio cancer genomics portal: an open platform for exploring multidimensional cancer genomics data. *Cancer Discovery* (2012) 2(5):401–4. doi: 10.1158/2159-8290.CD-12-0095
162. Lonsdale J, Thomas J, Salvatore M, Phillips R, Lo E, Shad S, et al. The Genotype-Tissue Expression (GTEx) project. *Nat Genet* (2013) 45(6):580–5. doi: 10.1038/ng.2653
163. Canning M, Guo G, Yu M, Myint C, Groves MW, Byrd JK, et al. Heterogeneity of the Head and Neck Squamous Cell Carcinoma Immune Landscape and Its Impact on Immunotherapy. *Front Cell Dev Biol* (2019) 7:52. doi: 10.3389/fcell.2019.00052
164. Tang Z, Li C, Kang B, Gao G, Li C, Zhang Z. GEPIA: a web server for cancer and normal gene expression profiling and interactive analyses. *Nucleic Acids Res* (2017) 45(W1):W98–102. doi: 10.1093/nar/gkx247
165. Brinkmann K, Zigrino P, Witt A, Schell M, Ackermann L, Broxtermann P, et al. Ubiquitin C-terminal hydrolase-L1 potentiates cancer chemosensitivity by stabilizing NOXA. *Cell Rep* (2013) 3(3):881–91. doi: 10.1016/j.celrep.2013.02.014
166. Piva F, Santoni M, Matrana MR, Satti S, Giulietti M, Occhipinti G, et al. BAP1, PBRM1 and SETD2 in clear-cell renal cell carcinoma: molecular diagnostics and possible targets for personalized therapies. *Expert Rev Mol Diagn* (2015) 15(9):1201–10. doi: 10.1586/14737159.2015.1068122
167. D'Arcy P, Brnjic S, Olofsson MH, Fryknas M, Lindsten K, De Cesare M, et al. Inhibition of proteasome deubiquitinating activity as a new cancer therapy. *Nat Med* (2011) 17(12):1636–40. doi: 10.1038/nm.2536
168. Ventz S, Trippa L, Schoenfeld JD. Lessons Learned from De-escalation trials in favorable risk HPV-associated Squamous Cell Head and Neck Cancer - A Perspective on future trial designs. *Clin Cancer Res* (2019) 25(24):7281–6. doi: 10.1158/1078-0432.CCR-19-0945
169. Mehanna H, Robinson M, Hartley A, Kong A, Foran B, Fulton-Lieuw T, et al. Radiotherapy plus cisplatin or cetuximab in low-risk human papillomavirus-positive oropharyngeal cancer (De-ESCALaTE HPV): an open-label randomised controlled phase 3 trial. *Lancet* (2019) 393(10166):51–60. doi: 10.1016/S0140-6736(18)32752-1
170. Bi H-L, Zhang X-L, Zhang Y-L, Xie X, Xia Y-L, Du J, et al. The deubiquitinase UCHL1 regulates cardiac hypertrophy by stabilizing epidermal growth factor receptor. *J Sci Adv* (2020) 6(16):eaax4826. doi: 10.1126/sciadv.aax4826
171. Azoury SC, Gilmore RC, Shukla V. Molecularly targeted agents and immunotherapy for the treatment of head and neck squamous cell cancer (HNSCC). *Discovery Med* (2016) 21(118):507–16. doi: 10.1016/S0140-6736(18)32752-1
172. Ferris RL. Immunology and Immunotherapy of Head and Neck Cancer. *J Clin Oncol Off J Am Soc Clin Oncol* (2015) 33(29):3293–304. doi: 10.1200/JCO.2015.61.1509
173. Whiteside TL. Head and Neck Carcinoma Immunotherapy: Facts and Hopes. *Clin Cancer Res An Off J Am Assoc Cancer Res* (2017). doi: 10.1158/1078-0432.CCR-17-1261
174. Gotwals P, Cameron S, Cipolletta D, Cremasco V, Crystal A, Hewes B, et al. Prospects for combining targeted and conventional cancer therapy with immunotherapy. *Nat Rev Cancer* (2017) 17(5):286–301. doi: 10.1038/nrc.2017.17
175. Sun SC. Deubiquitylation and regulation of the immune response. *Nat Rev Immunol* (2008) 8(7):501–11. doi: 10.1038/nri2337
176. Farshi P, Deshmukh RR, Nwankwo JO, Arkwright RT, Cvek B, Liu J, et al. Deubiquitinases (DUBs) and DUB inhibitors: a patent review. *Expert Opin Ther Pat* (2015) 25(10):1191–208. doi: 10.1517/13543776.2015.1056737
177. Harrigan JA, Jacq X, Martin NM, Jackson SP. Deubiquitylating enzymes and drug discovery: emerging opportunities. *Nat Rev Drug Discovery* (2018) 17(1):57–78. doi: 10.1038/nrd.2017.152
178. Islam MT, Zhou X, Chen F, Khan MA, Fu J, Chen H. Targeting the signalling pathways regulated by deubiquitinases for prostate cancer therapeutics. *Cell Biochem Funct* (2019) 37(5):304–19. doi: 10.1002/cbf.3401
179. Schauer NJ, Magin RS, Liu X, Doherty LM, Buhrlage SJ. Advances in Discovering Deubiquitinating Enzyme (DUB) Inhibitors. *J Med Chem* (2020) 63(6):2731–50. doi: 10.1021/acs.jmedchem.9b01138

Conflict of Interest: The authors declare that the research was conducted in the absence of any commercial or financial relationships that could be construed as a potential conflict of interest.

frontiers in Oncology

REVIEW
published: 11 February 2021
doi: 10.3389/fonc.2020.621294

Ubiquitination of Nonhistone Proteins in Cancer Development and Treatment

Xiuzhen Zhang[1], Tong Meng[2], Shuaishuai Cui[1], Ling Feng[1], Dongwu Liu[1,3], Qiuxiang Pang[1] and Ping Wang[1]**

[1] School of Life Sciences, Shandong University of Technology, Zibo, China, [2] Tongji University Cancer Center, Shanghai Tenth People's Hospital of Tongji University, School of Medicine, Tongji University, Shanghai, China, [3] School of Agricultural Engineering and Food Science, Shandong University of Technology, Zibo, China

Ubiquitination, a crucial post-translation modification, regulates the localization and stability of the substrate proteins including nonhistone proteins. The ubiquitin-proteasome system (UPS) on nonhistone proteins plays a critical role in many cellular processes such as DNA repair, transcription, signal transduction, and apoptosis. Its dysregulation induces various diseases including cancer, and the identification of this process may provide potential therapeutic targets for cancer treatment. In this review, we summarize the regulatory roles of key UPS members on major nonhistone substrates in cancer-related processes, such as cell cycle, cell proliferation, apoptosis, DNA damage repair, inflammation, and T cell dysfunction in cancer. In addition, we also highlight novel therapeutic interventions targeting the UPS members (E1s, E2s, E3s, proteasomes, and deubiquitinating enzymes). Furthermore, we discuss the application of proteolysis-targeting chimeras (PROTACs) technology as a novel anticancer therapeutic strategy in modulating protein target levels with the aid of UPS.

Keywords: ubiquitination, E3 ligase, deubiquitinase, nonhistone protein, cancer, proteolysis-targeting chimeras

OPEN ACCESS

Edited by:
Yi Sun,
Zhejiang University, China

Reviewed by:
Huabo Su,
Augusta University, United States
Qingping Dou,
Wayne State University, United States

***Correspondence:**
Qiuxiang Pang
pangqiuxiang@sdut.edu.cn
Ping Wang
wangp@tongji.edu.cn

Specialty section:
This article was submitted to Cancer Molecular Targets and Therapeutics, a section of the journal Frontiers in Oncology

Received: *26 October 2020*
Accepted: *24 December 2020*
Published: *11 February 2021*

Citation:
Zhang X, Meng T, Cui S, Feng L, Liu D, Pang Q and Wang P (2021) Ubiquitination of Nonhistone Proteins in Cancer Development and Treatment. Front. Oncol. 10:621294. doi: 10.3389/fonc.2020.621294

INTRODUCTION

Post-translational modification with ubiquitin plays an important role in the regulation of protein degradation and turnover. Ubiquitin, a small protein of 76 amino acids, can be covalently attached to target proteins to form mono- or polyubiquitinated types. This process occurs by a cascade of enzymatic reactions including E1-activating enzymes, E2-conjugating enzymes, and E3 ubiquitin ligases. Polyubinquitin with different chain topologies on specific lysine residues on substrates is related to different functional consequences (1). Generally, polyubiquitin chains linked at the 48 lysine site (K48) or K11 site lead to 26S proteasome-mediated proteolysis, which plays an essential role in maintaining protein homeostasis, regulating cell cycle, and apoptosis. On the other hand, chains with K63 site, as well as monoubiquitination, representing non-proteolytic ubiquitination, participate in diverse cellular processes, such as signal transduction, autophagy, and DNA damage repair (2, 3). As for most substrates, they are first covalently modified by ubiquitin and then directed to the proteasome to be degraded. Also, the function of ubiquitin ligases can be reversed by deubiquitinating enzymes (DUBs), which remove ubiquitin from substrate proteins and participate in the regulation of various cellular pathways (4).

Ubiquitination is ubiquitous, and second only to phosphorylation in abundance (5). Some reports have shown that histone ubiquitination regulating DNA-driven processes such as gene transcription and DNA damage repair (6, 7), and aberrant histone ubiquitination frequently occurs in cancers (8). Accumulating evidences indicate that ubiquitylation of nonhistone proteins plays an important role in many cellular processes, including DNA repair, transcription, signal transduction, autophagy, apoptosis, and so on (9). Nonhistone protein substrates for ubiquitination include general transcription factors, transcriptional activators or repressors, nonhistone chromatin-associated protein, and nuclear receptor coactivators. Dysregulation of nonhistone lysine ubiquitination is closely associated with various human cancers (10). Therefore, it is more important to study the role of nonhistone ubiquitination in tumorigenesis and tumor treatment. Moreover, interrogating the regulatory networks of UPS can offer a strategy for delineating the mechanism of cancer development and facilitate the identification of therapeutic targets. Meanwhile, the UPS exhibits high substrate specificity, which makes targeting it a promising strategy for cancer treatment. Nowadays, many UPS inhibitors such as bortezomib, carfilzomib and ixazomib, have been well applied in cancer treatment (11, 12). In this review, we summarize the regulatory roles of key UPS members on major nonhistone substrates in cancer-related processes.

Recently, a novel strategy named proteolysis-targeting chimeras (PROTACs) has been developed. PROTAC is a strategy that utilizes a hybrid molecule (a short peptide or a small molecule) to link a specific protein to an E3 ubiquitin ligase and induces the targeted protein degradation by the UPS in the cell (13). PROTACs link the target protein to an E3 ubiquitin ligase by a designed hybrid molecule, providing a path for ubiquitinating undruggable proteins such as transcription factors, scaffolding proteins and nonenzymatic proteins. Due to their high selectivities, low working concentrations, and less off-target toxicities, PROTACs may boost the development of drug discovery (14).

Considering the importance of UPS in the regulation of cancer development and treatment, we focus on the regulatory roles of key UPS members on nonhistone proteins in cancer development and highlight the novel therapeutic options targeting them. In addition, we also discuss and summarize the applications and recent advances of PROTAC technology focusing on nonhistone proteins.

THE UBIQUITINATION CASCADE AND DEUBIQUITINATION

The enzymes of Ubiquitination and Deubiquitination

The UPS contains a series of essential components: ubiquitin, E1s, E2s, E3s, DUBs, and the 26S proteasome. Until now, two E1s and about 40 E2s have been discovered, with more than 600 E3s conferring the diversity of protein substrates (15). Generally, E3 ligases are structurally classified into three subtypes: really interesting new gene (RING), homologous to E6-associated protein C-terminus (HECT) and RING-in-between-RING (RBR) E3s. RING E3 ligases are most abundant with more than 600 members in humans. About 30 HECT E3 ligases have been found in humans, including the NEDD4 family, the HERC family and other HECTs. RBR E3s have 14 members and work as hybrids of RING E3s and HECT E3s (16). In addition, there are approximate 100 DUBs and they are subdivided into 6 families based on sequence and structural similarity namely ubiquitin-specific proteases (USPs), ubiquitin carboxy-terminal hydrolases (UCHs), ovarian-tumor proteases (OTUs), Machado-Joseph disease protein proteases (MJD), JAB1/MPN/MOV34 metalloenzymes (JAMMs), and monocyte chemotactic protein-induced proteases (MCPIPs) (17). To date, more than 40 DUBs have been implicated in tumorigenesis (4).

The Process of Ubiquitination and Deubiquitination

The process of ubiquitylation contains three steps (**Figure 1**). Initially, the α-carboxyl group of the C-terminal glycine residue of ubiquitin links to a cysteine residue on E1 in an ATP-dependent manner, and a thioester bond is formed. Subsequently, E2 binds to the activated ubiquitin, and the complex of E1 and ubiquitin is transferred to the catalytic cysteine of E2 *via* a trans(thio) esterification reaction. Finally, E3 recognizes the substrate and catalyzes the linking of ubiquitin to a specific lysine residue on the substrate. The function of E3 ligases can be reversed by DUBs, which mediate the removal and processing of ubiquitin. DUBs regulate multiple biological processes including the cell cycle, DNA repair, apoptosis, inflammation, and signaling pathways.

THE ROLES OF E3 LIGASES AND DUBS IN REGULATING CANCER DEVELOPMENT

The UPS regulates diverse important cellular processes including cell cycle arrest, cell proliferation, and apoptosis. Thus, dysregulation of its key members and their regulatory network is often associated with human diseases, particularly cancer. Increasing studies have revealed that E3 ligases and DUBs are involved in cancer development through various biological processes, such as cell cycle, cell proliferation, apoptosis, DNA damage repair, inflammation, and T cell dysfunction in cancer and some of them are shown in **Tables 1** and **2** (15).

E3 ligases and DUBs Regulate Cell Cycle

Cell cycle progression and arrest are commonly deregulated in cancer (73). Increasing evidence indicates that multiple E3s participate in regulating cell cycle progression (**Figure 2**). Thus, the deregulation of E3s leads to the sustained proliferation and genomic instability of cancer cells. The anaphase-promoting complex named the cyclosome (APC/C) is the most sophisticated RING E3 ligase. It precisely governs cell cycle progression by recruiting cell division cycle 20 (CDC20) and CDC20-like protein 1 (CDH1) in turns. APC/C-CDC20 regulates cell cycle transition from metaphase to anaphase, while

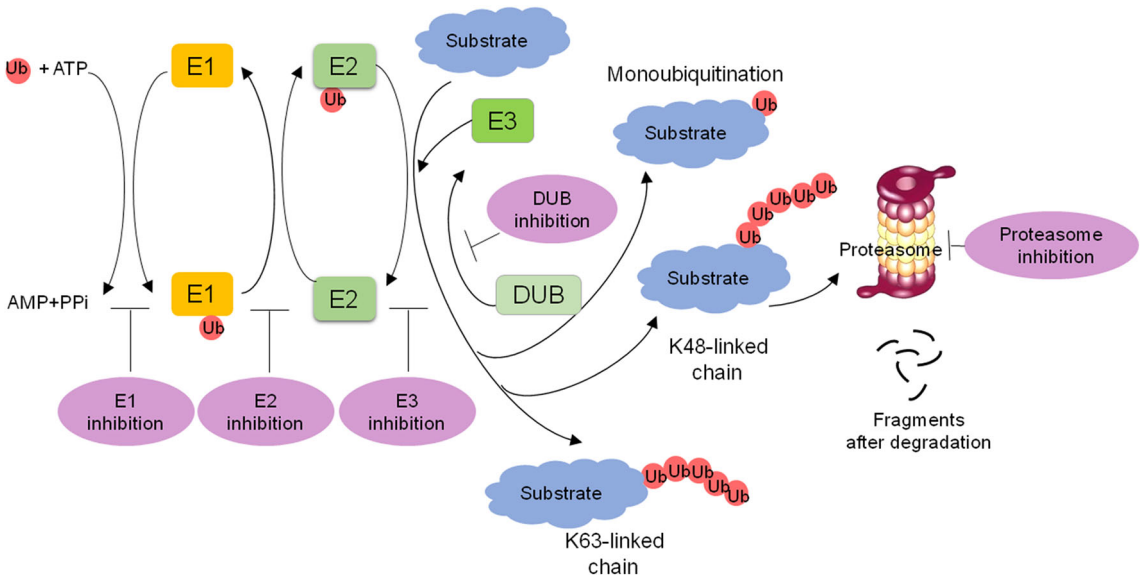

FIGURE 1 | Overview of the ubiquitin-proteasome system (UPS) and targeting strategies for the UPS. The ubiquitin is activated with E1 in an ATP dependent manner, transferred to E2, and then transferred to the substrate through E3 ligase recognization, forming a mono- or polyubiquitinated protein. K48 or K11 polyubiquitin chains lead to 26S proteasome-mediated degradation. Monoubiquitination or K63 polyubiquitin chains are nonproteolytic ubiquitination signals and participate in many biological processes. DUBs remove or edit ubiquitins from substrate proteins. The targeting of E1s, E2s, E3s, proteasome and DUBs is a promising strategy for cancer treatment.

APC/C-CDH1 mediates mitotic exit and early G1 entry. Many studies indicate that Cdh1 functions as a tumor suppressor, whereas CDC20 may function as an oncoprotein to promote the development and progression of cancers (18, 74).

Another representative example is SCF E3 ligases, which consist of four components: S-phase kinase-associated protein 1 (SKP1), cullin 1, Roc1/Rbx1/Hrt1 and an F-box protein (FBP). Commonly, FBPs serve for substrate recognition in the complexes and selectively regulate diverse biological processes (19). FBXW7, F-box/WD repeat-containing protein 7 (FBXW7), S-phase kinase associated protein2 (SKP2), and β-transducin repeat containing proteins (β-TrCPs) are well-studied FBPs. FBXW7 a tumor suppressor, works on many oncogenes including Myc, c-Jun, cyclin E, mTOR, Notch-1 and Mcl-1. It is often mutated or deleted in lots of cancers such as metastatic colorectal adenocarcinoma, T-cell acute lymphoblastic leukemia, and cholangiocarcinomas (20–22, 75). SKP2 plays a critical role during S and G2/M phases through regulating some cell cycle proteins, such as p21, p57, cyclin A, cyclin E, cyclin D1, and CDK inhibitors (e.g. p27). SKP2 is an important oncogene and is widely overexpressed in various cancers, such as breast cancer (23) and hepatocellular carcinoma (26). β-TrCPs-containing SCF complexes play a dual role in cell cycle checkpoint control: mediating and relieving cell cycle arrest *via* bonding different substrates (28, 76). Thus, the SCF complexes work on a subset of cyclins and CDK inhibitors to regulate the progression from G1 to the onset of mitosis. In addition, Parkin, a well-known RBR E3 ligase, controls the cell cycle by downregulating some G1/S kinases such as cyclin D and cyclin E (29, 30).

DUBs also participate in the regulation of cell-cycle progression (**Figure 2**) (31). For instance, E2F transcription factors play a key role in cell-cycle progression through G1 and into S-phase (77). The tumor suppressor retinoblastoma protein (Rb) maintains the cell in G1 through inhibiting E2F (78). However, hyperphosphorylated Rb dissociates from E2F, leading to the transcription of S-phase genes. The E3 ligase MDM2 promotes Rb degradation *via* ubiquitylation (79). On the contrary, the DUB USP7 directly reverses MDM2-mediated polyubiquitylation of Rb, stalling the cell cycle in G1 and inhibiting cell proliferation (32). Tumor suppressor BRCA1-associated protein 1 (BAP1), whose mutations can be seen in many cancers (62), has been found that it also could promote cell proliferation through deubiquitylating host cell factor 1 (HCF-1). HCF-1, an important transcriptional co-regulator of E2F, promotes cell cycle progression at the G1/S boundary by activating the E2F1 transcription factor. Therefore, BAP1 regulates cell proliferation at G1/S by co-regulating transcription from HCF-1/E2F-governed promoters. Moreover, BAP1 knockdown leads to G1 arrest and decreases the expression of S phase genes in OCM1 cells and NCI-H226 lung carcinoma cell line (47, 48, 80). It is well known that APC/C plays a crucial role in the completion of mitosis and maintenance of G1. Recently, OTUD7B/Cezanne has been reported to deubiquitinate and stabilize the APC/C substrates, as well as promote mitotic progression and cell proliferation. Cezanne is upregulated in multiple tumors, suggesting a potential role in cancer cell proliferation (49). Besides, the transcription factor FOXM1 participates in cell cycle progression and is upregulated in basal-like breast cancer. Arceci et al. reveal that USP21 directly binds to FOXM1, makes it deubiquitinate, and increases its expression level *in vitro* and *in vivo*. Suppression of USP21 causes a mitotic entry

TABLE 1 | Some E3s involved in cancers.

E3	Substrate	Category	Associated cancer or cancer line	Biological functions	Model	Alteration in tumors	Reference
APC/C-CDC20	Cyclin A, cycin B1, securin,	Oncogene	Colorectal cancer	Cell cycle regulation	*In vivo*	Overexpression	(18)
APC/C-CDH1	CDC20, CDC25A	Tumor suppressor	Breast cancer	Cell cycle regulation	*In vivo*		(19)
SCF^{FBXW7}	c-Myc, c-Jun, cyclin E, mTOR, Notch-1, Mcl-1,	Tumor suppressor	Metastatic colorectal denocarcinoma, T-cell acute lymphoblastic leukemia, and cholangiocarcinomas	Cell cycle regulation,	*In vivo*	Mutation	(20–23)
	c-Myc	Tumor suppressor	Leukemia-initiating cell	Cell proliferation	*In vitro*	Mutation	(24, 25)
SCF^{SKP2}	p27, p21, p57, cyclin A, cyclin E, cyclin D1	Oncogene	Breast cancer lung cancer	Cell cycle regulation	*In vivo*	Overexpression	(26)
	c-Myc,			Cell proliferation	*In vivo*	Overexpression	(27)
$SCF^{\beta TrCPs}$	Mcl-1, BimEL, PDCD4, STAT1	depends on substrates	Colorectal cancer, pancreatic cancer	Cell cycle regulation	*In vivo*	Overexpression	(28, 29)
Parkin	cyclin D, cyclin E	Tumor suppressor	Glioma, colorectal cancer	Cell cycle regulation	*In vivo*	Mutation	(30, 31)
MDM2	Retinoblastoma protein, p53	Oncogene	Lung cancer, colorectal cancer, cutaneous melanoma, breast cancer	Cell cycle control, Apoptosis	*In vivo*	Overexpression, Mutation	(32, 33) (34),
TRPC4AP/ TRUSS	c-Myc		IMR5 neuroblastoma cells, U2OS, HeLa cells	Cell proliferation	*In vitro*		(35)
KCTD2	c-Myc		Glioma stem cells	Cell proliferation	*In vitro*	Suppression	(36)
CHIP	c-Myc		Glioma	Cell proliferation			(37)
HectH9	c-Myc	Oncogene	HeLa, T47D, MCF7, MRC5 cells	Cell proliferation	*In vivo*, *In vitro*	Overexpression	(38)
hUTP14a	c-Myc	Oncogene	Colorectal cancer	Cell proliferation	*In vivo*	Upregulation	(39)
	p53, retinoblastoma protein	Oncogene	U2OS cell, H1299, HCT116 cell	Apoptosis	*In vitro*, *In vivo*	Upregulation	(40, 41)
TRAF6	TAB2			Inflammation			(42)
Fbxo38	PD-1	Tumor suppressor		T cell dysfunction in cancer	*In vivo*	Downregulation	(43)
Stub1,Cbl-b	Foxp3	Tumor suppressor	Colitis	Inflammation	*In vivo*	Downregulation	(44, 45)
VHL	HIF-1α	Tumor suppressor	Pancreatic cancer	Inflammation			(46)

delay to slow proliferation and sensitivity to paclitaxel in cell culture and animal xenografts (50). The deubiquitinating enzyme USP5 is overexpressed in numerous malignancies, promoting tumor growth *via* modulating cell cycle regulators such as FoxM1. USP5 deficiency also induces DNA damage, cell cycle arrest and apoptosis in pancreatic ductal adenocarcinoma cells (51, 53). Besides, USP2 and USP14 regulate the cancer cell cycle *via* deubiquitinating cyclin D1 (54) and Cyclin B1 (55), respectively. Knocking down USP14 arrests cell cycle at the G2/M phase and inhibits the proliferation and migration of breast cancer cells (55), USP44 deubiquitinates the APC-inhibitory Mad2-Cdc20 complex, thereby preventing anaphase onset (57, 58). USP37 deubiquitinates and stabilizes Cyclin A and promotes S phase entry (59).

E3 Ligases and DUBs Regulate Cell Proliferation

Many oncogenes can induce cancer cell proliferation, and UPS mediates their transcription by modulating general transcription factors, transcriptional activators and transcriptional coactivators *via* proteolytic and nonproteolytic ubiquitination (60). Here, we take the oncogene c-Myc as an example to show how ubiquitination regulates the transcription of oncogenes in cancer.

The overexpression of c-Myc is widely found in many cancers and is related to cell growth, proliferation, apoptosis and metabolic pathways (81). Its accumulation is also associated with poor cancer outcomes (82). Myc levels are controlled through targeted degradation by UPS (83). Multiple E3s are involved in modulating c-Myc activity in a tissue-specific manner. For instance, the ubiquitin ligase SCF-FBXW7 directly catalyzes c-Myc ubiquitination in a glycogen synthase kinase 3 phosphorylation-3-dependent manner and leads to c-Myc degradation *in vitro* (84). Furthermore, FBXW7 regulates the ubiquitylation of c-Myc protein and mediates leukemia-initiating cell activity (24). TRPC4AP (transient receptor potential cation channel, subfamily C, member 4-associated protein)/TRUSS (tumor necrosis factor receptor-associated ubiquitous scaffolding and signaling protein) binds to c-Myc

TABLE 2 | Some DUBs involved in cancers.

DUB	Substrate	Category	Associated cancer or cancer line	Biological functions	Model	Alteration in tumors	Reference
BAP1	HCF-1	Tumor suppressor	OCM1 cell, NCI-H226 lung carcinoma cell line	Cell proliferation	*In vitro*	Loss, mutation	(47–49)
OTUD7B/ Cezanne	APC/C	Oncogene	HCT116, RPE1, HeLaS3, U2OS cells	Cell proliferation	*In vitro*	Overexpression	(50)
USP21	FOXM1, p53	Oncogene	Breast cancer	Cell cycle progression, NF-κB signing	*In vitro*, *In vivo*	Overexpression	(51)
	BRCA2	Oncogene	Hepatocellular carcinoma	DNA damage repair, NF-κB signaling	*In vivo*	Overexpression	(52)
USP5	FoxM1	Oncogene	Pancreatic cancer	Cell cycle regulation		Overexpression	(53, 54)
USP2	Cyclin D1, MDM2	Oncogene	Hepatoma and breast cancer cells	Cell cycle regulation, apoptosis	*In vitro*	Overexpression	(55, 56)
USP14	Cyclin B1		Breast cancer, colorectal cancer, non-small cell lung cancer	Cell cycle regulation	*In vitro*		(57)
USP44	Cdc20	Oncogene	HeLa cell, T-cell leukemias	Cell cycle regulation	*In vitro*, *In vivo*	Overexpression	(58, 59)
USP37	Cyclin A,		U2OS cells, HeLa cells, lung cancer	Cell cycle regulation, apoptosis	*In vitro*, *In vivo*	Overexpression	(60, 61)
USP7	Retinoblastoma protein, p53, MDM2, FOXO4	Tumor suppressor	HEK293, prostate cancer, colon cancer, non-small cell lung cancer	Cell cycle arrest, apoptosis, Cell proliferation	*In vitro*, *In vivo*	Downregulation	(62, 63) (32, 34),
USP11	BRCA2	Oncogene	U2OS cell, breast cancer	DNA damage repair,	*In vitro*, *In vivo*	Upregulation	(64, 65)
USP13	RAP80	Oncogene	Ovarian cancer	DNA damage response	*In vivo*	Overexpression	(66)
USP22	c-Myc	Tumor promoter	Breast cancer	apoptosis	*In vivo*	Overexpression	(67)
USP28	c-Myc	Oncogene	Colon cancer, breast cancer	Cell cycle regulation, apoptosis, DNA damage repair	*In vivo*	Overexpression	(68)
USP36	c-Myc	Oncogene	Breast cancer, lung cancer	Apoptosis	*In vivo*	Overexpression	(69)
USP10	p53	Tumor suppressor	HCT116 cell	DNA damage repair	*In vitro*	Downregulation	(70)
A20	TRAF2, TRAF6, RIP1	Tumor suppressor	B-cell lymphomas	inflammation, apoptosis inflammation	*In vivo*	Downregulation	(71)
CYLD	IκK	Tumor suppressor	Cylindromatosis	inflammation	*In vivo*	Downregulation	(72)

and promotes its ubiquitination and degradation in multiple cancer cells (25). CRL3-potassium channel tetramerization domain-containing 2 (KCTD2) mediates c-Myc protein degradation by ubiquitination and suppresses gliomagenesis (35). E3 ligase CHIP interacts and degrades c-Myc by ubiquitination in glioma cells (36). In addition, 11S proteasomal activator REGγ has been reported to induce the degradation of c-Myc in cancer cells (37). On the other hand, SCF-SKP2 enhances c-Myc transcriptional activity by enabling the formation of c-Myc activator complexes (85). The E3 ligase HectH9 regulates the transcriptional activation of Myc through forming a lysine 63-linked polyubiquitin chain and promotes tumor cell proliferation *in vivo* and *in vitro* (27).

The deubiquitinating enzymes can prevent c-Myc degradation, maintain its stability, and then promote cancer progression. USP28 was the first DUB shown to regulate c-Myc stability. It is highly expressed in colon and breast carcinomas and binds to Myc through interacting with FBW7alpha to stabilize Myc in the nucleus (38). USP22 increased c-Myc stability *via* deubiquitination in breast cancer cells (68). We previously found that USP37 was significantly upregulated in human lung cancer tissues, and directly deubiquitinated and stabilized c-Myc independent of Fbw7 (67). USP36, a highly expressed USP in a subset of human breast and lung cancers, could interact with the nucleolar Fbw7γ and maintain c-Myc stability in the nucleolus (61). Recently, a novel E3 ligase, human U three protein 14a (hUTP14a) is upregulated in human colorectal cancer tissues, and it stabilizes c-Myc through forming a complex with USP36/Fbw7γ in the nucleolus and promote cancer progression (69).

E3 Ligases and DUBs Regulate Apoptosis

Apoptosis could inhibit aberrant cell cycle progression and prevent tumorigenesis (39). If apoptotic pathways are abrogated, the cells may not appropriately induce apoptosis, which may lead to tumorigenesis. As a tumor suppressor protein, p53 is frequently mutated in most cancers and plays a pivotal role in apoptosis, genome instability and mutation. Ubiquitination has been found to play a key role in regulating p53 degradation as well as its activity and localization. For instance, MDM2 (murine double minute 2) has been found to negatively regulate p53 with diverse mechanisms. It can interact directly and degrade p53 *via* ubiquitination. Besides, it can connect p53 and pRb to form an Rb-Mdm2-p53 trimeric complex for the regulation of p53-induced apoptosis (86). Mdm2 can also form a heterodimer

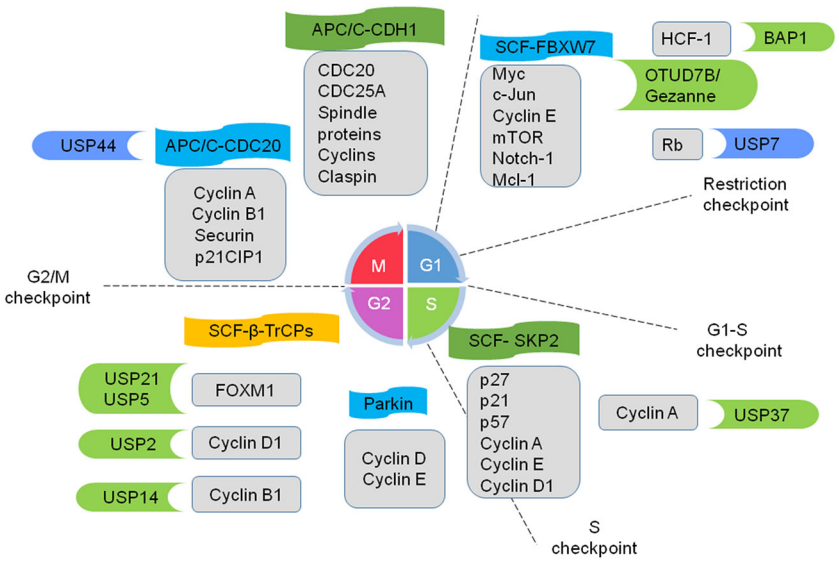

FIGURE 2 | Ubiquitin ligases and DUBs coordinate to regulate cell cycle progression. E3 ligase APC/C (anaphase-promoting complex; also named as the cyclosome) recruits cell division cycle 20 (cdc20) and CDC20-like protein 1 (CDH1). APC/C-CDC20 promotes cell cycle transition from metaphase to anaphase, while APC/C-CDH1 mediates mitotic exit and early G1 entry. E3 ligases SCF (S-phase kinase-associated protein 1-cullin 1-F-box protein) complexes work on a subset of cyclins and CDK inhibitors and regulate progression from G1 to the onset of mitosis. FBXW7, SKP2, and β-TrCPs are well-studied F-box proteins. E3 Parkin downregulates some G1/S kinases. Several DUBs play crucial roles in cell-cycle progression in cancers. Some example substrates of E3 and DUBs are shown in the gray boxes. The E3 and DUBs in green are tumor promoters and the ones in blue are tumor suppressors.

with MdmX (Mdm4) and participate in ubiquitin-mediated p53 degradation (33). Moreover, Mdm2 is upregulated in multiple cancers such as colorectal cancer, cutaneous melanoma and breast cancer (63). Therefore, the inhibition of p53-MDM2 interaction facilitates p53-mediated cell-cycle arrest or apoptosis in cancer cells.

Up to now, many DUBs are involved in the regulation of p53. For example, USP7 modulates the stability of both p53 and MDM2, and maintains the level of p53 ubiquitylation (34, 87); USP2 affects the stability of MDM2 (88); Otub1 inhibits p53 ubiquitination and activates p53 in cells (56); USP10 regulates the location and stability of p53, and stabilize both mutated and wild-type p53, thereby having a dual role in tumorigenesis (89).

Several E3s target anti-apoptotic protein myeloid cell leukemia 1 (MCL1) and sensitize cells to apoptosis. For example, DNA damage promotes HUWE1 bind to MCL1 and marks MCL1 for proteasomal degradation; the cell cycle regulators APC/C-CDC20 and SCF-FBXW7 degrade MCL1 and link apoptosis to prolonged mitotic arrest. Human UTP14a is upregulated in several types of tumors and involved in tumor progression *via* multiple mechanisms. It also exhibits an anti-apoptotic activity through the intrinsic apoptotic pathway, and protects tumor cells from chemotherapeutic drug-induced apoptosis (70). It binds p53 and induces p53 degradation through a ubiquitin-independent manner (40). Moreover, hUTP14a can also bind tumor suppressor pRb, and promote the polyubiquitination and degradation of pRb *in vitro* and *in vivo* (90). Thus hUTP14a might possess the potential as a target for anti-tumor therapy.

E3 ligases and DUBs Regulate DNA Damage Repair

Errors in DNA replication and repair often cause genomic instability (73). DNA damage repair is critical to maintain genome integrity and prevent cancer. Many E3s including MDM2 and BRCA1 participate in regulating the DNA damage response and cell cycle checkpoints to cancer development. In brief, DNA double-strand breaks (DSBs) induce the activation of DNA damage sensors, which leads to the inactivation of MDM2, maintenance of p53 stability, promotion of SCF-β-TrCP mediated degradation of CDK phosphatase, and decrease of CDK activity. In the meantime, DNA repair machines are recruited to DNA damage sites under the control of ubiquitination. The inhibition of homologous recombination (HR) during G1 is also dependent on ubiquitylation mediated by APC/C-CDH1 and cullin 3-RING-E3 ligase (CRL3)-kelch-like ECH-associated protein 1 (KEAP1). USP11 is also involved in the regulation of DNA double-strand break repair, which is often up-regulated in cancer, resulting in resistance to poly ADP ribose polymerase 1 (PARP) inhibitors (41, 64). USP21 deubiquitinates and stabilizes BRCA2, promotes HR efficiency, and enhances homologous recombination efficiency and tumor cell growth (65). USP13 deubiquitinates receptor-associated protein 80 (RAP80) and promotes DNA damage response. Therefore, inhibiting USP13 makes ovarian cancer cells sensitive to cisplatin and olaparib (a PARP inhibitor) (52).

E3 ligases and DUBs Regulate Inflammation

Cancer-related inflammation plays an important role in tumor development and progression. The transcription factor NF−κB

regulates multiple biological processes including inflammation, immunity, cell proliferation and apoptosis. Abnormal activation of NF-κB has been involved in tumorigenesis. Ubiquitination regulates NF-κB pathways in proteasome-dependent and independent mechanisms (**Figure 3**) (66). For example, NF-κB is activated by the inflammatory cytokine interleukin-1 (IL-1). Without simulation, NF-κB is inactive in the cytoplasm binding to the inhibitory proteins of the κB family (IκB). IL-1β activates the ubiquitin E3 ligase tumor necrosis factor receptor-associated factor 6 (TRAF6). TRAF6 cooperates with the E2 enzyme Ubc13-Uev1A to synthesize K63 polyubiquitin chains and adds them to the TAB2 (TGFβ-activated kinase 1 binding protein 2) subunit of the TGF-β activated kinase 1 (TAK1) kinase complex, resulting in TAK1 activation. TAK1 then phosphorylates the IκB kinase β (IκKβ). Phosphorylated IκB is subsequently ubiquitinated and degraded by 26S proteasome, thereby allowing NF-κB to translocate to the nucleus and activate gene expression.

Inappropriate activation of NF-κB has been linked to cancers. NF-κB activation could be tightly controlled by deubiquitinating enzymes as negative regulators of IκK. For example, DUB A20 inhibits IκK activation *via* three mechanisms, replacing K63 polyubiquitin chains from receptor-interacting protein 1(RIP1) with K48 polyubiquitin chains, blocking the interaction between Ubc13 and TRAFs, and inhibiting IκK phosphorylation by TAK1 (42). Another well-known DUB is the tumor suppressor CYLD, which inhibits NF-κB activation by cleaving K63 as well as linear polyubiquitin chains to inhibit IκK (71). Lack of CYLD in cells would elevate NF-κB activation, which likely contributes to tumor development.

E3 ligases and DUBs Regulate T Cell Dysfunction in Cancer

T cell activation is critical for the initiation and regulation of the immune response in cancer immunotherapy. It requires at least two signals to become fully activated. One occurs after the engagement of the T cell receptor (TCR) and major histocompatibility complex (MHC). Another is provided when co-stimulator CD28 binds to CD80 and CD86 that are expressed on antigen-presenting cells (APCs). However, the multifaceted suppressive signals that existed in the tumor microenvironment make intratumoral T cells dysfunctional. The main traits of T cell dysfunction include some inhibitory receptors (e.g., PD-1), inhibitory cells (e.g., Treg cells), suppressive soluble mediators (e.g., TGFβ), transcriptional factors (e.g., T-bet), etc (72). UPS has been found to play a key regulatory role in maintaining T cell dysfunction with diverse mechanisms (91).

Dysfunctional T cells usually have abnormally high expression of multiple inhibitory receptors such as PD-1. Inhibitory receptors binding to their ligands negatively regulate an immune response. A recent study has identified that E3 ligase Fbxo38 ubiquitinates and degrades PD-1 in activated intratumoral T cells, which proves a novel mechanism for cancer immunotherapy. Fbxo38 can be activated by IL-2-induced STAT5 in activated T cells. In the dysfunctional T cells, Fbxo38 is downregulated, leading to an increased PD-1 abundance and impressive tumor immune response (92).

Regulatory T (Treg) cells are a subpopulation of $CD4^+$ T cells that are crucial for maintaining immune tolerance. Treg cells usually produce immunosuppressive molecules such as TGFβ and inhibit the function of effector T cells. Treg cell development and function are determined by the transcription factor forkhead box protein 3 (Foxp3) and several E3s are involved in the process. For example, Stub1 and casitas B cell lymphoma protein b (Cbl-b) ubiquitinate Foxp3 and negatively regulate Treg cell development (43, 44). E3 ligase von Hippel-Lindau (VHL), Itchy homolog (Itch) and gene related to anergy in

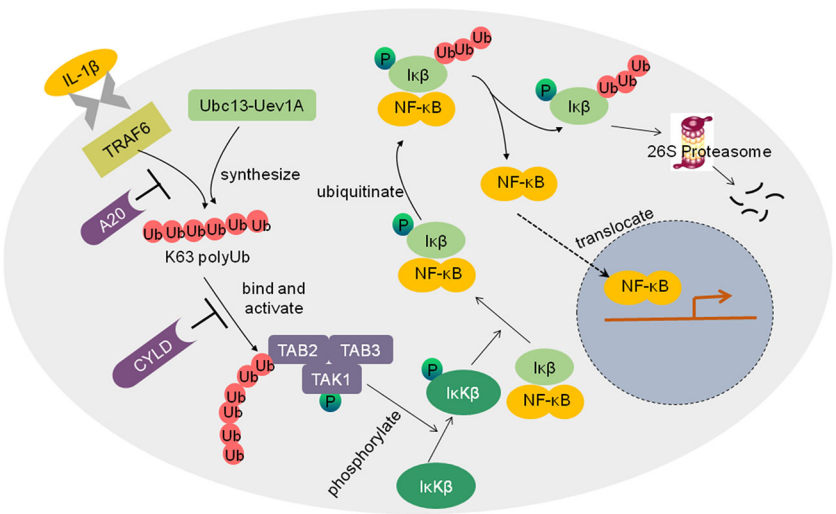

FIGURE 3 | Schematic diagram of the regulation of NF-κB activation by ubiquitin ligases and DUBs. IL-1β activates the ubiquitin E3 ligase TRAF6, TRAF6 cooperated with the E2 enzyme Ubc13-Uev1A to synthesize K63 polyubiquitin chains and add them to the TAB2 subunit of the TGF-β activated kinase 1 (TAK1) kinase complex, which results in TAK1 activation. TAK1 then phosphorylates IκKβ. Phosphorylated IκB is subsequently ubiquitinated and degraded by 26S proteasome, thus allowing NF-κB to translocate to the nucleus, and the NF-κB pathway is activated. Deubiquitinases such as A20 and CYLD inhibit the activation of the NF-κB pathway.

lymphocytes (Grail) participate in maintaining Treg cell repressive function (45, 46). Loss of VHL in Tregs leads to type 1 T helper (Th1)-like cell conversion and interferon-gamma (IFN-γ) production (45). Itch deficiency in Treg cells results in severe airway inflammation in mice, increasing TH2 cytokine production (46). Also, GRAIL-deficient Treg cells induce decreased suppressive function and increased Th17 cell-related gene expressions (93). Cbl-b and Grail have been found to play crucial roles in tumor immunosurveillance. Their loss inhibits tumor formation in mice. Cbl-b$^{-/-}$ and Grail$^{-/-}$ CD8^{+} T cells can be fully activated in the absence of costimulatory factors *in vitro*. They could promote tumor rejection and inhibit tumor formation when they are transferred into tumor-bearing mice (94, 95). These studies suggest that Cbl-b and Grail may serve as therapeutic targets to antitumor immunity.

TGFβ, a well-known immunosuppressor factor, plays an important role in immune tolerance (96). It not only promotes thymic Treg cell development by repressing T cell clonal deletion but also regulates peripheral Treg cell differentiation and maintains Treg cell function by inducing Foxp3 expression (96). Moreover, TGFβ inhibits T cell proliferation by decreasing IL-2 production and upregulating cell cycle inhibitors (97). It also blocks CD4^{+} T cell differentiation by modulating T-bet or GATA expression (97). Besides, TGFβ downregulates the expressions of cytolytic genes in cytotoxic T lymphocytes (98), costimulatory factors and MHC II molecules in dendritic cells and macrophages, reducing antigen resenting ability and regulating T cell function indirectly (99). In fact, as a versatile cytokine, TGFβ exerts pivotal functions in diverse processes of cancer development, such as proliferation, differentiation, apoptosis, and migration, depending on the target cells (100). Thus, TGFβ signaling has been regarded as a potential therapeutic target for the treatment of cancers.

Dynamic ubiquitination/deubiquitination plays a key role in the regulation of the TGFβ signaling pathway (**Figure 4**) (101). The TGFβ1-induced TGFβ pathway activation consists of receptors (TGF receptor I and II), receptor-SMADs (SMAD2 and SMAD3), co-SMAD (SMAD4), and inhibitor adaptor SMAD (SMAD7). TGFβ1 binding induces TGFRII to phosphate TGFRI, and then the activated-TGFRI phosphorylates SMAD2 and SMAD3. Subsequently, the phosphorylated SMAD2/3 dissociates from the receptor and oligomerizes with SMAD4. Following that, SMAD2/3/4 translocates to the nucleus and recruits other gene regulatory proteins and transcript specific genes. Many E3s and DUBs are reported to be involved in turning off the TGFβ pathway. For example, AIP4/Itch brings SMAD7 to TGFβRI and prevents the activation of SMAD2 (102). SMAD7 also serves as a scaffold to recruit E3 ligases SMURF1, SMURF2, Tuil1/WWP1 and NEDD4-2 to ubiquitinate and degrade the receptor complex (103–106). On the contrary, USP26 stabilizes SMAD7 *via* deubiquitination (107). As for SMADs, SMURF2 and NEDD4-2 target SMAD2 for degradation (106, 108) whereas SMAD3 is targeted by E3 ligases CHIP and ROC1-SCFFbw1a (109, 110). SMAD4 is indirectly regulated by E3 ligases SMURF1, SMURF2, Tuil1/WWP1, and NEDD4-2 through forming a complex with SMAD7, SMAD6 or activated SMAD2 (111). SMAD4 has a point mutation in many cancers. In this case, these protein variants are degraded by E3 ligases SCF-Skp2 and SCF-β-TrCP1 (112, 113) In addition, the R-SMAD/SMAD4 complex can be dissociated by SMURF2 monoubiquitinates SMAD3 or Ectodermin/Tif1γ monoubiquitinates SMAD4. Once the R-SMAD/SMAD4 complex enters the nucleus, the DNA-binding proteins SnoN and TGIF direct NEDD4-2 and Tiul/WWP1 to degrade SMAD2 and inhibit the signaling.

On the other hand, lots of E3s and DUBs participate in turning on the TGFβ pathway. At the receptor level, USP4 interacts directly with TGFβRI to maintain its stability (114). DUBs such as USP11 and USP15, stabilize the receptor complex by being associated with the scaffold protein SMAD7 (115, 116). SMAD7 can be degraded by E3 ligases Arkadia, AIP4/Itch and RNF12 mediated ubiquitination (117). OTUB1 maintains the stability of SMAD2/3 by reversing the ubiquitination of SMAD2 and USP9X, and also promotes the R-SMAD/SMAD4 complex formation by preventing ubiquitination on R-SMAD (118). In the nucleus, transcriptional repressor SnoN can be degraded by E3s Arkadia, SMURF2 and CDH1-APC mediated ubiquitination (119, 120). Monoubiquitination of R-SMADs prevents the R-SMAD/SMAD4 complex binding with the DNA, while USP15 reverses the modification and promotes TGFβ dependent transcription.

The T-box family transcription factor T-bet regulates the Th1 cell differentiation and induces the production of IFN-γ. Recently, it has been shown that it is expressed in Treg and participates in relevant immunosuppressive function (121). It has been suggested that T-bet is required in T cell dysfunction (72). Although the underlying mechanism of T-bet ubiquitination is unknown, USP10 has been found to stabilize T-bet *via* deubiquitination and enhance the secretion of IFN-γ (122).

Furthermore, UPS could regulate TCR activation. For instance, E3 ligases Cbl, Itch, and Grail degrade the TCR complex and inhibit T cell activation through proteolysis-dependent mechanisms (91, 123). In contrast, USP12 has been found to stabilize the TCR complex and promote TCR signaling through deubiquitylating TCR adaptor proteins LAT and Trat1 in primary mouse T lymphocytes (124). Naik et al. found that USP9X regulated TCR signaling and tolerance induction, and also the USP9X-deficient T cells were hyperproliferative (125). Therefore, E3 ligases and deubiquitinases keep the delicate balance between immunity and tolerance.

THE THERAPEUTIC TARGETS OF UPS AND DUBS

Numerous evidence indicates that every component of UPS can be regarded as valuable therapeutic targets in the development of anti-cancer drugs. Several drugs such as bortezomib (a proteasome inhibitor), have been approved by the FDA in cancer, and many other inhibitors are in development (**Table 3**) (138).

Targeting the E1 Enzyme

The E1 enzyme is responsible for activating ubiquitin molecules in the UPS, and several compounds have been identified to target E1. For example, adenosine sulfamate analogs, such as MLN7243

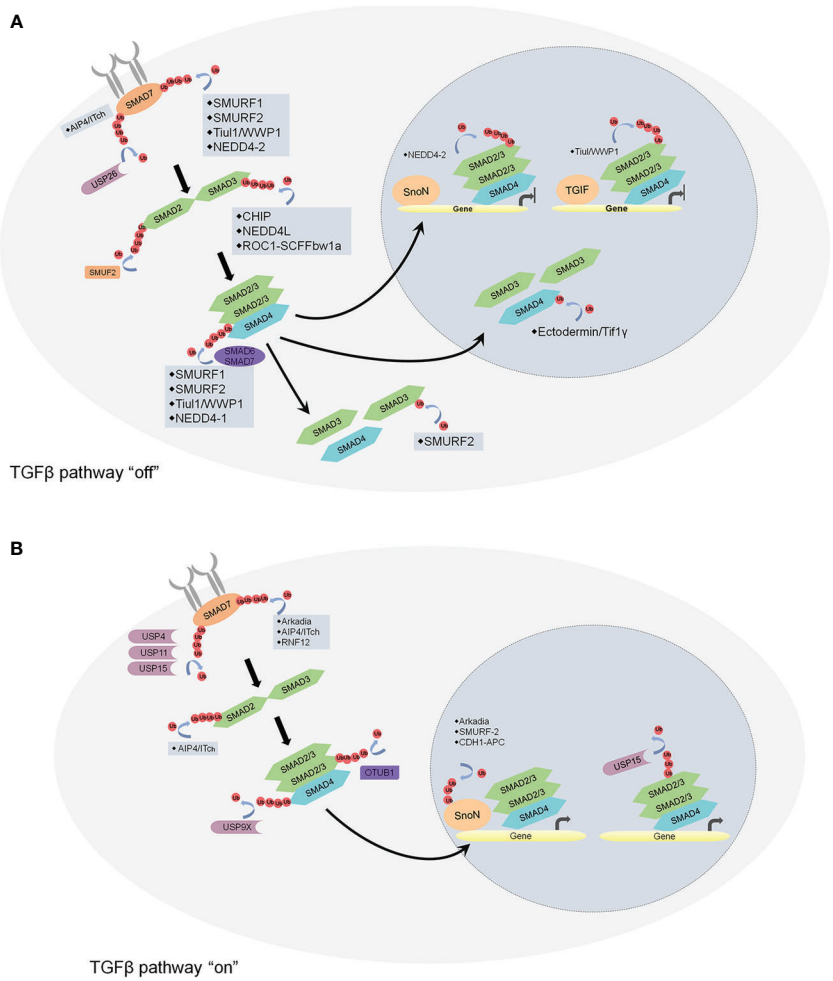

FIGURE 4 | Schematic overview of the regulation of TGFβ pathway by ubiquitin ligases and DUBs. **(A)** factors that turn off the TGFβ pathway. AIP4/Itch brings SMAD7 to TGFβRI and prevents the activation of SMAD2. SMAD7 recruits E3 ligases SMURF1, SMURF2, Tuil1/WWP1, and NEDD4-2 to ubiquitinate and degrade the receptor complex. On the contrary, USP26 stabilizes SMAD7 *via* deubiquitination. As for SMADs, SMURF2, and NEDD4-2 target SMAD2 for degradation whereas SMAD3 is targeted by E3 ligases CHIP and ROC1-SCFFbw1a. SMAD4 is regulated by E3 ligases SMURF1, SMURF2, Tuil1/WWP1, and NEDD4-2 through forming a complex with SMAD7, SMAD6 or activated SMAD2. The R-SMAD/SMAD4 complex can be dissociated by SMURF2 monoubiquitinates SMAD3 or Ectodermin/Tif1γ monoubiquitinates SMAD4. Once the R-SMAD/SMAD4 complex enters the nucleus, the DNA-binding proteins SnoN and TGIF direct NEDD4-2 and Tiul/WWP1 to degrade SMAD2 and inhibit the signaling. **(B)** factors that turn on the TGFβ pathway. At the receptor level, USP4, USP11, and USP15 stabilize the receptor complex. E3s Arkadia, AIP4/Itch and RNF12 induce SMAD7 degradation. OTUB1 maintains the stability of SMAD2/3 and also promotes the R-SMAD/SMAD4 complex formation by preventing ubiquitination on R-SMAD. In the nucleus, transcriptional repressor SnoN can be degraded induced by E3s Arkadia, SMURF2 and CDH1-APC. Monoubiquitination of R-SMADs prevents the R-SMAD/SMAD4 complex binding with the DNA, while USP15 reverses the modification and promotes TGFβ-dependent transcription.

(126) and MLN4924, function as the ubiquitin-activating enzyme and NEDD8-activating enzyme inhibitors, respectively. They are currently undergoing Phase I/II and Phase I clinical trials (127, 139). Recently, TAK-243 was reported to induce leukemic cell death in preclinical models of acute myeloid leukemia cells through inhibition of the ubiquitin-like modifier-activating enzyme 1 (128). Experimental inhibitors of E1 have also been reported. For example, PYR-41, an irreversible inhibitor of ubiquitin E1, can inhibit the ubiquitylation of TRAF6 and decrease nuclear factor-kappa B activation. PYR-41 can also inhibit the degradation of p53 and activate its transcriptional activity (140). Due to lacking specificity, inhibition of E1 would cause remarkable side effects.

Targeting the E2 Enzyme

The E2 enzyme binds to E1, and then the activated ubiquitin is transferred to a cysteine of the E2 enzyme from the E1 enzyme. Thus, E2 enzymes mediate the conjugation of ubiquitin to substrates. Nowadays, several E2 inhibitors have been found to interfere with the process. For instance, Leucettamol A and manadosterols A and B, which are isolated from the sea sponges, inhibit the Ubc13-Uev1A interaction and block the

TABLE 3 | Anti-cancer compounds in clinical trials targeting the ubiquitin-proteasome system and DUBs.

Classification	Compound	Target	Cancer/cancer cell line	Status	References
E1 inhibitor	MLN7243	Ubiquitin-activating enzyme	Acute myeloid leukemia	Phase I/II	(65)
	MLN4924	NEDD8-activating enzyme	Malignant melanoma	Phase I	(52)
	TAK-243	Ubiquitin-like modifier-activating enzyme 1	Acute myeloid leukemia	PreClinical	(42)
	PYR-41	Ubiquitin-activating enzyme	HCT116 cells, H522 cells	PreClinical	(71)
E2 inhibitor	Leucettamol A	Ubc13-Uev1A		Research	(72)
	manadosterols A and B	Ubc13-Uev1A		Research	(91)
	CC0651	Human Cdc34	PC-3 prostate cancer cells, HCT116 cells	PreClinical	(92)
E3 inhibitor	RG7112	MDM2/HDM2	Liposarcoma, acute Leukemia	Clinical	(43)
	RG7388	MDM2	Human osteosarcoma SJSA cells	Clinical	(44)
	SAR405838	MDM2/HDM2	Liposarcoma, gastrointestinal, Melanoma, non-small cell lung cancer	Phase I	(45, 46)
	MK-8242	MDM2/HDM2	Acute myeloid leukemia, Advanced solid tumors	Phase I	(93, 94)
	NVP-CG097	MDM2	SJSA-1 cells	Phase I	(95)
	HDM201	MDM2	Acute myeloid leukemia	Phase I	(96)
	AMG232	MDM2	Solid tumors and lymphomas	Phase I	(97)
	RITA	MDM2	HCT116 cells	Research	(98)
	PRIMA1	MDM2	SW480 tumor, Saos-2 osteosarcoma cells	Research	(99)
	HLI373	HDM2	RPE cells, U2OS cells, MDA-MB-468 breast cancer cell	Research	(100)
	HLI98	MDM2	RPE cells, U2OS cells, LOX-IMVI cells, A549 cells, HT1080 cells	Research	(101)
	MEL23/MEL24	MDM2	U2OS cells, HCT116 cells, RKO cells, HT-1080 cells, H1299 cells, MCF7 cells	Research	(102)
	RO8994	MDM2	SJSA-1 cells, RKO cells, HCT116 cells	Research	(103)
	NSC207895	MDMX	MCF7 cells	Research	(105)
	ATSP-7041	MDM2 & MDMX	SJSA-1 cells, RKO cells, HCT116 cells, MCF7 cell,	Research	(106)
	ALRN-6924	MDM2 & MDMX	Solid tumors and lymphomas	Phase I	(107)
	oridonin	c-Myc	Leukemia and lymphoma cells	Research	(109)
	compound ZL25	SKP2	Prostate cancer cell PC-3 & LNCaP cell, H3255 cells, H1299 cells, Hep3B cells & U2OS cells	Research	(106)
	compound A	SKP2	Hematologic malignancies	Research	(111)
	Erioflorin	Pdcd4	RKO cells, HeLa cells, MCF7 cells	Research	(112)
	GS143	β-TrCP1		Research	(113)
	TAME	Cdh1 and Cdc20	HeLa cells	Research	(114)
	apcin	Cdc20	RPE1 cells	Research	(115)
	Clomipramine	Itch	Breast, prostate and bladder cancer cells	Approved	(118)
Proteasome inhibitor	Bortezomib	Proteasome	Multiple meloma, nonsmall cell lung cancer, pancreatic cancer, mantle cell lymphoma	Approved	(119, 120, 123, 124)
	Carfilzomib	Proteasome	Multiple meloma, Waldenstrom's Macroglobulinemia	Approved	(7)
	Ixazomib	Proteasome	Multiple meloma	Approved	(8)
	Oprozomib	Proteasome	Multiple meloma, solid tumors, Waldenstrom Macroglobulinemia	Phase Ib/II	(126)
	Delanzomib	Proteasome	Multiple Myeloma, solid tumors, Lymphoma, Non-Hodgkin	Phase I/II	(127)
	Marizomib	Proteasome	Refractory and relapsed multiple myeloma, malignant glioblastoma	Phase III	(126, 128, 129)
DUB inhibitor	WP1130	USP9X	HCT116 cells	Research	(129)

(Continued)

TABLE 3 | Continued

Classification	Compound	Target	Cancer/cancer cell line	Status	References
	WP1130	UCH37	Multiple myeloma MM1.S & Mantle cell lymphoma Z138 cells	Research	(130)
	HBX 41,108	USP7	Prostatic adenocarcinoma PC3 cells, Colon carcinoma HCT116 cells	Research	(131)
	P5091	USP7	Multiple myeloma cells	Research	(132)
	b-AP15	USP14 & UCHL5	Multiple myeloma cells	Research	(133)
	Protac-1	MetAP-2		Research	(134)
	ARV-825	BRD4	Multiple myeloma cells	Research	(135)
	ARV-771	pan-BET	Castration-resistant prostate cancer	Research	(136)
	QCA570	BET	Human acute leukemia cells	Research	(137)

E1-E2 complex formation (141, 142). Another example is CC0651, a small molecule inhibitor of the E2 enzyme hCdc34 (130). The E2 enzyme hCdc34 can ubiquitylate SCF (Skp2) substrate p27, and CC0651 decreases tumor cell growth by inhibiting p27 ubiquitylation and degradation.

Targeting the E3 Enzyme

E3 ligase recognizes substrate proteins and catalyzes the transfer of ubiquitin from E2 to target protein lysine. Therefore, E3 ligase has high substrate specificity which makes targeting E3 ligase become a promising tumor treatment strategy. So far, many studies have identified some compounds that could target specific E3 ligases and disturb UPS.

MDM2/p53

Due to the critical roles of p53 in regulating the genome, many efforts have been made to find the antagonists of E3 ligase MDM2/HDM2 to restore the function of p53. To date, a large number of inhibitors have been discovered based on MDM2-p53 interaction. Some of them are undergoing clinical assessment with different stages, such as RG7112 (129), RG7388 (131), SAR405838 (132, 143), MK-8242 (144, 145), NVP-CG097 (133), HDM201 (146), and AMG232 (147). Besides, more MDM2 inhibitors, such as RITA (134), PRIMA1 (135) HLI373 (148), HLI98 (149), MEL23 and MEL24 (150), and RO8994 (136) have been discovered to target MDM2 directly, thereby enhancing p53 activity and exhibiting anti-cancer ability.

MDMX/HDMX (murine/humans double minute X) shares significant homology with MDM2 and is also a negative regulator of p53. Though nutlin-3 has been found to inhibit MDM2-p53 but not MDMX-p53 interaction (151), NSC207895 targets MDMX specifically and acts addictively with nutlin-3a to activate p53 and induce apoptosis (137). Moreover, ATSP-7041 (152) and ALRN-6924 (153) decrease p53-dependent tumor growth as dual inhibitors of MDM2 and MDMX.

SCF E3 Ligases

SCF (Skp1/cullin/F-box) E3 ligases are the largest family of E3 ubiquitin ligases. Their substrates play important roles in regulating the cell cycle, DNA replication, and signal transduction. Therefore, the dysregulation of these E3s often leads to cancer (154). Since FBPs are responsible for the specificity of SCFs, many small molecules are designed to target them. For instance, the natural compound oridonin enhances the ubiquitination and degradation of c-Myc mediated by FBW7, inducing apoptosis in leukemia and lymphoma cells (155). Furthermore, compound ZL25 inhibits SKP2 directly, resulting in the p53-independent cellular senescence in cancer cells (156). Another SKP2 inhibitor, compound A, induces p27-dependent cell cycle arrest and cell death by inhibition of SCF-SKP2 complexes formation (157). Erioflorin stabilizes the tumor suppressor Pdcd4 by blocking its interaction with β-TrCP1, suppresses the activity of AP-1 and NF-κB, and decelerates cancer cell proliferation (158). Another inhibitor, GS143, was shown to markedly decrease IκB ubiquitination by targeting β-TrCP1 and suppress the NF-κB signaling pathway (159).

Since Cdc20 is an oncogenic cofactor in the APC/C complex, many efforts have been made to find Cdc20 inhibitors to anti-cancer. TAME (tosyl-L-arginine methyl ester) was reported to bind to the APC complex. It could inhibit its activation by targeting both Cdh1 and Cdc20 and arrest cells in metaphase (160). Moreover, Apcin was found to bind directly to Cdc20, inhibiting the ubiquitylation of D-box-containing substrates, and subsequently inducing tumor cell death (161).

E3 ligase Cbl-b has been identified as a negative regulator of TCR signaling. When Cbl-b is inhibited, the T cell-mediated antitumor activity will be enhanced. Autologous peripheral blood mononuclear cells (PBMCs) from patients were collected and transfected with Cbl-b-siRNA, which were called APN401. The results of the Phase I clinical trial for APN401 revealed that its intravenous infusion in patients with refractory solid tumors was feasible and safe (162). Several small-molecule Cbl-b inhibitors have been discovered to decrease the ubiquitylation of TAM receptors and promote the activation of T cells as well as natural killer cells. They are expected to be utilized in combination with other approved agents in immunotherapy (163).

Itch, a HECT domain-containing E3 ligase, promotes the ubiquitylation of several proteins (e.g. p70, p63, c-Jun, JunB, Notch, and c-FLIP) and shows a potential target for cancer therapy. Rossi et al. identified that antidepressant drug clomipramine and its homologs could inhibit Itch auto-ubiquitylation and p73 ubiquitylation to reduce breast, prostate and bladder cancer cell growth by blocking autophagy (164).

Targeting Proteasome Activity

Among all the UPS components, the proteasome has been successfully used as a target for cancer treatment. The proteasome is a large multi-protein complex containing multicatalytic proteases (e.g., chymotrypsin- and caspase-like enzyme) and is responsible

for the degradation or processing of intracellular proteins. As such, it regulates the levels of some important mediators for cell-cycle progression and apoptosis in normal and malignant cells, such as cyclins, caspases, BCL2 and nuclear factor of κB (165). Bortezomib is the first proteasome inhibitor approved for recurrent refractory multiple meloma (MM) in 2003 (166, 167). It reversibly inhibits the activities of chymotrypsin- and caspase-like enzymes, leads to the apoptosis of MM cells, and suppresses the activation of NF-κB, production of cytokines (e.g., IL-6, IGF-1, and VEGF) in the tumor microenvironment, and adherence of myeloma cells to bone marrow stromal cells (165, 168). Later, it was extended to patients with non-small cell lung cancer, pancreatic cancer, and mantle cell lymphoma (169, 170). Although bortezomib has antitumor activity, it can cause side effects such as neuropathy and autophagy in some cases (171, 172). Besides, bortezomib resistance often occurred in about one year (173, 174). Carfilzomib, a second-in-class proteasome inhibitor drug, was approved in 2012 for MM by the US FDA (11). It irreversibly inhibits the chymotrypsin-like activities and shows improved safety in maintaining its cytotoxic potential in the bortezomib resistant cell lines (12). Carfilzomib treatment also causes adverse effects such as cardiovascular complications, hypertension, and heart failure, but they are reversible and manageable with careful monitoring. Both bortezomib and carfilzomib are not suitable for oral administration. Ixazomib is the first oral bioavailable proteasome inhibitor and was approved by the FDA in 2015. It reversibly inhibits the chymotrypsin-like activities and shows improved safety profiles over bortezomib, but its therapeutic advantages still need further investigation by randomized clinical trials (12).

The clinical successes of existing proteasome inhibitors encourage great efforts to discover more proteasome inhibitors with improved efficacy and safety. Thus, a lot of proteasome inhibitors have been identified including oprozomib, delanzomib and marizomib. Oprozomib is an orally available inhibitor with a homologous structure to carfilzomib. It is currently being studied in several clinical trials including a multicenter phase Ib/II trial for MM patients. Oprozomib can effectively decrease the viability of MM cells both *in vitro* and *in vivo* (175). Delanzomib, a reversible oral bioavailability of bortezomib analog, overcomes bortezomib's resistance to peripheral neuropathy. But it causes severe skin toxicity to many patients (176). Marizomib, a novel proteasome inhibitor with a better therapeutic ratio, overcomes bortezomib resistance and exhibits broader anti-cancer activities (177). Moreover, marizomib has synergistic effects on refractory and recurrent MM patients with BTZ, linedoxamine, bormadoxamine and low dose dexamethasone (175, 178). In addition, marizomib can penetrate the blood-brain barrier and induces apoptosis in glioma cells with low toxicity on normal cells (179). Marizomib is currently being assessed in a phase III trial for the treatment of malignant glioblastoma in combination with temozolomide and radiotherapy.

Targeting DUBs Activity

Ubiquitination is a dynamic and reversible process and DUBs catalyze the removal of ubiquitin or polyubiquitin chains from the target protein. DUBs are actively involved in regulating tumorigenesis. Thus, DUB inhibitors are regarded as potential anti-cancer agents (180) To date, a number of DUB inhibitors have been identified to inhibit tumorigenesis (4, 10, 181).

WP1130, an inhibitor of DUBs, can suppress the activities of USP9X, USP5, USP14 and UCH37, deregulate anti-apoptotic protein MCL-1 and upregulate pro-apoptotic protein p53. It exhibits high anti-tumor activity (182). For example, the transcription factor E-twenty-six related gene (ERG) is overexpressed and promotes prostate carcinogenesis. Inhibition of USP9X by WP1130 leads to ERG degradation and inhibits tumor growth (183).

Recently, HBX 41,108, a small-molecule inhibitor of USP7, was reported to inhibit USP7-mediated p53 deubiquitination, stabilizing p53 and inducing p53-dependent apoptosis in cancer cells (184). Besides, P5091, a selective USP7 inhibitor, was found to induce apoptosis and overcome bortezomib resistance in MM cells. What's more, it can inhibit tumor growth and exhibit synergistic anti-MM activity in combination with lenalidomide, HDAC inhibitor SAHA, or dexamethasone (185). A class of dual small molecule inhibitors of USP7 and USP47 has been identified to promote p53 activity and apoptosis in MM and B-cell leukemia cells *in vitro* and xenograft models (186).

Moreover, USP14 can inhibit the degradation of ubiquitin-protein conjugates *in vitro* and *in vivo* (187). The inhibitors of USP14 have been found to stimulate the proteasomal degradation of oxidized proteins, causing resistance to oxidative stress (188). Consistently, b-AP15 was shown to inhibit cell growth and overcome bortezomib resistance in MM cells by selectively blocking the deubiquitylating activity of USP14 and UCHL5 (189). These studies indicate that inhibiting specific oncogenic DUBs may be an effective anti-cancer approach.

PROTACs TECHNOLOGY

Recently, emerging technologies based on PROTACs attract increasing attention in the pharmaceutical industry (190). PROTACs are heterobifunctional molecules that simultaneously bind a target protein and an E3 ubiquitin ligase, enabling ubiquitination and degradation of the target by the UPS in the cell (**Figure 5**) (13). PROTACs link the target protein to an E3 ubiquitin ligase by a designed hybrid molecule, providing a path for ubiquitinating undruggable proteins such as transcription factors, scaffolding proteins and nonenzymatic proteins. The first PROTACs were reported in 2001 by the Crews group and Ray Deshaies (191). They artificially synthesized a chimeric compound named Protac-1. Protac-1 has two domains: one domain contains the IκBa phosphopeptide that could recruit the F-box protein β-TrCP, and the other domain contains ovalicin which could bind to the target protein methionine aminopeptidase-2 (MetAP-2). As a result, MetAP-2 was ubiquitinated and degraded in a Protac-1-induced proteolysis manner.

Due to the excellent permeability and low working concentrations, small molecule-based PROTACs, which utilize small molecules to recruit E3 ubiquitin ligases, have more potential to be developed into drugs than peptide-based PROTACs (13). The PROTAC technology broadens the range of target proteins degraded by the UPS.

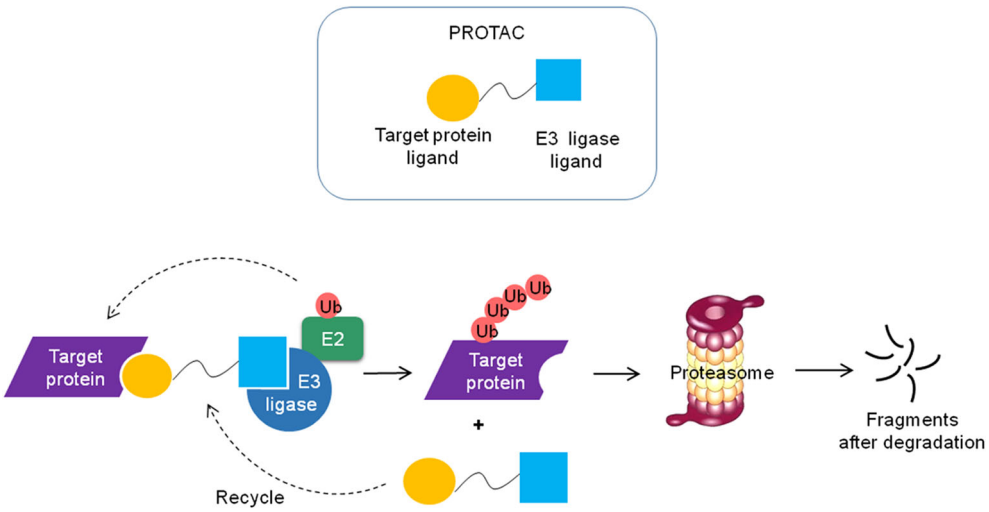

FIGURE 5 | Schematic diagram of the PROTAC technology. The PROTC is a chimeric molecule that consists of two ligands, one is to interact with E3 ligase and the other is to bind the target protein. The target protein is polyubiquitinated and degraded by the proteasome and the PROTC molecule can be recycled.

Recently, some transcriptional regulators (such as BRD4, TRIM24 and Smad3) have been reported to be targeted by PROTAC technologies (13). BRD4, a bromodomain and extraterminal domain (BET) family member, usually resides upstream of important oncogenes such as c-Myc, BCL-xL and BCL-6, and regulates their expressions. Therefore, BRD4 has become a promising therapeutic target in multiple cancer types. Preclinical studies of BRD4 inhibitors, JQ1 and OTX015, demonstrate their value in suppressing c-Myc expression and BL cell proliferation. However, owing to the reversible binding of inhibitors, the suppression is incomplete and requires high drug concentrations. Crews groups developed a bifunctional molecule, ARV-825, connecting the BRD4 inhibitor OTX015 to an E3 ligase cereblon binding moiety (pomalidomide) using PROTAC technology. As a result, ARV-825 actively recruits BRD4 to cereblon, leading to BRD4 efficient degradation *via* the proteasome in Burkitt's Lymphoma cells. Moreover, ARV-825 treatment produces a more pronounced effect on the inhibition of c-Myc than that of the BRD4 inhibitors in five MM cell lines [SKO-007(J3), U266, RPMI-8226, ARP-1, JJN3] and an MM patient-derived $CD138^{+}$ MM cells (192). In addition, Zengerle et al. designed another PROTAC, connecting JQ1 for BET family proteins and a ligand for VHL. Interestingly, the PROTAC not only triggered the degradation of BET family proteins particularly BRD4, but also regulated the transcription of BRD4 downstream genes such as Myc, p21 and AREG (193). In this way, it can also dampen the pro-inflammatory response in microglia, because BET proteins control the transcription of NF-κB-depended genes (194). These findings demonstrate that BRD4 PROTACs is a promising novel strategy to efficiently target BRD4 (195).

Raina and his colleagues reported that ARV-771 (another pan-BET inhibitor)-based PROTAC, dramatically suppressed androgen receptor (AR) protein level and AR signaling. It could lead to tumor regression in castration-resistant prostate cancer (CRPC) mouse xenograft model with more efficiency than BET inhibitors. This study provides evidence that small molecule-based PROTAC functions in a solid-tumor malignancy of CRPC (196). The results of BET-PROTACs ARV-825 and ARV-771 in the treatment of MCL cells demonstrate that they induce more apoptosis than BET inhibitors. Also, the results show that they can overcome the resistance of ibrutinib and exert a synergistic effect on apoptosis induction in the combination of other drugs such as ibrutinib, venetoclax (a BCL2-antagonist) and palbociclib (a CDK4/6 inhibitor) (197).

Recently, more BET-PROTACs have been designed. For instance, Qin et al. synthesized a BET-PROTAC called QCA570, utilizing a new class of BET inhibitors Oxazepines to recruit BET proteins. It could inhibit human acute leukemia cell proliferation at low picomolar concentrations, and abolish tumor growth in leukemia xenograft models in mice (198). Zhang and his colleagues demonstrated that BET-specific PROTACs were active against preclinical models of MM (199). Interestingly, the activity of BRD4-specific PROTACs can be improved over 100-fold through modification of hydroxylation of proline (200). In addition to the BET family, a functional PROTAC against TRIM24, another bromodomain-containing transcriptional regulator, has been designed and provides a path to find new undruggable targets (201). Wang et al. designed new PROTACs to prevent renal fibrosis by targeting SMAD3. They used hypoxia-inducible factor-1α to recruit VHL and screened compounds to bind SMAD3 from the Enamine library using the GLIDE molecular docking program. SMAD3 was degraded by PROTAC mediated ubiquitination (202). Thus, transcription factors can be targeted *via* PROTAC technology.

In addition, the undruggable transcription factors also can be degraded *via* alteration of the activity of an E3 ubiquitin ligase. For instance, Thalidomide and its derivatives Lenalidomide and Pomalidomide are effective drugs for the treatment of multiple

myeloma and other B cell lymphomas. Thalidomide analogs bind Cereblon (CRBN), the substrate receptor of the CUL4-RBX1-DDB1-CRBN (CRL4CRBN) E3 ubiquitin ligase and alter its substrate selectivity to recruit, ubiquitinate and degrade unrelated transcription factors, such as Ikaros (IKZF1), Aiolos (IKZF3) and Casein kinase 1 alpha (CK1α) (203, 204). These findings provide a novel way to selective degrade specific targets through modulating the activity of an E3 ubiquitin ligase.

To date, it remains an obstacle for the discovery of small molecule moiety to different targets. Another obstacle is specificity, how to get tissue-specific or disease-specific induced protein degradation? How to realize conditional triggered induced protein degradation? A deeper understanding of the tissue expression of E3 ligase and tumor microenvironment may provide a larger therapeutic window for appropriate PROTAC.

CONCLUSIONS

Ubiquitination of nonhistone proteins plays an important role in many cellular processes, including cell cycle, cell proliferation, DNA repair, apoptosis, inflammation, immune response, etc. Dysregulation of nonhistone lysine ubiquitylation is closely associated with the development of various human cancers. Therefore, UPS has been evolved as promising therapeutic targets for novel anti-cancer drugs. Nowadays, many proteasome inhibitors and E3 ligase modulators have been approved for anticancer treatment, whereas small-molecule inhibitor therapeutic strategies usually need high drug exposures and potentially increase the risk of off-target adverse effects. Fortunately, PROTAC technologies provide a path to target many undruggable proteins with UPS such as transcription factors.

AUTHOR CONTRIBUTIONS

XZ wrote and drafted this article. TM and LF revised the manuscript critically. SC and DL drew the figures and prepared the table. QP and PW contributed to the drafting of the article and are responsible for the integrity of the work as a whole. All authors contributed to the article and approved the submitted version.

FUNDING

This work was supported by the Natural Science Foundation of Shandong Province (No. ZR2016CM46).

REFERENCES

1. Suryadinata R, Roesley SN, Yang G, Sarcevic B. Mechanisms of generating polyubiquitin chains of different topology. *Cells* (2014) 3:674–89. doi: 10.3390/cells3030674
2. Erpapazoglou Z, Walker O, Haguenauer-Tsapis R. Versatile roles of k63-linked ubiquitin chains in trafficking. *Cells* (2014) 3:1027–88. doi: 10.3390/cells3041027
3. Haglund K, Di Fiore PP, Dikic I. Distinct monoubiquitin signals in receptor endocytosis. *Trends Biochem Sci* (2003) 28:598–603. doi: 10.1016/j.tibs.2003.09.005
4. Wei R, Liu X, Yu W, Yang T, Cai W, Liu J, et al. Deubiquitinases in cancer. *Oncotarget* (2015) 6:12872–89. doi: 10.1007/s10555-016-9640-2
5. Gross S, Rahal R, Stransky N, Lengauer C, Hoeflich KP. Targeting cancer with kinase inhibitors. *J Clin Invest* (2015) 125:1780–9. doi: 10.1172/JCI76094
6. Uckelmann M, Sixma TK. Histone ubiquitination in the DNA damage response. *DNA Repair (Amst)* (2017) 56:92–101. doi: 10.1016/j.dnarep.2017.06.011
7. Osley MA, Fleming AB, Kao CF. Histone ubiquitylation and the regulation of transcription. *Results Probl Cell Differ* (2006) 41:47–75. doi: 10.1007/400_006
8. Jeusset LM, McManus KA-O. Developing Targeted Therapies That Exploit Aberrant Histone Ubiquitination in Cancer. *Cells* (2019) 8:165. doi: 10.3390/cells8020165
9. Deng L, Meng T, Chen L, Wei W, Wang P. The role of ubiquitination in tumorigenesis and targeted drug discovery. *Signal Transduct Target Ther* (2020) 5. doi: 10.1038/s41392-020-0107-0
10. Morrow JK, Lin HK, Sun SC, Zhang S. Targeting ubiquitination for cancer therapies. *Future Med Chem* (2015) 7:2333–50. doi: 10.4155/fmc.15.148
11. Piva R, Ruggeri B, Williams M, Costa G, Tamagno I, Ferrero D, et al. CEP-18770: A novel, orally active proteasome inhibitor with a tumor-selective pharmacologic profile competitive with bortezomib. *Blood* (2008) 111:2765–75. doi: 10.1182/blood-2007-07-100651
12. Park JE, Miller Z, Jun Y, Lee W, Kim KB. Next-generation proteasome inhibitors for cancer therapy. *Transl Res* (2018) 198:1–16. doi: 10.1016/j.trsl.2018.03.002
13. Zou Y, Ma D, Wang Y. The PROTAC technology in drug development. *Cell Biochem Funct* (2019) 37:21–30. doi: 10.1002/cbf.3369
14. Neklesa TK, Winkler JD, Crews CM. Targeted protein degradation by PROTACs. *Pharmacol Ther* (2017) 174:138–44. doi: 10.1016/j.pharmthera.2017.02.027
15. Wang D, Ma L, Wang B, Liu J, Wei W. E3 ubiquitin ligases in cancer and implications for therapies. *Cancer Metastasis Rev* (2017) 36:683–702. doi: 10.1007/s10555-017-9703-z
16. Senft D, Qi J, Ronai ZA. Ubiquitin ligases in oncogenic transformation and cancer therapy. *Nat Rev Cancer* (2018) 18:69–88. doi: 10.1038/nrc.2017.105
17. Bhattacharya S, Ghosh MK. Cell death and deubiquitinases: perspectives in cancer. *BioMed Res Int* (2014) 2014:435197. doi: 10.1155/2014/435197
18. Fujita T, Liu W, Doihara H, Date H, Wan Y. Dissection of the APCCdh1-Skp2 cascade in breast cancer. *Clin Cancer Res* (2008) 14:1966–75. doi: 10.1158/1078-0432.CCR-07-1585
19. Wang Z, Liu P, Inuzuka H, Wei W. Roles of F-box proteins in cancer. *Nat Rev Cancer* (2014) 14:233–47. doi: 10.1038/nrc3700
20. Aydin IT, Melamed RD, Adams SJ, Castillo-Martin M, Demir A, Bryk D, et al. FBXW7 mutations in melanoma and a new therapeutic paradigm. *J Natl Cancer Inst* (2014) 106:dju107. doi: 10.1093/jnci/dju107
21. Xu J, Wu W, Wang J, Huang C, Wen W, Zhao F, et al. miR-367 promotes the proliferation and invasion of non-small cell lung cancer via targeting FBXW7. *Oncol Rep* (2017) 37:1052–8. doi: 10.3892/or.2016.5314
22. Gong J, Cui Z, Li L, Ma Q, Wang Q, Gao Y, et al. MicroRNA-25 promotes gastric cancer proliferation, invasion, and migration by directly targeting F-box and WD-40 Domain Protein 7, FBXW7. *Tumour Biol* (2015) 36 (10):7831–40. doi: 10.1007/s13277-015-3510-3
23. Zhang W, Cao L, Sun Z, Xu J, Tang L, Chen W, et al. Skp2 is over-expressed in breast cancer and promotes breast cancer cell proliferation. *Cell Cycle* (2016) 15:1344–51. doi: 10.1080/15384101.2016.1160986
24. King B, Trimarchi T, Reavie L, Xu L, Mullenders J, Ntziachristos P, et al. The ubiquitin ligase FBXW7 modulates leukemia-initiating cell activity by

regulating MYC stability. *Cell* (2013) 153:1552–66. doi: 10.1016/j.cell.2013.05.041
25. Choi SH, Wright JB, Gerber SA, Cole MD. Myc protein is stabilized by suppression of a novel E3 ligase complex in cancer cells. *Genes Dev* (2010) 24:1236–41. doi: 10.1101/gad.1920310
26. Hung WC, Tseng WL, Shiea J, Chang HC. Skp2 overexpression increases the expression of MMP-2 and MMP-9 and invasion of lung cancer cells. *Cancer Lett* (2010) 288:156–61. doi: 10.1016/j.canlet.2009.06.032
27. Adhikary S, Marinoni F, Hock A, Hulleman E, Popov N, Beier R, et al. The ubiquitin ligase HectH9 regulates transcriptional activation by Myc and is essential for tumor cell proliferation. *Cell* (2005) 123:409–21. doi: 10.1016/j.cell.2005.08.016
28. Müerköster S, Arlt A, Sipos B, Witt M, Grossmann M, Klöppel G, et al. Increased expression of the E3-ubiquitin ligase receptor subunit betaTRCP1 relates to constitutive nuclear factor-kappaB activation and chemoresistance in pancreatic carcinoma cells. *Cancer Res* (2005) 65:1316–24. doi: 10.1158/0008-5472.CAN-04-1626
29. Veeriah S, Taylor BS, Meng S, Fang F, Yilmaz E, Vivanco I, et al. Somatic mutations of the Parkinson's disease-associated gene PARK2 in glioblastoma and other human malignancies. *Nat Genet* (2010) 42:77–82. doi: 10.1038/ng.491
30. Poulogiannis G, McIntyre RE, Dimitriadi M, Apps JR, Wilson CH, Ichimura K, et al. PARK2 deletions occur frequently in sporadic colorectal cancer and accelerate adenoma development in Apc mutant mice. *Proc Natl Acad Sci USA* (2010) 107:15145–50. doi: 10.1073/pnas.1009941107
31. Darling S, Fielding AB, Sabat-Pospiech D, Prior IA, Coulson JM. Regulation of the cell cycle and centrosome biology by deubiquitylases. *Biochem Soc Trans* (2017) 45:1125–36. doi: 10.1042/BST2017008
32. Bhattacharya S, Ghosh MK. HAUSP, a novel deubiquitinase for Rb - MDM2 the critical regulator. *FEBS J* (2014) 281(13):3061–78. doi: 10.1111/febs.12843
33. Marine JC. MDM2 and MDMX in cancer and development. *Curr Top Dev Biol* (2011) 94:45–75. doi: 10.1016/B978-0-12-380916-2.00003-6
34. Brooks CL, Li M, Hu M, Shi Y, Gu W. The p53–Mdm2–HAUSP complex is involved in p53 stabilization by HAUSP. *Oncogene* (2007) 26:7262–6. doi: 10.1038/sj.onc.1210531
35. Kim EJ, Kim SH, Jin X, Kim H. KCTD2, an adaptor of Cullin3 E3 ubiquitin ligase, suppresses gliomagenesis by destabilizing c-Myc. *Cell Death Differ* (2017) 24:649–59. doi: 10.1038/cdd.2016.151
36. Paul I, Ahmed SF, Bhowmik A, Deb S, Ghosh MK. The ubiquitin ligase CHIP regulates c-Myc stability and transcriptional activity. *Oncogene* (2013) 32:1284–95. doi: 10.1038/onc.2012.144
37. Li S, Jiang C, Pan J, Wang X, Jin J, Zhao L, et al. Regulation of c-Myc protein stability by proteasome activator REGγ. *Cell Death Differ* (2015) 22:1000–11. doi: 10.1038/cdd.2014.188
38. Popov N, Wanzel M, Madiredjo M, Zhang D, Beijersbergen R, Bernards R, et al. The ubiquitin-specific protease USP28 is required for MYC stability. *Nat Cell Biol* (2007) 9:765–74. doi: 10.1038/ncb1601
39. Hassan M, Watari H, AbuAlmaaty A, Ohba Y, Sakuragi N. Apoptosis and molecular targeting therapy in cancer. *BioMed Res Int* (2014) 2014:150845. doi: 10.1155/2014/150845
40. Hu L, Wang J, Liu Y, Zhang Y, Zhang L, Kong R, et al. A small ribosomal subunit (SSU) processome component, the human U3 protein 14A (hUTP14A) binds p53 and promotes p53 degradation. *J Biol Chem* (2011) 286:3119–28. doi: 10.1074/jbc.M110.157842
41. Wiltshire TD, Lovejoy CA, Wang T, Xia F, O'Connor MJ, Cortez D. Sensitivity to poly(ADP-ribose) polymerase (PARP) inhibition identifies ubiquitin-specific peptidase 11 (USP11) as a regulator of DNA double-strand break repair. *J Biol Chem* (2010) 285:14565–71. doi: 10.1074/jbc.M110.104745
42. da Silva CG, Minussi DC, Ferran C, Bredel M. A20 expressing tumors and anticancer drug resistance. *Adv Exp Med Biol* (2014) 809:65–81. doi: 10.1007/978-1-4939-0398-6_5
43. Chen Z, Barbi J, Bu S, Yang H-Y, Li Z, Gao Y, et al. The ubiquitin ligase Stub1 negatively modulates regulatory T cell suppressive activity by promoting degradation of the transcription factor Foxp3. *Immunity* (2013) 39:272–85. doi: 10.1016/j.immuni.2013.08.006
44. Zhao Y, Guo H, Qiao G, Zucker M, Langdon WY, Zhang J. E3 Ubiquitin Ligase Cbl-b Regulates Thymic-Derived CD4+CD25+ Regulatory T Cell Development by Targeting Foxp3 for Ubiquitination. *J Immunol (Baltimore Md 1950)* (2015) 194:1639–45. doi: 10.4049/jimmunol.1402434
45. Lee JH, Elly C, Park Y, Liu Y-C. E3 Ubiquitin Ligase VHL Regulates Hypoxia-Inducible Factor-1α to Maintain Regulatory T Cell Stability and Suppressive Capacity. *Immunity* (2015) 42:1062–74. doi: 10.1016/j.immuni.2015.05.016
46. Jin H-S, Park Y, Elly C, Liu Y-C. Itch expression by Treg cells controls Th2 inflammatory responses. *J Clin Invest* (2013) 123:4923–34. doi: 10.1172/JCI69355
47. Eletr ZM, Wilkinson KD. An emerging model for BAP1's role in regulating cell cycle progression. *Cell Biochem Biophys* (2011) 60:3–11. doi: 10.1007/s12013-011-9184-6
48. Machida YJ, Machida Y, Vashisht AA, Wohlschlegel JA, Dutta A. The deubiquitinating enzyme BAP1 regulates cell growth via interaction with HCF-1. *J Biol Chem* (2009) 284:34179–88. doi: 10.1074/jbc.M109.046755
49. Bonacci T, Suzuki A, Grant GD, Stanley N, Cook JG, Brown NG, et al. Cezanne/OTUD7B is a cell cycle-regulated deubiquitinase that antagonizes the degradation of APC/C substrates. *EMBOJ* (2018) 37. doi: 10.15252/embj.201798701
50. Arceci A, Bonacci T, Wang X, Stewart K, Damrauer JS, Hoadley KA, et al. FOXM1 Deubiquitination by USP21 Regulates Cell Cycle Progression and Paclitaxel Sensitivity in Basal-like Breast Cancer. *Cell Rep* (2019) 26:3076–86.e3076. doi: 10.1016/j.celrep.2019.02.054
51. Kaistha BP, Krattenmacher A, Fredebohm J, Schmidt H, Behrens D, Widder M, et al. The deubiquitinating enzyme USP5 promotes pancreatic cancer via modulating cell cycle regulators. *Oncotarget* (2017) 8:66215–25. doi: 10.18632/oncotarget.19882
52. Li Y, Luo K, Yin Y, Wu C, Deng M, Li L, et al. USP13 regulates the RAP80-BRCA1 complex dependent DNA damage response. *Nat Commun* (2017) 8:15752. doi: 10.1038/ncomms15752
53. Li XY, Wu HY, Mao XF, Jiang LX, Wang YX. USP5 promotes tumorigenesis and progression of pancreatic cancer by stabilizing FoxM1 protein. *Biochem Biophys Res Commun* (2017) 492:48–54. doi: 10.1016/j.bbrc.2017.08.040
54. Nepal S, Shrestha A, Park PH. Ubiquitin specific protease 2 acts as a key modulator for the regulation of cell cycle by adiponectin and leptin in cancer cells. *Mol Cell Endocrinol* (2015) 412:44–55. doi: 10.1016/j.mce.2015.05.029
55. Liu B, Liu Y, Wang Y, Xie C, Gan M, Han T, et al. CyclinB1 deubiquitination by USP14 regulates cell cycle progression in breast cancer. *Pathol Res Pract* (2019) 215:152592. doi: 10.1016/j.prp.2019.152592
56. Sun X-X, Challagundla KB, Dai M-S. Positive regulation of p53 stability and activity by the deubiquitinating enzyme Otubain 1. *EMBO J* (2012) 31:576–92. doi: 10.1038/emboj.2011.434
57. Stegmeier F, Rape M, Draviam VM, Nalepa G, Sowa ME, Ang XL, et al. Anaphase initiation is regulated by antagonistic ubiquitination and deubiquitination activities. *Nature* (2007) 446:876–81. doi: 10.1038/nature05694
58. Zhang Y, van Deursen J, Galardy PJ. Overexpression of ubiquitin specific protease 44 (USP44) induces chromosomal instability and is frequently observed in human T-cell leukemia. *PloS One* (2011) 6:e23389. doi: 10.1371/journal.pone.0023389
59. Huang X, Summers MK, Pham V, Lill JR, Liu J, Lee G, et al. Deubiquitinase USP37 is activated by CDK2 to antagonize APC(CDH1) and promote S phase entry. *Mol Cell* (2011) 42:511–23. doi: 10.1016/j.molcel.2011.03.027
60. Geng F, Wenzel S, Tansey WP. Ubiquitin and proteasomes in transcription. *Annu Rev Biochem* (2012) 81:177–201. doi: 10.1146/annurev-biochem-052110-120012
61. Sun XX, He X, Yin L, Komada M, Sears RC, Dai MS. The nucleolar ubiquitin-specific protease USP36 deubiquitinates and stabilizes c-Myc. *Proc Natl Acad Sci USA* (2015) 112:3734–9. doi: 10.1073/pnas.1411713112
62. Murali R, Wiesner T, Scolyer RA. Tumours associated with BAP1 mutations. *Pathology* (2013) 45:116–26. doi: 10.1097/PAT.0b013e32835d0efb
63. Wade M, Li YC, Wahl GM. MDM2, MDMX and p53 in oncogenesis and cancer therapy. *Nat Rev Cancer* (2013) 13:83–96. doi: 10.1038/nrc3430
64. Schoenfeld AR, Apgar S, Dolios G, Wang R, Aaronson SA. BRCA2 is ubiquitinated in vivo and interacts with USP11, a deubiquitinating enzyme that exhibits prosurvival function in the cellular response to DNA damage. *Mol Cell Biol* (2004) 24:7444–55. doi: 10.1128/MCB.24.17.7444-7455.2004
65. Liu J, Kruswick A, Dang H, Tran AD, Kwon SM, Wang XW, et al. Ubiquitin-specific protease 21 stabilizes BRCA2 to control DNA repair and tumor growth. *Nat Commun* (2017) 8:137. doi: 10.1038/s41467-017-00206-2

66. Chen J, Chen ZJ. Regulation of NF-κB by ubiquitination. *Curr Opin Immunol* (2013) 25:4–12. doi: 10.1016/j.coi.2012.12.005
67. Pan J, Deng Q, Jiang C, Wang X, Niu T, Li H, et al. USP37 directly deubiquitinates and stabilizes c-Myc in lung cancer. *Oncogene* (2015) 34:3957–67. doi: 10.1038/onc.2014.327
68. Kim D, Hong A, Park HI, Shin WH, Yoo L, Jeon SJ, et al. Deubiquitinating enzyme USP22 positively regulates c-Myc stability and tumorigenic activity in mammalian and breast cancer cells. *J Cell Physiol* (2017) 232:3664–76. doi: 10.1002/jcp.25841
69. Zhang J, Ren P, Xu D, Liu X, Liu Z, Zhang C, et al. Human UTP14a promotes colorectal cancer progression by forming a positive regulation loop with c-Myc. *Cancer Lett* (2019) 440-441:106–15. doi: 10.1016/j.canlet.2018.10.010
70. Ma T, Lu C, Guo Y, Zhang C, Du X. Human U3 protein 14a plays an anti-apoptotic role in cancer cells. *Biol Chem* (2017) 398:1247–57. doi: 10.1515/hsz-2017-0121
71. Kovalenko A, Chable-Bessia C, Cantarella G, Israel A, Wallach D, Courtois G. The tumour suppressor CYLD negatively regulates NF-kappaB signalling by deubiquitination. *Nature* (2003) 424:801–5. doi: 10.1038/nature01802
72. Xia A, Zhang Y, Xu J, Yin T, Lu X-J. T Cell Dysfunction in Cancer Immunity and Immunotherapy. *Front Immunol* (2019) 10:1719. doi: 10.3389/fimmu.2019.01719
73. Abbas T, Keaton MA, Dutta A. Genomic instability in cancer. *Cold Spring Harb Perspect Biol* (2013) 5:a012914. doi: 10.1101/cshperspect.a012914
74. Wu WJ, Hu KS, Wang DS, Zeng ZL, Zhang DS, Chen DL, et al. CDC20 overexpression predicts a poor prognosis for patients with colorectal cancer. *J Transl Med* (2013) 11:142. doi: 10.1186/1479-5876-11-142
75. Korphaisarn K, Morris VK, Overman MJ, Fogelman DR, Kee BK, Raghav KPS, et al. FBXW7 missense mutation: a novel negative prognostic factor in metastatic colorectal adenocarcinoma. *Oncotarget* (2017) 8:39268–79. doi: 10.18632/oncotarget.16848
76. Ougolkov A, Zhang B, Yamashita K, Bilim V, Mai M, Fuchs SY, et al. Associations among beta-TrCP, an E3 ubiquitin ligase receptor, beta-catenin, and NF-kappaB in colorectal cancer. *J Natl Cancer Inst* (2004) 96:1161–70. doi: 10.1093/jnci/djh219
77. Johnson DG, Schneider-Broussard R. Role of E2F in cell cycle control and cancer. *Front Biosci* (1998) 3:d447–8. doi: 10.2741/a291
78. Helin K, Harlow E, Fattaey A. Inhibition of E2F-1 transactivation by direct binding of the retinoblastoma protein. *Mol Cell Biol* (1993) 13:6501–8. doi: 10.1128/mcb.13.10.6501
79. Miwa S, Uchida C, Kitagawa K, Hattori T, Oda T, Sugimura H, et al. Mdm2-mediated pRB downregulation is involved in carcinogenesis in a p53-independent manner. *Biochem Biophys Res Commun* (2006) 340:54–61. doi: 10.1016/j.bbrc.2005.11.148
80. Pan H, Jia R, Zhang L, Xu S, Wu Q, Song X, et al. BAP1 regulates cell cycle progression through E2F1 target genes and mediates transcriptional silencing via H2A monoubiquitination in uveal melanoma cells. *Int J Biochem Cell Biol* (2015) 60:176–84. doi: 10.1016/j.biocel.2015.01.001
81. Dang CV. c-Myc target genes involved in cell growth, apoptosis, and metabolism. *Mol Cell Biol* (1999) 19:1–11. doi: 10.1128/mcb.19.1.1
82. Dang CV. MYC on the path to cancer. *Cell* (2012) 149:22–35. doi: 10.1016/j.cell.2012.03.003
83. Farrell AS, Sears RC. MYC degradation. *Cold Spring Harb Perspect Med* (2014) 4:a014365. doi: 10.1101/cshperspect.a014365
84. Welcker M, Orian A, Jin J, Grim JE, Grim JA, Harper JW, et al. The Fbw7 tumor suppressor regulates glycogen synthase kinase 3 phosphorylation-dependent c-Myc protein degradation. *Proc Natl Acad Sci USA* (2004) 101:9085–90. doi: 10.1073/pnas.0402770101
85. Kim SY, Herbst A, Tworkowski KA, Salghetti SE, Tansey WP. Skp2 regulates Myc protein stability and activity. *Mol Cell* (2003) 11:1177–88. doi: 10.1016/S1097-2765(03)00173-4
86. Yap DB, Hsieh JK, Chan FS, Lu X. mdm2: a bridge over the two tumour suppressors, p53 and Rb. *Oncogene* (1999) 18:7681–9. doi: 10.1038/sj.onc.1202954
87. Kon N, Kobayashi Y, Li M, Brooks CL, Ludwig T, Gu W. Inactivation of HAUSP in vivo modulates p53 function. *Oncogene* (2010) 29:1270–9. doi: 10.1038/onc.2009.427
88. Stevenson LF, Sparks A, Allende-Vega N, Xirodimas DP, LaneDP, Fau - Saville MK, Saville MK. The deubiquitinating enzyme USP2a regulates the p53 pathway by targeting Mdm2. *EMBO J* (2007) 26:976–86. doi: 10.1038/sj.emboj.7601567
89. Yuan J, Luo K, Zhang L, Cheville JC, Lou Z. USP10 regulates p53 localization and stability by deubiquitinating p53. *Cell* (2010) 140:384–96. doi: 10.1016/j.cell.2009.12.032
90. Liu H, Wang J, Liu Y, Hu L, Zhang C, Xing B, et al. Human U3 protein14a is a novel type ubiquitin ligase that binds RB and promotes RB degradation depending on a leucine-rich region. *Biochim Biophys Acta Mol Cell Res* (2018) 1865:1611–20. doi: 10.1016/j.bbamcr.2018.08.016
91. Fujita Y, Tinoco R, Li Y, Senft D, Ronai Z. Ubiquitin Ligases in Cancer Immunotherapy - Balancing Antitumor and Autoimmunity. *Trends Mol Med* (2019) 25:428–43. doi: 10.1016/j.molmed.2019.02.002
92. Meng X, Liu X, Guo X, Jiang S, Chen T, Hu Z, et al. FBXO38 mediates PD-1 ubiquitination and regulates anti-tumour immunity of T cells. *Nature* (2018) 564:130–5. doi: 10.1038/s41586-018-0756-0
93. Nurieva RI, Zheng S, Jin W, Chung Y, Zhang Y, Martinez GJ, et al. The E3 ubiquitin ligase GRAIL regulates T cell tolerance and regulatory T cell function by mediating T cell receptor-CD3 degradation. *Immunity* (2010) 32:670–80. doi: 10.1016/j.immuni.2010.05.002
94. Chiang JY, Jang IK, Hodes R, Gu H. Ablation of Cbl-b provides protection against transplanted and spontaneous tumors. *J Clin Invest* (2007) 117:1029–36. doi: 10.1172/JCI29472
95. Haymaker C, Yang Y, Wang J, Zou Q, Sahoo A, Alekseev A, et al. Absence of Grail promotes CD8 T cell anti-tumour activity. *Nat Commun* (2017) 8:239. doi: 10.1172/JCI29472
96. Zhang L, Yi H, Xia X-P, Zhao Y. Transforming growth factor-beta: an important role in CD4+CD25+ regulatory T cells and immune tolerance. *Autoimmunity* (2006) 39:269–76. doi: 10.1080/08916930600753903
97. Gorelik L, Flavell RA. Transforming growth factor-beta in T-cell biology. *Nat Rev Immunol* (2002) 2:46–53. doi: 10.1038/nri704
98. Thomas DA, Massagué J. TGF-beta directly targets cytotoxic T cell functions during tumor evasion of immune surveillance. *Cancer Cell* (2005) 8:369–80. doi: 10.1016/j.ccr.2005.10.012
99. Li MO, Wan YY, Sanjabi S, Robertson A-KL, Flavell RA. Transforming growth factor-beta regulation of immune responses. *Annu Rev Immunol* (2006) 24:99–146. doi: 10.1146/annurev.immunol.24.021605.090737
100. Massagué J. TGFbeta in Cancer. *Cell* (2008) 134:215–30. doi: 10.1016/j.cell.2008.07.001
101. Kumari N, Jaynes PW, Saei A, Iyengar PV, Richard JLC, Eichhorn PJA. The roles of ubiquitin modifying enzymes in neoplastic disease. *Biochim Biophys Acta Rev Cancer* (2017) 1868:456–83. doi: 10.1016/j.bbcan.2017.09.002
102. Lallemand F, Seo SR, Ferrand N, Pessah M, L'Hoste S, Rawadi G, et al. AIP4 restricts transforming growth factor-beta signaling through a ubiquitination-independent mechanism. *J Biol Chem* (2005) 280:27645–53. doi: 10.1074/jbc.M500188200
103. Seo SR, Lallemand F, Ferrand N, Pessah M, L'Hoste S, Camonis J, et al. The novel E3 ubiquitin ligase Tiul1 associates with TGIF to target Smad2 for degradation. *EMBO J* (2004) 23:3780–92. doi: 10.1038/sj.emboj.7600398
104. Komuro A, Imamura T, Saitoh M, Yoshida Y, Yamori T, Miyazono K, et al. Negative regulation of transforming growth factor-beta (TGF-beta) signaling by WW domain-containing protein 1 (WWP1). *Oncogene* (2004) 23:6914–23. doi: 10.1038/sj.onc.1207885
105. Ebisawa T, Fukuchi M, Murakami G, Chiba T, Tanaka K, Imamura T, et al. Smurf1 interacts with transforming growth factor-beta type I receptor through Smad7 and induces receptor degradation. *J Biol Chem* (2001) 276:12477–80. doi: 10.1074/jbc.C100008200
106. Kuratomi G, Komuro A, Goto K, Shinozaki M, Miyazawa K, Miyazono K, et al. NEDD4-2 (neural precursor cell expressed, developmentally down-regulated 4-2) negatively regulates TGF-beta (transforming growth factor-beta) signalling by inducing ubiquitin-mediated degradation of Smad2 and TGF-beta type I receptor. *Biochem J* (2005) 86:461–70. doi: 10.1042/BJ20040738
107. Kit Leng Lui S, Iyengar PV, Jaynes P, Isa Z, Pang B, Tan TZ. Eichhorn PA-OX: USP26 regulates TGF-β signaling by deubiquitinating and stabilizing SMAD7. *EMBO Rep* (2017) 18:797–808. doi: 10.15252/embr.201643270
108. Lin X, Liang M Fau - Feng XH, Feng XH. Smurf2 is a ubiquitin E3 ligase mediating proteasome-dependent degradation of Smad2 in transforming growth factor-beta signaling. *J Biol Chem* (2000) 275:36818–22. doi: 10.1074/jbc.C000580200

109. Fukuchi M, Imamura T, Chiba T, Ebisawa T, Kawabata M, Tanaka K, et al. Ligand-dependent degradation of Smad3 by a ubiquitin ligase complex of ROC1 and associated proteins. *Mol Biol Cell* (2001) 12:1431–43. doi: 10.1091/mbc.12.5.1431
110. Xin H, Xu X, Li L, Ning H, Rong Y, Shang Y, et al. CHIP controls the sensitivity of transforming growth factor-beta signaling by modulating the basal level of Smad3 through ubiquitin-mediated degradation. *J Biol Chem* (2005) 280:20842–50. doi: 10.1074/jbc.M412275200
111. Morén A, Hellman U, Inada Y, Imamura T, Heldin CH, Moustakas A. Differential ubiquitination defines the functional status of the tumor suppressor Smad4. *J Biol Chem* (2003) 278:33571–82. doi: 10.1074/jbc.M300159200
112. Liang M, Liang YY, Wrighton K, Ungermannova D, Wang XP, Brunicardi FC, et al. Ubiquitination and proteolysis of cancer-derived Smad4 mutants by SCFSkp2. *Mol Cell Biol* (2004) 24:7524–37. doi: 10.1128/MCB.24.17.7524-7537.2004
113. Wan M, Tang Y, Tytler EM, Lu C, Jin B, Vickers SM, et al. Smad4 protein stability is regulated by ubiquitin ligase SCF beta-TrCP1. *J Biol Chem* (2004) 279:14484–7. doi: 10.1074/jbc.C400005200
114. Zhang L, Zhou F, Drabsch Y, Gao R, Snaar-Jagalska BE, Mickanin C, et al. USP4 is regulated by AKT phosphorylation and directly deubiquitylates TGF-β type I receptor. *Nat Cell Biol* (2012) 14:717–26. doi: 10.1038/ncb2522
115. Al-Salihi MA, Herhaus L, Macartney T, Sapkota GP. USP11 augments TGFβ signalling by deubiquitylating ALK5. *Open Biol* (2012) 2:120063. doi: 10.1098/rsob.120063
116. Eichhorn PJ, Rodón L, Gonzàlez-Juncà A, Dirac A, Gili M, Martínez-Sáez E, et al. USP15 stabilizes TGF-β receptor I and promotes oncogenesis through the activation of TGF-β signaling in glioblastoma. *Nat Med* (2012) 18:429–35. doi: 10.1038/nm.2619
117. Briones-Orta MA, Levy L, Madsen CD, Das D, Erker Y, Sahai E, et al. Arkadia regulates tumor metastasis by modulation of the TGF-β pathway. *Cancer Res* (2013) 73:1800–10. doi: 10.1158/0008-5472.CAN-12-1916
118. Herhaus L, Al-Salihi M, Macartney T, Weidlich S, Sapkota GP. OTUB1 enhances TGFβ signalling by inhibiting the ubiquitylation and degradation of active SMAD2/3. *Nat Commun* (2013) 4:2519. doi: 10.1038/ncomms3519
119. Nagano Y, Mavrakis KJ, Lee KL, Fujii T, Koinuma D, Sase H, et al. Arkadia induces degradation of SnoN and c-Ski to enhance transforming growth factor-beta signaling. *J Biol Chem* (2007) 282:20492–501. doi: 10.1074/jbc.M701294200
120. Bonni S, Wang HR, Causing CG, Kavsak P, Stroschein SL, Luo K, et al. TGF-beta induces assembly of a Smad2-Smurf2 ubiquitin ligase complex that targets SnoN for degradation. *Nat Cell Biol* (2001) 3:587–95. doi: 10.1038/35078562
121. Levine AG, Mendoza A, Hemmers S, Moltedo B, Niec RE, Schizas M, et al. Stability and function of regulatory T cells expressing the transcription factor T-bet. *Nature* (2017) 546:421–5. doi: 10.1038/nature22360
122. Pan L, Chen Z, Wang L, Chen C, Li D, Wan H, et al. Deubiquitination and stabilization of T-bet by USP10. *Biochem Biophys Res Commun* (2014) 449:289–94. doi: 10.1016/j.bbrc.2014.05.037
123. Sitaram P, Uyemura B, Malarkannan S, Riese MJ. Beyond the Cell Surface: Targeting Intracellular Negative Regulators to Enhance T cell Anti-Tumor Activity. *Int J Mol Sci* (2019) 20:5821. doi: 10.3390/ijms20235821
124. Jahan AS, Lestra M, Swee LK, Fan Y, Lamers MM, Tafesse FG, et al. Usp12 stabilizes the T-cell receptor complex at the cell surface during signaling. *Proc Natl Acad Sci U S A* (2016) 113:E705–14. doi: 10.1073/pnas.1521763113
125. Naik E, Webster JD, DeVoss J, Liu J, Suriben R, Dixit VM. Regulation of proximal T cell receptor signaling and tolerance induction by deubiquitinase Usp9X. *J Exp Med* (2014) 211:1947–55. doi: 10.1084/jem.20140860
126. Hyer ML, Milhollen MA, Ciavarri J, Fleming P, Traore T, Sappal D, et al. A small-molecule inhibitor of the ubiquitin activating enzyme for cancer treatment. *Nat Med* (2018) 24:186–93. doi: 10.1038/nm.4474
127. Nawrocki ST, Griffin P, Kelly KR, Carew JS. MLN4924: a novel first-in-class inhibitor of NEDD8-activating enzyme for cancer therapy. *Expert Opin Invest Drugs* (2012) 21:1563–73. doi: 10.1517/13543784.2012.707192
128. Barghout SH, Patel PS, Wang X, Xu GW, Kavanagh S, Halgas O, et al. Preclinical evaluation of the selective small-molecule UBA1 inhibitor, TAK-243, in acute myeloid leukemia. *Leukemia* (2019) 33:37–51. doi: 10.1038/s41375-018-0167-0
129. Vu B, Wovkulich P, Pizzolato G, Lovey A, Ding Q, Jiang N, et al. Discovery of RG7112: A Small-Molecule MDM2 Inhibitor in Clinical Development. *ACS Med Chem Lett* (2013) 4:466–9. doi: 10.1021/ml4000657
130. Ceccarelli DF, Tang X, Pelletier B, Orlicky S, Xie W, Plantevin V, et al. An allosteric inhibitor of the human Cdc34 ubiquitin-conjugating enzyme. *Cell* (2011) 145:1075–87. doi: 10.1016/j.cell.2011.05.039
131. Ding Q, Zhang Z, Liu J-J, Jiang N, Zhang J, Ross TM, et al. Discovery of RG7388, a potent and selective p53-MDM2 inhibitor in clinical development. *J Med Chem* (2013) 56:5979–83. doi: 10.1021/jm400487c
132. Wang S, Sun W, Zhao Y, McEachern D, Meaux I, Barrière C, et al. SAR405838: an optimized inhibitor of MDM2-p53 interaction that induces complete and durable tumor regression. *Cancer Res* (2014) 74:5855–65. doi: 10.1158/0008-5472.CAN-14-0799
133. Holzer P, Masuya K, Furet P, Kallen J, Valat-Stachyra T, Ferretti S, et al. Discovery of a Dihydroisoquinolinone Derivative (NVP-CGM097): A Highly Potent and Selective MDM2 Inhibitor Undergoing Phase 1 Clinical Trials in p53wt Tumors. *J Med Chem* (2015) 58:6348–58. doi: 10.1021/acs.jmedchem.5b00810
134. Issaeva N, Bozko P, Enge M, Protopopova M, Verhoef LG, Masucci M, et al. Small molecule RITA binds to p53, blocks p53-HDM-2 interaction and activates p53 function in tumors. *Nat Med* (2004) 10:1321–8. doi: 10.1038/nm1146
135. Bykov VJ, Issaeva N, Shilov A, Hultcrantz M, Pugacheva E, Chumakov P, et al. Restoration of the tumor suppressor function to mutant p53 by a low-molecular-weight compound. *Nat Med* (2002) 8:282–8. doi: 10.1038/nm0302-282
136. Zhang Z, Ding Q, Liu J-J, Zhang J, Jiang N, Chu X-J, et al. Discovery of potent and selective spiroindolinone MDM2 inhibitor, RO8994, for cancer therapy. *Bioorg Med Chem* (2014) 22:4001–9. doi: 10.1016/j.bmc.2014.05.072
137. Wang H, Ma X, Ren S, Buolamwini JK, Yan C. A small-molecule inhibitor of MDMX activates p53 and induces apoptosis. *Mol Cancer Ther* (2011) 10:69–79. doi: 10.4161/cc.9.6.11067
138. Nalepa G, Rolfe M, Harper JW. Drug discovery in the ubiquitin-proteasome system. *Nat Rev Drug Discovery* (2006) 5:596–613. doi: 10.1038/nrd2056
139. Soucy TA, Smith PG, Milhollen MA, Berger AJ, Gavin JM, Adhikari S, et al. An inhibitor of NEDD8-activating enzyme as a new approach to treat cancer. *Nature* (2009) 458:732–6. doi: 10.1038/nature07884
140. Yang Y, Kitagaki J, Dai RM, Tsai YC, Lorick KL, Ludwig RL, et al. Inhibitors of ubiquitin-activating enzyme (E1), a new class of potential cancer therapeutics. *Cancer Res* (2007) 67:9472–81. doi: 10.1158/0008-5472.CAN-07-0568
141. Tsukamoto S, Takeuchi T, Rotinsulu H, Mangindaan RE, van Soest RW, Ukai K, et al. Leucettamol A: a new inhibitor of Ubc13-Uev1A interaction isolated from a marine sponge, Leucetta aff. microrhaphis. *Bioorg Med Chem Lett* (2008) 18:6319–20. doi: 10.1016/j.bmcl.2008.10.110
142. Ushiyama S, Umaoka H, Kato H, Suwa Y, Morioka H, Rotinsulu H, et al. Manadosterols A and B, sulfonated sterol dimers inhibiting the Ubc13-Uev1A interaction, isolated from the marine sponge Lissodendryx fibrosa. *J Nat Prod* (2012) 75:1495–9. doi: 10.1021/np300352u
143. de Jonge M, de Weger VA, Dickson MA, Langenberg M, Le Cesne A, Wagner AJ, et al. A phase I study of SAR405838, a novel human double minute 2 (HDM2) antagonist, in patients with solid tumours. *Eur J Cancer (Oxford Engl 1990)* (2017) 76:144–51. doi: 10.1016/j.ejca.2017.02.005
144. Ravandi F, Gojo I, Patnaik MM, Minden MD, Kantarjian H, Johnson-Levonas AO, et al. A phase I trial of the human double minute 2 inhibitor (MK-8242) in patients with refractory/recurrent acute myelogenous leukemia (AML). *Leuk Res* (2016) 48:92–100. doi: 10.1016/j.leukres.2016.07.004
145. Wagner AJ, Banerji U, Mahipal A, Somaxiah N, Hirsch H, Fancourt C, et al. Phase I Trial of the Human Double Minute 2 Inhibitor MK-8242 in Patients With Advanced Solid Tumors. *J Clin Oncol* (2017) 35:1304–11. doi: 10.1200/JCO.2016.70.7117
146. Seipel K, Marques MAT, Sidler C, Mueller BU, Pabst T. MDM2- and FLT3-inhibitors in the treatment of -ITD acute myeloid leukemia, specificity and efficacy of NVP-HDM201 and midostaurin. *Haematologica* (2018) 103:1862–72. doi: 10.3324/haematol.2018.191650
147. Sun D, Li Z, Rew Y, Gribble M, Bartberger MD, Beck HP, et al. Discovery of AMG 232, a potent, selective, and orally bioavailable MDM2-p53 inhibitor in clinical development. *J Med Chem* (2014) 57:1454–72. doi: 10.1021/jm401753e
148. Kitagaki J, Agama KK, Pommier Y, Yang Y, Weissman AM. Targeting tumor cells expressing p53 with a water-soluble inhibitor of Hdm2. *Mol Cancer Ther* (2008) 7:2445–54. doi: 10.1158/1535-7163.MCT-08-0063
149. Yang Y, Ludwig RL, Jensen JP, Pierre SA, Medaglia MV, Davydov IV, et al. : Small molecule inhibitors of HDM2 ubiquitin ligase activity stabilize and activate p53 in cells. *Cancer Cell* (2005) 7:547–59. doi: 10.1016/j.ccr.2005.04.029

150. Herman AG, Hayano M, Poyurovsky MV, Shimada K, Skouta R, Prives C, et al. Discovery of Mdm2-MdmX E3 ligase inhibitors using a cell-based ubiquitination assay. *Cancer Discovery* (2011) 1:312–25. doi: 10.1158/2159-8290.CD-11-0104
151. Joseph TL, Madhumalar A, Brown CJ, Lane DP, Verma CS. Differential binding of p53 and nutlin to MDM2 and MDMX: computational studies. *Cell Cycle* (2010) 9:1167–81. doi: 10.4161/cc.9.6.11067
152. Chang YS, Graves B, Guerlavais V, Tovar C, Packman K, To KH, et al. Stapled alpha-helical peptide drug development: a potent dual inhibitor of MDM2 and MDMX for p53-dependent cancer therapy. *Proc Natl Acad Sci USA* (2013) 110:E3445–3454. doi: 10.1073/pnas.1303002110
153. Carvajal LA, Neriah DB, Senecal A, Benard L, Thiruthuvanathan V, Yatsenko T, et al. Dual inhibition of MDMX and MDM2 as a therapeutic strategy in leukemia. *Sci Trans Med* (2018) 10:eaao3003. doi: 10.1126/scitranslmed.aao3003
154. Nakayama KI, Nakayama K. Ubiquitin ligases: cell-cycle control and cancer. *Nat Rev Cancer* (2006) 6:369–81. doi: 10.1038/nrc1881
155. Huang HL, Weng HY, Wang LQ, Yu CH, Huang QJ, Zhao PP, et al. Triggering Fbw7-mediated proteasomal degradation of c-Myc by oridonin induces cell growth inhibition and apoptosis. *Mol Cancer Ther* (2012) 11:1155–65. doi: 10.1158/1535-7163.MCT-12-0066
156. Chan CH, Morrow JK, Li CF, Gao Y, Jin G, Moten A, et al. Pharmacological inactivation of Skp2 SCF ubiquitin ligase restricts cancer stem cell traits and cancer progression. *Cell* (2013) 154:556–68. doi: 10.1016/j.cell.2013.06.048
157. Chen Q, Xie W, Kuhn DJ, Voorhees PM, Lopez-Girona A, Mendy D, et al. Targeting the p27 E3 ligase SCF(Skp2) results in p27- and Skp2-mediated cell-cycle arrest and activation of autophagy. *Blood* (2008) 111:4690–9. doi: 10.1182/blood-2007-09-112904
158. Blees JS, Bokesch HR, Rübsamen D, Schulz K, Milke L, Bajer MM, et al. Erioflorin stabilizes the tumor suppressor Pdcd4 by inhibiting its interaction with the E3-ligase β-TrCP1. *PloS One* (2012) 7:e46567. doi: 10.1371/journal.pone.0046567
159. Nakajima H, Fujiwara H, Furuichi Y, Tanaka K, Shimbara N. A novel small-molecule inhibitor of NF-kappaB signaling. *Biochem Biophys Res Commun* (2008) 368:1007–13. doi: 10.1016/j.bbrc.2008.01.166
160. Zeng X, Sigoillot F, Gaur S, Choi S, Pfaff KL, Oh DC, et al. Pharmacologic inhibition of the anaphase-promoting complex induces a spindle checkpoint-dependent mitotic arrest in the absence of spindle damage. *Cancer Cell* (2010) 18:382–95. doi: 10.1016/j.ccr.2010.08.010
161. Sackton KL, Dimova N, Zeng X, Tian W, Zhang M, Sackton TB, et al. Synergistic blockade of mitotic exit by two chemical inhibitors of the APC/C. *Nature* (2014) 514:646–9. doi: 10.1038/nature13660
162. Triozzi PK,M, Alistar A, Bitting R, Neal A, Lametschwandtner G, Loibner H. : Phase I clinical trial of adoptive cellular immunotherapy with APN401 in patients with solid tumors. *J Immunother Cancer* (2015) 3:175. doi: 10.1186/2051-1426-3-S2-P175
163. Riling CS,III., Cunnion B, Todd E, Mattern M, Wu J, Kambayashi T, et al. Small-molecule Cbl-b inhibitors as novel intracellular checkpoint inhibitors for cancer immunotherapy. *Mol Targets Cancer Ther* (2018) 17:A206. doi: 10.1158/1535-7163.TARG-17-A206
164. Rossi M RB, Ansell K, Amelio I, Caraglia M, Misso G, Bernassola F, et al. High throughput screening for inhibitors of the HECT ubiquitin E3 ligase ITCH identifies antidepressant drugs as regulators of autophagy. *Cell Death Dis* (2014) 5:e1203. doi: 10.1038/cddis.2014.113
165. Adams J. The proteasome: a suitable antineoplastic target. *Nat Rev Cancer* (2004) 4:349–60. doi: 10.1038/nrc1361
166. Richardson PG, Hideshima T, Anderson KC. Bortezomib (PS-341): a novel, first-in-class proteasome inhibitor for the treatment of multiple myeloma and other cancers. *Cancer Control* (2003) 10:361–9. doi: 10.1177/107327480301000502
167. Kouroukis TC, Baldassarre FG, Haynes AE, Imrie K, Reece DE, Cheung MC. Bortezomib in multiple myeloma: systematic review and clinical considerations. *Curr Oncol* (2014) 21:e573–603. doi: 10.3747/co.21.1798
168. Chen D, Frezza M, Schmitt S, Kanwar J, Dou QP. Bortezomib as the first proteasome inhibitor anticancer drug: current status and future perspectives. *Curr Cancer Drug Targ* (2011) 11:239–53. doi: 10.2174/156800911794519752
169. Frankland-Searby S, Bhaumik SR. The 26S proteasome complex: an attractive target for cancer therapy. *Biochim Biophys Acta* (2012) 1825:64–76. doi: 10.1016/j.bbcan.2011.10.003
170. Bonvini P, Zorzi E, Basso G, Rosolen A. Bortezomib-mediated 26S proteasome inhibition causes cell-cycle arrest and induces apoptosis in CD-30+ anaplastic large cell lymphoma. *Leukemia* (2007) 21:838–42. doi: 10.1038/sj.leu.2404528
171. Richardson PG, Briemberg H, Jagannath S, Wen PY, Barlogie B, Berenson J, et al. Frequency, characteristics, and reversibility of peripheral neuropathy during treatment of advanced multiple myeloma with bortezomib. *J Clin Oncol* (2006) 24:3113–20. doi: 10.1200/JCO.2005.04.7779
172. Gelman JS, Sironi J, Berezniuk I, Dasgupta S, Castro LM, Gozzo FC, et al. Alterations of the intracellular peptidome in response to the proteasome inhibitor bortezomib. *PloS One* (2013) 8:e53263. doi: 10.1371/journal.pone.0053263
173. Richardson PG, Barlogie B, Berenson J, Singhal S, Jagannath S, Irwin D, et al. A phase 2 study of bortezomib in relapsed, refractory myeloma. *N Engl J Med* (2003) 348:2609–17. doi: 10.1056/NEJMoa030288
174. Suzuki E, Demo S, Deu E, Keats J, Arastu-Kapur S, Bergsagel PL, et al. Molecular mechanisms of bortezomib resistant adenocarcinoma cells. *PloS One* (2011) 6:e27996. doi: 10.1371/journal.pone.0027996
175. Chauhan D, Singh AV, Aujay M, Kirk CJ, Bandi M, Ciccarelli B, et al. A novel orally active proteasome inhibitor ONX 0912 triggers in vitro and in vivo cytotoxicity in multiple myeloma. *Blood* (2010) 116:4906–15. doi: 10.1182/blood-2010-04-276626
176. Vogl DT, Martin TG, Vij R, Hari P, Mikhael JR, Siegel D, et al. Phase I/II study of the novel proteasome inhibitor delanzomib (CEP-18770) for relapsed and refractory multiple myeloma. *Leukemia Lymphoma* (2017) 58:1872–9. doi: 10.1080/10428194.2016.1263842
177. Potts BC, Albitar MX, Anderson KC, Baritaki S, Berkers C, Bonavida B, et al. Marizomib, a proteasome inhibitor for all seasons: preclinical profile and a framework for clinical trials. *Curr Cancer Drug Targ* (2011) 11:254–84. doi: 10.2174/156800911794519716
178. Spencer A, Harrison S, Zonder J, Badros A, Laubach J, Bergin K, et al. A phase 1 clinical trial evaluating marizomib, pomalidomide and low-dose dexamethasone in relapsed and refractory multiple myeloma (NPI-0052-107): final study results. *Br J Haematol* (2018) 180:41–51. doi: 10.1111/bjh.14987
179. Di K, Lloyd GK, Abraham V, MacLaren A, Burrows FJ, Desjardins A, et al. Marizomib activity as a single agent in malignant gliomas: ability to cross the blood-brain barrier. *Neuro-oncology* (2016) 18:840–8. doi: 10.1093/neuonc/nov299
180. Fang Y, Fu D, Shen XZ. The potential role of ubiquitin c-terminal hydrolases in oncogenesis. *Biochim Biophys Acta* (2010) 1806:1–6. doi: 10.1016/j.bbcan.2010.03.001
181. Liu J, Shaik S, Dai X, Wu Q, Zhou X, Wang Z, et al. Targeting the ubiquitin pathway for cancer treatment. *Biochim Biophys Acta* (2015) 1855:50–60. doi: 10.1016/j.bbcan.2014.11.005
182. Kapuria V, Peterson LF, Fang D, Bornmann WG, Talpaz M, Donato NJ. Deubiquitinase inhibition by small-molecule WP1130 triggers aggresome formation and tumor cell apoptosis. *Cancer Res* (2010) 70:9265–76. doi: 10.1158/0008-5472.CAN-10-1530
183. Wang S, Kollipara RK, Srivastava N, Li R, Ravindranathan P, Hernandez E, et al. Ablation of the oncogenic transcription factor ERG by deubiquitinase inhibition in prostate cancer. *Proc Natl Acad Sci U S A* (2014) 111:4251–6. doi: 10.1073/pnas.1322198111
184. Colland F, Formstecher E, Jacq X, Reverdy C, Planquette C, Conrath S, et al. Small-molecule inhibitor of USP7/HAUSP ubiquitin protease stabilizes and activates p53 in cells. *Mol Cancer Ther* (2009) 8:2286–95. doi: 10.1158/1535-7163.MCT-09-0097
185. Chauhan D, Tian Z, Nicholson B, Kumar KG, Zhou B, Carrasco R, et al. A small molecule inhibitor of ubiquitin-specific protease-7 induces apoptosis in multiple myeloma cells and overcomes bortezomib resistance. *Cancer Cell* (2012) 22:345–58. doi: 10.1016/j.ccr.2012.08.007
186. Weinstock J, Wu J, Cao P, Kingsbury WD, McDermott JL, Kodrasov MP, et al. Selective Dual Inhibitors of the Cancer-Related Deubiquitylating Proteases USP7 and USP47. *ACS Med Chem Lett* (2012) 3:789–92. doi: 10.1021/ml200276j
187. Lee BH, Lee MJ, Park S, Oh DC, Elsasser S, Chen PC, et al. Enhancement of proteasome activity by a small-molecule inhibitor of USP14. *Nature* (2010) 467:179–84. doi: 10.1038/nature09299
188. Lee BH, Finley D, King RW. A High-Throughput Screening Method for Identification of Inhibitors of the Deubiquitinating Enzyme USP14. *Curr Protoc Chem Biol* (2012) 4:311–30. doi: 10.1002/9780470559277.ch120078

189. Tian Z, D'Arcy P, Wang X, Ray A, Tai YT, Hu Y, et al. A novel small molecule inhibitor of deubiquitylating enzyme USP14 and UCHL5 induces apoptosis in multiple myeloma and overcomes bortezomib resistance. *Blood* (2014) 123:706–16. doi: 10.1182/blood-2013-05-500033
190. Lai AC, Crews CM. Induced protein degradation: an emerging drug discovery paradigm. *Nat Rev Drug Discovery* (2017) 16:101–14. doi: 10.1038/nrd.2016.211
191. Sakamoto KM, Kim KB, Kumagai A, Mercurio F, Crews CM, Deshaies RJ. Protacs: chimeric molecules that target proteins to the Skp1-Cullin-F box complex for ubiquitination and degradation. *Proc Natl Acad Sci USA* (2001) 98:8554–9. doi: 10.1073/pnas.141230798
192. Abruzzese MP, Bilotta MT, Fionda C, Zingoni A, Soriani A, Vulpis E, et al. Inhibition of bromodomain and extra-terminal (BET) proteins increases NKG2D ligand MICA expression and sensitivity to NK cell-mediated cytotoxicity in multiple myeloma cells: role of cMYC-IRF4-miR-125b interplay. *J Hematol Oncol* (2016) 9:134. doi: 10.1186/s13045-016-0362-2
193. Zengerle M, Chan KH, Ciulli A. Selective Small Molecule Induced Degradation of the BET Bromodomain Protein BRD4. *ACS Chem Biol* (2015) 10:1770–7. doi: 10.1021/acschembio.5b00216
194. DeMars KM, Yang C, Castro-Rivera CI, Candelario-Jalil E. Selective degradation of BET proteins with dBET1, a proteolysis-targeting chimera, potently reduces pro-inflammatory responses in lipopolysaccharide-activated microglia. *Biochem Biophys Res Commun* (2018) 497:410–5. doi: 10.1016/j.bbrc.2018.02.096
195. Lu J, Qian Y, Altieri M, Dong H, Wang J, Raina K, et al. Hijacking the E3 Ubiquitin Ligase Cereblon to Efficiently Target BRD4. *Chem Biol* (2015) 22:755–63. doi: 10.1016/j.chembiol.2015.05.009
196. Raina K, Lu J, Qian Y, Altieri M, Gordon D, Rossi AM, et al. PROTAC-induced BET protein degradation as a therapy for castration-resistant prostate cancer. *Proc Natl Acad Sci USA* (2016) 113:7124–9. doi: 10.1073/pnas.1521738113
197. Sun B, Fiskus W, Qian Y, Rajapakshe K, Raina K, Coleman KG, et al. BET protein proteolysis targeting chimera (PROTAC) exerts potent lethal activity against mantle cell lymphoma cells. *Leukemia* (2018) 32:343–52. doi: 10.1038/leu.2017.207
198. Qin C, Hu Y, Zhou B, Fernandez-Salas E, Yang CY, Liu L, et al. Discovery of QCA570 as an Exceptionally Potent and Efficacious Proteolysis Targeting Chimera (PROTAC) Degrader of the Bromodomain and Extra-Terminal (BET) Proteins Capable of Inducing Complete and Durable Tumor Regression. *J Med Chem* (2018) 61:6685–704. doi: 10.1021/acs.jmedchem.8b00506
199. Zhang X, Lee HC, Shirazi F, Baladandayuthapani V, Lin H, Kuiatse I, et al. Protein targeting chimeric molecules specific for bromodomain and extra-terminal motif family proteins are active against pre-clinical models of multiple myeloma. *Leukemia* (2018) 32:2224–39. doi: 10.1038/s41375-018-0044-x
200. Testa A, Lucas X, Castro GV, Chan KH, Wright JE, Runcie AC, et al. 3-Fluoro-4-hydroxyprolines: Synthesis, Conformational Analysis, and Stereoselective Recognition by the VHL E3 Ubiquitin Ligase for Targeted Protein Degradation. *J Am Chem Soc* (2018) 140:9299–313. doi: 10.1021/jacs.8b05807
201. Gechijian LN, Buckley DL, Lawlor MA, Reyes JM, Paulk J, Ott CJ, et al. Functional TRIM24 degrader via conjugation of ineffectual bromodomain and VHL ligands. *Nat Chem Biol* (2018) 14:405–12. doi: 10.1038/s41589-018-0010-y
202. Wang X, Feng S, Fan J, Li X, Wen Q, Luo N. New strategy for renal fibrosis: Targeting Smad3 proteins for ubiquitination and degradation. *Biochem Pharmacol* (2016) 116:200–9. doi: 10.1016/j.bcp.2016.07.017
203. Krönke J, Fink EC, Hollenbach PW, MacBeth KJ, Hurst SN, Udeshi ND, et al. Lenalidomide induces ubiquitination and degradation of CK1α in del (5q) MDS. *Nature* (2015) 523:183–8. doi: 10.1038/nature14610
204. Krönke J, Udeshi ND, Narla A, Grauman P, Hurst SN, McConkey M, et al. Lenalidomide causes selective degradation of IKZF1 and IKZF3 in multiple myeloma cells. *Sci (N Y NY)* (2014) 343:301–5. doi: 10.1126/science.1244851

Conflict of Interest: The authors declare that the research was conducted in the absence of any commercial or financial relationships that could be construed as a potential conflict of interest.

frontiers in Oncology

ORIGINAL RESEARCH
published: 25 February 2021
doi: 10.3389/fonc.2021.629327

Identification and Validation of Ubiquitin-Specific Proteases as a Novel Prognostic Signature for Hepatocellular Carcinoma

Wenkai Ni[1,2†], Saiyan Bian[1,3†], Mengqi Zhu[3†], Qianqian Song[4], Jianping Zhang[3], Mingbing Xiao[3] and Wenjie Zheng[3*]*

[1] Department of Gastroenterology, Affiliated Hospital of Nantong University, Nantong, China, [2] Endoscopy Center and Endoscopy Research Institute, Zhongshan Hospital, Fudan University, Shanghai, China, [3] Research Center of Clinical Medicine, Affiliated Hospital of Nantong University, Nantong, China, [4] Department of Radiology, Wake Forest School of Medicine, One Medical Center Boulevard, Winston-Salem, NC, United States

OPEN ACCESS

Edited by:
Jean Borges Bertoldo, Martin Luther University of Halle-Wittenberg, Germany

Reviewed by:
Rozangela Curi Pedrosa, Federal University of Santa Catarina, Brazil
Pirjo Spuul, Tallinn University of Technology, Estonia

***Correspondence:**
Wenjie Zheng
zwj007008009@163.com
Mingbing Xiao
xmb73@163.com

[†]These authors have contributed equally to this work

Specialty section:
This article was submitted to Cancer Molecular Targets and Therapeutics, a section of the journal Frontiers in Oncology

Received: *14 November 2020*
Accepted: *18 January 2021*
Published: *25 February 2021*

Citation:
Ni W, Bian S, Zhu M, Song Q, Zhang J, Xiao M and Zheng W (2021) Identification and Validation of Ubiquitin-Specific Proteases as a Novel Prognostic Signature for Hepatocellular Carcinoma. Front. Oncol. 11:629327. doi: 10.3389/fonc.2021.629327

Purpose: Ubiquitin-specific proteases (USPs), as a sub-family of deubiquitinating enzymes (DUBs), are responsible for the elimination of ubiquitin-triggered modification. USPs are recently correlated with various malignancies. However, the expression features and clinical significance of USPs have not been systematically investigated in hepatocellular carcinoma (HCC).

Methods: Genomic alterations and expression profiles of USPs were investigated in CbioPortal and The Cancer Genome Atlas (TCGA) Liver hepatocellular carcinoma (LIHC) dataset. Cox regression and least absolute shrinkage and selection operator (LASSO) analyses were conducted to establish a risk signature for HCC prognosis in TCGA LIHC cohort. Subsequently, Kaplan-Meier analysis, receiver operating characteristic (ROC) curves and univariate/multivariate analyses were performed to evaluate the prognostic significance of the risk signature in TCGA LIHC and international cancer genome consortium (ICGC) cohorts. Furthermore, we explored the alterations of the signature genes during hepatocarcinogenesis and HCC progression in GSE89377. In addition, the expression feature of USP39 was further explored in HCC tissues by performing western blotting and immunohistochemistry.

Results: Genomic alterations and overexpression of USPs were observed in HCC tissues. The consensus analysis indicated that the USPs-overexpressed sub-Cluster was correlated with aggressive characteristics and poor prognosis. Cox regression with LASSO algorithm identified a risk signature formed by eight USPs for HCC prognosis. High-risk group stratified by the signature score was correlated with advanced tumor stage and poor survival HCC patients in TCGA LIHC cohort. In addition, the 8-USPs based signature could also robustly predict overall survival of HCC patients in ICGC(LIRI-JP) cohort. Furthermore, gene sets enrichment analysis (GSEA) showed that the high-risk score was associated with tumor-related pathways. According to the observation in GSE89377, USP39 expression was dynamically increased with hepatocarcinogenesis

and HCC progression. The overexpression of USP39 was further determined in a local HCC cohort and correlated with poor prognosis. The co-concurrence analysis suggested that USP39 might promote HCC by regulating cell-cycle- and proliferation- related genes.

Conclusion: The current study provided a USPs-based signature, highlighting its robust prognostic significance and targeted value for HCC treatment.

Keywords: ubiquitin-specific proteases, hepatocellular carcinoma, prognosis, risk signature, molecular target

INTRODUCTION

Hepatocellular carcinoma is one of the most common malignancies worldwide with significant clinical, economic, and psychological burdens (1). Liver resection, ablation, and liver transplantation are potentially curative strategies for HCC patients at early stage, while a major proportion of HCC patients are diagnosed with intermediate and advanced stages with limited approaches (2). Currently, systemic therapy remains essential for advanced-stage HCC, including targeted agents and immune checkpoint inhibitors (3). However, HCC patients are generally inclined to poor prognosis with recurrence and chemoresistance. With the advancements in multi-omics profiling, recent studies have provided prognostic candidates for potential application of clinic. For the current status, it is of great significant to identifying robust molecular biomarkers to predict HCC patients' outcome.

Ubiquitination (Ub) is one of the most common post-translational protein modifications that has been implicated in multiple biological processes, including embryonic development, cell cycle, and even oncogenesis (4). The dominant forms of Ub are recognized as mono-ubiquitination and Lys48/Lys63-linked polyubiquitination (5). The Ub processes are commonly mediated by E1-ubiquitin-activating enzymes, E2-ubiquitin-binding enzymes, E3-ubiquitin ligases, and deubiquitinating enzymes (DUBs) (6). DUBs, as proteolytic enzymes, are responsible for the elimination of ubiquitin-triggered modification, which could be further classified into eight sub-families such as ubiquitin-specific proteases (USPs), ubiquitin COOH terminal hydrolases (UCHs), Machado-Josephine domain-containing proteases (MJDs), ovarian tumor-associated proteases (OTUs), zinc finger–containing ubiquitin peptidases (ZUFSPs), and motif interacting with ubiquitin-containing novel DUB family (MINDY), Jab1/MPN domain-associated metallopeptidase (JAMM) domain proteins, and monocyte chemotactic protein-induced protein (MCPIP) (7). Of them, through deubiquitinating a wide range of substrates, USPs family members are involved in various physiological and pathological processes. Our previous study has suggested USP7 as a drug-able target that promoted chemoresistance of HCC (8). Recently, increasing studies indicate that USPs are implicated in the progression of HCC. USP22 could facilitate the hypoxia-induced stemness of HCC cells by regulating HIF1α/P53 signaling (9). USP5 enhanced epithelial-mesenchymal transition (EMT)-induced metastasis by stabilizing SLUG (10). Moreover, USP21 could promote the malignant transformation of the normal human hepatocytes and increased the tumorigenicity of the HCC cells by activating the ERK signaling through the stabilization of MEK2 (11). In contrast, USPs may also act as tumor suppressors in HCC progression. USP10 was reported to inhibit tumor growth and inactivate mTORC1/AKT signaling by stabilizing AMPKα and PTEN in HCC cells (12). Besides of regulating malignant behaviors, USPs were also considered as prognostic markers. Previous studies suggested that USP4, USP7, USP11, and USP33 were correlated with poor survival of HCC patients (13–16).

However, none integrated analysis of USPs has been performed for HCC till now. The current study systematically investigated the expression features and clinical significance of USP family members in HCC. Additionally, we established a USP family-based prognostic model from TCGA datasets and further validated it in ICGC (LIRI-JP) cohort. Considering the specific role of the USP family in HCC, we further explored the relationship between the signature genes and the landscape of HCC progression in GSE89377. Moreover, the expression features and clinical implications of USP39 were explored in a local HCC cohort.

METHODS AND MATERIALS

Patients Information

HCC and adjacent tissues were obtained from 16 HCC patients who received hepatectomy at Affiliated Hospital of Nantong University (Nantong, Jiangsu, China) in 2018, which were frozen for western blotting. Liver specimens were collected from 106 patients with HCC underwent surgery at Affiliated Hospital of Nantong University between March 2012 and June 2017. Clinical information was recorded in detail, including each patient' clinical parameters and post-surgery follow-up. All sections were pre-checked histologically. Written informed consent was obtained from each patient. This study was approved by the Ethics Committee of Affiliated Hospital of Nantong University.

Data Acquisition and Preprocessing

The expression profiles of the 57 USPs in 374 HCC patients with clinical information was downloaded from TCGA LIHC datasets (https://cancergenome.nih.gov/) through the R package "TCGA-Assembler". Heatmap was performed to visualize the expression levels of the USPs in HCC and normal tissues in TCGA LIHC cohort. The RNA-seq data of 232 HCC cases was also extracted from ICGC cohort (https://dcc.icgc.org/projects/LIRI-JP). The

clinical parameters of the TCGA and ICGC cohort were shown in **Table 1**. The mRNA profiles of USPs in HCC-related stratified groups were extracted from GSE89377 and multiple GSE datasets.

PPI Network Construction, Correlation Analysis, and Consensus Clustering Analysis

An interaction network of 57 USPs was recapitulated by STRING (http://string-db.org). NetworkAnalyst (networkanalyst.ca) was used to predict the liver-specific protein-protein interaction (PPI) of the USPs. In addition, the Pearson correlation analysis was performed to calculate the associations among the 57 USPs. The LIHC cohort was stratified into sub-groups by consensus expression of USPs with "ConsensusClusterPlus" R package. Principal component analysis (PCA) was carried out with the "prcomp" function of the "stats" R package.

TABLE 1 | The clinical characteristic information of the HCC patients in TCGA and ICGC.

Characteristics	TCGA(%)	ICGC (%)
Number of Patients	374	232
Age		
<60	177 *(47.32)*	64*(27.59)*
≥60	196*(52.41)*	168*(72.41)*
NA	1*(0.27)*	NA
Gender		
Male	253*(67.65)*	171 *(73.71)*
Female	121*(32.35)*	61 *(26.29)*
Survival status		
Alive	238*(63.64)*	189*(81.47)*
Dead	130*(34.76)*	43 *(18.53)*
NA	6*(1.60)*	NA
Stage		
I	173*(46.26)*	36*(15.52)*
II	87*(23.26)*	106*(45.69)*
III	85*(22.73)*	71*(30.60)*
IV	5*(1.34)*	19*(8.19)*
NA	24*(6.42)*	NA
Histological grade		
G1	55*(14.71)*	NA
G2	178*(47.59)*	NA
G3	124*(33.16)*	NA
G4	12*(3.21)*	NA
NA	5*(1.34)*	NA
T classification		
T1	183*(48.93)*	NA
T2	95*(25.40)*	NA
T3	80*(21.39)*	NA
T4	13*(3.48)*	NA
NA	3*(0.80)*	NA
N classification		
N0	254*(67.91)*	NA
N1	4*(1.07)*	NA
NX	115*(30.75)*	NA
NA	1*(0.27)*	NA
M classification		
M0	268*(71.66)*	NA
M1	4*(1.07)*	NA
MX	102*(27.27)*	NA

NA, not available.

Construction of Prognostic Signature

The correlation of USPs with clinical outcome of HCC patients was evaluated by Univariate Cox regression test. USPs with $P<0.05$ were further enrolled into Univariate Cox regression test by using the least absolute shrinkage and selection operator (LASSO) algorithm with the "glmnet" R package. An 8-gene prognostic signature was screened based on the minimum criteria. The risk score of each patient was calculated according to the normalized expression level of each gene and its coefficients. The formula was listed as follows: The coefficient ($gene_i$) was derived from the Cox proportional hazards regression analysis. The TCGA LIHC cohort was divided into two sub-groups based on the median value of the risk score. t-SNE were performed to explore the distribution of different risk groups by using the "Rtsne" R package. In addition, to explore the potential function, gene ontology (GO) was performed based on the differential gene profiles of the two groups ($|\log_2 FC| \geq 1$, FDR <0.05).

Evaluating the Prognostic Value of the Gene Signature

The correlation of risk score with clinicopathological features (age, gender, grade, stage, T, N, and M status) was evaluated by Chi-square test and visualized with heatmap. Kaplan-Meier analysis with log-rank test was conducted to compare the difference of overall survival between patients at high- or low-risk group. Stratified analysis was performed to evaluate the prognostic significance of the risk score in cases at different stages and grades. Receiver operating characteristic (ROC) curve was conducted to assess the predictive performance of the signature model. Univariate and Multivariate Cox regression analyses were performed to define the risk score as an independent prognosis predictor for HCC patients in the TCGA cohort. To validate the prognostic value of the USPs-based signature, the Kaplan-Meier analysis, ROC analysis, Univariate and Multivariate Cox regression analyses were also performed in ICGC cohort.

Gene Sets Enrichment Analysis

To identify enriched pathways associated with the signature, gene set enrichment analysis (GSEA) was performed on the high-risk sub-groups of the TCGA and ICGC cohorts, respectively. The analysis was based on GSEA v.3.0. Molecular Signatures Database v.7.0. Gene sets with P value < 0.05 and FDR < 25% were considered significantly enriched.

Expression Profiles and Functional Prediction for USP39

The mRNA profiles of USP39 in Pan-cancers and the correlation of USP39 with proliferation and cell cycle-related genes was analyzed by TIMER database (cistrome.shinyapps.io/timer). The significantly correlated genes with USP39 in TCGA LIHC dataset and corresponding GSEA were analyzed by LinkedOmics (www.linkedomics.org). The mRNA profiles of USP39 in HCC cases at different stages and grades were obtained from Ualcan (ualcan.path.uab.edu).

Immunohistochemistry (IHC) and Evaluation

The sections of HCC tissues were deparaffinized in xylene, dehydrated in gradient concentrations of ethanol. After incubated in sodium citrate buffer for antigen retrieval, the slides were blocked in BSA for 1 h at room temperature. Then the samples were sequentially incubated with the indicated primary antibody (USP39, 1:200, Santa Cruz, USA) and secondary antibody. At last, the sections were visualized by 3,3′-diaminobenzidine (DAB, Kem-En-Tec Diagnostics, Denmark). Staining of USP39 was independently scored by two pathologists. The statistical analysis of the IHC results were performed as previously described (17). The IHC score was calculated by combining staining intensity and positive percentages. The positive percentages were scored as follows: 0 (0%); 1(1–10%), 2 (11–50%), 3 (51–80%), and 4 (≥81%). The staining intensity was scored as 0 (negative), 1 (weak), 2 (moderate), and 3 (strong). The final score was calculated by multiplying the percentage score with the intensity score. Score of 4-12 was considered high expression of USP39, while score less than 4 was defined as low expression.

Western Blotting

The total protein of each sample was extracted by using radioimmunoprecipitation assay buffer (RIPA) and separated by a sodium dodecyl sulfate (SDS) gel. Following transferred onto polyvinylidene difluoride (PVDF) membranes, the samples were subsequently blocked in 5% BSA for 2 h and incubated in primary antibody (USP39, Santa, USA; GAPDH, Abcam, USA) at a concentration of 1:1,000 overnight. Then the membranes were rinsed in TBST for three times, followed by exposing to horseradish peroxidase (HPR) -conjugated secondary antibodies (Abcam, USA) for 2 h at room temperature. Ultimately, the intensity of the membranes was detected by using the enhanced chemiluminescence (ECL) kit (Millipore, USA).

Statistical Analyses

The statistics in this study were performed by using R software (Version 3.5), GraphPad Prism software (Version 7.0), and SPSS (Version 23.0). The survival difference of overall survival between two groups was compared by Kaplan-Meier analysis with a log-rank test. Univariate and multivariate analyses were conducted by using the Cox proportional hazards regression model. The chi-square test was used to evaluate the relationship between the risk score and clinicopathological variables. One-way ANOVA and multiple comparison were used to determine the differential expression of USPs among sub-groups in GSE89377. $P < 0.05$ was considered as statistically significant.

RESULTS

Genomic Alterations of the USP Family in TCGA LIHC Cohort

The genomic alterations of USPs are presented in **Figure 1**. A total of 57 USPs were involved in this study. According to the OncoPrint analyzed by CbioPortal, USP36 (15%), USP7 (14%), and USP32(14%) were three top-altered genes (**Figure 1A**).

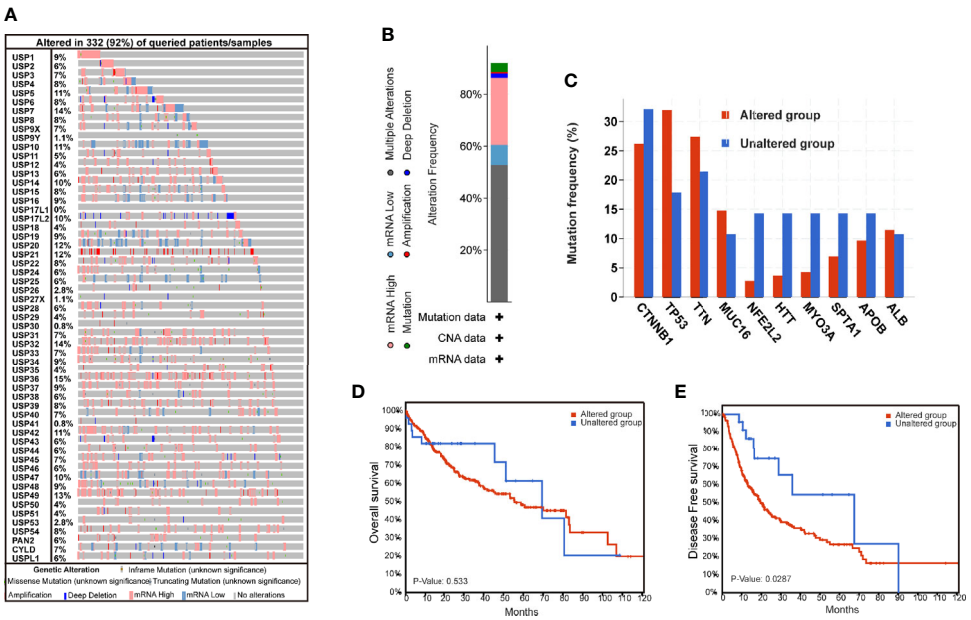

FIGURE 1 | The genomic alterations of ubiquitin-specific proteases in HCC tissues. **(A)** The Oncoprint of 57 ubiquitin-specific proteases (USPs) in TCGA LIHC dataset by CbioPortal. **(B)** Integrated analysis of the USPs genomic alteration proportion in LIHC dataset. **(C)** The top mutated genes in the USPs-altered group and USPs-unaltered groups. **(D, E)** The Kaplan-Meier curves of the overall survival and disease-free survival for the HCC patients in USPs-altered group and USPs-unaltered groups.

Generally, USP family members altered in 91.8% of the whole HCC cases (**Figure 1B**). Of them, the frequency of mutation, amplification, deep deletion, mRNA high, mRNA low, and multiple alteration was 3.44%, 0.57%, 1.72%, 25.78%, 7.74%, and 52.72%, respectively. As shown in **Figure 1C**, five well-known HCC-related genes had higher alteration frequency in the USPs-altered group. Furthermore, the altered group showed poorer disease-free survival (DFS, P=0.0287), though the difference of the overall survival was not statistically significant (**Figure 1D, E**).

The Expression Features of USPs in HCC

The expression profiles of USPs in 374 HCC tissues and 50 normal liver tissue were extracted from TCGA LIHC cohort. Compared with normal liver tissues, a majority of USPs (45/57) presented higher expression in HCC tissues (**Figure 2A**). As shown in **Figure 2B**, the correlation analysis showed that the most relevance among all the USPs was observed in USP34/USP37 (r = 0.79) and USP1/USP24 (r = 0.79). Furthermore, we used STRING to establish the interactive network among the 57 USPs, in which USP1, USP39, USP5, USP13, and USP25 seemed to be the hub genes (**Figure 2C**). In addition, NetworkAnalyst (networkanalyst.ca) was used to predict the liver-specific protein-protein interaction (PPI) of the 57 USPs (**Figure 2D**). GO and KEGG analyses further indicated that the nodules in this PPI network were enriched in biological processes like cellular protein catabolic process, and protein ubiquitination, as well as pathways like cell cycle, necroptosis, viral carcinogenesis, Hippo signaling pathway, and NF-kappa B signaling pathway (**Table 2**).

Consensus Clustering of the USPs in TCGA LIHC Cohort

Based on the expression features of USPs and CDF value, 374 HCC samples of TCGA cohort were stratified into two clusters by using the Consensus ClusterPlus package (k = 2, **Figures 3A–C**). Furthermore, the PCA showed that the two clusters could be well- distinguished in the whole TCGA LIHC cohort (**Figure 3D**). Then, we further explored the association between the USPs-based clusters and the clinicopathological parameters of HCC patients in LIHC cohort. As the heatmap illustrated in **Figure 3E**, USPs-overexpressed cluster 2 was significantly correlated with age, neoplasm stage, tumor growth, and survival status. Consistently, the patients at cluster 2 with USPs overexpression had poorer overall survival than cases of cluster 1 (**Figure 3F**, P<0.001), suggesting the prognostic potential of USP family for HCC patients.

Construction of the USPs-Based Signature in TCGA LIHC Cohort

With the implications in HCC prognosis, we further conducted the univariate Cox regression analyses to evaluate the prognostic significance of USPs. As listed in **Supplementary Table 1**, 21

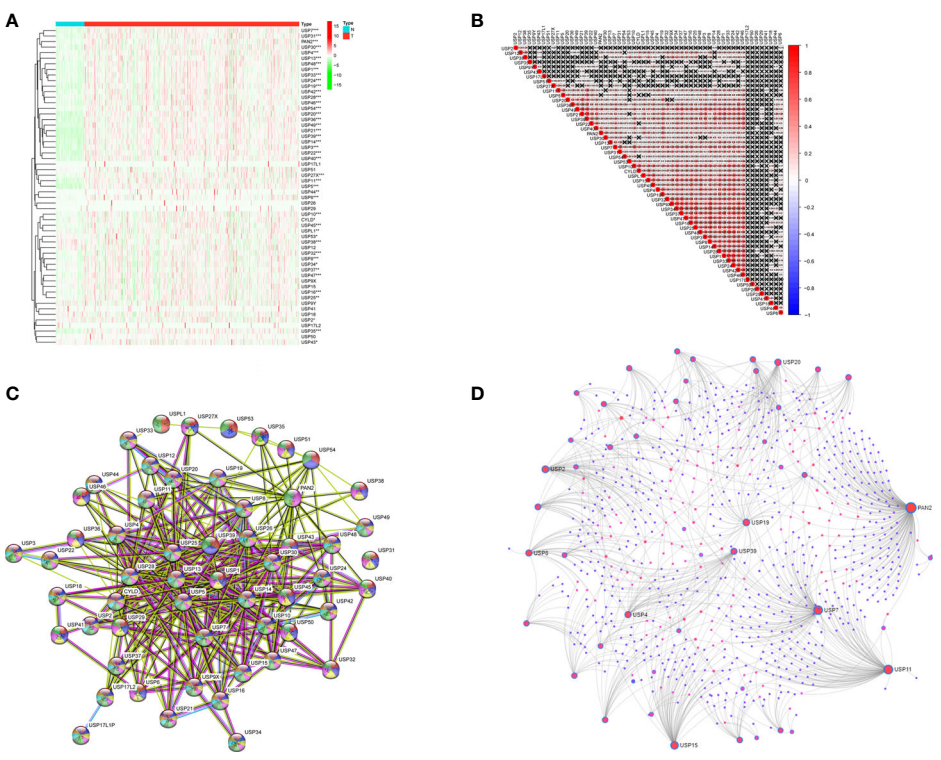

FIGURE 2 | The expression features and interactions of ubiquitin-specific proteases family in HCC. **(A)** The expression levels of 57 USPs in HCC tissues and normal liver tissues evaluated in TCGA datasets. **(B)** Spearman correlation analyses of the 57 USPs in LIHC cohort. **(C)** The interactions among the 57 USPs was analyzed by STRING. **(D)** Liver specific interaction of the 57 USPs was predicted by Networkanalyst. ***P < 0.001; **P < 0.01; *P < 0.05.

TABLE 2 | GO_BP and KEGG analyses of the liver-specific interaction of USPs.

Pathway	Total	Expected	Hits	P Value	FDR
GO_BP analysis					
Cellular protein catabolic process	518	25.6	114	5.77E-44	4.73E-41
Protein catabolic process	644	31.8	121	3.12E-39	1.28E-36
Cellular macromolecule catabolic process	849	42	138	1.44E-37	3.92E-35
Macromolecule catabolic process	1070	52.9	148	4.12E-32	6.76E-30
Proteolysis	1100	54.1	133	3.10E-23	4.24E-21
Protein modification	713	35.2	96	8.08E-20	9.47E-18
Protein ubiquitination	658	32.5	88	5.17E-18	5.30E-16
Cellular catabolic process	2140	106	189	7.86E-17	7.16E-15
Catabolic process	2560	127	205	8.42E-14	6.90E-12
Interphase of mitotic cell cycle	435	21.5	61	1.14E-13	8.47E-12
KEGG analysis					
Ubiquitin mediated proteolysis	137	8.02	32	7.18E-12	2.28E-09
Cell cycle	124	7.26	29	6.92E-11	1.10E-08
Necroptosis	162	9.49	31	3.13E-09	3.32E-07
Endocytosis	244	14.3	39	6.46E-09	5.14E-07
Epstein-Barr virus infection	201	11.8	32	1.71E-07	9.76E-06
Oocyte meiosis	125	7.32	24	1.84E-07	9.76E-06
Viral carcinogenesis	201	11.8	30	1.72E-06	7.80E-05
Hippo signaling pathway	154	9.02	25	2.74E-06	0.000109
Pathways in cancer	530	31	57	3.97E-06	0.000133
NF-kappa B signaling pathway	100	5.85	19	4.17E-06	0.000133

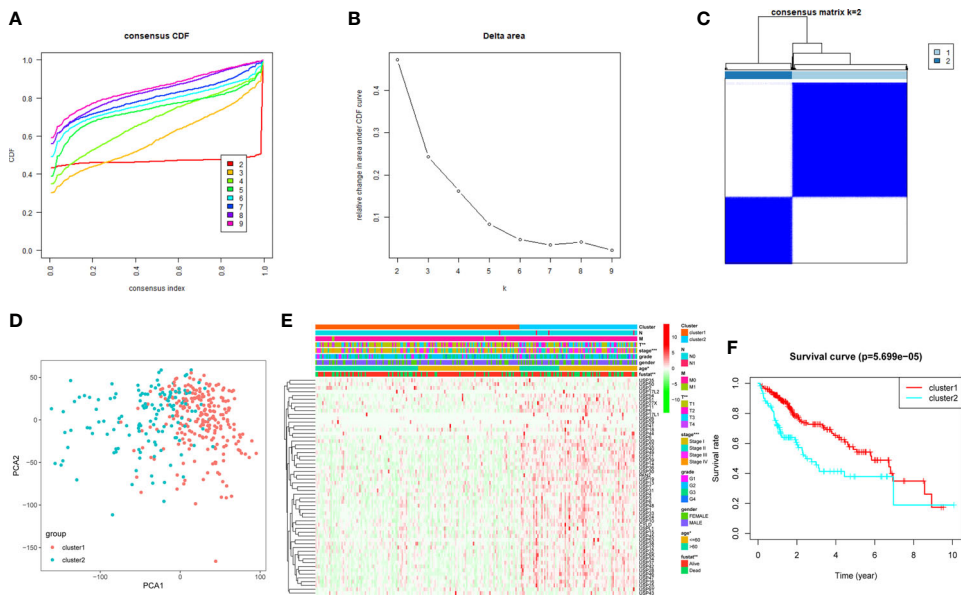

FIGURE 3 | Consensus clusters of the USPs. **(A, B)** Consensus clustering model with cumulative distribution function (CDF) with k from 2 to 9; **(C)** The LIHC cohort stratified into two clusters (k = 2); **(D)** principal component analysis (PCA) of the total mRNA profiles of the two clusters; **(E)** Heatmap indicated the correlation of cluster 2 with clinicopathologic parameters. **(F)** The Kaplan-Meier curves of the overall survival of HCC patients in the two clusters. ***$P < 0.001$; **$P < 0.01$; *$P < 0.05$.

USPs were significantly correlated with poor overall survival of the HCC patients, including USP1, USP10, USP11, USP13, USP14, USP15, USP19, USP21, USP22, USP24, USP28, USP29, USP32, USP33, USP36, USP37, USP39, USP42, USP46, USP48, and USP54. Next, the 21 USPs were enrolled into the Cox proportional hazards regression analysis with LASSO algorithm (**Figure 4A**). Eight genes, including USP1, USP13, USP22, USP24, USP29, USP39, USP48, and USP54, were ultimately screened to establish the signature based on the minimum criteria. According to the expression level of the USPs and coefficients, we stratified the TCGA LIHC cohort into a high-risk group and a low-risk group based on the median risk score. t-SNE analysis indicated the efficiency to distinguish different risk group (**Figure 4B**). As shown in **Figure 4C**, patients

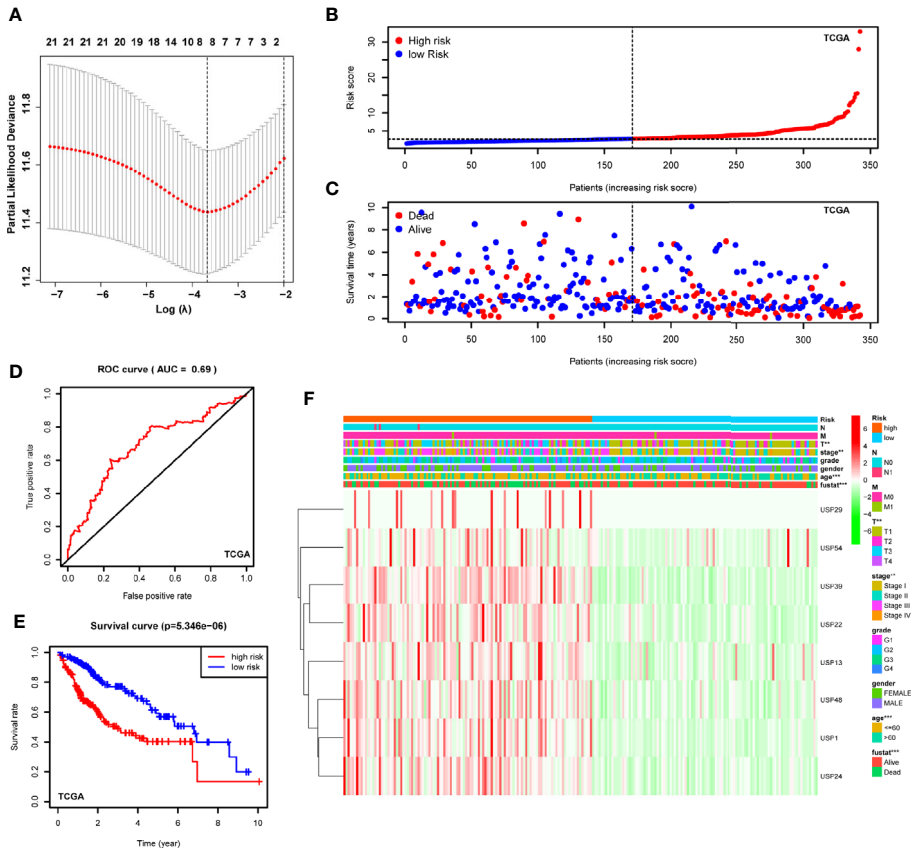

FIGURE 4 | Construction of the USPs-based signature in TCGA LIHC cohort. **(A)** The coefficients of the 8-gene signature were calculated by multivariate Cox analysis with LASSO. **(B)** The distribution and median value of the risk scores in the TCGA LIHC cohort. **(C)** The distributions of OS status and risk score in the TCGA LIHC cohort. **(D)** The ROC curve was calculated to evaluate the predictive efficiency of the USPs-based signature in TCGA. **(E)** The Kaplan–Meier curves of overall survival for HCC patients at high-risk group and low-risk group in TCGA. **(F)** The correlation of the high or low risk score with clinicopathologic parameters in the TCGA LIHC cohort. ROC, receiver operator curve. ***$P < 0.001$; **$P < 0.01$.

at high-risk group had a probability of poor survival than that in low-risk group. Next, the ROC analysis suggested that the risk signature could robustly predict OS for HCC patients in TCGA LIHC cohort (AUC = 0.69, **Figure 4D**). In addition, Kaplan-Meier analysis demonstrated that HCC patients with high-risk score had shorter overall survival compared to the cases with low-risk score (P<0.001, **Figure 4E**). Then we analyzed the correlation of the risk signature with clinical parameters in TCGA cohort. High-risk group was significantly correlated with aggressive phenotypes such as tumor size, neoplasm stage, and survival status (**Figure 4F**). Additionally, we conducted stratified analysis in the sub-groups of TCGA LIHC cohort. For HCC patients at stage I and II, high-risk score led to a poorer overall survival (**Supplementary Figure 1A**, P<0.001). However, though the general survival time was obviously shorter in high-risk group, the difference was not statistically significant for patients at stage III and IV (**Supplementary Figure 1B**, P=0.103). In contrast, patients at high-risk score displayed a significantly poorer OS in sub-groups of grade I&II (**Supplementary Figure 1C**, P<0.001) or grade III &IV (**Supplementary Figure 1D**, P=0.026).

Validating the Signature in ICGC Cohort

To confirm the robustness of the signature, we further evaluated the risk model in ICGC cohort (LIRI-JP). The patients from the ICGC cohort were also categorized into two groups according to the median risk score calculated by the formula established in the TCGA cohort. The t-SNE analysis demonstrated that patients in two high- and low-groups were distributed in discrete dots (**Figure 5A**). In consistent with the results of TCGA, the cases in the high-risk group had a probability of poorer survival (**Figure 5B**). The ROC analysis also confirmed the predictive performance of the risk model in ICGC cohort (**Figure 5C**, AUC=0.674). In addition, Kaplan-Meier analyses indicated that HCC patients with high-risk score had reduced overall survival time (**Figure 5D**, P<0.001). As shown in **Figures 5E, F**, the stratified analysis showed that high-risk score was correlated with shorter OS in cases both of I&II stages (**Figure 5E**,

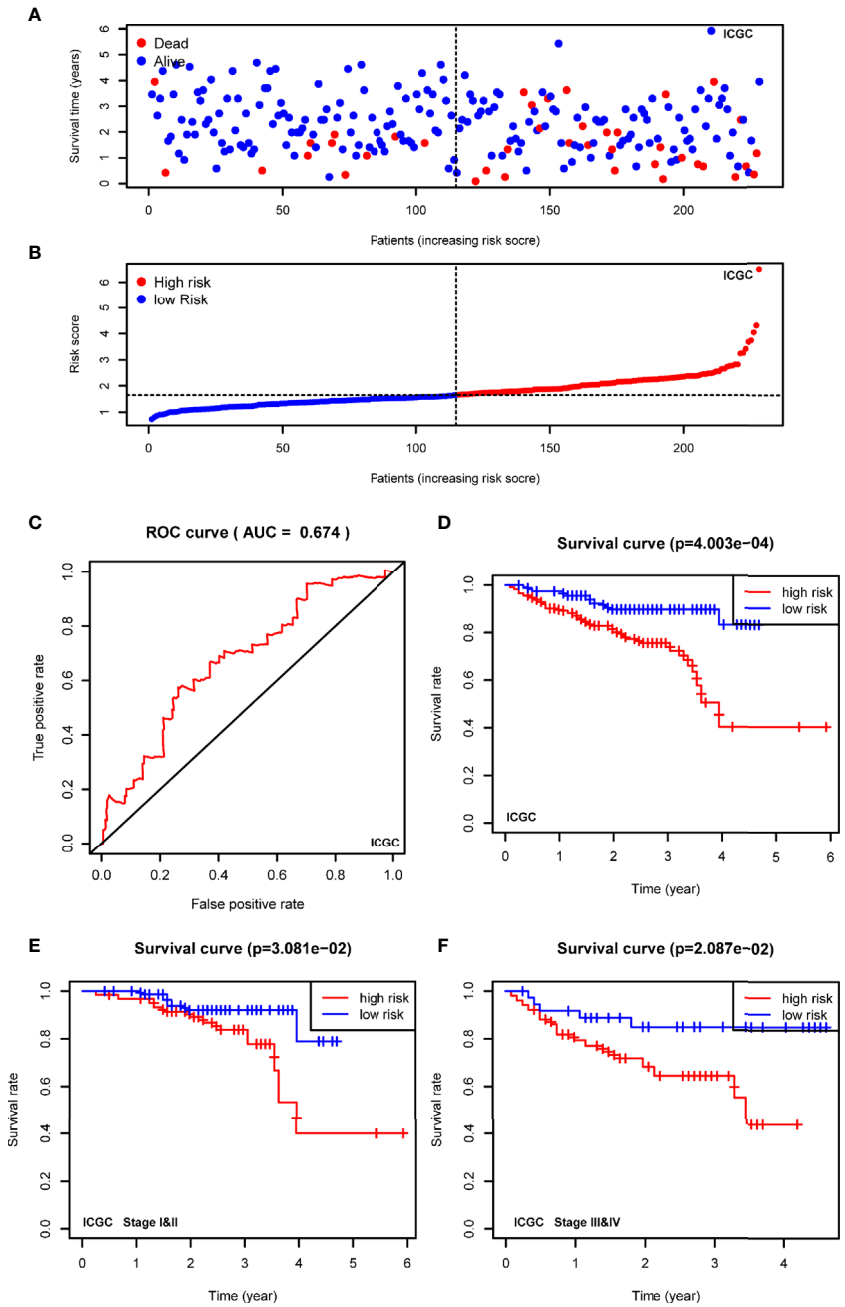

FIGURE 5 | Validating the prognostic value of the USPs-based signature in ICGC cohort. **(A)** The distribution and median value of the risk scores in the ICGC cohort. **(B)** The distributions of OS status and risk score in the ICGC cohort. **(C)** The ROC curve was calculated to evaluate the predictive efficiency of the USPs-based signature in ICGC cohort. **(D)** The Kaplan–Meier curves of overall survival for HCC patients at high-risk group and low-risk group in ICGC cohort. **(E, F)** The Kaplan–Meier curves of HCC patients at stage I&II and stage III&IV in ICGC cohort. ICGC, International Cancer Genome Consortium.

P=0.0308) and III&IV stages (**Figure 5F**, *P*=0.0209) in the ICGC cohort.

Identify the USPs-Based Signature as an Independent Prognostic Factor of HCC

Furthermore, the univariate and multivariate Cox regression analyses were conducted to evaluate the risk signature as an independent prognostic factor in the two cohorts. For TCGA cohort, the univariate Cox analysis demonstrated that the risk score (*P*<0.001, HR = 1.157, 95% CI = 1.112–1.205), neoplasm stage, T status, and M status were potential hazard factors (**Figure 6A**). Further multivariate Cox regression analysis elucidated that the risk score was an independent factor (*P*<0.001, HR = 1.152, 95% CI = 1.101–1.205) of HCC

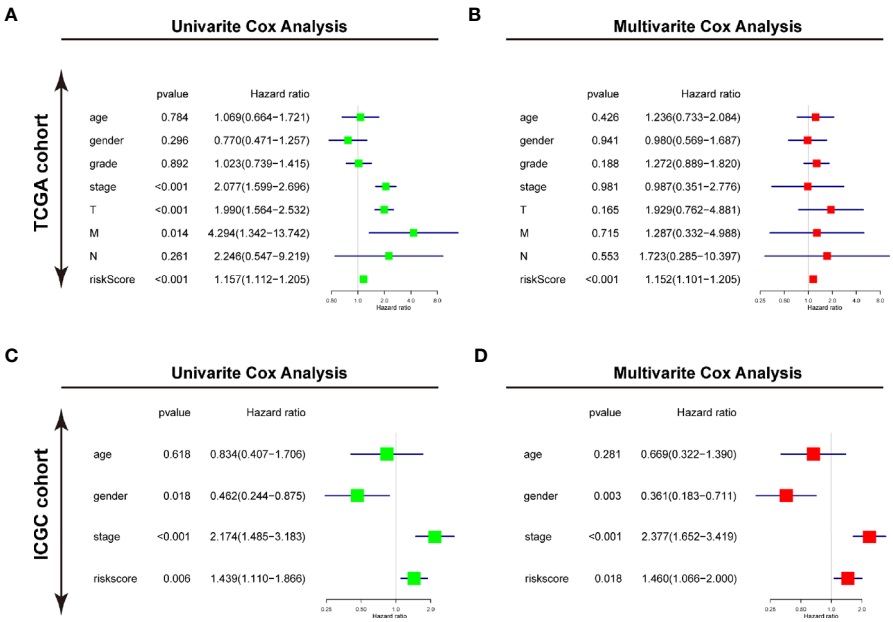

FIGURE 6 | Identifying the USPs-based signature as an independent factor for HCC prognosis. **(A)** Univariate Cox analyses of the clinicopathological factors (including the risk score) and overall survival in the TCGA LIHC cohort. **(B)** Multivariate Cox analyses of the clinicopathological factors (including the risk score) and overall survival in the TCGA LIHC cohort. **(C)** Univariate Cox analyses in the ICGC cohort. **(D)** Multivariate Cox analyses in the ICGC cohort. ICGC, International Cancer Genome Consortium.

(**Figure 6B**). For ICGC cohort, the univariate Cox analysis the risk score (P=0.006, HR = 1.439, 95% CI = 1.110–1.866) and neoplasm stage were candidate factors (**Figure 6C**). In accordance with the observation in TCGA cohort, the risk score was also recommended as an independent predictor for OS by the multivariate Cox regression analysis in the ICGC cohort (**Figure 6D**, P=0.018, HR = 1.460, 95% CI = 1.066–2.000).

Functions and Pathways Correlated With the USPs-Based Signature

To predict the biological functions, we conducted GO analyses in differential expression genes (DEGs) between high-risk and low-risk groups in both of TCGA cohort and ICGC cohort. the DEGs were enriched in biological process like DNA replication, nuclear division, ECM constituent, small molecule catabolic process, collagen-containing ECM, and peptidase inhibitor activity (**Supplementary Figures 2A, B**). Furthermore, we conducted GSEA with KEGG and Hallmarks to unravel the molecular mechanisms underlying the USPs-based signature (**Supplementary Table 2**). As shown in **Figure 7A**, the ubiquitin mediated proteolysis, cell cycle, DNA replication, ERBB signaling, MYC targets, G2/M checkpoints, PI3K/AKT/mTOR signaling, and Wnt/β-catenin pathway were enriched in the high-risk group of the TCGA cohort. For the ICGC cohort, in addition to the pathways mentioned above, the significantly enriched pathways also included regulation of autophagy and E2F targets (**Figure 7B**).

Expression Features of the Risk Genes in HCC Progression

Then, we extracted the mRNA profiles from GSE89377 to analyze the expression of the 8 USPs in the HCC progression. At first, we compared the expression of the USPs in HCC staging, in which only USP39 presented the dynamically increasing characteristics (**Figure 8A**). It was consistent with the observation in Ualcan databases, by which USP39 expression was significantly upregulated in advanced stages and grades of HCC patients (**Supplementary Figures 3A, B**). Interestingly, among the eight signature genes, USP39 was found elevated from normal control, dysplastic nodules with low grade, dysplastic nodules with high grade, to HCC cases, suggesting an enhanced expression tendency in hepatocarcinogenesis (**Figure 8B**). The observation above suggested the potential role of USP39 in HCC progression and hepatocarcinogenesis.

The Expression Feature of USP39 in HCC

Based on the observation in GSE89377 dataset, we further explored the potential functions and mechanisms regulated by

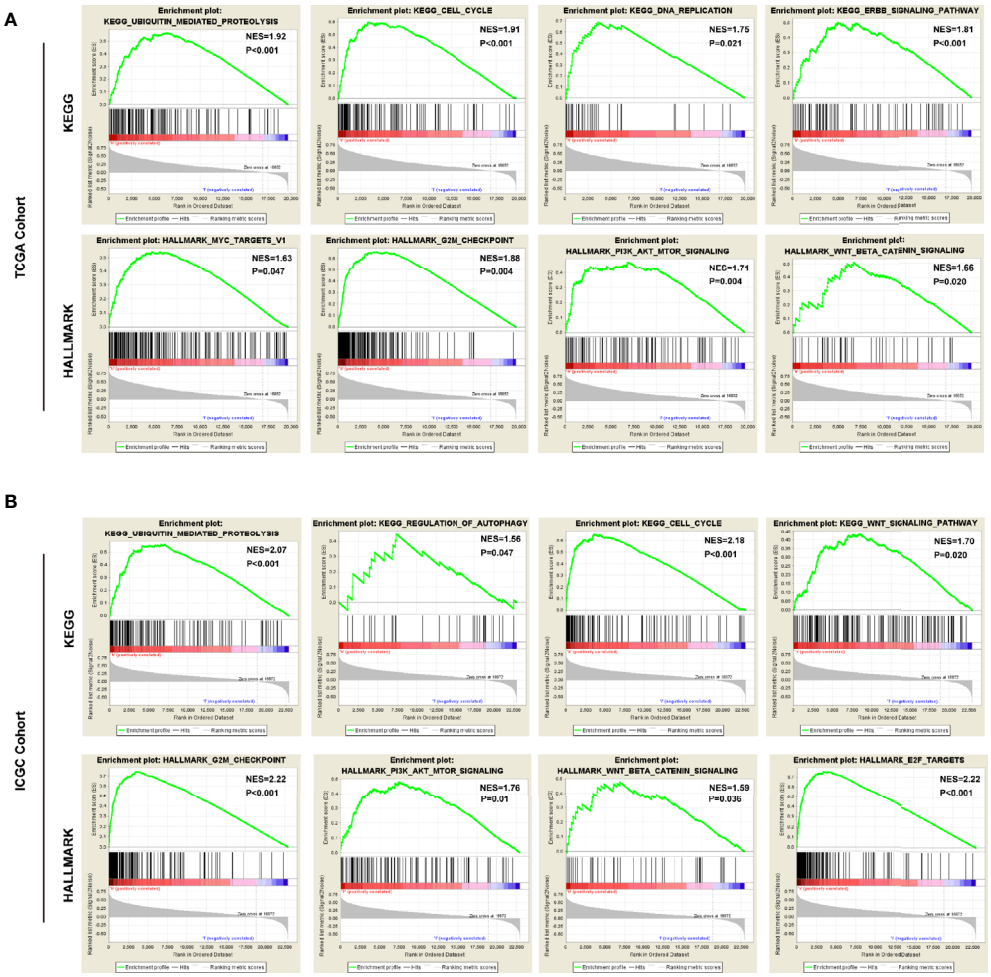

FIGURE 7 | The pathways correlated with the high-risk score. The gene set enrichment analysis (GSEA) was performed in the TCGA and ICGC cohorts to explore mechanisms underlying the 8-USPs based signature. **(A)** Four representative KGEE pathways and hallmarks in the high–risk group of TCGA cohort; **(B)** Four representative KGEE pathways and hallmarks in the high–risk group of ICGC cohort. NES, Normalized enrichment score.

USP39 (**Supplementary Table 3**). According to the pan-cancers analysis in TIMER dataset, the most significant difference of USP39 between pan-cancers and normal tissues was observed in HCC (**Supplementary Figure 4A**). In a serials of mRNA expression datasets, most of them (10/11) confirmed the overexpression of USP39 in HCC tissues (**Supplementary Figure 4B**). In protein level, as shown in **Figure 9A**, significantly elevated expression of USP39 was determined in 15/16 HCC tissues compared with the self-paired adjacent tissues analyzed by western blotting. Then we further explored the expression feature of USP39 in a local cohort including 106 HCC tissues by performing immunohistochemistry. USP39 was mainly distributed in the nucleus of HCC tissues. HCC cases with metastasis presented higher staining intensity of USP39 than the cases without metastasis (**Figure 9B**). Additionally, higher expression of USP39 was detected in poorly differentiated tissues than well differentiated HCC cases (**Figure 9C**). Furthermore, Kaplan-Meier analyses suggested that HCC patients with higher USP39 expression might have shorter overall survival (**Figure 9D**).

The Clinical Implications and Mechanisms of USP39 in HCC

For the clinical investigation, USP39 overexpression was correlated with neoplasm stage, histological grade, and tumor size of HCC patients in LIHC cohort (**Table 3**). To further explore the biological functions mediated by USP39, we used LinkedOmics to examine USP39 co-expression mode in TCGA LIHC cohort (**Figure 10A**). The top 50 genes significantly correlated with USP39 in TCGA were elucidated in the heatmap (**Figure 10B**). GO term annotation by GSEA indicated that USP39 co-expressed genes were enriched in processes like cell cycle checkpoint, G0/G1 and G2/M transition, DNA replication, and cytokines (**Figure 10C**). The KEGG analysis showed the enrichment in cell cycle, DNA

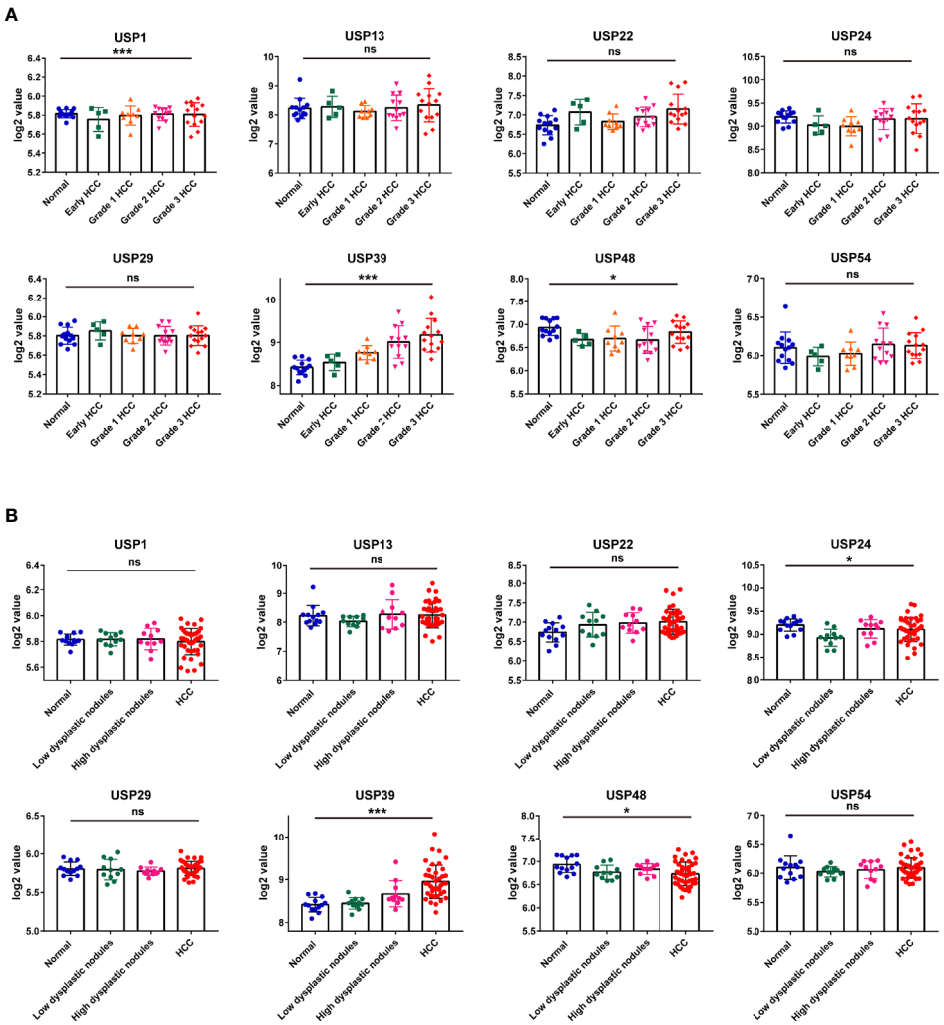

FIGURE 8 | The expression features of the 8 risk genes in hepatocarcinogenesis and HCC cases at different grades in GSE89377 cohort. **(A)** The expression features of the eight USPs in cases at different tumor grades in GSE89377 cohort. **(B)** The expression features of the eight USPs in patients with dysplastic nodules and HCC in GSE89377 cohort. *$P < 0.05$; ***$P < 0.001$; ns, non-significance.

replication, and ubiquitin mediated proteolysis. Based on these, we analyzed the correlation of USP39 with cell cycle and proliferation-related genes in TCGA LIHC cohort (**Figure 10D**). As elucidated in **Figure 10E**, USP39 was significantly correlated with PCNA, FEN1, MKI67, CDK1/2, Cyclin B1/2, CHEK1/2, and BUB1/1B/3.

DISCUSSION

Ubiquitination is a critical post-translational mechanism that plays multifaceted roles in multiple biological processes like apoptosis, cell-cycle progression, inflammatory responses, and transcriptional activities (18, 19). DUBs can inactivate the Ub signal from target proteins by trimming Ub chains (20). However, dysregulation of the DUBs may induce the malfunction of the ubiquitin system, which could subsequently regulate a serial of oncogenes or tumor suppressor genes (21, 22). A growing body of evidence suggests that USP sub-family is implicated in various malignancies (23). In the current study, we focused on the expression features and prognostic value of USPs for HCC. According to the hepatic expression levels in TCGA cohort, most of the USPs were overexpressed in HCC tissues. As elucidated in the liver-specific PPI, the nodules in this network were enriched in tumor or inflammation-related processes and pathways. Of them, Hippo signaling pathway and NF-kappa B signaling pathway have been frequently implicated in the genesis and progression of HCC.

Furthermore, the Consensus cluster analysis further indicated the correlation of USPs-enriched sub-cluster with neoplasm stage, tumor growth, and overall survival, suggesting the prognostic potential of the USP family for HCC patients. Then

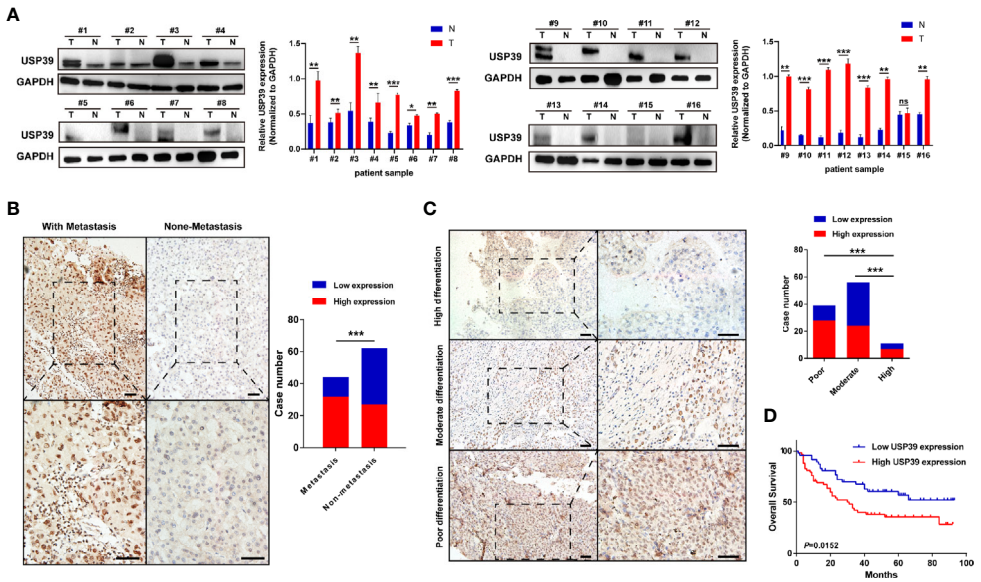

FIGURE 9 | The protein expression features and prognostic significance of USP39 in HCC tissues. **(A)** The expression of USP39 in 16 pairs of HCC and adjacent tissues analyzed by western blotting. **(B)** Representative immunostaining images of USP39 in HCC cases with or without metastasis. **(C)** Representative immunostaining images of USP39 in HCC cases with high, moderate, or poor differentiation. **(D)** The Kaplan–Meier curves of HCC patients with high or low USP39 expression identified by immunohistochemistry. T, tumor tissues; N, adjacent tissues; ns, non-significance. ***P < 0.001; **P < 0.01; *P < 0.05.

TABLE 3 | Correlation of USP39 expression with clinical parameters of HCC patients in TCGA.

Clinical characteristics	Total(N)	Odds ratio in USP39	P value
Age (≥65 vs.<65)	370	1.54 (1.01,2.33)	0.044
Gender (female vs. male)	371	0.72 (0.47,1.11)	0.14
Stage (I/II vs. III/IV)	347	1.88 (1.15,3.07)	1.10E-02
Histological grade (G1/G2 vs. G3/G4)	366	1.8 (1.17,2.77)	7.00E-03
T (T1/T2 vs. T3/T4)	368	1.71 (1.06,2.76)	2.60E-02
N (N0 vs. N1)	256	2.73 (0.28,26.57)	0.356
M (M0 vs. M1)	270	2.87 (0.29,27.92)	0.331
Survival status (alive vs. dead)	371	0.65 (0.42,0.99)	0.046

we screened the USPs with prognostic value evaluated in TCGA LIHC cohort, which were subsequently enrolled into multivariate analysis with LASSO algorithm. Ultimately, USP1, USP13, USP22, USP24, USP29, USP39, USP48, and USP54 were used to establish the risk signature. As shown in the survival analyses, the signature-derived risk score could robustly predict the overall survival in the entire TCGA LIHC cohort and sub-groups stratified by different stages and grades. To further confirm the prognostic value of the signature, we chose another HCC cohort ICGC (LIRI-JP). In consistence with the observation in TCGA cohort, it also had excellent performance in predicting the overall survival of HCC patients in the ICGC cohort. Remarkably, the univariate and multivariate Cox analyses in the two cohorts draw a consistent result that the USPs-based signature-derived risk score was an independent factor for the prognosis of HCC patients. For the potential mechanisms modulated by the USPs-based signature, we conducted the GO analysis on the DEGs and GSEA in the two cohorts. Interestingly, some well-known HCC-related pathways were correlated with the high-risk score, including cell cycle, DNA replication, ERBB signaling, MYC signaling, G2/M checkpoints, PI3K/AKT/mTOR signaling, Wnt/β-catenin pathway, autophagy, and E2F signaling. It was speculated that the activation in these tumorigenesis pathways might contribute to the poor survival of the patients with high-risk score.

Hepatocarcinogenesis is known as a multi-center and multi-step process, in which USPs played crucial roles (24, 25). Then GSE89377, a dataset with different HCC- related sub-groups, was used to investigate the expression characteristics of the USPs in HCC staging and hepatocarcinogenesis. For the eight signature USPs, only USP39 presented significantly enhanced expression with the advancing of histological grade. Subsequently, we also explored the expression levels of the eight genes in normal, dysplastic nodes (low and high grade), and HCC tissues. In accordance with the data in cases at different grades, USP39 displayed a dynamic increasing from pre-HCC status to HCC. However, USP13, USP22, and USP39, previously correlated with the malignant phenotypes of HCC cells (26–28), showed less differences among the sub-groups. It could be speculated that these USPs might be not key driver genes for HCC progression though they enhance aggressive behaviors of HCC cells. Instead, based on the observation in this GSE dataset, USP39 might serve as a hub gene that participates in tumorigenesis and HCC progression.

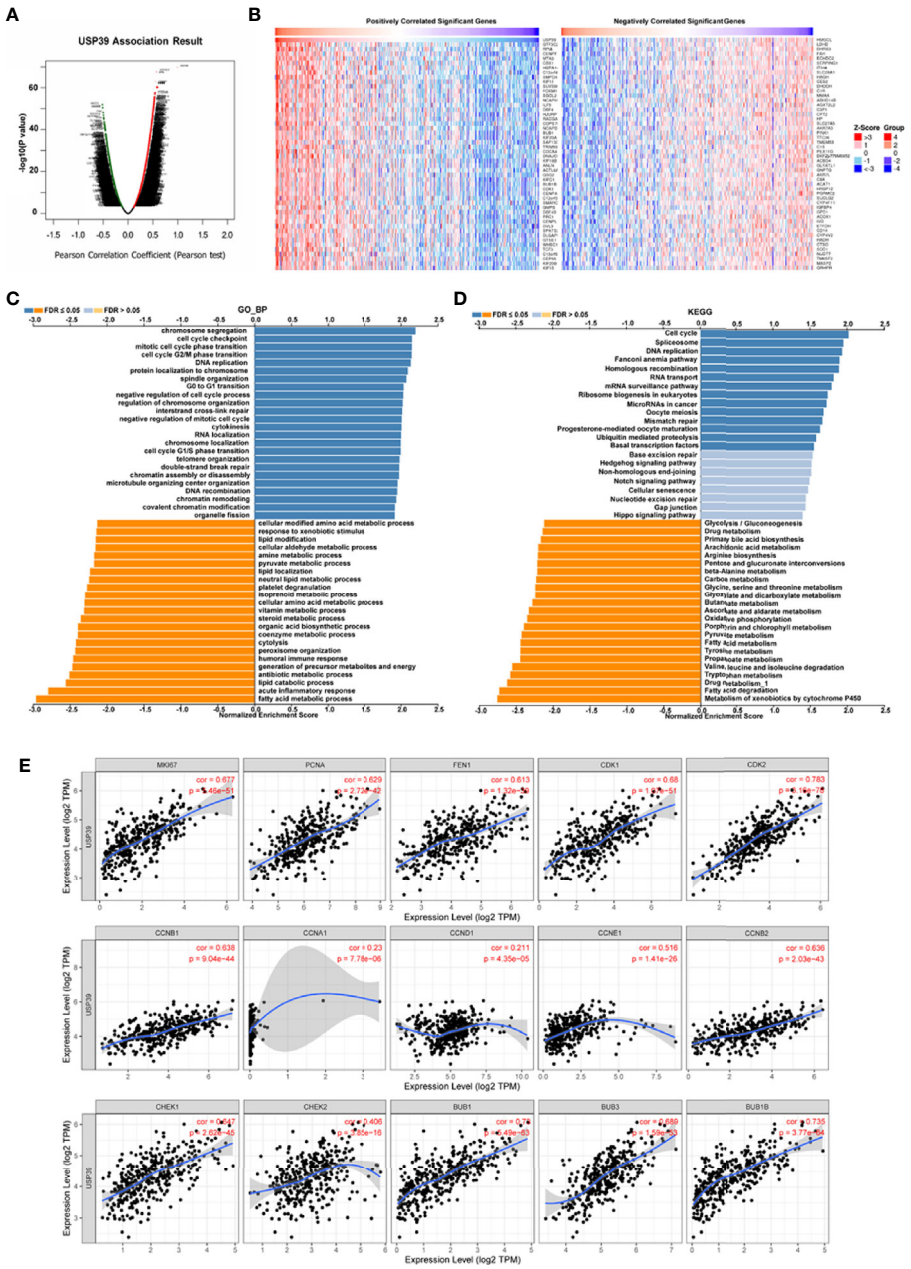

FIGURE 10 | The potential function of USP39 in HCC. **(A, B)** The significantly positively- or negatively- correlated genes with USP39 in the TCGA LIHC cohort. **(C, D)** The USP39-regulated functions and pathways were calculated by GSEA with GO analysis and KEGG analysis. **(E)** The correlation of USP39 with cell cycle and proliferation-related genes in TCGA LIHC cohort were calculated by TIMER.

We further focused on exploring the clinical significance and potential function of USP39 in HCC. USP39 is a cysteine deubiquitinating enzyme belonging to the USP family. Overexpression of USP39 was observed in approximately half of the pan-cancers in TCGA dataset, of which HCC displayed the most differences between normal and tumor tissues. In addition, combining analyses of multiple datasets and experimental detection further confirmed the overexpression of USP39 in HCC tissues. Interestingly, the expression of USP39 also increased from pre-cancerous stage to HCC, which was consistent with the observation above and further suggested the implications of USP39 in hepatocarcinogenesis. Currently, the clinical significance of USP39 has not been investigated in HCC. Herein, we found that overexpression of USP39 was significantly correlated with neoplasm stage, histological grade, and tumor size. Through the co-concurrence analysis, we found

that USP39 might be involved in cell cycle and DNA replication pathways. As is known, the proteins such as Cyclin family, CDKs, and checkpoint molecules are highly important to ensure proper proliferation, while deregulation of these proteins can result in various types of tumors. As expected, according to the analysis in TIMER, USP39 was significantly correlated with cell cycle- and proliferation- related genes. Accordantly, a previous study suggested the tumor-promotive role of USP39 in HCC cell lines. USP39 knockdown has been found to inhibit the proliferation and colony formation through downregulating the transcription factor Forkhead Box M1 (29). The observation above suggested that USP39 might be a potential molecular target for HCC treatment.

Despite of the encouraging performance of the USPs-based signature, there were certain limitations for the current study. The establishment and validation of the signature were based on the public sequence data. Further validation, such as prospective studies and clinical trials of HCC patients in multi-centers, might make the signature more convincing. In addition, the current study preliminarily predicted the functions and pathways modulated by USPs. The exact biological roles and mechanisms of UPSs in HCC remained to be investigated by more experimental assays.

CONCLUSION

In conclusion, the current study investigated the expression features and potential functions of USPs in HCC. An 8-USPs-formed signature could robustly predict the prognosis of HCC patients in TCGA LIHC cohort and ICGC (LIRI-JP) cohort. In addition, USP39, one of the eight signature genes, might be a potential molecular target for hepatocarcinogenesis and HCC progression. Our study provided evidence for the future investigation into USP family in the prognostic significance and targeted value for HCC treatment.

DATA AVAILABILITY STATEMENT

The datasets presented in this study can be found in online repositories. The names of the repository/repositories and accession number(s) can be found in the article/**Supplementary Material**.

ETHICS STATEMENT

The studies involving human participants were reviewed and approved by the Ethics Committee of Affiliated Hospital of Nantong University. The patients/participants provided their written informed consent to participate in this study.

AUTHOR CONTRIBUTIONS

WZ and MX conceived and designed the study. QS, WN, and JZ analyzed the data. SB and MZ drafted the paper. WZ revised the manuscript. All authors contributed to the article and approved the submitted version.

FUNDING

This study was supported by grants from the National Natural Science Foundation (82070622, 81702419), the Key Research and Development Plan of Jiangsu Province (BE2020668, BE2019692), and the Nantong Science and Technology Project (MS12019013, MS12020020, MS22020005).

SUPPLEMENTARY MATERIAL

The Supplementary Material for this article can be found online at: https://www.frontiersin.org/articles/10.3389/fonc.2021.629327/full#supplementary-material

REFERENCES

1. Villanueva A. Hepatocellular Carcinoma. *N Engl J Med* (2019) 380(15):1450–62. doi: 10.1056/NEJMra1713263
2. Yang JD, Hainaut P, Gores GJ, Amadou A, Plymoth A, Roberts LR. A global view of hepatocellular carcinoma: trends, risk, prevention and management. *Nat Rev Gastroenterol Hepatol* (2019) 16(10):589–604. doi: 10.1038/s41575-019-0186-y
3. Huang A, Yang XR, Chung WY, Dennison AR, Zhou J. Targeted therapy for hepatocellular carcinoma. *Signal Transduct Target Ther* (2020) 5(1):146. doi: 10.1038/s41392-020-00264-x
4. Craney A, Rape M. Dynamic regulation of ubiquitin-dependent cell cycle control. *Curr Opin Cell Biol* (2013) 25(6):704–10. doi: 10.1016/j.ceb.2013.07.004
5. Kim W, Bennett EJ, Huttlin EL, Guo A, Li J, Possemato A, et al. Systematic and quantitative assessment of the ubiquitin-modified proteome. *Mol Cell* (2011) 44(2):325–40. doi: 10.1016/j.molcel.2011.08.025
6. Reyes-Turcu FE, Ventii KH, Wilkinson KD. Regulation and cellular roles of ubiquitin-specific deubiquitinating enzymes. *Annu Rev Biochem* (2009) 78:363–97. doi: 10.1146/annurev.biochem.78.082307.091526
7. Mevissen TET, Komander D. Mechanisms of Deubiquitinase Specificity and Regulation. *Annu Rev Biochem* (2017) 86:159–92. doi: 10.1146/annurev-biochem-061516-044916
8. Zhang W, Zhang J, Xu C, Zhang S, Bian S, Jiang F, et al. Ubiquitin-specific protease 7 is a drug-able target that promotes hepatocellular carcinoma and chemoresistance. *Cancer Cell Int* (2020) 20:28. doi: 10.1186/s12935-020-1109-2
9. Ling S, Shan Q, Zhan Q, Ye Q, Liu P, Xu S, et al. USP22 promotes hypoxia-induced hepatocellular carcinoma stemness by a HIF1alpha/USP22 positive feedback loop upon TP53 inactivation. *Gut* (2020) 69(7):1322–34. doi: 10.1136/gutjnl-2019-319616
10. Meng J, Ai X, Lei Y, Zhong W, Qian B, Qiao K, et al. USP5 promotes epithelial-mesenchymal transition by stabilizing SLUG in hepatocellular carcinoma. *Theranostics* (2019) 9(2):573–87. doi: 10.7150/thno.27654
11. Li W, Cui K, Prochownik EV, Li Y. The deubiquitinase USP21 stabilizes MEK2 to promote tumor growth. *Cell Death Dis* (2018) 9(5):482. doi: 10.1038/s41419-018-0523-z
12. Lu C, Ning Z, Wang A, Chen D, Liu X, Xia T, et al. USP10 suppresses tumor progression by inhibiting mTOR activation in hepatocellular carcinoma. *Cancer Lett* (2018) 436:139–48. doi: 10.1016/j.canlet.2018.07.032
13. Qiu C, Liu Y, Mei Y, Zou M, Zhao Z, Ye M, et al. Ubiquitin-speci fi c protease 4 promotes metastasis of hepatocellular carcinoma by increasing TGF-beta signaling-induced epithelial-mesenchymal transition. *Aging (Albany NY)* (2018) 10(10):2783–99. doi: 10.18632/aging.101587
14. Wang X, Zhang Q, Wang Y, Zhuang H, Chen B. Clinical Significance of Ubiquitin Specific Protease 7 (USP7) in Predicting Prognosis of

Hepatocellular Carcinoma and its Functional Mechanisms. *Med Sci Monit* (2018) 24:1742–50. doi: 10.12659/msm.909368
15. Zhang S, Xie C, Li H, Zhang K, Li J, Wang X, et al. Ubiquitin-specific protease 11 serves as a marker of poor prognosis and promotes metastasis in hepatocellular carcinoma. *Lab Invest* (2018) 98(7):883–94. doi: 10.1038/s41374-018-0050-7
16. Gan Q, Shao J, Cao Y, Lei J, Xie P, Ge J, et al. USP33 regulates c-Met expression by deubiquitinating SP1 to facilitate metastasis in hepatocellular carcinoma. *Life Sci* (2020) 261:118316. doi: 10.1016/j.lfs.2020.118316
17. Wu J, Chen Y, Geng G, Li L, Yin P, Nowsheen S, et al. USP39 regulates DNA damage response and chemo-radiation resistance by deubiquitinating and stabilizing CHK2. *Cancer Lett* (2019) 449:114–24. doi: 10.1016/j.canlet.2019.02.015
18. Swatek KN, Komander D. Ubiquitin modifications. *Cell Res* (2016) 26(4):399–422. doi: 10.1038/cr.2016.39
19. Vu LD, Gevaert K, De Smet I. Protein Language: Post-Translational Modifications Talking to Each Other. *Trends Plant Sci* (2018) 23(12):1068–80. doi: 10.1016/j.tplants.2018.09.004
20. Haglund K, Dikic I. Ubiquitylation and cell signaling. *EMBO J* (2005) 24 (19):3353–9. doi: 10.1038/sj.emboj.7600808
21. Shi D, Grossman SR. Ubiquitin becomes ubiquitous in cancer: emerging roles of ubiquitin ligases and deubiquitinases in tumorigenesis and as therapeutic targets. *Cancer Biol Ther* (2010) 10(8):737–47. doi: 10.4161/cbt.10.8.13417
22. Clague MJ, Urbe S, Komander D. Breaking the chains: deubiquitylating enzyme specificity begets function. *Nat Rev Mol Cell Biol* (2019) 20(6):338–52. doi: 10.1038/s41580-019-0099-1
23. Young MJ, Hsu KC, Lin TE, Chang WC, Hung JJ. The role of ubiquitin-specific peptidases in cancer progression. *J BioMed Sci* (2019) 26(1):42. doi: 10.1186/s12929-019-0522-0
24. Chen S, Cao Q, Wen W, Wang H. Targeted therapy for hepatocellular carcinoma: Challenges and opportunities. *Cancer Lett* (2019) 460:1–9. doi: 10.1016/j.canlet.2019.114428
25. Zongyi Y, Xiaowu L. Immunotherapy for hepatocellular carcinoma. *Cancer Lett* (2020) 470:8–17. doi: 10.1016/j.canlet.2019.12.002
26. Huang J, Gu ZL, Chen W, Xu YY, Chen M. Knockdown of ubiquitin-specific peptidase 13 inhibits cell growth of hepatocellular carcinoma by reducing c-Myc expression. *Kaohsiung J Med Sci* (2020) 36(8):615–21. doi: 10.1002/kjm2.12209
27. Ling S, Li J, Shan Q, Dai H, Lu D, Wen X, et al. USP22 mediates the multidrug resistance of hepatocellular carcinoma via the SIRT1/AKT/MRP1 signaling pathway. *Mol Oncol* (2017) 11(6):682–95. doi: 10.1002/1878-0261.12067
28. Yuan X, Sun X, Shi X, Jiang C, Yu D, Zhang W, et al. USP39 promotes the growth of human hepatocellular carcinoma in vitro and in vivo. *Oncol Rep* (2015) 34(2):823–32. doi: 10.3892/or.2015.4065
29. Yuan X, Sun X, Shi X, Jiang C, Yu D, Zhang W, et al. USP39 regulates the growth of SMMC-7721 cells via FoxM1. *Exp Ther Med* (2017) 13(4):1506–13. doi: 10.3892/etm.2017.4115

Conflict of Interest: The authors declare that the research was conducted in the absence of any commercial or financial relationships that could be construed as a potential conflict of interest.

frontiers in Oncology

ORIGINAL RESEARCH
published: 09 March 2021
doi: 10.3389/fonc.2021.625169

NEDD4 Induces K48-Linked Degradative Ubiquitination of Hepatitis B Virus X Protein and Inhibits HBV-Associated HCC Progression

Tao Wan, Zhao Lei, Biao Tu, Tianyin Wang, Jiale Wang and Feizhou Huang *

Department of Hepatobiliary Surgery, The Third Xiangya Hospital of Central South University, Changsha, China

Neural precursor cell expressed developmentally downregulated gene 4 (NEDD4) plays two opposite roles in carcinogenesis. It has been reported that NEDD4 inhibits hepatocellular carcinoma (HCC) progression; however, little is known about its potential function and molecular mechanism in HCC in the context of hepatitis B virus (HBV) infection. In this study, we analyzed NEDD4 expression in 199 HCC specimens with or without HBV infection and observed that NEDD4 expression was unrelated to HBV exposure in HCC tumor tissue but that high NEDD4 expression conferred better overall survival (OS) and progression-free survival (PFS) than low NEDD4 expression in patients with HBV-associated HCC. Upregulation of NEDD4 inhibited proliferation, migration and invasion in HBV-related HCC cell lines. We demonstrated that NEDD4 interacts with HBV X protein (HBx) and that HBx upregulation could reverse the suppression of proliferation and mobility induced by NEDD4 overexpression. Furthermore, we confirmed that NEDD4 induced the degradation of HBx in a ubiquitin/proteasome-dependent manner via K48-linked ubiquitination. Our findings suggest that NEDD4 exerts a tumor-suppressive effect in HBV-associated HCC by acting as an E3 ubiquitin ligase for HBx degradation and provide new insights into the function of NEDD4.

Keywords: NEDD4, hepatocellular carcinoma, HBx, HBV-associated HCC, ubiquitin-proteasome pathway

OPEN ACCESS

Edited by:
Yi Sun,
Zhejiang University, China

Reviewed by:
Yogesh Chawla,
Mayo Clinic, United States
Hui-Kuan Lin,
Wake Forest Baptist Medical Center, United States

***Correspondence:**
Feizhou Huang
huangfeizhou@csu.edu.cn

Specialty section:
This article was submitted to Cancer Molecular Targets and Therapeutics, a section of the journal Frontiers in Oncology

Received: *02 November 2020*
Accepted: *01 February 2021*
Published: *09 March 2021*

Citation:
Wan T, Lei Z, Tu B, Wang T, Wang J and Huang F (2021) NEDD4 Induces K48-Linked Degradative Ubiquitination of Hepatitis B Virus X Protein and Inhibits HBV-Associated HCC Progression. Front. Oncol. 11:625169. doi: 10.3389/fonc.2021.625169

INTRODUCTION

Hepatocellular carcinoma (HCC) is the major subtype of primary liver cancer (1). With the characteristics of insidious onset, rapid progression, and frequent recurrence, HCC ranks third in terms of cancer-related death worldwide (1, 2). Extensive investigations have provided overwhelming evidence that the development of HCC is closely related to metabolic syndrome, alcohol abuse, aflatoxin B1 exposure, and chronic hepatitis B or C virus (HBV or HCV) infection (1). Chronic HBV infection represents the most common pathogenic factor, accounting for up to 54% of HCC cases (3). In the early stage of HBV infection, HBV DNA integrates into the host genome, which results in genomic instability and direct insertional mutagenesis of various oncogenes (4). Persistent expression of HBV regulatory proteins can facilitate the oncogenic

transformation of liver cells (3). The HBV X protein (HBx), an HBV-genome-encoded multifunctional regulator, has been proven to be involved in several cellular processes leading to HCC (5). For instance, HBx interferes with the nucleotide excision repair pathway (6); HBx exerts antiapoptotic effects through the PI3K/Akt pathway and p38/MAPK pathway (7, 8); HBx acts as an epigenetic deregulation agent to modulate the transcription of DNA methyltransferase (DNMT) 1 and DNMT3 (9); HBx promotes telomerase activity by increasing the expression of TERT (10). In addition, it has been reported that anti-HBV drugs, such as telbivudine, entecavir, and interferon-α2b, suppress the growth of HBV-related HCC via downregulation of HBx (11).

Ubiquitination, a posttranslational modification, is responsible for numerous complex cellular processes, including protein degradation, protein-protein interactions, and cellular pathway regulation. During the ubiquitination process, ubiquitin (Ub) is covalently attached to lysine residues on the protein substrate through sequential enzymatic reactions accomplished by ubiquitin-activating enzyme E1, ubiquitin-conjugating enzyme E2, and ubiquitin-protein ligase E3 (12). Neural precursor cell expressed developmentally downregulated gene 4 (NEDD4) is one of E3 Ub ligases that has been identified to exert numerous vital cellular processes, such as proteasomal degradation, membrane protein endocytosis, endosomal trafficking and autophagy regulation (13). Recently, NEDD4 has been reported to play either oncogenic or suppressive roles in multiple human cancers. For example, p21 is the substrate of NEDD4 as well as a key regulator of tumor proliferation in colorectal cancer. NEDD4 could target p21 protein for degradation by increasing the ubiquitylation of p21, and promote cell proliferation. N-myc downstream-regulated gene 1 (NDRG1) inhibits colorectal cancer cell proliferation through emulatively antagonizing NEDD4-mediated ubiquitylation of p21, which suggests an oncogenic role of NEDD4 in colorectal cancer (14). In malignant glioma, researchers found that NEDD4 directly promotes cell migration and invasion, but does not affect the proliferation and apoptosis. Besides, NEDD4 could interact with cyclic nucleotide Ras guanine nucleotide exchange facto (CNrasGEF), increase CNrasGEF polyubiquitination and target CNrasGEF for degradation. Downregulated CNrasGEF promotes cell migration and invasion, and facilitates the effect of NEDD4-induced cell motility, which indicates that NEDD4 exerts an oncogenic function in glioma cell motility through ubiquitination of CNrasGEF (15). However, previous study has reported that NEDD4 interacts with Myc oncoproteins, and targets Myc oncoproteins for ubiquitination and degradation by the ubiquitin conjugating enzymes (E2) UbcH5a and UbcH5b. The histone deacetylase Sirtuin 2 (SIRT2) reduces ubiquitin-proteasome pathway-induced N-Myc protein degradation in neuroblastoma and C-Myc protein degradation in pancreatic cancer through repressing NEDD4 gene transcription by directly binding to NEDD4 gene promoter, which contributes to upregulation of Myc oncoproteins and results in cancer cell proliferation (16). From this perspective, NEDD4 exercises a tumor suppressive function. Recent studies have also found that negative regulation of LATS1 and PTEN might be the mechanisms by which NEDD4 promotes HCC progression (17, 18). However, here we described the opposite function of NEDD4 in HBV-associated HCC.

In this study, we first found that HBV-infected HCC patients with high tumor NEDD4 expression experienced superior cumulative survival over those with low tumor NEDD4 expression and that high NEDD4 expression in HBV-positive cell lines inhibited proliferation, migration, and invasion. Second, we identified 245 proteins that may interact with NEDD4 in HepG2.215 cell lines and found that NEDD4 and HBx interact with each other. Finally, our study demonstrated that NEDD4 induced the degradation of HBx in an ubiquitin-proteasome-dependent manner via K48-linked ubiquitination, which suppressed tumor progression in HBV-positive HCC.

METHODS AND MATERIALS

Patients and Specimens

Samples from a total of 199 HCC patients who underwent surgery were obtained from Department of Hepatobiliary Surgery, The Third Xiangya Hospital, Central South University. The clinical characteristics of the patients were collected and are shown in **Supplementary Table S1**. We divided the patients into two groups: HBV-positive patients (N = 104) and HBV-negative patients (N = 95). For RNA extraction, the tissues were immediately stored in liquid nitrogen until further investigation. All experiments were conducted with the approval of the Ethical Committee of The Third Xiangya Hospital, Central South University.

Cell Culture

HEK293T and HBV-related HCC cell lines, including HepG2.215, HepG3B, SNU182, SNU387, PLC/PRF/5, and MHCC97H, were obtained from the Chinese Academy of Sciences (Shanghai, China). Cells were maintained in Dulbecco's modified Eagle's medium (DMEM) (Gibco, USA) supplemented with 10% fetal bovine serum (FBS) (Gibco, USA) and 1% penicillin/streptomycin (Gibco, USA) at 37°C with 5% CO_2.

Quantitative Reverse Transcription Polymerase Chain Reaction (qRT-PCR)

Total RNA was extracted from liver samples or HCC cells with TRIzol Reagent (Takara, Japan). We then separated and purified total RNA with chloroform, isopropanol, and ethanol. One microgram of RNA was reverse-transcribed into cDNA by the PrimeScript RT reagent Kit (Takara, Japan) according to the manufacturer's instructions, and qRT-PCR analysis was performed using SYBR® Green Master Mix (Takara, Japan). The relative expression of target genes was analyzed and shown as the fold change (2-ΔΔCt). The primer sequences of the target genes were as follows: NEDD4, 5′-GGAGT TGCCAGAGAATGGTT-3′ (forward); 5′-TTGCCATGATAA ACTGCCAT-3′ (reverse). HBX, 5'- TGTCAACAACCGAC CTTGAG-3' (forward); 5'-AAAGTTGCATGGTGCTGGTG-3' (reverse). GAPDH, 5'-GGACCTGACCTGCCGTCTAG-3' (forward); 5'-GTAGCCCAGGATGCCCTTGA-3' (reverse).

Plasmid Construction and Transfection

Expression plasmid constructs, including full-length pcDNA3.1 (+)-Flag-HBx, full-length pcDNA3.1(+)-Myc-NEDD4 (*Homo sapiens*), pcDNA3.1(+)-Myc-NEDD4 catalytic inactive mutant (cysteine 1197 to alanine, *Homo sapiens*), full-length pcDNA3.1 (+)-HA-Ubiquitin (ubiquitin B, UBB, *Homo sapiens*), full-length pcDNA3.1(+)-HA-K48-Ubiquitin (ubiquitin B, UBB, *Homo sapiens*), pcDNA3.1(+)-HA-K63-Ubiquitin (ubiquitin B, UBB, *Homo sapiens*) were all constructed by and purchased from Obio Technology (Shanghai) Corp, Ltd. NEDD4 small-interfering RNA (siRNA) was designed and synthesized by GenePharma (Shanghai, China). A Lipofectamine 3000 Transfection Kit (Invitrogen, L3000-015) was used for transfection. Transfection was performed according to the manufacturer's instructions with minor modifications. Briefly, 293T cells were seeded in 6-well plates at a density of 3×10^5 cells/well. The use of each plasmid was 2.5 μg/well with 5 μl Lipo3000 and 5 μl P3000 according to the manufacturer's instructions. The total amount of transfected plasmids in each well was equalized by adding empty pcDNA3.1(+)-vector.

MTT Assay

We used a 3-(4,5-dimethylthiazol-2-yl)-2,5-diphenyltetrazolium bromide (MTT) kit (Abcam, ab211091) to evaluate cell viability. Cells were inoculated in 96-well plates (1,500 cells per well) for 48 h, and then 20 μl of MTT solution was added to each well and incubated at 37°C for 4 h. After removing the supernatants, 150 μl of DMSO was added to each well, and the absorbance was measured at 570 nm with an automated microplate reader (Thermo Fisher Scientific, USA).

EdU Proliferation Assay

HepG2.215 cells were seeded into 24-well plates and treated for 48 h. Subsequently, according to the instructions of BeyoClick™ EdU Cell Proliferation Kit with Alexa Fluor 488 (Beyotime, Jiangsu, China), EdU solution was added into each well and the cells were incubated for a further 2 h. Then, the cells were washed by PBS and fixed with 4% paraformaldehyde for 20 min. After that, 0.5% Triton X-100 was added to increase the permeability of the cells. Subsequently, the cells were incubated with Click Reaction Mixture for 30 min and stained with Hoechst (1:1000) for 2 min. Finally, the cells were observed using a fluorescence microscope. Edu positive cell rate = number of green fluorescence-labeled cells/number of blue fluorescence-labeled cells × 100%.

Transwell Assay

We used the serum-free DMEM cell suspension at a density of 1×10^5/ml.

Fibronectin and BD™ Matrigel (BD, USA) were precoated on Transwell inserts for the migration assays and invasion assays, respectively.

We added 100 μl of the cell suspension to the upper chamber of the Transwell inserts and 600 μl of DMEM with 10% FBS to the lower chamber. Cells were incubated at 37°C for 24 h for the migration assay and 48 h for the invasion assay. Then, we fixed the cells on the lower insert surface with 4% paraformaldehyde and stained them with 1% crystal violet. Six different microscopic fields of three independent inserts were captured to count the cells.

Western Blotting

Cells were harvested and lysed in RIPA buffer containing protease and phosphatase inhibitors for 30 min on ice. After centrifugating lysates at 14,000 rpm at 4°C for 15 min, we collected the supernatants and determined protein concentrations using the BCA protein assay (Thermo Scientific). Equal amounts of each sample diluted in 5x SDS loading buffer were subjected to SDS-polyacrylamide gel electrophoresis and then transferred to polyvinylidene fluoride (PVDF) membranes (Millipore) for 2 h. Five percent nonfat dry milk dissolved in TBST (150 mM NaCl, 50 mM Tris-HCl, pH 7.5, and 0.05% Tween-20) was used to block the membranes for 2 h, and then the membranes were incubated with primary antibodies overnight at 4°C. The primary antibodies used in this study were GAPDH (1:1000, Abcam, ab8245), NEDD4 (1:1000, Cell Signaling Technology, 2740), HBX (1:1000, Abcam, ab235), and Ki-67 (1:1000, Abcam, ab16667). Then, we washed the membranes three times in TBST and incubated the membranes with the appropriate HRP-conjugated secondary antibodies (1:3000, Beyotime Institute of Biotechnology, A0216, A0208, A0192) for 1.5 h at room temperature. Then, the membranes were washed an additional three times with TBST. The bands on membranes were visualized using an ECL western blotting kit (Millipore).

Coimmunoprecipitation and LC-MS/MS

HepG2.215 cell lines were harvested on ice in modified RIPA buffer containing 50 mM Tris•HCl (pH 7.5), 150 mM NaCl, 0.1% (vol/vol) Triton X-100, 0.5% (wt/vol) sodium deoxycholate, 0.1% (wt/vol) SDS, 1 mM EDTA, 50 mM N-ethylmaleimide, 1 mM NaF, 1 mM Na3VO4, 1 mM PMSF, and 1 μg/ml each of aprotinin, leupeptin, and pepstatin. The cell lysates (approximately 400 μg of total protein) were incubated with an antibody against NEDD4 (4 μl, Cell Signaling Technology, 3607), HBX (4 μl, Abcam, ab2741), Flag-Tag (4 μl, Cell Signaling Technology, 14793) or their IgG control (Cell Signaling Technology, 3452 or 37988) at 4°C overnight. Then, protein-G agarose beads (40 L, Beyotime Biotechnology) were added, and the mixture was incubated at 4°C for another 3 h. The agarose beads were collected, washed, and resuspended in 60 μl of sample buffer containing 50 mM Tris•HCl, pH 7.6, 2% (wt/vol) SDS, 10% (vol/vol) glycerol, 10 mM DTT, and 0.2% bromophenol blue. Afterward, the samples were boiled for 10 min. Liquid chromatography with tandem mass spectrometry (LC-MS/MS) was used to analyze the interacting proteins of NEDD4 in HepG2.215 cell lines. The entire LC-MS/MS procedure was performed by Applied Protein Technology (ATP) Company. The western blotting protocols were reported above. A special secondary antibody (1:1000, Abcam, ab131366), which only recognizes native (nonreduced) antibodies to highly minimize the detection of heavy and light chains, was used to test the IP samples to avoid the influence of the IP antibodies in the IP samples.

Immunofluorescence Staining

HepG2.215 cell lines were seeded on sterile glass coverslips. When cells reached approximately 60% confluence, the growth medium was aspirated. Cells were washed with ice-cold PBS three times before fixing in 4% paraformaldehyde for 30 min. To permeabilize the cells, 0.1% Triton X-100 was added for 15 min at room temperature, and 5% normal goat serum was used to block cells for 30 min. A primary antibody against NEDD4 (1:100, Cell Signaling Technology, 2740) and HBX (1:100, Abcam, ab235) was added, and the cells were incubated overnight at 4°C. After the cells were washed with PBS three times, anti-rabbit IgG (1:500, Cell Signaling Technology, 4413) and anti-mouse IgG (1:500, Cell Signaling Technology, 4408) were added, and the cells were incubated for another 1 h at room temperature. 4',6-diamidino-2-phenylindole (DAPI) was used to counterstain the nuclei. Thereafter, the coverslips were mounted on glass slides with antifade mounting medium (Beyotime, P0126). Thereafter, the samples were viewed under a laser scanning confocal microscope at different wavelengths of 488 nm, 555 nm, and 405 nm. Images were observed under a confocal microscope (Carl Zeiss LSM710, Jena, Germany).

Flag-HBX Degradation Assay

HepG2.215 cell lines were seeded in 6-well plates at a density of 3 × 105 cells/well and transfected with Flag-HBX+empty vector plasmids or Flag-HBX+Myc-NEDD4 plasmids for 72 h. Protein lysates were prepared at the indicated time points after the addition of cycloheximide (CHX) (10 μM). Equal amounts of protein were separated by SDS-PAGE. The levels of Flag-HBX were determined by immunoblotting and quantified at the indicated time points. HepG2.215 cells were seeded in 6-well plates at a density of 3 × 105 cells/well and transfected with Flag-HBX and Myc-NEDD4 plasmids for 72 h. Cells were treated with chloroquine (CQ, 50 μM, Cell Signaling Technology, 14774) or MG132 (20 μM, Selleck, S2619) for another 12 h to block the autophagy-lysosome or ubiquitin-proteasome pathway, respectively. Protein lysates were harvested after that, and the protein level of Flag-HBX was evaluated by western blotting.

In Vivo Ubiquitination Assay

To prepare cell lysates, HepG2.215 cell lines were solubilized in ice-cold modified lysis buffer (50 mM Tris, pH 7.4, 150 mM NaCl, 10% glycerol, 1 mM EDTA, 1 mM EGTA, 1% SDS, 1 mM Na3VO4, 1 mM DTT and 10 mM NaF) supplemented with a protease inhibitor cocktail after transfection with different combinations of plasmids for 72 h. The cell lysate was incubated at 60°C for 10 min. The lysate was then diluted 10 times with modified lysis buffer without SDS. The lysate was incubated with Flag-Tag primary antibody (1:100, Cell Signaling Technology, 14793) for 3 h at 4°C. Protein-G agarose beads (40 L, Beyotime Biotechnology) were added, and the lysate was rotated gently for 8 h at 4°C. The immunoprecipitates were washed at least three times in wash buffer (50 mM Tris, pH 7.4, 150 mM NaCl, 10% glycerol, 1 mM EDTA, 1 mM EGTA, 0.1% SDS, 1 mM DTT and 10 mM NaF). Proteins were recovered by boiling the beads in 5X SDS sample buffer and analyzed by western blotting using the HA-Tag primary antibody (1:1000, Cell Signaling Technology, 3724).

In Vivo Experiments

We used HepG2.215 cells and NEDD4-overexpressing HepG2.215 cells to further verify the function of NEDD4 *in vivo*. Cells suspensions at a concentration of 1×10^7 cells per 100 μl serum-free medium were prepared. *In vivo* experiments were performed in the Animal Laboratory Center, and ethics approval was obtained from the Committee for Experimental Animal Studies of Central South University. Four- to six-week-old male nude (BALB/c nu/nu) mice were subcutaneously injected with 100 μl of cell suspension in the left armpits. Tumor volumes were measured and recorded each week. The mice were sacrificed one month after injection. The tumors were excised, photographed, and weighed.

Immunohistochemistry

Xenograft tumor tissues were fixed in formalin for 48 h and were prepared into paraformaldehyde-fixed, paraffin-embedded sections. The sections were deparaffinized in xylene, rehydrated in ethanol and rinsed in PBS before being treated with TE (10 mM Tris/1 mM EDTA, [pH 9.0]). Then, sections were incubated with 3% hydrogen peroxide. After blocking with 200 μl of normal goat serum (ZSGB-BIO, China) for 1 h at 37°C, sections were incubated with 200 μl Ki-67 primary antibody (1:200, Abcam, ab16667) overnight at 4°C. Then, the sections were washed with PBS three times and incubated with diluted streptavidin-peroxidase HRP conjugates. After that, immunohistochemical staining was performed with hematoxylin before analysis under a microscope. The numbers of Ki-67 positive cells were counted in three random fields of view per slide, and the percentage of Ki-67 positive cells was calculated.

Statistical Analysis

All results were determined from three independent experiments under the same conditions. All data are expressed as the mean ± standard deviation (SD). Differences among groups were compared by Student's t-tests and one-way ANOVA. The Kaplan-Meier test was used to evaluate overall survival (OS) and progression-free survival (PFS). Differences were considered statistically significant when p values were less than 0.05 ($p < 0.05$).

RESULTS

NEDD4 Overexpression Is Associated With Increased OS and PFS in HBV-Positive HCC Patients

Previous studies have revealed that the role of NEDD4 in human cancers remains controversial. Although it has been proven that NEDD4 acts as a proto-oncogene in HCC, studies have not made a distinction between HBV-positive and HBV-negative HCC. Therefore, we first investigated the correlation between NEDD4 expression and HBV exposure through analyzing tumor samples from 104 patients with HBV-positive HCC and 95 patients with HBV-negative HCC using qRT-PCR. We found that there was

no significant difference in NEDD4 expression between HBV-positive and -negative HCC (**Figure 1A**). However, Kaplan-Meier analysis revealed that HBV-positive HCC patients with high NEDD4 expression had significantly longer OS and PFS times (p = 0.0009 and p = 0.017, **Figures 1B, C**). There was no relationship between NEDD4 expression and OS and PFS for patients with HBV-negative HCC (**Figures 1D, E**). These results indicated that NEDD4 might play a tumor-suppressive role in HBV-associated HCC.

NEDD4 Overexpression Inhibits Proliferation and Mobility in HBV-Associated HCC Cell Lines

The role of NEDD4 in HBV-associated HCC remains unclear. Therefore, we first detected basic NEDD4 expression levels in HBV-associated HCC cell lines, including HepG2.215, HepG3B, SNU182, SNU387, PLC/PRF/5, and MHCC97H (**Figures 1F, G**). Next, we selected PLC/PRF/5 cells (high NEDD4 expression) and HepG2.215 cells (low NEDD4 expression) to investigate the regulatory effect of NEDD4 in HBV-associated HCC. We generated NEDD4 knockdown PLC/PRF/5 cells and NEDD4 overexpression HepG2.215 cells (si-NEDD4 and OE-NEDD4) as well as their negative controls (si-Vector; OE-Vector). The expression of NEDD4 in these cells was identified at the mRNA level (**Figure 2A**). The EdU assays were performed to determine the regulatory effect of NEDD4 on proliferation. The results demonstrated that si-NEDD4 significantly increase the ratio of proliferating cells to 36.3% compared with the control (21.1%) in PLC/PRF/5 cells. Conversely, over-expression of NEDD4 markedly decreased the proliferation ability in HepG2.215 cells (**Figure 2B**). In addition, the MTT assay implied that NEDD4 knockdown

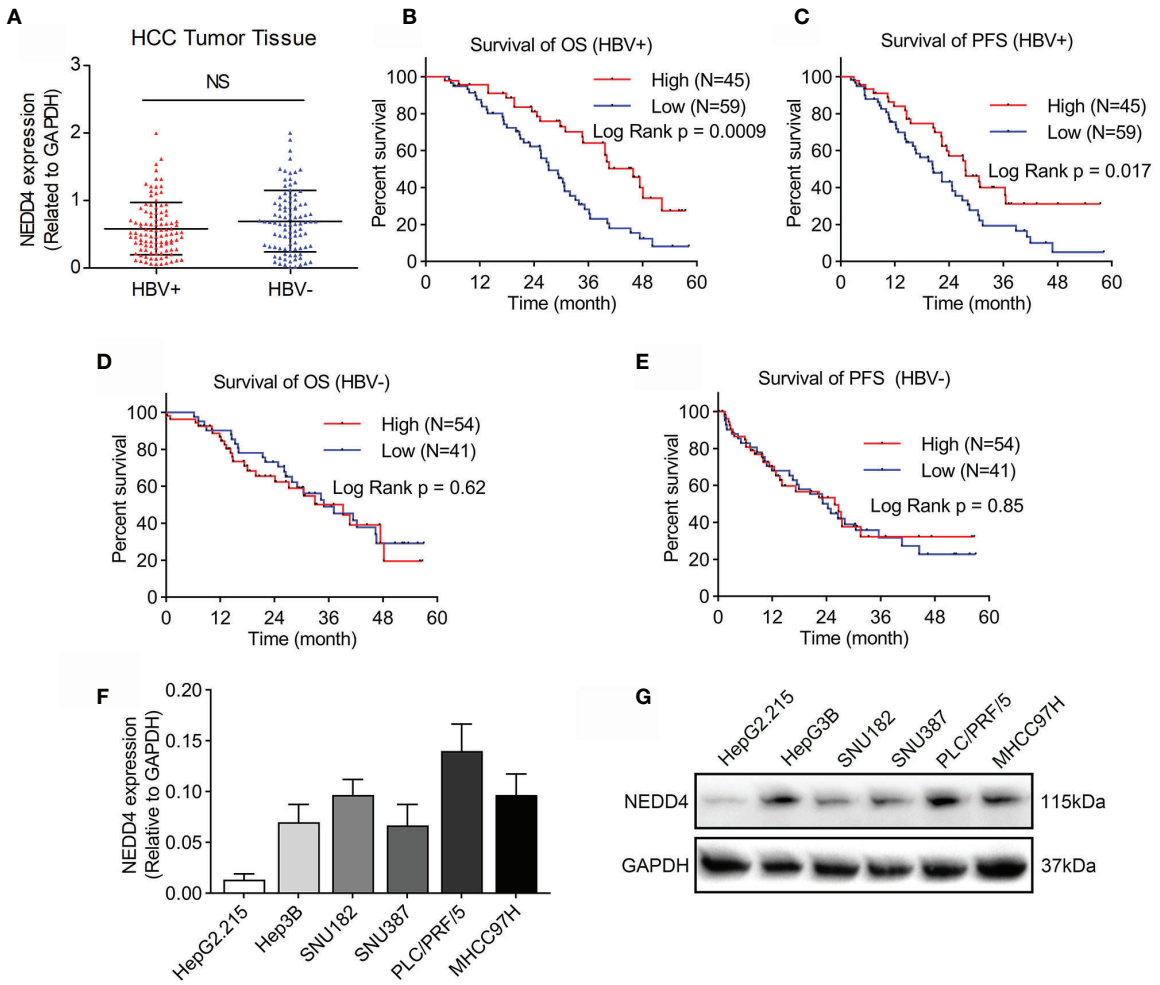

FIGURE 1 | NEDD4 expression in HCC tissues and cell lines. **(A)** NEDD4 expression in HCC specimens with or without HBV infection was evaluated through qRT-PCR. There was no correlation between NEDD4 expression and HBV exposure in HCC tissue. **(B)** and **(C)** High NEDD4 expression was related to better OS and PFS than low NEDD4 expression in patients with HBV-associated HCC. **(D)** NEDD4 expression was unrelated to OS for patients with HBV-negative HCC. **(E)** NEDD4 expression was unrelated to PFS for patients with HBV-negative HCC. **(F)** NEDD4 mRNA expression in HBV-associated cell lines. **(G)** NEDD4 protein expression in HBV-associated cell lines. (Data are presented as the mean ± SD. NS, no significance ($p < 0.05$).

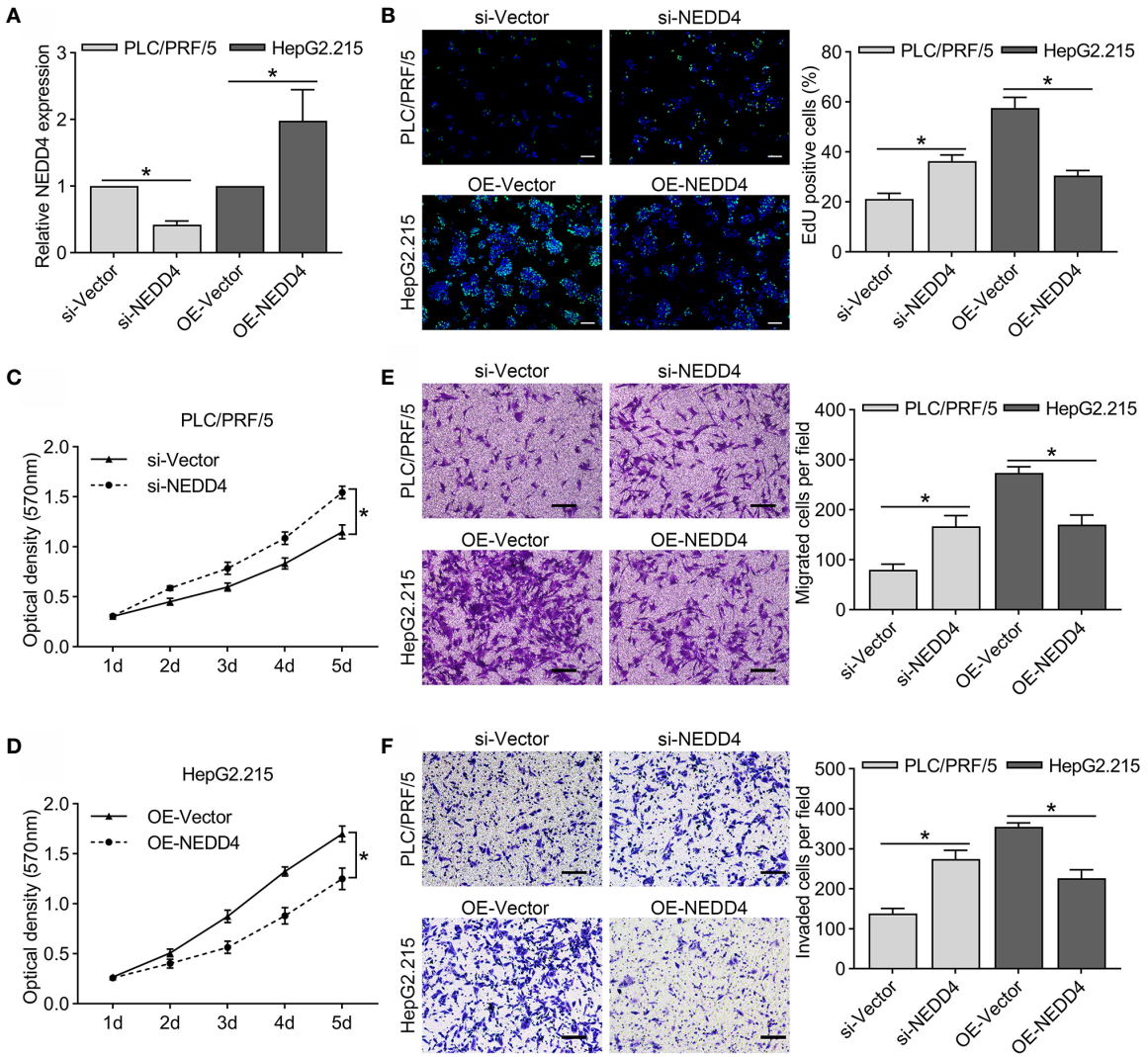

FIGURE 2 | Regulatory effect of NEDD4 in HBV-associated HCC cell lines. **(A)** NEDD4 mRNA expression in NEDD4 knockdown PLC/PRF/5 cells and NEDD4 overexpression HepG2.215 cells as well as their negative controls. **(B)** Edu assay was performed to compare the cell growth ability in NEDD4 knockdown PLC/PRF/5 cells and NEDD4 overexpression HepG2.215 cells with their negative controls (Green fluorescence: EdU, Blue fluorescence: Hoechst). **(C)** Downregulated NEDD4 in PLC/PRF/5 cells promoted proliferation. **(D)** NEDD4 overexpression in HepG2.215 cells inhibited proliferation. **(E)** Downregulated NEDD4 promoted migration in PLC/PRF/5 cells, while upregulated NEDD4 inhibited migration in HepG2.215 cells. **(F)** NEDD4 depletion promoted invasion in PLC/PRF/5 cells, whereas NEDD4 overexpression inhibited invasion in HepG2.215 cells. Data are presented as the mean ± SD. *$p < 0.05$. (si-NEDD4 represents NEDD4 knockdown PLC/PRF/5 cells, and si-Vector represents the negative control; OE-NEDD4 represents NEDD4 overexpression HepG2.215 cells, and OE-Vector represents the negative control) (n = 3 independently replicated experiments; white scale bars: 100 μm, black scale bars: 50 μm).

promoted the proliferation of HBV-associated HCC cells, while NEDD4 overexpression inhibited their growth in a time-dependent manner (**Figures 2C, D**).

We further conducted a Transwell assay to detect cell migration and invasion *in vitro*. We found that the expression of NEDD4 inhibited both migration and invasion in HBV-associated HCC cells (**Figures 2E, F**). Surprisingly, our results were completely opposite to those of previous studies showing that NEDD4 promotes the proliferation and mobility of HBV-negative HCC cells, including SMMC-7721, QGY-7703, and Huh-7 cells (17, 18). These results suggested that molecular interactions between NEDD4 and HBV-associated proteins might exist.

NEDD4 Interacts With HBx in HBV-Associated HCC Cell Lines

To validate the interplay of NEDD4 and proteins relative to HBV infection, we performed coimmunoprecipitation (Co-IP) and LC-MS/MS experiments in HBV-associated hepatocellular cells. We identified 245 proteins that may interact with NEDD4 in HepG2.215 cell lines (**Supplementary document 1**). Surprisingly, we noticed that HBx was involved in the

Co-IP complex (**Supplementary document 1**). HBx is a 17-kDa transcriptional coactivator produced by HBV virus that plays a significant role in HBV-associated hepatocarcinogenesis. Therefore, we further conducted reciprocal Co-IP/western blot assays to confirm again that endogenous NEDD4 and HBx interact with each other in the HepG2.215 cell line (**Figures 3A, B**). Moreover, immunofluorescence assays showed NEDD4 and HBx colocalization in the HepG2.215 cell line (**Figure 3C**).

NEDD4 Diminishes the Expression of HBx at the Protein Level but Not at the mRNA Level

As mentioned above, NEDD4 mostly acts as an E3 ubiquitin ligase that interacts with other proteins to play a role in certain physiological and pathological conditions. Therefore, we conducted qRT-PCR and western blotting assays to investigate HBx expression in NEDD4-overexpressing cells. The results showed that NEDD4 upregulation did not affect the mRNA level of HBx (**Figure 4A**). However, the protein level of HBx was downregulated after NEDD4 overexpressed (**Figure 4B**). These results indicated that NEDD4 negatively regulates HBx in the process of posttranslational modification.

HBx Overexpression Reverses the Suppression of Proliferation and Mobility Induced by NEDD4 Overexpression in HBV-Associated HCC Cells

To determine whether the interplay of NEDD4 and HBx attenuates HBV-associated HCC progression, we upregulated HBx expression in NEDD4-overexpressing cells (OE-HBx+OE-NEDD4) and generated HBx-overexpressing cells (OE-HBx) as a control group (**Figure 4C**). Our results showed that upon upregulation of HBx, NEDD4-induced proliferation suppression was recovered (**Figure 4D**). Similar results were also found for cell metastatic capacity. HBx upregulation compensated for NEDD4-induced migration and invasion inhibition (**Figures 4E, F**). These results suggested that NEDD4 might attenuate the expression of HBx protein to suppress HBV-associated HCC progression.

NEDD4 Induces the Degradation of HBx in a Ubiquitin/Proteasome-Dependent Manner *via* K48-Linked Ubiquitination

Since NEDD4 suppresses the expression of HBx at the protein level and mostly acts as an E3 ubiquitin ligase, we speculated that NEDD4 might affect the degradation of HBx protein. We then evaluated the degradation kinetics of Flag-HBx coexpressed with Myc-NEDD4 or NEDD4 knockdown in 293T cells, and we demonstrated that the Flag-HBx degradation rate was significantly higher when coexpressed with Myc-NEDD4 while significantly lower when knocking down NEDD4 simultaneously (**Figures 5A, B**). The degradation of proteins occurs mainly through the autophagy-lysosome or ubiquitin-proteasome pathway. Thus, we added chloroquine (CQ, 50 μM) or MG132 (10 μM) to block the autophagy-lysosome pathway or ubiquitin-proteasome pathway, respectively. We demonstrated that MG132 reversed the degradation of Flag-HBx mediated by Myc-NEDD4, while CQ had little effect (**Figure 5C**). This result indicated that NEDD4 degraded HBx through the ubiquitin-proteasome pathway instead of the autophagy-lysosome pathway. We further coexpressed HA-ubiquitin, Myc-NEDD4 and Flag-HBx in 293T cells and found that Myc-NEDD4 significantly induced the ubiquitination of Flag-HBx (**Figure 5D**), and the type of HBx ubiquitination modulated by NEDD4 was K48-linked instead of K63-linked (**Figures 5E, F**). Finally, we constructed a plasmid with a catalytically inactive mutant NEDD4 (cysteine 1197 to alanine). The results demonstrated that the catalytically inactive NEDD4 mutant did not induce the ubiquitination of HBx (**Figure 5G**). In summary,

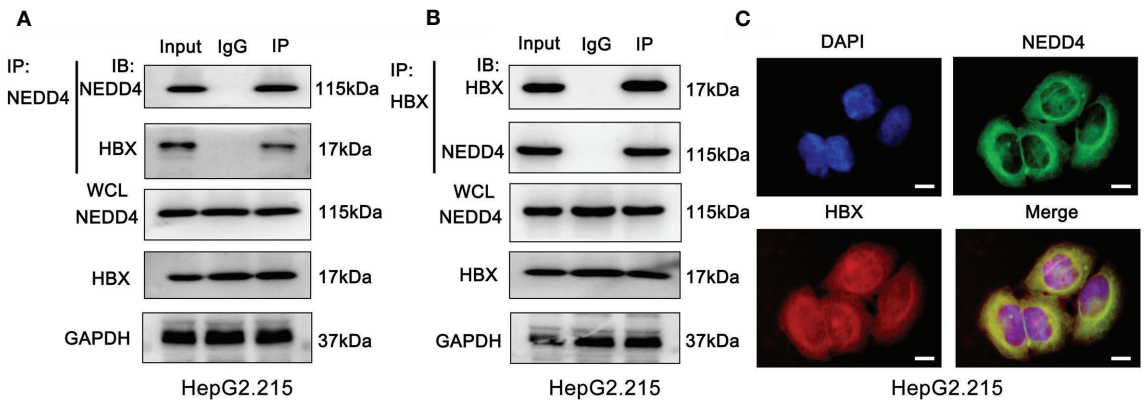

FIGURE 3 | NEDD4 interacts with HBx in HBV-associated hepatocellular cells. **(A)** and **(B)** Coimmunoprecipitation was conducted with NEDD4 and HBx antibodies. The coimmunoprecipitated mixture was separated by SDS-PAGE and evaluated by immunoblotting. NEDD4 and HBx interact with each other in HepG2.215 cells. **(C)** Immunofluorescence assay demonstrated the colocalization of NEDD4 and HBx in HepG2.215 cells (green NEDD4, red HBx, blue, DAPI) (n = 3 independently replicated experiments; white scale bars: 10 μm). IP, Immunoprecipitation; IB, immunoblot; WCL, whole cells lysate.

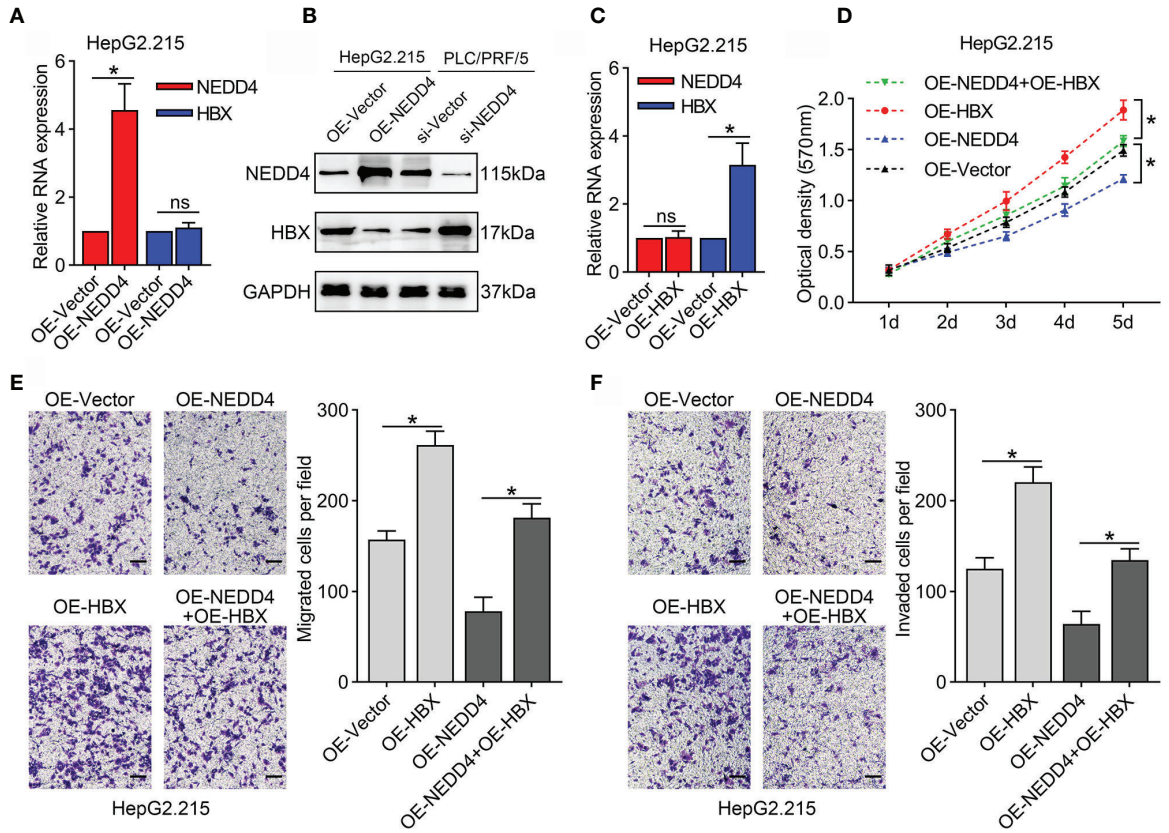

FIGURE 4 | HBx upregulation reverses the suppression of proliferation and mobility induced by NEDD4 overexpression in HBV-associated HCC cells in HepG2.215 cell line. **(A)** NEDD4 upregulation did not affect the mRNA level of HBx. **(B)** The protein level of HBx was downregulated after NEDD4 overexpressed. **(C)** HBx mRNA expression in HBx-overexpressing cells, NEDD4-overexpressing cells, cells overexpressing both HBx and NEDD4, and negative control cells. **(D)** Upon upregulation of HBx, NEDD4-induced proliferation suppression was recovered. **(E)** HBx upregulation compensated for NEDD4-induced migration inhibition. **(F)** NEDD4-induced invasion suppression was reversed after HBx upregulation. Data are presented as the mean ± SD. *$p < 0.05$, NS, no significance ($p > 0.05$). (OE-HBx+OE-NEDD4 represents upregulated HBx in NEDD4 overexpression HepG2.215 cells; OE-HBx represents HBx overexpression HepG2.215 cells; OE-NEDD4 represents NEDD4 overexpression HepG2.215 cells and OE-Vector represents the negative control) (n = 3 independently replicated experiments; scale bars: 50 μm).

NEDD4 might act as an E3 ubiquitin ligase to ubiquitinate HBx through the K48 ubiquitin chain and thus degrade HBx.

NEDD4 Overexpression Inhibits HBV-Associated HCC Progression *In Vivo*

To verify whether NEDD4 upregulation could attenuate the malignant features of HBV-associated HCC *in vivo*, xenograft tumor models were established in nude mice. We noticed that NEDD4 overexpression sharply decreased tumor size compared to that in the control group (**Figure 6A**). Both tumor volume and tumor weight in the OE-NEDD4 group were significantly smaller than those of the control group (**Figures 6B, C**). Subsequently, we measured the expression of Ki-67 (a protein related to proliferation) in xenograft tumors through immunohistochemistry and western blotting. We found that the expression of Ki-67 was diminished in NEDD4-overexpressing xenograft tumors compared to control tumors (**Figures 6D, E**). Taken together, these results further confirmed that NEDD4 upregulation inhibited HBV-associated HCC progression.

DISCUSSION

Here, we used HBV-associated HCC cells to further explore the potential function of NEDD4 in the context of HBV infection. We have clearly described that NEDD4 contributes to inhibiting HBV-associated HCC progression via the NEDD4-HBx interaction, which results from the K48-linked ubiquitination and degradation of HBx by NEDD4.

NEDD4 is frequently overexpressed in many different human malignancies and can act as either an oncogene or a tumor suppressor (19). Recently, several studies revealed that NEDD4 is highly expressed in HCC and participates in HCC progression (17, 18). However, few studies have focused on the correlation between NEDD4 and HBV-associated HCC. In this study, we compared NEDD4 expression between HBV-positive and HBV-negative HCC tumor tissues. Although there was no correlation between NEDD4 expression and HBV exposure, we noticed that HBV-associated HCC patients with high NEDD4 expression had better survival than those with low NEDD4 expression. This result was

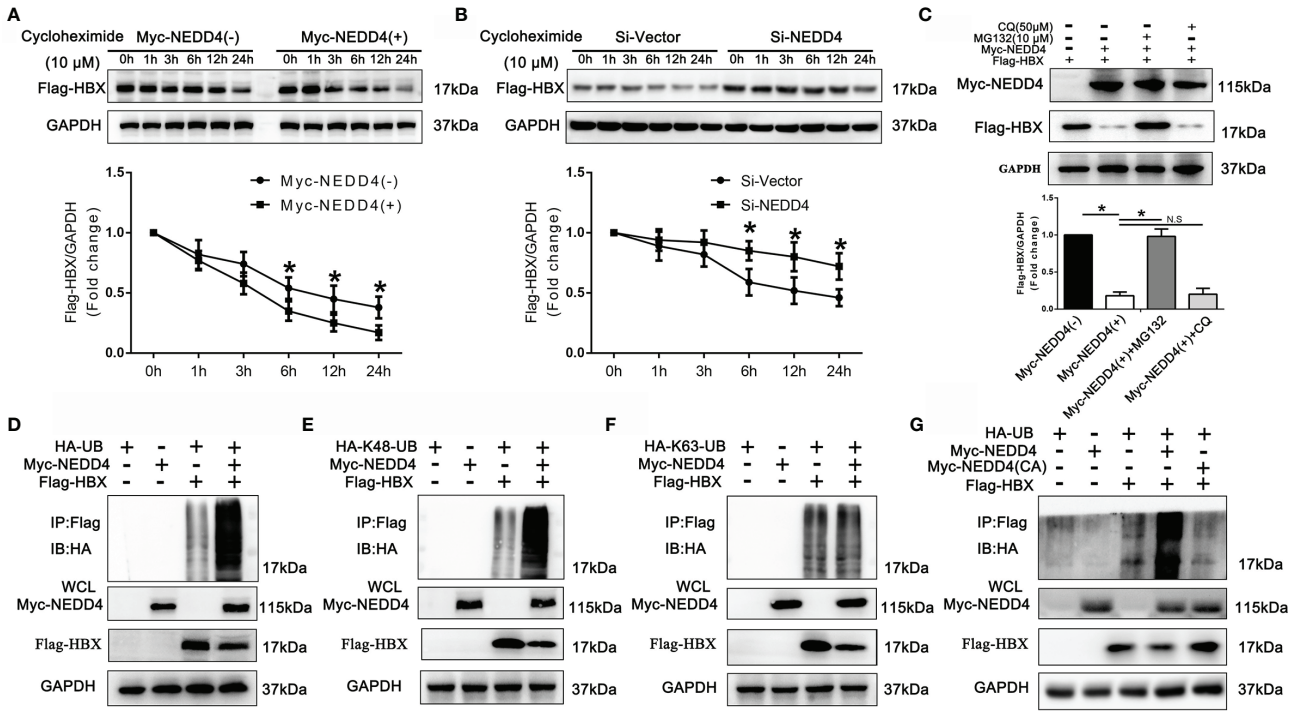

FIGURE 5 | NEDD4 induced the degradation of HBx in a ubiquitin/proteasome-dependent manner via K48-linked ubiquitination. **(A)** Flag-HBx was transfected into 293T cells with Myc-NEDD4 or empty vectors. After transfection of plasmids for 48 h, protein lysates were prepared at the indicated time points after treatment with 10 μM cycloheximide, and the Flag-HBx protein levels were evaluated by western blotting. The results demonstrated that the Flag-HBx degradation rate was significantly higher when HBx was coexpressed with Myc-NEDD4. **(B)** Flag-HBx was transfected into 293T cells with Si-Vector or Si-NEDD4. After transfection for 48 h, protein lysates were prepared at the indicated time points after treatment with 10 μM cycloheximide, and the Flag-HBx protein levels were evaluated by western blotting. The results demonstrated that the Flag-HBx degradation rate was significantly lower with NEDD4 knockdown. **(C)** Flag-HBx and Myc-NEDD4 expression vectors were cotransfected into 293T cells for 48 h, after which 293T cells were treated with chloroquine (CQ, 50 μM) or MG132 (10 μM) for another 12 h. Western blotting demonstrated that MG132 reversed the degradation of Flag-HBx induced by Myc-NEDD4, while CQ had little effect. **(D)** Flag-HBx and HA-Ubiquitin was transfected into 293T cells with Myc-NEDD4 or empty vectors. After transfection of plasmids for 48 h, protein lysates were harvested and Flag-HBx was immunoprecipitated with anti-Flag antibody. Western blotting demonstrated that Myc-NEDD4 significantly induced the ubiquitination of Flag-HBx. **(E)** Flag-HBx and HA-K48-Ubiquitin was transfected into 293T cells with Myc-NEDD4 or empty vectors. After transfection of plasmids for 48 h, protein lysates were harvested and Flag-HBx was immunoprecipitated with anti-Flag antibody. Western blotting demonstrated that Myc-NEDD4 significantly induced the K48-linked ubiquitination of Flag-HBx. **(F)** Flag-HBx and HA-K63 -Ubiquitin was transfected into 293T cells with Myc-NEDD4 or empty vectors. After transfection of plasmids for 48 h, protein lysates were harvested and Flag-HBx was immunoprecipitated with anti-Flag antibody. Western blotting demonstrated that Myc-NEDD4 did not induce the K63-linked ubiquitination of Flag-HBx. **(G)** Flag-HBx and HA-Ubiquitin was transfected into 293T cells with Myc-NEDD4 or Myc-NEDD4 catalytically inactive mutant (cysteine 1197 to alanine). After transfection of plasmids for 48 h, protein lysates were harvested and Flag-HBx was immunoprecipitated with anti-Flag antibody. Western blotting demonstrated that Myc-NEDD4 catalytically inactive mutant did not induce the ubiquitination of Flag-HBx. Data in A and B are presented as the mean ± SD. *$p < 0.05$, NS, no significance ($p > 0.05$). (n = 3 independently replicated experiments). HA-UB, full-length pcDNA3.1(+)-HA tagged-Ubiquitin (ubiquitin B, UBB, *Homo sapiens*); HA-K48-UB, full-length pcDNA3.1(+)-HA tagged-Lys48 Ubiquitin (ubiquitin B, UBB, *Homo sapiens*); HA-K63-UB, pcDNA3.1(+)-HA tagged-Lys63-Ubiquitin (ubiquitin B, UBB, *Homo sapiens*).

quite different from that of Xiaofeng Hang et al., who analyzed 219 HCC patients and demonstrated that NEDD4 overexpression is associated with decreased overall survival (18). Therefore, our focus was to investigate whether the function of NEDD4 was different in HBV-associated HCC. Our findings indicated that NEDD4 upregulation in HBV-associated HCC cell lines inhibited proliferation, migration, and invasion. Although these results were completely opposite to those of previous studies using HBV-negative cell lines, they were not incomprehensible because the regulatory effect of NEDD4 in cancer remains elusive. It has been reported that NEDD4 could negatively regulate the tumor suppressor PTEN via polyubiquitination for degradation or positively modulate PTEN nuclear transport through monoubiquitination (20, 21). However, there may be no correlations between NEDD4 and PTEN (22, 23). In breast cancer, Jia Liu et al. found that depletion of β-TRCP or inactivation of CKIδ increased NEDD4 abundance, leading to the downregulation of PTEN, which activated the oncogenic mTOR/Akt pathway and promoted cell proliferation (24). In contrast, NEDD4 reduced the PIP5Kα-dependent PIP2 pool to inhibit breast cancer cell proliferation through the PI3K/Akt pathway (25). NEDD4 downregulation in breast cancer cells elevated HER3 expression and enhance AKT and ERK signaling, resulting in cell proliferation and invasion (26). In gastric carcinoma, the role of

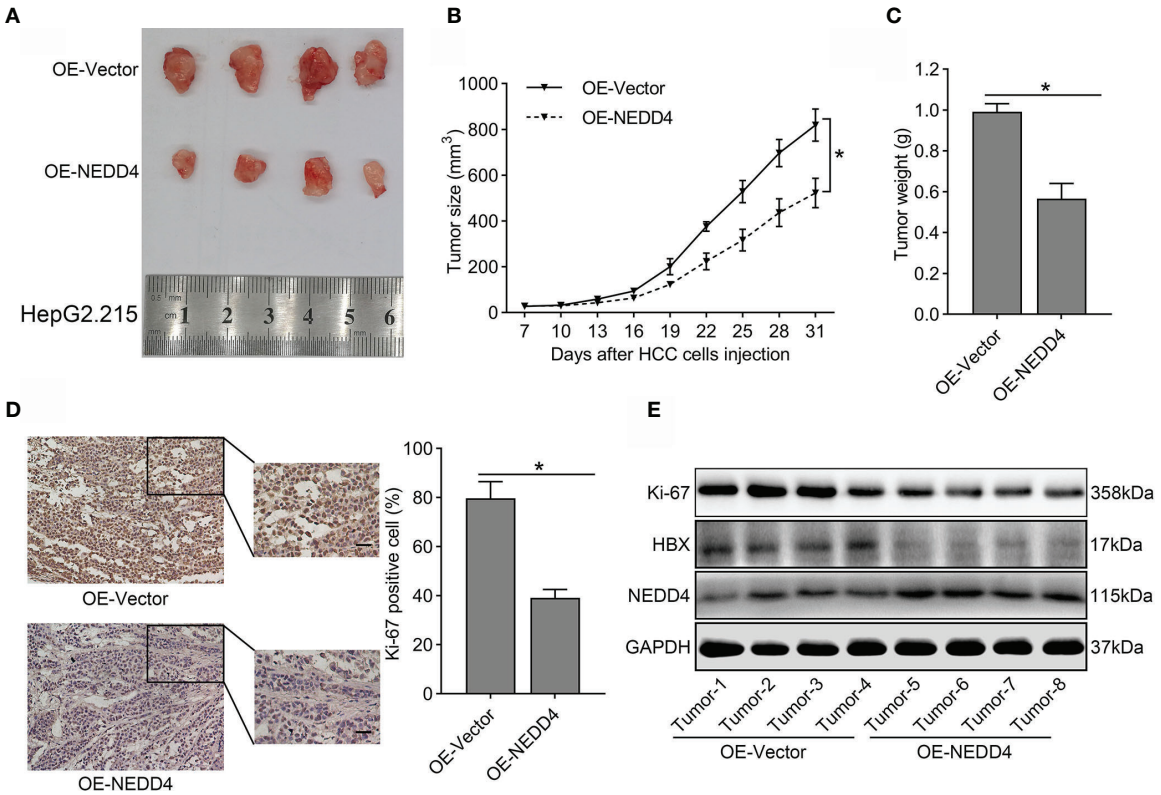

FIGURE 6 | The tumor suppressor role of NEDD4 in HBV-associated HCC *in vivo*. **(A)** A representative photograph of xenograft tumors from mice injected with NEDD4-overexpressing HepG2.215 cells and negative control cells. **(B)** A tumor size curve shows the volume variation of the xenografts from mice injected with NEDD4-overexpressing HepG2.215 cells and control cells. **(C)** Weight of the tumors from mice injected with NEDD4-overexpressing HepG2.215 cells and control cells were measured after the mice were killed. **(D)** Representative images of immunohistochemical staining patterns and western blotting bands for Ki-67 in xenograft tumors in the NEDD4 overexpression group and control group. **(E)** Western blot results showed that over-expression of NEDD4 could markedly inhibit the expression of HBX and Ki-67 in xenograft tumors. Data are presented as the mean ± SD. *p < 0.05 (OE-NEDD4 represents the NEDD4 overexpression group, and OE-Vector represents the control group.) (n = 3 independently replicated experiments; scale bars: 50 μm).

NEDD4 is equally controversial. Kim et al. found that NEDD4 was expressed in the majority of gastric cancer tissue, while Zhen Yang et al. observed no significant difference in NEDD4 expression between primary gastric tumors and tumor adjacent tissues (23, 27). The expression level of NEDD4 was decreased from gastric dysplasia to gastric carcinoma (23). Based on the ambiguous function of NEDD4 in human cancers and our discrepant discovery in HBV-associated HCC, we speculated that NEDD4 might participate in favorable regulation during the process of hepatocarcinogenesis induced by HBV infection.

To further explore the mechanism of NEDD4 in HBV-associated HCC, we screened 245 proteins interacting with NEDD4 and noticed that HBx was a downstream target in this process. HBx is one of the proteins encoded by the HBV genome, which participates in viral replication and infection, the transactivation of cellular promoters and enhancers through protein-protein interaction, and the regulation of host cellular genes and signal transduction cascades (5). There is growing evidence that Hbx is responsible for the pathogenesis of HBV-related liver diseases, and downregulation of HBx is one of the therapeutic mechanisms for HBV-related HCC (11). In this study, we observed that NEDD4 interacted with HBx and negatively controlled the protein expression of HBx. HBx upregulation could reverse the suppression of proliferation and mobility induced by NEDD4 overexpression. These findings indicate that the different regulatory effects of NEDD4 in HBV-associated HCC cells might be attributed to the NEDD4-HBx interaction.

Thus, the question remains regarding how NEDD4 regulates HBx. NEDD4 is a member of the E3 ubiquitin ligase family and exerts its functions to some extent through degradative ubiquitination of its downstream substrates in both physiological and pathological conditions (13, 19–21, 28). However, only a few previous studies have concentrated on the role of the E3 ubiquitin ligase in HCC. Susie A. Lee et al. found that upregulated NEDD4 was correlated with low Spry2 protein levels in HCC and confirmed that depletion of NEDD4 decreased ubiquitinated levels of Spry2, which suggested a possible role of NEDD4 in Spry2 degradation (29). Another study indicated that NEDD4 regulated the degradation of GUCD1, whose function is to regulate normal and abnormal cell growth in the liver, through the ubiquitin-proteasome system (30). Neither study directly explained the association between NEDD4-induced degradative ubiquitination

and hepatocarcinogenesis. On the other hand, previous studies demonstrated that HBx could be recognized as a substrate by E3 ubiquitin ligases for degradation (31). For example, TRIM5γ could recruit TRIM31 and form a TRIM5γ-TRIM31-HBx complex that promotes proteasomal degradation of HBx (32). These findings indicated that Hbx may be a downstream substrate of NEDD4 and regulated through ubiquitination-dependent degradation. In addition, protein degradation can be mediated by the ubiquitin-proteasome pathway or the autophagy-lysosome pathway (33, 34). The type of ubiquitin chain linkage determines the fate of the target substrate. Lys48-linked polyubiquitin chains often label proteins for degradation, while K63-linked ubiquitination usually regulates protein functions or degradation through the lysosomal pathway (28). In this study, for the first time, we verified that NEDD4 promotes the degradation of HBx. We used chloroquine or MG132 to block the autophagy-lysosome pathway or ubiquitin-proteasome pathway, respectively, and confirmed that NEDD4 degrades HBx through the ubiquitin-proteasome pathway. Our in-depth analysis indicated that NEDD4 ubiquitinates and degrades HBx via a K48 ubiquitin chain. These findings suggested that Hbx may be an unveiled substrate of NEDD4 and could explain the discrepant function of NEDD4 in HBV-associated HCC.

In summary, our study first demonstrated that NEDD4 expression was irrelevant to HBV exposure in HCC tumor tissue but that high NEDD4 expression was related to a better OS and PFS than low expression in patients with HBV-associated HCC. Second, we found that NEDD4 inhibited proliferation, migration, and invasion in HBV-related HCC cell lines. Moreover, we identified that NEDD4 interacts with HBx and negatively controls HBx expression at the protein level but not at the mRNA level. HBx upregulation reversed the suppression of proliferation and mobility induced by NEDD4 overexpression. Furthermore, we confirmed that NEDD4 induced the degradation of HBx in a ubiquitin/proteasome-dependent manner via K48-linked ubiquitination. Finally, the tumor suppressor role of NEDD4 in HBV-associated HCC was observed *in vivo*. Our research provides new insight into the function of NEDD4 in HCC. However, there are still some limitations to this study. First, evaluating the upstream and/or downstream signal transduction pathways associated with the NEDD4-HBx complex is of great importance. Second, the discrepant role of NEDD4 in human cancers is attributed to the dual regulation of PTEN, but the regulatory effect of NEDD4 on PTEN in HBV-associated HCC remains unclear. These limitations will be the focus of our future study.

DATA AVAILABILITY STATEMENT

The raw data supporting the conclusions of this article will be made available by the authors, without undue reservation.

ETHICS STATEMENT

The studies involving human participants were reviewed and approved by the Ethical Committee of The Third Xiangya Hospital, Central South University. The patients/participants provided their written informed consent to participate in this study. The animal study was reviewed and approved by the Committee for Experimental Animal Studies of Central South University.

AUTHOR CONTRIBUTIONS

TW performed the experiments. TW wrote the initial draft of the manuscript. TW, ZL, BT, TyW, JW, and FH contributed to the conceptual idea, the experimental design of the study, and the editing of the manuscript. All authors contributed to the article and approved the submitted version.

FUNDING

This study was financially supported by the Provincial Natural Science Foundation of Hunan (2017JJ2336) and the Changzhutan National Independent Innovation Demonstration Zone special project (2017XK2108).

SUPPLEMENTARY MATERIAL

The Supplementary Material for this article can be found online at: https://www.frontiersin.org/articles/10.3389/fonc.2021.625169/full#supplementary-material

REFERENCES

1. Forner A, Reig M, Bruix J. Hepatocellular carcinoma. *Lancet* (2018) 391:1301–14. doi: 10.1016/S0140-6736(18)30010-2
2. Bray F, Ferlay J, Soerjomataram I, Siegel RL, Torre LA, Jemal A. Global cancer statistics 2018: GLOBOCAN estimates of incidence and mortality worldwide for 36 cancers in 185 countries. *CA Cancer J Clin* (2018) 68:394–424. doi: 10.3322/caac.21492
3. Ringelhan M, O'Connor T, Protzer U, Heikenwalder M. The direct and indirect roles of HBV in liver cancer: prospective markers for HCC screening and potential therapeutic targets. *J Pathol* (2015) 235:355–67. doi: 10.1002/path.4434
4. Bouchard MJ, Schneider RJ. The enigmatic X gene of hepatitis B virus. *J Virol* (2004) 78:12725–34. doi: 10.1128/JVI.78.23.12725-12734.2004
5. Ali A, Abdel-Hafiz H, Suhail M, Al-Mars A, Zakaria MK, Fatima K, et al. Hepatitis B virus, HBx mutants and their role in hepatocellular carcinoma. *World J Gastroenterol* (2014) 20:10238–48. doi: 10.3748/wjg.v20.i30.10238
6. Qadri I, Fatima K, Abde LHH. Hepatitis B virus X protein impedes the DNA repair via its association with transcription factor, TFIIH. *BMC Microbiol* (2011) 11:48. doi: 10.1186/1471-2180-11-48
7. Lee YI, Kang-Park S, Do SI, Lee YI. The hepatitis B virus-X protein activates a phosphatidylinositol 3-kinase-dependent survival signaling cascade. *J Biol Chem* (2001) 276:16969–77. doi: 10.1074/jbc.M011263200
8. Kuo TC, Chao CC. Hepatitis B virus X protein prevents apoptosis of hepatocellular carcinoma cells by upregulating SATB1 and HURP expression. *Biochem Pharmacol* (2010) 80:1093–102. doi: 10.1016/j.bcp.2010.06.003

9. Pogribny IP, Rusyn I. Role of epigenetic aberrations in the development and progression of human hepatocellular carcinoma. *Cancer Lett* (2014) 342:223–30. doi: 10.1016/j.canlet.2012.01.038
10. Liu YC, Chen CJ, Wu HS, Chan DC, Yu JC, Yang AH, et al. Telomerase and c-myc expression in hepatocellular carcinomas. *Eur J Surg Oncol* (2004) 30:384–90. doi: 10.1016/j.ejso.2004.01.003
11. Zhang S, Gao S, Zhao M, Liu Y, Bu Y, Jiang Q, et al. Anti-HBV drugs suppress the growth of HBV-related hepatoma cells via down-regulation of hepatitis B virus X protein. *Cancer Lett* (2017) 392:94–104. doi: 10.1016/j.canlet.2017.02.003
12. Pickart CM, Eddins MJ. Ubiquitin: structures, functions, mechanisms. *Biochim Biophys Acta* (2004) 1695:55–72. doi: 10.1016/j.bbamcr.2004.09.019
13. Boase NA, Kumar S. NEDD4: The founding member of a family of ubiquitin-protein ligases. *Gene* (2015) 557:113–22. doi: 10.1016/j.gene.2014.12.020
14. Zhang S, Yu C, Yang X, Hong H, Lu J, Hu W, et al. N-myc downstream-regulated gene 1 inhibits the proliferation of colorectal cancer through emulative antagonizing NEDD4-mediated ubiquitylation of p21. *J Exp Clin Cancer Res* (2019) 38:490. doi: 10.1186/s13046-019-1476-5
15. Zhang H, Nie W, Zhang X, Zhang G, Li Z, Wu H, et al. NEDD4-1 regulates migration and invasion of glioma cells through CNrasGEF ubiquitination in vitro. *PloS One* (2013) 8:e82789. doi: 10.1371/journal.pone.0082789
16. Liu PY, Xu N, Malyukova A, Scarlett CJ, Sun YT, Zhang XD, et al. The histone deacetylase SIRT2 stabilizes Myc oncoproteins. *Cell Death Differ* (2013) 20:503–14. doi: 10.1038/cdd.2012.147
17. Zheng H, Ke X, Li D, Wang Q, Wang J, Liu X, et al. NEDD4 promotes cell growth and motility in hepatocellular carcinoma. *Cell Cycle* (2018) 17:728–38. doi: 10.1080/15384101.2018.1440879
18. Hang X, Zhu S, Di H, Wu Z, Chu K, Wang J, et al. NEDD4 Depletion Inhibits Hepatocellular Carcinoma Growth via Targeting PTEN. *Cell Physiol Biochem* (2016) 39:768–79. doi: 10.1159/000445667
19. Wang ZW, Hu X, Ye M, Lin M, Chu M, Shen X. NEDD4 E3 ligase: Functions and mechanism in human cancer. *Semin Cancer Biol* (2020). 67(2):92–101. doi: 10.1016/j.semcancer.2020.03.006
20. Wang X, Trotman LC, Koppie T, Alimonti A, Chen Z, Gao Z, et al. NEDD4-1 is a proto-oncogenic ubiquitin ligase for PTEN. *Cell* (2007) 128:129–39. doi: 10.1016/j.cell.2006.11.039
21. Trotman LC, Wang X, Alimonti A, Chen Z, Teruya-Feldstein J, Yang H, et al. Ubiquitination regulates PTEN nuclear import and tumor suppression. *Cell* (2007) 128:141–56. doi: 10.1016/j.cell.2006.11.040
22. Chen Y, van de Vijver MJ, Hibshoosh H, Parsons R, Saal LH. PTEN and NEDD4 in Human Breast Carcinoma. *Pathol Oncol Res* (2016) 22:41–7. doi: 10.1007/s12253-015-9971-2
23. Yang Z, Yuan XG, Chen J, Lu NH. Is NEDD4-1 a negative regulator of phosphatase and tensin homolog in gastric carcinogenesis? *World J Gastroenterol* (2012) 18:6345–8. doi: 10.3748/wjg.v18.i43.6345
24. Liu J, Wan L, Liu P, Inuzuka H, Liu J, Wang Z, et al. SCF(beta-TRCP)-mediated degradation of NEDD4 inhibits tumorigenesis through modulating the PTEN/Akt signaling pathway. *Oncotarget* (2014) 5:1026–37. doi: 10.18632/oncotarget.1675
25. Tran MH, Seo E, Min S, Nguyen QT, Choi J, Lee UJ, et al. NEDD4-induced degradative ubiquitination of phosphatidylinositol 4-phosphate 5-kinase alpha and its implication in breast cancer cell proliferation. *J Cell Mol Med* (2018) 22:4117–29. doi: 10.1111/jcmm.13689
26. Huang Z, Choi BK, Mujoo K, Fan X, Fa M, Mukherjee S, et al. The E3 ubiquitin ligase NEDD4 negatively regulates HER3/ErbB3 level and signaling. *Oncogene* (2015) 34:1105–15. doi: 10.1038/onc.2014.56
27. Kim SS, Yoo NJ, Jeong EG, Kim MS, Lee SH. Expression of NEDD4-1, a PTEN regulator, in gastric and colorectal carcinomas. *APMIS* (2008) 116:779–84. doi: 10.1111/j.1600-0463.2008.00999.x
28. Zou X, Levy-Cohen G, Blank M. Molecular functions of NEDD4 E3 ubiquitin ligases in cancer. *Biochim Biophys Acta* (2015) 1856:91–106. doi: 10.1016/j.bbcan.2015.06.005
29. Lee SA, Ladu S, Evert M, Dombrowski F, De Murtas V, Chen X, et al. Synergistic role of Sprouty2 inactivation and c-Met up-regulation in mouse and human hepatocarcinogenesis. *Hepatology* (2010) 52:506–17. doi: 10.1002/hep.23681
30. Bellet MM, Piobbico D, Bartoli D, Castelli M, Pieroni S, Brunacci C, et al. NEDD4 controls the expression of GUCD1, a protein upregulated in proliferating liver cells. *Cell Cycle* (2014) 13:1902–11. doi: 10.4161/cc.28760
31. Minor MM, Slagle BL. Hepatitis B virus HBx protein interactions with the ubiquitin proteasome system. *Viruses* (2014) 6:4683–702. doi: 10.3390/v6114683
32. Tan G, Yi Z, Song H, Xu F, Li F, Aliyari R, et al. Type-I-IFN-Stimulated Gene TRIM5gamma Inhibits HBV Replication by Promoting HBx Degradation. *Cell Rep* (2019) 29:3551–3563 e3553. doi: 10.1016/j.celrep.2019.11.041
33. Lecker SH, Goldberg AL, Mitch WE. Protein degradation by the ubiquitin-proteasome pathway in normal and disease states. *J Am Soc Nephrol* (2006) 17:1807–19. doi: 10.1681/ASN.2006010083
34. Klionsky DJ, Emr SD. Autophagy as a regulated pathway of cellular degradation. *Science* (2000) 290:1717–21. doi: 10.1126/science.290.5497.1717

Conflict of Interest: The authors declare that the research was conducted in the absence of any commercial or financial relationships that could be construed as a potential conflict of interest.

frontiers in Oncology

REVIEW
published: 31 March 2021
doi: 10.3389/fonc.2021.659049

Exploring the Roles of HERC2 and the NEDD4L HECT E3 Ubiquitin Ligase Subfamily in p53 Signaling and the DNA Damage Response

*Nicholas A. Mathieu, Rafael H. Levin and Donald E. Spratt**

Gustaf H. Carlson School of Chemistry and Biochemistry, Clark University, Worcester, MA, United States

OPEN ACCESS

Edited by:
Jean Borges Bertoldo, Martin Luther University of Halle-Wittenberg, Germany

Reviewed by:
Arun Upadhyay, Northwestern University, United States
Khosrow Rezvani, University of South Dakota, United States
Jason Luke Parsons, University of Liverpool, United Kingdom

***Correspondence:**
Donald E. Spratt
dspratt@clarku.edu

Specialty section:
This article was submitted to Cancer Molecular Targets and Therapeutics, a section of the journal Frontiers in Oncology

Received: *26 January 2021*
Accepted: *16 March 2021*
Published: *31 March 2021*

Citation:
Mathieu NA, Levin RH and Spratt DE (2021) Exploring the Roles of HERC2 and the NEDD4L HECT E3 Ubiquitin Ligase Subfamily in p53 Signaling and the DNA Damage Response. Front. Oncol. 11:659049. doi: 10.3389/fonc.2021.659049

Cellular homeostasis is governed by the precise expression of genes that control the translation, localization, and termination of proteins. Oftentimes, environmental and biological factors can introduce mutations into the genetic framework of cells during their growth and division, and these genetic abnormalities can result in malignant transformations caused by protein malfunction. For example, p53 is a prominent tumor suppressor protein that is capable of undergoing more than 300 posttranslational modifications (PTMs) and is involved with controlling apoptotic signaling, transcription, and the DNA damage response (DDR). In this review, we focus on the molecular mechanisms and interactions that occur between p53, the HECT E3 ubiquitin ligases WWP1, SMURF1, HECW1 and HERC2, and other oncogenic proteins in the cell to explore how irregular HECT-p53 interactions can induce tumorigenesis.

Keywords: HECT E3 ubiquitin ligases, WWP1, HERC2, HECW1, SMURF1, p53, DNA damage response

INTRODUCTION

Cell growth and division is controlled by the regulated synthesis and degradation of proteins that signal for and carry out the replication of DNA. This requires the timely expression and removal of proteins at specific checkpoints during the cell cycle to ensure proper cell division and homeostasis (1). When this delicate cellular equilibrium becomes imbalanced, unregulated cell division can occur and lead to the development of cancer. To protect against the formation of cancers, the cell has evolved an intricate network of proteins that work to recognize, target, and repair genetic abnormalities prior to its division. If significant cellular stress is recognized by these surveillance proteins, they will initiate a caspase cascade that activates lethal regulatory cell death (RCD) pathways, thereby preventing that cell from undergoing replication (2–9). Perhaps the most important protein involved in regulating these vital cellular activities is the tumor suppressor protein p53. Generally considered the "guardian of the genome", p53 is a 43.7 kDa protein capable of undergoing more than 300 unique post translational modifications (i.e. phosphorylation (10), acetylation (11), methylation (12), SUMOylation (13), O-GlcNAcylation (14)) and interacts with a variety of proteins to dictate cellular fate following S-phase DNA duplication (15–20). One prominent PTM involved with regulating p53 activity under genotoxic and carcinogenic

environments is ubiquitylation—a catalytic process that is carried out on p53 by select members of the homologous to E6AP *C*-terminus (HECT) E3 ubiquitin ligase family (21–24).

Over the past two decades, HECT-related cancer research has focused on the founding member of the HECT E3 ligase family, E6 associate protein (E6AP) (25–30). There are many studies that have cemented E6AP as a critical regulator of biochemical processes involved in the development of cervical and prostate cancer. For example, E6AP has been shown to interact with the human papilloma virus (HPV) protein E6 to target p53 for cellular degradation to produce unregulated cell division in the female cervical tissues (25). *In vivo* studies have also linked E6AP to metastatic forms of prostate cancer by acting to reduce tumor suppressor protein p27 expression levels in prostate gland cells (26, 30). Recent studies have also found that the members of the NEDD4L subfamily of the HECT E3 ubiquitin ligases—specifically WWP1, SMURF1, and HECW1—as well as the large HECT E3 ubiquitin ligase HERC2, are linked to the pathogenesis of prostate (31), lung (32–34), colon (35–38), breast (39, 40), thyroid (41), gastric (42), liver (43), oral (44), and ovarian cancers (45, 46).

This review aims to consolidate and examine the mounting literature on how additional members of the HECT E3 ubiquitin ligase family play integral roles in regulating DNA repair and p53 cellular activities. Here we explore and summarize the specific pathways, structures, and catalytic mechanisms used by WWP1, SMURF1, HECW1 and HERC2, and how their malfunction can result in oncogenesis. We also discuss developing a framework for future HECT-based cancer research that builds toward an improved overall understanding of oncogenic processes in the cell. Research on the interplay between these important protein networks will provide the necessary knowledge for developing novel treatment methods that can slow or even prevent the progression of HECT-dependent p53-related cancers.

Abbreviations: APC, Anaphase promoting complex; ATM, Ataxia telangiectasia mutated kinase; ATR, Ataxia telangiectasia and Rad3 related kinase; BARD1, BRCA1 associated RING domain protein 1; Bax, Bcl-2 associated X protein; Bcl2 - B-cell lymphoma 2; BRCA1, Breast cancer gene 1; ChIP, Chromatin immunoprecipitation assays; CPH, Cullin-7-PARC-HERC2 domain; Cyt-b5, Cytochrome-b5 like domain; DDR, DNA damage response; DOC, Downregulated in ovarian cancer domain; DSB, Double strand break; E1, Ubiquitin activating enzyme; E2, Ubiquitin conjugating enzyme; E3, Ubiquitin ligase; H2AX, Histone 2A family member X; HECT, Homologous to E6AP C-terminus; HECW1, HECT, C2, and WW-domain containing protein 1; HECW2, HECT, C2, and WW-domain containing protein 2; HERC, HECT and RLD containing; HERC2 - HECT and RLD containing protein 2; LATS1, Large tumor suppressor kinase 1; MAPK8, Mitogen activated protein kinase 8; MDC1, Mediator of DNA damage checkpoint 1; MDM2, Mouse double minute 2; MDMX, Mouse double minute 4 (aka MDM4); MIB, Mind bomb domain; MMP2, Matrix metallopeptidase 2; MMP9, Matrix metallopeptidase 9; MRE11, Meiotic recombination 11; NBS1, Nijmegen breakage syndrome 1; NEDD4, Neuronal precursor cell-expressed developmentally downregulated 4; NEURL4, Neuralized E3 ubiquitin protein ligase 4; p53, Tumor suppressor protein p53; PIKK, Phosphatidylinositol 3-kinase-like protein kinase; PPxY or PY, proline-rich motif; PTM, Post translational modification; RAD50, Radiation sensitive protein 50; RAP80, Receptor associated protein 80; RBR, RING-between-RING, RING-BRcat-Rcat; RCD, Regulatory cell death; RING, Really interesting new gene; RLD, Regulator of chromosome condensation 1-like domain; RNF11, RING finger protein 11; RNF8, RING finger protein 8; RUNX2, Runt-related transcription factor 2; Smad2, Mothers against decapentplegic homolog 2; Smad7, Mothers against decapentplegic homolog 7; SMURF1, SMAD ubiquitylation regulatory factor 1; SMURF2, SMAD ubiquitylation regulatory factor 2; TGF-β, Transforming growth factor beta; TRAIL, TNR-related apoptosis-inducing ligand; TβR-I, TGF-β receptor I; UBE2N, Ubiquitin conjugating E2 enzyme UBE2N (aka Ubc13); WW, Tryptophan-tryptophan domain; WWP1, WW-domain containing protein 1; WWP2, WW-domain containing protein 2; ZF, Zinc finger.

UBIQUITYLATION—A BRIEF OVERVIEW

Ubiquitylation involves the post-translational attachment of ubiquitin, a small 8.6 kDa protein, on to a substrate protein by an E1-E2-E3 enzymatic cascade (47–49). The human genome codes for two ubiquitin specific E1 enzymes (i.e. UBE1 and UBE1L2), 38 distinct E2 enzymes (ex. UBE2D3, UBE2L3, UBE2C, etc.) and over 1,000 unique E3 ligases (50). As ubiquitin is passed along the ubiquitylation signaling enzyme cascade (E1 to E2 to E3), the attachment of ubiquitin becomes more specific to ensure that the precise target protein is modified. This specificity from the ubiquitylation-signaling pathway can regulate various intracellular processes including protein turnover, cell cycle progression (51), apoptosis (52), cell differentiation and development (51), immune response and inflammation (53), intracellular trafficking (54), signal transduction (23), DNA transcription and repair (55), viral infection (53) and more. For the cell to carry out these processes, ubiquitin is first activated by an ubiquitin activating enzyme (E1; EC 6.2.1.45) through an ATP-dependent mechanism to form a thioester bond between the *C*-terminal carboxyl of ubiquitin and the catalytic cysteine of the E1. The ubiquitin is then transferred to an ubiquitin conjugating enzyme (E2; EC 2.3.2.23) *via* a trans-thiolation reaction to form a thioester bond between the *C*-terminus of ubiquitin and the conserved catalytic cysteine residue of the E2 (47, 56–58). The E2~ubiquitin complex next interacts with an ubiquitin ligase (E3) to properly coordinate the transfer of ubiquitin on to a specific lysine of the target substrate protein. Recent studies have also demonstrated that under specific cellular conditions the E3 ligases are able to catalyze the attachment of ubiquitin on to cysteine, threonine and *N*-terminal methionine residues of select target proteins (59–61). While the specific function of these alternative ubiquitin substrate attachments is not fully understood and requires further examination, they do add a further dimension to the permutations that can occur with the cellular ubiquitin machinery.

There are several different classes of E3 ubiquitin ligases found in humans that include the really interesting new gene finger domain-containing (RING; EC 2.3.2.27) (62), U-box (63), RING-between-RING (RBR; also known as RING-BRcat-Rcat; EC 2.3.2.31) (64) and HECT (E.C. 2.3.2.26) E3 ubiquitin ligases. The RING E3 ubiquitin ligases are the largest and most widely studied family of E3 ligases with over 600 members identified in the human genome (65). During ubiquitylation, these enzymes act as protein scaffolds that orient the E2~ubiquitin thiolester complex and target substrate to allow for efficient ubiquitin

transfer (62, 66). In contrast, the RBRs catalyze substrate ubiquitylation by using a RING-like mechanism to coordinate an ubiquitin charged E2 cognate enzyme, followed by the formation of a HECT-like thiolester intermediate between ubiquitin and the enzyme's Rcat domain to complete the ubiquitin cargo transfer onto the substrate (64, 67–69). Lastly, the HECT E3 ubiquitin ligases play a catalytic role in the final attachment of ubiquitin by forming a thiolester intermediate with its conserved catalytic cysteine prior to transferring the ubiquitin to a substrate protein (70–74).

In the context of p53 ubiquitylation, several HECT E3 ubiquitin ligases have been shown to play a role in the final attachment of ubiquitin to p53. The specific HECT E3 ubiquitin ligase that attaches ubiquitin onto p53 decides the isopeptide linkages formed in a mono-, multi mono- or polyubiquitin chain (i.e., linear *via* *N*-terminal M1, or K6, K11, K27, K29, K33, K48, and/or K63) to modulate p53 activity and dictate its cellular function (47–49). For example, a K48-linked polyubiquitin chain attached to p53 signals for p53 turnover by the 26S proteasome (47–49), while K63-linked polyubiquitin chains control p53 intracellular trafficking (75) and transcriptional regulation of the complex between p53 and the RING E3 ubiquitin ligase mouse double minute 2 (MDM2) (76). Recent studies have also demonstrated that the HECT E3 ubiquitin ligases SMURF1 and HERC2 can regulate the activity of p53 independent of their ubiquitylation activities (i.e., no ubiquitin transfer or chain formation) (77, 78).

HECT E3 UBIQUITIN LIGASES—IMPORTANT ENZYMES IN ONCOGENESIS

The HECT E3 ubiquitin ligase family is comprised of 28 enzymes that contain a characteristic ~350 residue catalytic HECT domain found near their *C*-termini (70, 79, 80). The HECT domain is bi-lobal, where the *N*-lobe (~250 residues) is responsible for recruiting and binding the E2~ubiquitin complex, while the *C*-lobe contains the absolutely conserved catalytic cysteine responsible for the ubiquitin transfer onto a target substrate (81, 82). Structures of the isolated HECT domains from different HECT family members have revealed unique conformational orientations for the *C*-lobe, with some showing the *C*-lobe in close proximity to the *N*-lobe while others showing a large distance of separation. These findings suggest that a flexible linker exists between the *N*-lobe and *C*-lobe of the HECT domain that allows for the free rotation of the *C*-lobe for accepting ubiquitin from the E2 and subsequently transferring it to a target substrate.

Apart from the highly conserved HECT domain, there is remarkable diversity in the protein-protein interaction domains found at the *N*-termini of members in the HECT family. Through the biochemical and structural distinction of these *N*-terminal domains, the family of 28 enzymes has been classified into three different HECT subfamilies i) neuronal precursor cell-expressed developmentally downregulated 4 (NEDD4), ii) HECT and RLD containing (HERC), and iii) "Other" (70, 83). Focusing specifically on the NEDD4 subfamily, each of the nine members have been shown to contain an *N*-terminal C2 calcium binding domain involved with binding phospholipids through a calcium dependent mechanism (84), and two, three or four tryptophan-tryptophan (WW) domains involved in recognition of substrates with proline-rich motifs (i.e., PPxY or PY) (85) (**Figure 1**). Additionally, NEDD4 family members HECT, C2 and WW-domain containing protein 1 (HECW1) and HECW2 contain a unique HECW1/2 *N*-terminal domain thought to be involved in substrate recognition but has yet to be documented in the literature. Another HECT E3 ubiquitin ligase member belonging to the HERC subfamily, HECT and RLD containing protein 2 (HERC2), illustrates the vast diversity in *N*-terminal interaction domains (**Figure 1**). The HERC2 *N*-terminal protein-protein interaction domains include three regulator of chromosome condensation 1-like domains (RLDs) that are suggested to be involved in chromatin binding, centrosome assembly and guanine nucleotide exchange (101, 102), a zinc finger (ZF) domain that is required for protein/DNA binding (103), a unique Cullin-7-PARC-HERC2 (CPH) domain predicted to be involved in binding to tetramerized p53 (104, 105), and a cytochrome-b5 like domain (cyt-b5) that binds to heme and acts as a redox potential interaction domain with electron transport like properties (106). HERC2 also contains a mind bomb (MIB) domain that is thought to be involved in regulating the Notch signaling pathway to ensure proper intercellular communication during embryonic stem cell differentiation (107) and a downregulated in ovarian cancer (DOC) domain, which is similar to the anaphase promoting complex (APC) and may have a role in in the ubiquitylation activity of HERC2 (108).

The variability at the *N*-terminal protein-protein interaction domains in members of the NEDD4 subfamily and HERC2 suggest that these enzymes bind and recognize a broad range of substrate proteins in the context of oncogenesis (70) (**Table 1**). For example, it has been shown that HECW1 (aka NEDL1), SMAD ubiquitylation regulatory factor 1 (SMURF1), WW-domain containing protein 1 (WWP1) and HERC2 each carryout unique interactions with p53 that involve either the direct K63 ubiquitylation of p53, as in the case of WWP1 (75) (89), and/or the formation of multiprotein enzymatic complexes that act to modulate p53 activity independent from HECT-dependent ubiquitylation (149). Collectively, these HECT-dependent interactions have been identified as critical regulators of p53 activity that impact apoptotic signaling (149), the transcription of p53 related genes (75), equilibrium of the MDM2-p53 feedback loop (105, 150), ataxia telangiectasia mutated (ATM) and ataxia telangiectasia and Rad3 related (ATR) dependent DNA double strand break responses (151), and other oncological-related cellular responses.

THE NEDD4 HECT E3 UBIQUITIN LIGASES PLAY DIVERSE ROLES IN P53 MODULATION

The NEDD4 subfamily has become increasingly important in the field of oncology, as various members have been found to upregulate and interact with important tumor suppressor network proteins such as p53. Here we describe how WWP1, HECW1 and SMURF1 regulate p53-dependent cellular functions.

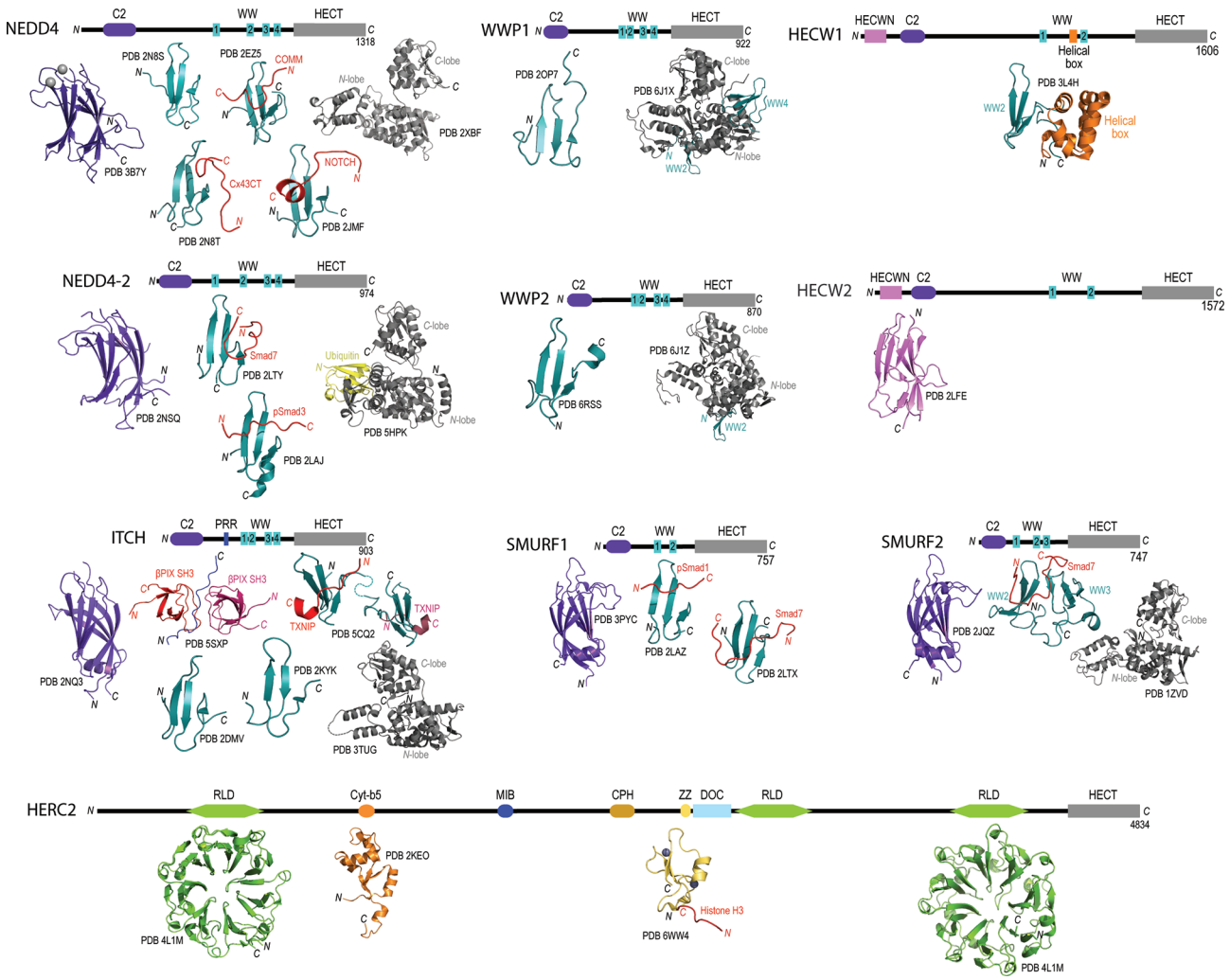

FIGURE 1 | Domain architecture and catalogue of three-dimensional structures of domains for members for the NEDD4L subfamily and HERC2. Domain architecture schematics are based upon annotated boundaries on Uniprot. All of the published or publicly available 3D structures were visualized using PyMol. NEDD4 – C2 domain bound to calcium (purple and silver spheres; PDB 3B7Y), WW domain 1 (PDB 2N8S) (86), WW domain 2 (cyan) in complex with phosphorylated Cx43CT (red; PBD 2N8T) (86), WW domain 3 (cyan) in complex with COMM (red; PDB 2EZ5) (87), WW domain 4 (cyan) in complex with NOTCH (red; PDB 2JMF) (88), and HECT domain (grey; PDB 2XBF) (89). NEDD4-2 – C2 domain (purple; PDB 2NSQ), WW domain 2 (cyan) in complex with Smad7 (red; PDB 2LTY) (90), WW domain 3 in complex with phosphorylated Smad3 (PDB 2LAJ) (91) HECT domain in complex with ubiquitin (PDB 5HPK) (92). ITCH – C2 domain (purple; PDB 2NQ3), proline-rich region (green) with βPix SH3 domains (reds; PDB 5SXP) (93), WW domain 1 (cyan; PDB 2DMV), WW domain 2 (cyan; PDB 2KYK), WW domains 3 and 4 (cyan) in complex with TXNIP peptide (red; PDB 5CQ2) (94), and HECT domain (grey; PDB 3TUG). WWP1 – WW domain 4 (cyan; PDB 2OP7), and WW domains 2, 3 and 4 (cyan) with HECT domain (grey; PDB 6J1X) (95). WWP2 – WW domain 4 (cyan; PDB 6RSS) (96), and WW domains 2, 3 and 4 (cyan) with HECT domain (grey; PDB 6J1Z) (95). SMURF1 – C2 domain (purple; PDB 3PYC), WW domain 1 (cyan) in complex with phosphorylated Smad1 (red; PDB 2LAZ) (91), and WW domain 2 (cyan) in complex with Smad7 (red; PDB 2LTX) (90). SMURF2 – C2 domain (purple; PDB 2JQZ) (97), WW domains 2 and 3 (cyan) in complex with Smad7 (red; PDB 2KXQ) (98), and HECT domain (grey; PDB 1ZVD) (99). HECW1 – Helical box (orange) with WW domain 2 (cyan; PDB 3L4H). HECW2 – HECWN domain (pink; PDB 2LFE). HERC2 – RLD domain 1 (green; PDB 4L1M), Cyt-b5 domain (orange; PDB 2KEO), ZZ domain bound to zinc ions (purple and grey spheres) in complex with Histone H3 tail (red; PDB 6WW4) (100), RLD domain 3 (green; PDB 3KCl).

WWP1 Facilitates p53 Aggregation in the Cytoplasm in Response to p53 Overexpression

WWP1 is a member of the NEDD4 subfamily that has been linked to colon, breast and oral cancers (31, 35, 39, 44, 152). WWP1 contains two WW domains that have been shown to recruit and modulate the activity of cancer related proteins like Runt-related transcription factor 2 (RUNX2) (153, 154), RING finger protein 11 (RNF11) (155, 156) and large tumor suppressor kinase 1 (LATS1) (157) *via* their proline-rich (PY) motifs (**Figure 1**). In addition to the interplay that occurs between WWP1 and these cancer-associated proteins, the enzyme can also interact with and regulate the activity of p53. Although p53 does contain a PY motif in its sequence (aa 68-91), WWP1 was

TABLE 1 | Examples of experimentally observed protein-protein interaction of oncogenic proteins with HECT E3 ubiquitin ligases.

Oncogenic Protein	HECT E3 ubiquitin ligase	Experimental detection method	Region of interaction	References
Cellular tumor antigen p53 (p53, TP53)	E6AP	2H, 3H, CE, CL, IF, IP, ITC, MS, PD, SPR, UbA, X-ray	280-781 aa	(71, 79, 109–130)
	HECW1	IP		(77)
	WWP1	IP, PD, UbA		(75)
	HERC2	IP, PD	CPH (2547-2640 aa)	(105)
Cellular tumor antigen p63 (p63, TP63)	WWP1	IP, UbA		(131)
	ITCH	IF, IP, NMR	WW domains 1&2	(132–136)
	NEDD4	2H, IP, UbA		(137)
Cellular tumor antigen p73 (p73, TP73)	HECW2	IP, PD, UbA	WW domains 1&2	(138)
	ITCH	IP, TAP, UbA		(139)
Apoptosis-stimulating of p53 protein 2 (TP53BP2)	E6AP	2H, 3H, IP		(115)
	ITCH	IF, IP, MS, PD, TAP	WW domains 1-4	(140, 141)
Melanoma-associated antigen 12 (MAGE12)	E6AP	2H, 3H		(115)
Promyelocytic leukemia protein (PML, MYL TRIM19)	E6AP	IF, IP, UbA		(142)
Mouse double minute 2 homolog (MDM2)	NEDD4	MS, PD, UbA		(143)
Breast cancer type 1 susceptibility protein (BRCA1)	HERC2	IP, MS, UbA	HECT domain (4252-4834 aa)	(144)
BCL-2-antagonist/killer (BAK)	HERC1	IF, PLISA	BH3 domain	(145)
Large tumor suppressor 1 (LATS1)	ITCH	IP, MS, PD, UbA	WW domains 1-4	(146, 147)
Protein Kinase B (AKT)	ITCH	MS	Phosphorylation @ S257	(148)

***Detection methods**: 2H, yeast or mammalian-two hybrid; 3H, yeast or mammalian-three hybrid; CE, co-elution during chromatography purification; CL, chemical crosslinking; IF, immunofluorescence; IP, immunoprecipitation; ITC, isothermal titration calorimetry; MS, liquid chromatography or MALDI MS/MS; NMR, nuclear magnetic resonance; PD, pulldown using GST, His or MBP tag; PLISA, proximity ligation in situ assay; SPR, surface plasmon resonance; TAP, tandem affinity purification; UbA, ubiquitylation assay; X-ray, X-ray crystallography. Given the HECT family's diverse regulation of p53 coupled with the well-established role of p53 in maintaining proper cell division and DNA integrity, members of the HECT E3 ubiquitin ligase family are promising oncological drug targets where their structural and mechanistic interactions with p53 can potentially be directed to modulate p53 activity and elicit precise HECT-p53 dependent anti-cancer cellular responses.*

observed to bind to p53's DNA binding domain and not with its WW domains (**Figure 2**). Intriguingly, this association was abolished when the PY motif of p53 was deleted, suggesting that the conformation p53 adopts in the presence of its PY motif is required for proper WWP1-p53 complex formation (75). This unusual interaction was also found to increase the stability of p53, in contrast to the destructive effects mediated by binding of other ubiquitin ligases such as the RING E3 ubiquitin ligase MDM2 (158). The ubiquitylation activity of WWP1 was required for p53 stabilization, as an inactive version of WWP1 with its catalytic cysteine substituted with an alanine reduced p53 stability in a dominant negative fashion (75). Surprisingly, the WWP1-dependent stability of p53 was inversely proportional to the transcriptional activities of p53, which can attributed to the WWP1-p53 complex translocation from the nucleus to the cytoplasm and its subsequent aggregation (75).

The observation that WWP1 interacts with p53 suggests that WWP1 might be involved in tumor suppressor networks. For example, WWP1 silencing in two osteosarcoma cell lines promoted apoptosis and reduced cell invasion (159). This suppression also resulted in decreased expression of B-cell lymphoma 2 (Bcl2), matrix metallopeptidase 2 (MMP2), matrix metallopeptidase 9 (MMP9) and β-catenin, while pro-apoptotic proteins Bcl-2 associated X protein (Bax) and E-cadherin expression levels increased indicating that WWP1 may play a role in pro-apoptotic pathways (159). Studies have also demonstrated that WWP1 contributes to extrinsic apoptosis. For instance, the inhibition of WWP1 correlated with elevated levels of apoptosis initiator caspases 8 and 9, mitogen activated protein kinase 8 (MAPK8), as well as executioner caspase 7 *via* the TNR-related apoptosis-inducing ligand (TRAIL) death receptor (160). This change in phenotype was shown to be reversible with the overexpression of wild-type WWP1 but could not be rescued with an inactive version of the protein (160). Taken together, these results show that the ubiquitylation activity of WWP1 is required to inhibit apoptosis and promote the progression of particular colon and thyroidal cancers.

Studies have also demonstrated that WWP1 is involved in prostate cancer. For example, WWP1 overexpression caused by chromosomal duplication events was observed in prostate xenografts (31). Knockout studies also revealed that the loss of WWP1 resulted in increased transforming growth factor beta (TGF-β) receptor 1 (TβR-I) and mothers against decapentaplegic homolog 2 (Smad2) protein levels, which in turn enhanced the inhibitory effect of TGF-β (31). These results are consistent with previous studies highlighting the role of WWP1 as a negative regulator of TGF-β. In this regulatory pathway, WWP1 binds to Smad7 *via* a WW/PY interaction, independent of its ubiquitylation activity (161). This binding and regulation of Smad7 has also been observed with other members of the NEDD4 family (i.e. SMURF1 and SMURF2) (162–165). Co-immunoprecipitation experiments revealed that Smad7, WWP1 and TβR-I are in close proximity within the cell and

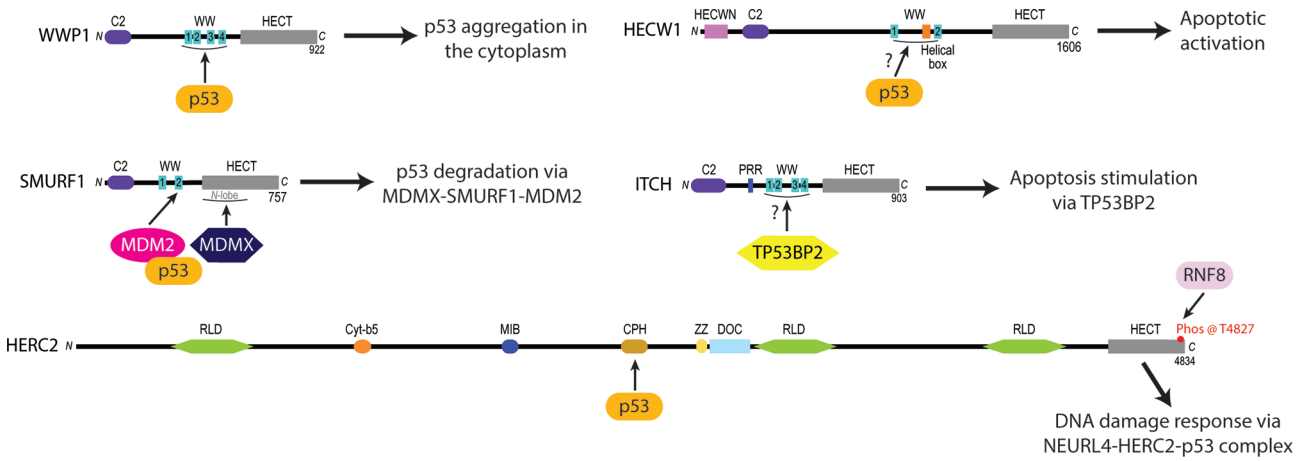

FIGURE 2 | Experimentally identified p53 protein-protein interaction sites of certain NEDD4L and HERC subfamily HECT E3 ligases linked to oncogenesis. The WW domains of WWP1 are required to recruit p53 and induce its cytoplasmic aggregation (75). HECW1 uses an unknown domain to interact with p53 and upregulate apoptotic cellular activity (149). SMURF1 coordinates the heterodimerization of MDM2 and MDMX *via* its second WW domain and the *N*-lobe of its HECT domain to increase the MDM2-dependent K48 polyubiquitylation and subsequent degradation of p53 (78). ITCH is a NEDD4L subfamily E3 ligase that stimulates apoptotic pathways by the WW1-4 domain-dependent activation of Tumor protein p53-binding protein 2 (TP53BP2) (140, 141). HERC2 interacts with p53 through its CPH domain to monitor the p53-MDM2 feedback loop in NEURL4 DDR pathways (105).

may form a complex that allows for WWP1 to ubiquitylate TβR-1 and target it for proteasomal degradation (161).

These cumulative studies demonstrate that WWP1 is an important enzyme in the regulation p53 mediated gene transcription and apoptosis. With research that implicates WWP1 in prostate and osteosarcoma, it is critical that additional studies be conducted to investigate possibilities of modulating the activity of WWP1 to elicit specific anti-cancer responses in the cell. For example, by using structural techniques to determine how p53 is bound and stabilized by an active form of WWP1 in the cytoplasm, it will become possible to elucidate the biochemical and biophysical properties of the WWP1-p53 complex as well as the mechanism of ubiquitin transfer. This newfound knowledge will aid in the design of artificial molecular machinery that acts to repress WWP1 interactions with p53 and hence regain normal p53 anti-tumor activity in active cancer cells. Additionally, by expanding our knowledge of other important WWP1-substrate interactions, including the recognition and binding of WWP1 to TGF-β receptors, the successful elucidation and categorization of the WWP1 interactome can be achieved to provide a clearer map of the pathological role(s) of WWP1.

HECW1 Positively Regulates p53 to Induce Apoptotic Pathway Activation

Recent biochemical studies have demonstrated that HECW1 possesses tumor suppressive activity by interacting with the *C*-terminus of p53 to upregulate the activation of p53-cisplatin dependent apoptotic cellular pathways (77, 149). This study also found that both the wild-type and isolated HECT constructs of HECW1 interact with p53, suggesting that the HECW1-dependent pro-apoptotic activation of p53 is independent of its ubiquitylation activity (77). Additionally, chromatin immunoprecipitation assays (ChIP) have demonstrated that HECW1 directs p53 to the p21wafi promoter region to induce the transcriptional activation of p53-related genes in response to carcinogenic cellular signals (149). There are currently no structural or mechanistic studies to explain how HECW1 forms a complex with p53 to regulate apoptotic anticancer activities within the cell. Taken together, these findings demonstrate the need for new structural and interactor-based studies on HECW1 to begin elucidating the exact mechanisms used by the enzyme to catalyze the activation of p53-induced apoptosis in cancerous cell lines. It will be important to determine the specific domains that HECW1 uses to recognize p53, define the conformational changes that HECW1 and p53 undergo to modulate p53 cellular activity, and decipher how the HECW1-p53 complex signals for the upregulation of p53 apoptotic signaling. Studies are also needed to examine how the HECW1-p53 interaction directs the migration of HECW1 to the nucleus where it promotes p53 activation of apoptotic related genes. By addressing these unknowns about the interplay between HECW1 and p53 cellular interplay, we may be able to fine tune the design of small molecule drugs that stimulate, activate, and enhance the HECW1-dependent activation of p53-induced apoptotic pathways in malignant cells.

SMURF1-Dependent MDM2/MDMX Heterodimerization Negatively Regulates p53 Activity

SMURF1 is another member of the NEDD4 subfamily that acts to negatively regulate p53 activity during breast (40), ovarian (46), gastric (42), and glioblastoma (166) tumorigenesis by augmenting the ubiquitylation activity of MDM2 – a RING E3

ligase that specifically targets p53 for proteasomal degradation (76, 158, 167, 168). Previous findings have demonstrated that SMURF1 uses its WW domains to recognize and bind target substrates before carrying out their HECT-dependent ubiquitylation (169–171). Contrary to this traditional HECT E3 function, recent studies have discovered a unique function of SMURF1 whereby it promotes the cellular stability of MDM2 substrates by facilitating the heterodimerization of MDM2 and its homolog mouse double minute 4 protein (MDMX, aka MDM4) (78). The ability of SMURF1 to mediate MDM2-MDMX heterodimerization is thought to rely on the coordination of MDM2 with its second WW domain while MDMX interacts with the HECT *N*-lobe of SMURF1 (78) (**Figure 2**). A consequence of these multiprotein interactions is the structural inhibition of the MDM2 auto degradation pathway by MDMX. Not surprisingly, this interaction has been shown to result in the prolonged stability of MDM2 *in vivo* with an increase in the K48-polyubiquitylation activity of MDM2 on p53 (78).

To date, MDM2 and MDMX are the only substrates known to interact with the second WW domain and HECT domain of SMURF1 and not be targeted for ubiquitylation. It remains unresolved how the unusual stabilization effects that SMURF1 provides for MDM2 and MDMX occur on the mechanistic and molecular level. Of interesting note is that MDM2 and MDMX are bound by SMURF1 at its second WW domain and HECT domain, the same enzymatic regions used by the SMURF1 to carry out the ubiquitylation of its target substrates (76, 78, 158, 167, 168). These findings make it conceivable that SMURF1 might bind MDMX in an analogous fashion to an E2 cognate enzyme at the *N*-lobe of its HECT domain. Likewise, with MDM2 bound by SMURF1 by its second WW domain, it is possible that the coordination of MDM2 to MDMX is facilitated by conformational shifts in the SMURF1 domain architecture that are similar to the mechanisms used by the SMURF1 to carry out the ubiquitylation of its target substrates.

Recent studies have determined that MDM2 and MDMX form a ternary complex with SMURF1 to promote MDM2/MDMX heterodimerization, which subsequently can recruit p53 to the complex with MDM2 serving as the bridging molecule within the MDMX-SMURF1-MDM2-p53 multiprotein complex (76, 78). While the exact function of this ternary intermediate remains unclear in the context of p53 signaling, biochemical pull-down assays have shown that p53 does not associate with the MDMX-SMURF1-MDM2 heterotrimer if the *N*-terminus of MDM2 is truncated (a.a. 1-76) (78), and that SMURF1 does not interact with p53 in the absence from MDM2 (78). These findings suggest that the *N*-terminus of MDM2 functions to recognize and bind p53 in addition to being the point of interaction for the second WW domain of SMURF1. It is critical that follow up structural studies be performed to examine if the *N*-terminal domain of MDM2 causes any conformational changes within the MDMX-SMURF1-MDM2 ternary complex and how these conformational changes may play a role in MDM2-MDMX heterodimerization and p53 regulation. Likewise, it will be important to examine how the unique structural interactions that occur between SMURF1, MDM2, and MDMX impact the ability of SMURF1 to stabilize MDM2, and how the subsequent regulation of MDM2 activity by SMURF1 plays a role in p53-dependent cancer development.

SMURF1's tight regulation of MDM2-dependent p53 ubiquitylation makes it a promising candidate for oncological drug development. An improved understanding of the mechanisms used by SMURF1 to promote MDM2-MDMX heterodimerization at the molecular level can be applied pharmacologically to regulate MDM2 p53 ubiquitylation activity in cancer cells, and therefore serve as a powerful tool to activate pro-apoptotic pathways and interrupt cell division.

HERC2—A NOVEL HECT E3 UBIQUITIN LIGASE LINKED TO CANCER DEVELOPMENT

Recent biochemical studies have identified HECT E3 ligases outside of the NEDD4 subfamily that regulate p53 activity. Here we describe how new research is beginning to reveal that HERC2 is a major player in mediating DNA repair by regulating p53 activity.

HERC2 Mediates p53 Activity Through the Formation of a Multiprotein Ternary Complex in Response to DNA Damage

HERC2 is a large 500 kDa multidomain E3 ubiquitin ligase that interacts with neuralized E3 ubiquitin protein ligase 4 (NEURL4) and MDM2 to modulate p53-dependent gene expression during the ATM and ATR induced DNA double strand break (DSB) repair response (105, 150). The HERC2-dependent activation of p53 is initiated by HERC2-NEURL4 complex formation that induces an allosteric conformational shift in the unique CPH domain of HERC2 (105, 150) (**Figure 3**). This change in conformation allows HERC2 to recruit oligomerized p53 with its CPH domain to form a NEURL4-HERC2-p53 ternary complex (105, 150). The NEURL4-HERC2-p53 complex then coordinates with the RING E3 ubiquitin ligase MDM2 that is usually responsible for targeting p53 for cytosolic trafficking *via* monoubiquitylation (172) and/or proteasomal degradation *via* K48-polyubiquitylation (57, 63, 64) under normal cellular conditions. However, during the ATM and ATR-activated DSB repair process, HERC2 is phosphorylated at T4827 on its *C*-terminal tail by phosphatidylinositol 3-kinase-like protein kinase (PIKK) to recruit the kinases ataxia telangiectasia mutated (ATM) and ataxia telangiectasia and Rad3 related (ATR) to the higher order NEURL4-HERC2-p53 complex where they catalyze the phosphorylation of oligomerized p53 and MDM2 (105, 150, 173). Following phosphorylation, MDM2 releases itself from the complex and carries out auto-polyubiquitylation to signal for its proteasomal degradation. Simultaneously, p53 is further stabilized by the CPH domain of HERC2 following its ATM and ATR-mediated phosphorylation and is no longer a target of MDM2 for polyubiquitylation (105, 150). The activated p53

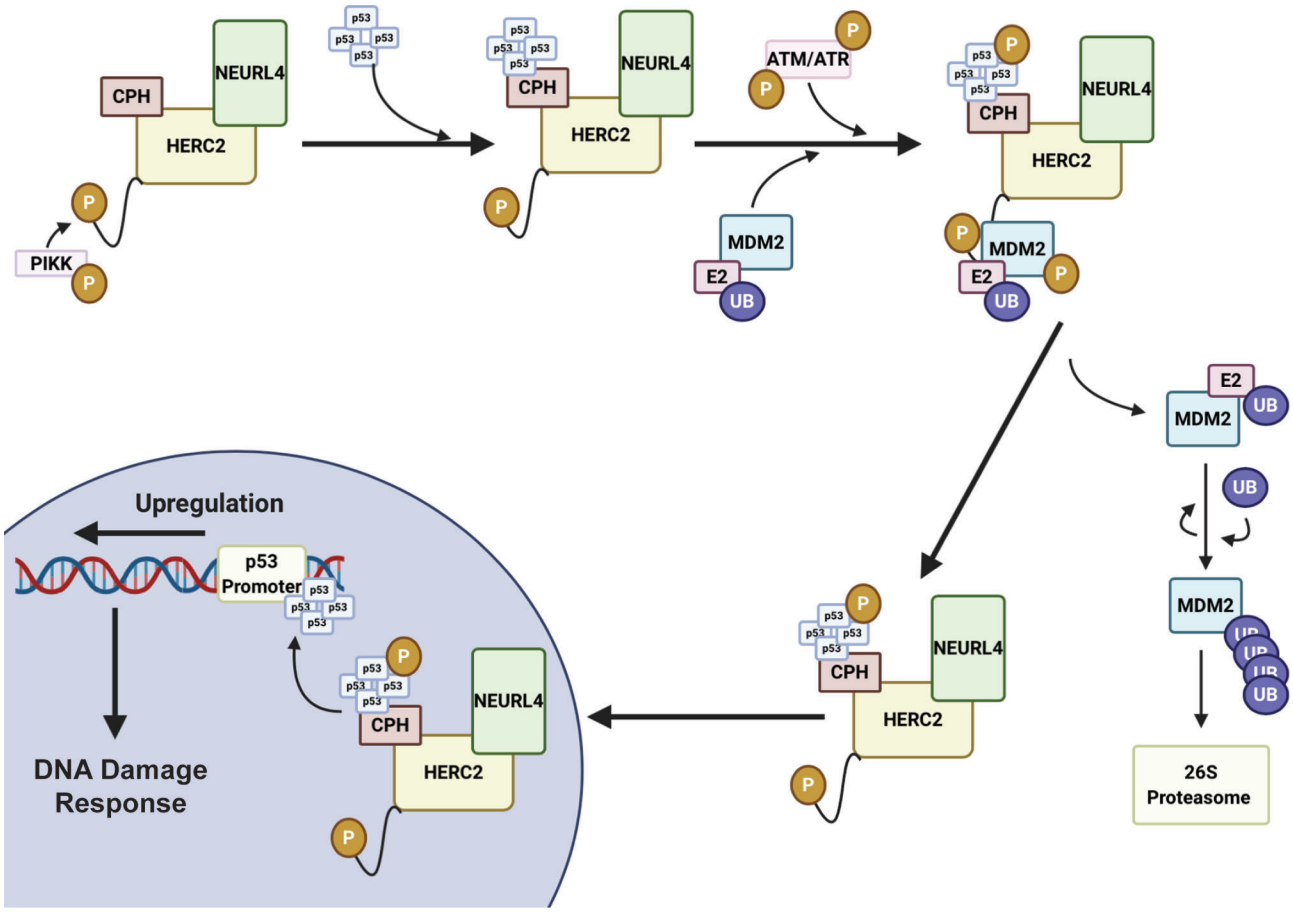

FIGURE 3 | HERC2 serves as a master regulator of p53 gene transcription in response to DNA damage. HERC2 recruits oligomerized p53 with its CPH domain to form a NEURL4-HERC2-p53 ternary complex and is phosphorylated at T4827 on its C-terminal tail by phosphatidylinositol 3-kinase-like protein kinase (PIKK). The HERC2-NEURL4-p53 ternary complex coordinates with the RING E3 ubiquitin ligase MDM2. The kinases Ataxia telangiectasia mutated (ATM) and Ataxia telangiectasia and Rad3 related (ATR) are also recruited to the multiprotein structure. ATR and ATM carry out the phosphorylation of MDM2 and oligomerized p53. Phosphorylated MDM2 becomes unstable and dissociates from the HERC2 scaffolding to allow for its K48 auto-polyubiquitylation and the cytoplasmic stability of the HERC2-NEURL4-p53 ternary complex. The HERC2-NEURL4-p53 ternary complex migrates to the nucleus where it releases oligomerized p53. p53 binds to the p53 promoter regions where it initiates the upregulation of genes to aid in cellular DNA repair and the DNA damage response. This figure was created with BioRender.com.

oligomers are then transported by the HERC2-NEURL4 complex to the nucleus and bind to p53 promoter regions where p53-regulated genes including p53, p21 and MDM2 become upregulated to aid in cellular DNA repair (105, 150). Once the cell's DNA damage response (DDR) is complete, ATM and ATR become targets of E3 ligases for proteasomal degradation and the HERC2-NEURL4 complex coordinates the MDM2-dependent degradation of p53 (167). Taken together, HERC2 acts as a master regulator of p53 transcriptional activation by selectively recruiting ATM and ATR kinases to modulate MDM2 and p53 stability throughout the DDR cycle. It remains unclear what specific structural conformations and mechanisms are used by HERC2 to control p53 stabilization by ATM and ATR dependent phosphorylation, or how p53 is targeted for degradation by MDM2-dependent ubiquitylation following its recruitment by the CPH domain of HERC2. Future studies are needed to clarify how the unique domains of HERC2 direct the ATM and ATR-dependent phosphorylation of p53 and p53-MDM2 regulation. An improved understanding of these mechanisms can potentially be exploited in novel oncological therapies that specifically target the p53-MDM2 feedback loop as a regulator of DNA replication and repair.

HERC2 Is a Novel Oncogenic Suppresser That Regulates the DNA Damage Responses and Screens the Genome Prior to Replication

In addition to regulating the MDM2-p53 transcriptional feedback loop, HERC2 can also prevent potentially oncogenic mutations from being passed into daughter cells by coordinating DNA double strand break (DSB) repair responses during the S and

G2-M phases of mitosis (174–179). The HERC2-DSB repair pathway is initiated when a double strand break is sensed by the MRN complex – meiotic recombination 11 (MRE11), Nijmegen breakage syndrome 1 (NBS1), and radiation sensitive protein 50 (RAD50) (151). After recognizing the DSB, NBS1 recruits ATM kinases to the damage site where they phosphorylate Histone 2A Family Member X (H2AX) and Mediator of DNA Damage Checkpoint 1 (MDC1) (151). These phosphorylation events promote H2AX and MDC1 complexation and signal for the recruitment of HERC2 and RNF8, a RING E3 ubiquitin ligase, to the DSB (176, 180). Once arriving to the damage site, HERC2's *C*-terminal tail is phosphorylated by PIKK at T4827 to promote its complexation with RING finger protein 8 (RNF8), an E3 ubiquitin ligase (**Figure 4**). Following RNF8 recruitment, HERC2 uses its *C*-terminal tail to stimulate the oligomerization of RNF8 and facilitates the formation of the HERC2-MDC1-RNF8 ternary complex. Phosphorylation signal cascades are used by these ternary complexes to carry out RNF8 mediated recruitment of RNF168, another RING E3 ubiquitin ligase, and its cognate E2 cognate enzyme UBE2N (aka Ubc13), to the DNA damage site (181). This multiprotein complex then works cooperatively to attach K63-polyubiquitin chains on to chromosomal histone proteins H2A and H2Ax. The K63 polyubiquitin linkages made on these histone sites are in close proximity to the DSB and serve as biochemical markers that recruit homologous DNA repair factors. These include breast cancer gene 1 (BRCA1), BRCA1 associated RING domain protein 1 (BARD1), receptor associated protein 80 (RAP80), and the non-homologous end joining repair factor 53BP1, all of which are required to carry out the full DDR response (176, 182, 183).

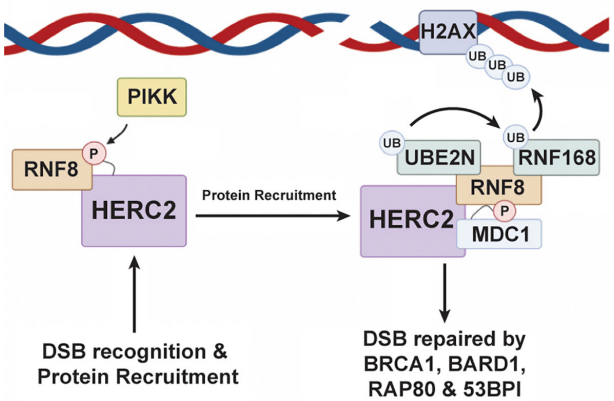

FIGURE 4 | HERC2 serves as a scaffold to facilitate H2A ubiquitylation in response to DNA double strand breaks. HERC2 initiates the repair response for DSBs by using its catalytic HECT domain as a binding scaffold for RING finger protein 8 (RNF8), a RING E3 ubiquitin ligase, to bring RNF8 into close proximity to a site of DNA damage. After binding RNF8 to its HECT domain, HERC2 coordinates the formation of a complex between UBE2N (aka Ubc13), an E2 ubiquitin conjugating enzyme, and RNF168 to catalyze the attachment of K63-polyubiquitin chains onto histones at the site of damaged DNA. This HERC2-mediated K63-polyubiquitylation activity then signals for the recruitment of healing factors like breast cancer gene 1 (BRCA1), receptor associate protein 80 (RAP80), and 53BP1 to elicit an effective DDR response. This figure was created with BioRender.com.

Recent studies indicate that HERC2 continues to play a role in the DSB repair pathway after the recruitment of these DNA repair factors. For example, it is suggested that HERC2 uses its phosphorylated *C*-terminal tail to help stabilize BRCA1, BARD1, and RAP80 by binding onto their degrons sites during the G2-M phase transition of cell replication thereby protecting these DDR proteins from proteasomal degradation while they carry out their DNA repair activities (176). This HERC2-dependent activity is critical to the prevention of cellular oncogenesis by acting to screen and repair the cell's genetic material at potentially carcinogenic mutation sites that were overlooked during S-phase DNA replication.

Collectively, studies on the onco-suppressive activities of HERC2 suggest it as a promising drug target for future immunotherapeutic treatments, particularly in cases of breast cancer development and pathogenesis. While HERC2 has been extensively characterized in a biochemical context, the mechanistic and structural basis for the involvement of HERC2 in the NEURL4-p53-MDM2 mediated DSB and DDR pathways remain largely unexplored. Intriguingly, in both pathways HERC2 serves as a scaffold that recruits and orchestrates the timely activities of regulatory proteins that are key to regulating p53-MDM2 intracellular concentration and/or DNA integrity. It is conceivable that HERC2 targeted drug development needs to be focused on enhancing the onco-suppressive activities of HERC2 to control the progression of cancer. As a prerequisite to developing these treatments, it will be paramount that structural studies be conducted to learn how HERC2 uses its different protein-protein interaction domains, including its catalytic HECT domain, to carry out specific molecular mechanisms that regulate p53 activity and the DDR response. For example, there are many unanswered questions on how the *N*-terminal variable domains of HERC2 contribute to substrate recognition and HERC2-dependent ubiquitylation. The mechanisms used by HERC2 in DNA maintenance/repair and p53-MDM2 modulation in the cell are also unknown. Additionally, studies on the role of conformationally flexible in the acidic *C*-terminal tail of HERC2 for building polyubiquitin chains during DDR and p53 oligomerization and clarifying how HERC2 recognizes and targets proteins to the p53 promoter region to regulate p53-related gene expression and/or a damaged DNA site to facilitate DNA repair are needed. Expanded studies on HERC2 could prove to be pivotal in the development of new immunotherapeutic treatments that target specific HECT E3 protein-protein interactions in the cell to elicit a specific intracellular immunological response against cancers.

HECT E3 UBIQUITIN LIGASES AS CANCER DRUG TARGETS—MOVING FORWARD

Recent advances in the biochemical and structural characterization of HECT E3 ubiquitin ligases have revealed

these enzymes are critical regulators of the p53-MDM2 and DDR pathways. To date, only one HECT E3 ubiquitin ligase specific cancer drug, Bortezomib, has been reported to effectively modulate the activity of the NEDD4L and HERC subfamily ligases discussed in this review (184). Intriguingly, a recent 2019 study used phage library analysis to identify a class of bicyclic peptides that demonstrate a general inhibitory effect on the HECT E3 ligases ITCH, WWP1, SMURF1 and HECW1 by competitively binding to the E2 interaction site on the *N*-lobe of the HECT domain (185). However, the activity of these small molecule competitive inhibitors provided no specific anticancer effects when tested in tumorigenic cell lines (185). Perhaps one of the largest obstacles for developing HECT specific anticancer therapeutics is the diversity of mechanisms and structures associated within each HECT subfamily and the reality that many of these mechanisms, structures, and their functional roles in cancer pathogenesis remain largely unknown. Concurrently, the amount of knowledge that remains to be uncovered on the NEDD4L subgroup, as well as other members of the broader HECT family, provide many opportunities for the generation of novel therapeutics to treat a broad range of cancers. As new discoveries continue to be made on this fascinating group of proteins, our knowledge into the scope of molecular mechanisms, protein-protein interactions, and identified substrates engaged by HECT E3 ubiquitin ligases in oncogenesis will continue to expand.

It will become increasingly important that new structural and biophysical studies be conducted on members of the HECT E3 ubiquitin ligases to clarify how the HECT domain architecture contributes to HECT catalytic dysfunction in p53 and related cellular pathways. For example, further examination of the mechanisms used by SMURF1 to catalyze MDM2/MDMX heterodimerization and increase the MDM2-dependent ubiquitylation of p53 could allow for the synthesis of small molecule inhibitors drugs that block MDMX-SMURF1 complex formation. Likewise, the development of therapies that promote the upregulation of p53 pro-apoptotic cellular signaling in SMURF1 overexpressed cells to disrupt tumor growth is another avenue that needs to be studied. An improved molecular understanding of how HERC2 uses its multidomain structure to direct the ATM and ATR-dependent phosphorylation of p53 and MDM2 will be pivotal to uncovering the HERC2-dependent mechanisms involved with p53-MDM2 regulation. Expanded studies on HECW1 and WWP1 will also be critical in the development of small molecule therapeutics to target these enzymes and their roles in p53 regulation. With so little known about the diverse structural, molecular, and mechanistic bases used by HECT E3 ligases to regulate the p53-MDM2, DDR, and other pathways implicated in oncogenesis, now is an exciting time to be researching this class of enzymes that are at the nexus for the development of new onco-therapeutic treatments.

AUTHOR CONTRIBUTIONS

Conceptualization, NM, RL, and DS. Writing—original draft preparation, review and editing, and revisions, NM, RL, and DS. Figures, NM, RL, and DS. Supervision, DS. All authors contributed to the article and approved the submitted version.

FUNDING

This research was supported by the National Institutes of Health, R15GM126432 (DS). NM was the recipient of an Arthur E. Martell and Thomas T. Sugihara Summer Undergraduate Scholarship from Clark University.

REFERENCES

1. Harashima H, Dissmeyer N, Schnittger A. Cell cycle control across the eukaryotic kingdom. *Trends Cell Biol* (2013) 23:345–56. doi: 10.1016/j.tcb.2013.03.002
2. Lacerda R, Menezes J, Candeias MM. Alternative Mechanisms of mRNA Translation Initiation in Cellular Stress Response and Cancer. *Adv Exp Med Biol* (2019) 1157:117–32. doi: 10.1007/978-3-030-19966-1_6
3. MacMillan CD, Leong HS, Dales DW, Robertson AE, Lewis JD, Chambers AF, et al. andStage of breast cancer progression influences cellular response to activation of the WNT/planar cell polarity pathway. *Sci Rep* (2014) 4:6315. doi: 10.1038/srep06315
4. Palmieri D, Scarpa M, Tessari A, Uka R, Amari F, Lee C, et al. Ran Binding Protein 9 (RanBP9) is a novel mediator of cellular DNA damage response in lung cancer cells. *Oncotarget* (2016) 7:18371–83. doi: 10.18632/oncotarget.7813
5. Raulf N, El-Attar R, Kulms D, Lecis D, Delia D, Walczak H, et al. Differential response of head and neck cancer cell lines to TRAIL or Smac mimetics is associated with the cellular levels and activity of caspase-8 and caspase-10. *Br J Cancer* (2014) 111:1955–64. doi: 10.1038/bjc.2014.521
6. Savina NV, Nikitchenko NV, Kuzhir TD, Rolevich AI, Krasny SA, Goncharova RI. The Cellular Response to Oxidatively Induced DNA Damage and Polymorphism of Some DNA Repair Genes Associated with Clinicopathological Features of Bladder Cancer. *Oxid Med Cell Longev* (2016) 2016:5710403. doi: 10.1155/2016/5710403
7. Sulli G, Di Micco R, d'Adda di Fagagna F. Crosstalk between chromatin state and DNA damage response in cellular senescence and cancer. *Nat Rev Cancer* (2012) 12:709–20. doi: 10.1038/nrc3344
8. Watanabe T, Morinaga S, Akaike M, Numata M, Tamagawa H, Yamamoto N, et al. The cellular level of histone H3 lysine 4 dimethylation correlates with response to adjuvant gemcitabine in Japanese pancreatic cancer patients treated with surgery. *Eur J Surg Oncol* (2012) 38:1051–7. doi: 10.1016/j.ejso.2012.08.008
9. Zhang K, Zhang B, Bai Y, Dai L. E2F1 promotes cancer cell sensitivity to cisplatin by regulating the cellular DNA damage response through miR-26b in esophageal squamous cell carcinoma. *J Cancer* (2020) 11:301–10. doi: 10.7150/jca.33983
10. Timofeev O, Koch L, Niederau C, Tscherne A, Schneikert J, Klimovich M, et al. Phosphorylation Control of p53 DNA-Binding Cooperativity Balances Tumorigenesis and Aging. *Cancer Res* (2020) 80:5231–44. doi: 10.1158/0008-5472.CAN-20-2002
11. Kim JH, Yoon EK, Chung HJ, Park SY, Hong KM, Lee CH, et al. p53 acetylation enhances Taxol-induced apoptosis in human cancer cells. *Apoptosis* (2013) 18:110–20. doi: 10.1007/s10495-012-0772-8
12. Fei Q, Shang K, Zhang J, Chuai S, Kong D, Zhou T, et al. Histone methyltransferase SETDB1 regulates liver cancer cell growth through methylation of p53. *Nat Commun* (2015) 6:8651. doi: 10.1038/ncomms9651
13. Ashikari D, Takayama K, Tanaka T, Suzuki Y, Obinata D, Fujimura T, et al. Androgen induces G3BP2 and SUMO-mediated p53 nuclear export in prostate cancer. *Oncogene* (2017) 36:6272–81. doi: 10.1038/onc.2017.225

14. Shaw P, Freeman J, Bovey R, Iggo R. Regulation of specific DNA binding by p53: evidence for a role for O-glycosylation and charged residues at the carboxy-terminus. *Oncogene* (1996) 12:921–30.
15. Appella E, Anderson CW. Post-translational modifications and activation of p53 by genotoxic stresses. *Eur J Biochem* (2001) 268:2764–72. doi: 10.1046/j.1432-1327.2001.02225.x
16. Di Ventura B, Funaya C, Antony C, Knop M, Serrano L. Reconstitution of Mdm2-dependent post-translational modifications of p53 in yeast. *PloS One* (2008) 3:e1507. doi: 10.1371/journal.pone.0001507
17. Saito S, Yamaguchi H, Higashimoto Y, Chao C, Xu Y, Fornace AJJr., et al. Phosphorylation site interdependence of human p53 post-translational modifications in response to stress. *J Biol Chem* (2003) 278:37536–44. doi: 10.1074/jbc.M305135200
18. Taira N, Yoshida K. Post-translational modifications of p53 tumor suppressor: determinants of its functional targets. *Histol Histopathol* (2012) 27:437–43. doi: 10.14670/HH-27.437
19. Tanaka T. Regulation of p53 function and promoter selectivity by post-translational modifications. *Seikagaku* (2010) 82:200–9.
20. Xu Y. Regulation of p53 responses by post-translational modifications. *Cell Death Differ* (2003) 10:400–3. doi: 10.1038/sj.cdd.4401182
21. Masuda Y, Saeki Y, Arai N, Kawai H, Kukimoto I, Tanaka K, et al. Stepwise multipolyubiquitination of p53 by the E6AP-E6 ubiquitin ligase complex. *J Biol Chem* (2019) 294:14860–75. doi: 10.1074/jbc.RA119.008374
22. Meng J, Tagalakis AD, Hart SL. Silencing E3 Ubiqutin ligase ITCH as a potential therapy to enhance chemotherapy efficacy in p53 mutant neuroblastoma cells. *Sci Rep* (2020) 10:1046. doi: 10.1038/s41598-020-57854-6
23. Michnov O, Solomayer E, Fehm T, Stubenrauch F, Iftner T. Knock down of p53 or its ubiquitin ligase E6AP does not affect the sensitivity of human papillomavirus-positive cervical cancer cells to cisplatin. *Am J Cancer Res* (2012) 2:309–21.
24. Rolfe M, Beer-Romero P, Glass S, Eckstein J, Berdo I, Theodoras A, et al. Reconstitution of p53-ubiquitinylation reactions from purified components: the role of human ubiquitin-conjugating enzyme UBC4 and E6-associated protein (E6AP). *Proc Natl Acad Sci USA* (1995) 92:3264–8. doi: 10.1073/pnas.92.8.3264
25. Beaudenon S, Huibregtse JM. HPV E6, E6AP and cervical cancer. *BMC Biochem* (2008) 9 Suppl 1:S4. doi: 10.1186/1471-2091-9-S1-S4
26. Gamell C, Bandilovska I, Gulati T, Kogan A, Lim SC, Kovacevic Z, et al. E6AP Promotes a Metastatic Phenotype in Prostate Cancer. *iScience* (2019) 22:1–15. doi: 10.1016/j.isci.2019.10.065
27. Gamell C, Gulati T, Levav-Cohen Y, Young RJ, Do H, Pilling P, et al. Reduced abundance of the E3 ubiquitin ligase E6AP contributes to decreased expression of the INK4/ARF locus in non-small cell lung cancer. *Sci Signal* (2017) 461:eaaf8223. doi: 10.1126/scisignal.aaf8223
28. Mani A, Oh AS, Bowden ET, Lahusen T, Lorick KL, Weissman AM, et al. E6AP mediates regulated proteasomal degradation of the nuclear receptor coactivator amplified in breast cancer 1 in immortalized cells. *Cancer Res* (2006) 66:8680–6. doi: 10.1158/0008-5472.CAN-06-0557
29. Owais A, Mishra RK, Kiyokawa H. The HECT E3 Ligase E6AP/UBE3A as a Therapeutic Target in Cancer and Neurological Disorders. *Cancers (Basel)* (2020) 12:2108. doi: 10.3390/cancers12082108
30. Raghu D, Paul PJ, Gulati T, Deb S, Khoo C, Russo A, et al. E6AP promotes prostate cancer by reducing p27 expression. *Oncotarget* (2017) 8:42939–48. doi: 10.18632/oncotarget.17224
31. Chen C, Sun X, Guo P, Dong XY, Sethi P, Zhou W, et al. Ubiquitin E3 ligase WWP1 as an oncogenic factor in human prostate cancer. *Oncogene* (2007) 26:2386–94. doi: 10.1038/sj.onc.1210021
32. Sakashita H, Inoue H, Akamine S, Ishida T, Inase N, Shirao K, et al. Identification of the NEDD4L gene as a prognostic marker by integrated microarray analysis of copy number and gene expression profiling in non-small cell lung cancer. *Ann Surg Oncol* (2013) 20 Suppl 3:S590–8. doi: 10.1245/s10434-013-3059-6
33. Li H, Xiao N, Wang Y, Wang R, Chen Y, Pan W, et al. Smurf1 regulates lung cancer cell growth and migration through interaction with and ubiquitination of PIPKIgamma. *Oncogene* (2017) 36:5668–80. doi: 10.1038/onc.2017.166
34. Bonanno L, Costa C, Majem M, Sanchez JJ, Rodriguez I, Gimenez-Capitan A, et al. Combinatory effect of BRCA1 and HERC2 expression on outcome in advanced non-small-cell lung cancer. *BMC Cancer* (2016) 16:312. doi: 10.1186/s12885-016-2339-5
35. Chen JJ, Zhang W. High expression of WWP1 predicts poor prognosis and associates with tumor progression in human colorectal cancer. *Am J Cancer Res* (2018) 8:256–65.
36. Qi H, Grenier J, Fournier A, Labrie C. Androgens differentially regulate the expression of NEDD4L transcripts in LNCaP human prostate cancer cells. *Mol Cell Endocrinol* (2003) 210:51–62. doi: 10.1016/j.mce.2003.08.009
37. Tanksley JP, Chen X, Coffey RJ. NEDD4L is downregulated in colorectal cancer and inhibits canonical WNT signaling. *PloS One* (2013) 8:e81514. doi: 10.1371/journal.pone.0081514
38. Yang H, Zhu J, Wang G, Liu H, Zhou Y, Qian J. STK35 Is Ubiquitinated by NEDD4L and Promotes Glycolysis and Inhibits Apoptosis Through Regulating the AKT Signaling Pathway, Influencing Chemoresistance of Colorectal Cancer. *Front Cell Dev Biol* (2020) 8:582695. doi: 10.3389/fcell.2020.582695
39. Chen C, Zhou Z, Ross JS, Zhou W, Dong JT. The amplified WWP1 gene is a potential molecular target in breast cancer. *Int J Cancer* (2007) 121:80–7. doi: 10.1002/ijc.22653
40. Yu L, Liu X, Cui K, Di Y, Xin L, Sun X, et al. SND1 Acts Downstream of TGFbeta1 and Upstream of Smurf1 to Promote Breast Cancer Metastasis. *Cancer Res* (2015) 75:1275–86. doi: 10.1158/0008-5472.CAN-14-2387
41. Bian S. miR-4319 inhibited the development of thyroid cancer by modulating FUS-stabilized SMURF1. *J Cell Biochem* (2020) 121:174–82. doi: 10.1002/jcb.29026
42. Tao Y, Sun C, Zhang T, Song Y. SMURF1 promotes the proliferation, migration and invasion of gastric cancer cells. *Oncol Rep* (2017) 38:1806–14. doi: 10.3892/or.2017.5825
43. Zhang Y, Wang W, Cai S, Chen Y, Wang Q, Pan Q, et al. Reciprocal regulation between betaTrCP and Smurf1 suppresses proliferative capacity of liver cancer cells. *J Cell Physiol* (2017) 232:3347–59. doi: 10.1002/jcp.25780
44. Lin JH, Hsieh SC, Chen JN, Tsai MH, Chang CC. WWP1 gene is a potential molecular target of human oral cancer. *Oral Surg Oral Med Oral Pathol Oral Radiol* (2013) 116:221–31. doi: 10.1016/j.oooo.2013.05.006
45. Yang Q, Zhao J, Cui M, Gi S, Wang W, Han X. Nedd4L expression is decreased in ovarian epithelial cancer tissues compared to ovarian non-cancer tissue. *J Obstet Gynaecol Res* (2015) 41:1959–64. doi: 10.1111/jog.12808
46. Chen X, Chen S, Li Y, Gao Y, Huang S, Li H, et al. SMURF1-mediated ubiquitination of ARHGAP26 promotes ovarian cancer cell invasion and migration. *Exp Mol Med* (2019) 51:1–12. doi: 10.1038/s12276-019-0236-0
47. Hershko A, Ciechanover A. The ubiquitin system. *Annu Rev Biochem* (1998) 67:425–79. doi: 10.1146/annurev.biochem.67.1.425
48. Komander D. The emerging complexity of protein ubiquitination. *Biochem Soc Trans* (2009) 37:937–53. doi: 10.1042/BST0370937
49. Komander D, Rape M. The ubiquitin code. *Annu Rev Biochem* (2012) 81:203–29. doi: 10.1146/annurev-biochem-060310-170328
50. Yu F, Wang S, Zhang W, Tang J, Wang H, Yu L, et al. Genome-wide identification of genes encoding putative secreted E3 ubiquitin ligases and functional characterization of PbRING1 in the biotrophic protist Plasmodiophora brassicae. *Curr Genet* (2019) 65:1355–65. doi: 10.1007/s00294-019-00989-5
51. Goto Y, Koyasu S, Kobayashi M, Harada H. The emerging roles of the ubiquitination/deubiquitination system in tumor radioresistance regarding DNA damage responses, cell cycle regulation, hypoxic responses, and antioxidant properties: Insight into the development of novel radiosensitizing strategies. *Mutat Res* (2017) 803-805:76–81. doi: 10.1016/j.mrfmmm.2017.07.007
52. Ditzel M, Meier P. Ubiquitylation in apoptosis: DIAP1's (N-)en(d)igma. *Cell Death Differ* (2005) 12:1208–12. doi: 10.1038/sj.cdd.4401711
53. Gomez-Martin D, Diaz-Zamudio M, Alcocer-Varela J. Ubiquitination system and autoimmunity: the bridge towards the modulation of the immune response. *Autoimmun Rev* (2008) 7:284–90. doi: 10.1016/j.autrev.2007.11.026

54. Smith VL, Jackson L, Schorey JS. Ubiquitination as a Mechanism To Transport Soluble Mycobacterial and Eukaryotic Proteins to Exosomes. *J Immunol* (2015) 195:2722–30. doi: 10.4049/jimmunol.1403186
55. Abbas T. The Role of Ubiquitination and SUMOylation in DNA Replication. *Curr Issues Mol Biol* (2020) 40:189–220. doi: 10.21775/cimb.040.189
56. Pickart CM. Mechanisms underlying ubiquitination. *Annu Rev Biochem* (2001) 70:503–33. doi: 10.1146/annurev.biochem.70.1.503
57. Pickart CM, Eddins MJ. Ubiquitin: structures, functions, mechanisms. *Biochim Biophys Acta* (2004) 1695:55–72. doi: 10.1016/j.bbamcr.2004.09.019
58. Capili AD, Lima CD. Taking it step by step: mechanistic insights from structural studies of ubiquitin/ubiquitin-like protein modification pathways. *Curr Opin Struct Biol* (2007) 17:726–35. doi: 10.1016/j.sbi.2007.08.018
59. Breslow E, Chauhan Y, Daniel R, Tate S. Role of methionine-1 in ubiquitin conformation and activity. *Biochem Biophys Res Commun* (1986) 138:437–44. doi: 10.1016/0006-291X(86)90300-1
60. Mihalik B, Gaborik Z, Varnai P, Clark AJ, Catt KJ, Hunyady L. Endocytosis of the AT1A angiotensin receptor is independent of ubiquitylation of its cytoplasmic serine/threonine-rich region. *Int J Biochem Cell Biol* (2003) 35:992–1002. doi: 10.1016/S1357-2725(02)00277-7
61. Amodio G, Margarucci L, Moltedo O, Casapullo A, Remondelli P. Identification of Cysteine Ubiquitylation Sites on the Sec23A Protein of the COPII Complex Required for Vesicle Formation from the ER. *Open Biochem J* (2017) 11:36–46. doi: 10.2174/1874091X01711010036
62. Deshaies RJ, Joazeiro CA. RING domain E3 ubiquitin ligases. *Annu Rev Biochem* (2009) 78:399–434. doi: 10.1146/annurev.biochem.78.101807.093809
63. Hatakeyama S, Nakayama KI. U-box proteins as a new family of ubiquitin ligases. *Biochem Biophys Res Commun* (2003) 302:635–45. doi: 10.1016/S0006-291X(03)00245-6
64. Spratt DE, Walden H, Shaw GS. RBR E3 ubiquitin ligases: new structures, new insights, new questions. *Biochem J* (2014) 458:421–37. doi: 10.1042/BJ20140006
65. Kraft E, Stone SL, Ma L, Su N, Gao Y, Lau OS, et al. Genome analysis and functional characterization of the E2 and RING-type E3 ligase ubiquitination enzymes of Arabidopsis. *Plant Physiol* (2005) 139:1597–611. doi: 10.1104/pp.105.067983
66. Metzger MB, Hristova VA, Weissman AM. HECT and RING finger families of E3 ubiquitin ligases at a glance. *J Cell Sci* (2012) 125:531–7. doi: 10.1242/jcs.091777
67. Marin I. RBR ubiquitin ligases: Diversification and streamlining in animal lineages. *J Mol Evol* (2009) 69:54–64. doi: 10.1007/s00239-009-9252-3
68. Marin I. Diversification and Specialization of Plant RBR Ubiquitin Ligases. *PloS One* (2010) 5:e11579. doi: 10.1371/journal.pone.0011579
69. Marin I, Lucas JI, Gradilla AC, Ferrus A. Parkin and relatives: the RBR family of ubiquitin ligases. *Physiol Genomics* (2004) 17:253–63. doi: 10.1152/physiolgenomics.00226.2003
70. Wang Y, Argiles-Castillo D, Kane EI, Zhou A, Spratt DE. HECT E3 ubiquitin ligases - emerging insights into their biological roles and disease relevance. *J Cell Sci* (2020) 133:jcs228072. doi: 10.1242/jcs.228072
71. Scheffner M, Nuber U, Huibregtse JM. Protein ubiquitination involving an E1-E2-E3 enzyme ubiquitin thioester cascade. *Nature* (1995) 373:81–3. doi: 10.1038/373081a0
72. Huang L, Kinnucan E, Wang G, Beaudenon S, Howley PM, Huibregtse JM, et al. Structure of an E6AP-UbcH7 complex: insights into ubiquitination by the E2-E3 enzyme cascade. *Science* (1999) 286:1321–6. doi: 10.1126/science.286.5443.1321
73. Kee Y, Huibregtse JM. Regulation of catalytic activities of HECT ubiquitin ligases. *Biochem Biophys Res Commun* (2007) 354:329–33. doi: 10.1016/j.bbrc.2007.01.025
74. Lorenz S. Structural mechanisms of HECT-type ubiquitin ligases. *Biol Chem* (2018) 399:127–45. doi: 10.1515/hsz-2017-0184
75. Laine A, Ronai Z. Regulation of p53 localization and transcription by the HECT domain E3 ligase WWP1. *Oncogene* (2007) 26:1477–83. doi: 10.1038/sj.onc.1209924
76. David D, Nair SA, Pillai MR. Smurf E3 ubiquitin ligases at the cross roads of oncogenesis and tumor suppression. *Biochim Biophys Acta* (2013) 1835:119–28. doi: 10.1016/j.bbcan.2012.11.003
77. Li Y, Ozaki T, Kikuchi H, Yamamoto H, Ohira M, Nakagawara A. A novel HECT-type E3 ubiquitin protein ligase NEDL1 enhances the p53-mediated apoptotic cell death in its catalytic activity-independent manner. *Oncogene* (2008) 27:3700–9. doi: 10.1038/sj.onc.1211032
78. Nie J, Xie P, Liu L, Xing G, Chang Z, Yin Y, et al. Smad ubiquitylation regulatory factor 1/2 (Smurf1/2) promotes p53 degradation by stabilizing the E3 ligase MDM2. *J Biol Chem* (2010) 285:22818–30. doi: 10.1074/jbc.M110.126920
79. Huibregtse JM, Scheffner M, Beaudenon S, Howley PM. A family of proteins structurally and functionally related to the E6-AP ubiquitin-protein ligase. *Proc Natl Acad Sci USA* (1995) 920:2563–7. doi: 10.1073/pnas.92.7.2563
80. Schwarz SE, Rosa JL, Scheffner M. Characterization of human hect domain family members and their interaction with UbcH5 and UbcH7. *J Biol Chem* (1998) 273:12148–54. doi: 10.1074/jbc.273.20.12148
81. Berndsen CE, Wolberger C. New insights into ubiquitin E3 ligase mechanism. *Nat Struct Mol Biol* (2014) 21:301–7. doi: 10.1038/nsmb.2780
82. Zheng N, Shabek N. Ubiquitin Ligases: Structure, Function, and Regulation. *Annu Rev Biochem* (2017) 86:129–57. doi: 10.1146/annurev-biochem-060815-014922
83. Rotin D, Kumar S. Physiological functions of the HECT family of ubiquitin ligases. *Nat Rev Mol Cell Biol* (2009) 10:398–409. doi: 10.1038/nrm2690
84. Plant PJ, Yeger H, Staub O, Howard P, Rotin D. The C2 domain of the ubiquitin protein ligase Nedd4 mediates Ca2+-dependent plasma membrane localization. *J Biol Chem* (1997) 272:32329–36. doi: 10.1074/jbc.272.51.32329
85. Staub O, Dho S, Henry P, Correa J, Ishikawa T, McGlade J, et al. WW domains of Nedd4 bind to the proline-rich PY motifs in the epithelial Na+ channel deleted in Liddle's syndrome. *EMBO J* (1996) 15:2371–80. doi: 10.1002/j.1460-2075.1996.tb00593.x
86. Spagnol G, Kieken F, Kopanic JL, Li H, Zach S, Stauch KL, et al. Structural Studies of the Nedd4 WW Domains and Their Selectivity for the Connexin43 (Cx43) Carboxyl Terminus. *J Biol Chem* (2016) 291:7637–50. doi: 10.1074/jbc.M115.701417
87. Kanelis V, Bruce MC, Skrynnikov NR, Rotin D, Forman-Kay JD. Structural determinants for high-affinity binding in a Nedd4 WW3* domain-Comm PY motif complex. *Structure* (2006) 14:543–53. doi: 10.1016/j.str.2005.11.018
88. Jennings MD, Blankley RT, Baron M, Golovanov AP, Avis JM. Specificity and autoregulation of Notch binding by tandem WW domains in suppressor of Deltex. *J Biol Chem* (2007) 282:29032–42. doi: 10.1074/jbc.M703453200
89. Maspero E, Mari S, Valentini E, Musacchio A, Fish A, Pasqualato S, et al. Structure of the HECT:ubiquitin complex and its role in ubiquitin chain elongation. *EMBO Rep* (2011) 12:342–9. doi: 10.1038/embor.2011.21
90. Aragon E, Goerner N, Xi Q, Gomes T, Gao S, Massague J, et al. Structural basis for the versatile interactions of Smad7 with regulator WW domains in TGF-beta Pathways. *Structure* (2012) 20:1726–36. doi: 10.1016/j.str.2012.07.014
91. Aragon E, Goerner N, Zaromytidou AI, Xi Q, Escobedo A, Massague J, et al. A Smad action turnover switch operated by WW domain readers of a phosphoserine code. *Genes Dev* (2011) 25:1275–88. doi: 10.1101/gad.2060811
92. Zhang W, Wu KP, Sartori MA, Kamadurai HB, Ordureau A, Jiang C, et al. System-Wide Modulation of HECT E3 Ligases with Selective Ubiquitin Variant Probes. *Mol Cell* (2016) 62:121–36. doi: 10.1016/j.molcel.2016.02.005
93. Desrochers G, Cappadocia L, Lussier-Price M, Ton AT, Ayoubi R, Serohijos A, et al. Molecular basis of interactions between SH3 domain-containing proteins and the proline-rich region of the ubiquitin ligase Itch. *J Biol Chem* (2017) 292:6325–38. doi: 10.1074/jbc.M116.754440
94. Liu Y, Lau J, Li W, Tempel W, Li L, Dong A, et al. Structural basis for the regulatory role of the PPxY motifs in the thioredoxin-interacting protein TXNIP. *Biochem J* (2016) 473:179–87. doi: 10.1042/BJ20150830
95. Wang Z, Liu Z, Chen X, Li J, Yao W, Huang S, et al. A multi-lock inhibitory mechanism for fine-tuning enzyme activities of the HECT family E3 ligases. *Nat Commun* (2019) 10:3162. doi: 10.1038/s41467-019-11224-7
96. Wahl LC, Watt JE, Yim HTT, De Bourcier D, Tolchard J, Soond SM, et al. Smad7 Binds Differently to Individual and Tandem WW3 and WW4 Domains of WWP2 Ubiquitin Ligase Isoforms. *Int J Mol Sci* (2019) 20:4682. doi: 10.3390/ijms20194682

97. Wiesner S, Ogunjimi AA, Wang HR, Rotin D, Sicheri F, Wrana JL, et al. Autoinhibition of the HECT-type ubiquitin ligase Smurf2 through its C2 domain. *Cell* (2007) 130:651–62. doi: 10.1016/j.cell.2007.06.050
98. Chong PA, Lin H, Wrana JL, Forman-Kay JD. Coupling of tandem Smad ubiquitination regulatory factor (Smurf) WW domains modulates target specificity. *Proc Natl Acad Sci USA* (2010) 107:18404–9. doi: 10.1073/pnas.1003023107
99. Ogunjimi AA, Briant DJ, Pece-Barbara N, Le Roy C, Di Guglielmo GM, Kavsak P, et al. Regulation of Smurf2 ubiquitin ligase activity by anchoring the E2 to the HECT domain. *Mol Cell* (2005) 19:297–308. doi: 10.1016/j.molcel.2005.06.028
100. Liu J, Xue Z, Zhang Y, Vann KR, Shi X, Kutateladze TG. Structural Insight into Binding of the ZZ Domain of HERC2 to Histone H3 and SUMO1. *Structure* (2020) 28:1225–30.e3. doi: 10.1016/j.str.2020.07.003
101. Dasso M. RCC1 in the cell cycle: the regulator of chromosome condensation takes on new roles. *Trends Biochem Sci* (1993) 18:96–101. doi: 10.1016/0968-0004(93)90161-F
102. Ohtsubo M, Okazaki H, Nishimoto T. The RCC1 protein, a regulator for the onset of chromosome condensation locates in the nucleus and binds to DNA. *J Cell Biol* (1989) 109:1389–97. doi: 10.1083/jcb.109.4.1389
103. Laity JH, Lee BM, Wright PE. Zinc finger proteins: new insights into structural and functional diversity. *Curr Opin Struct Biol* (2001) 11:39–46. doi: 10.1016/S0959-440X(00)00167-6
104. Kaustov L, Lukin J, Lemak A, Duan S, Ho M, Doherty R, et al. The conserved CPH domains of Cul7 and PARC are protein-protein interaction modules that bind the tetramerization domain of p53. *J Biol Chem* (2007) 282:11300–7. doi: 10.1074/jbc.M611297200
105. Cubillos-Rojas M, Amair-Pinedo F, Peiro-Jordan R, Bartrons R, Ventura F, Rosa JL. The E3 ubiquitin protein ligase HERC2 modulates the activity of tumor protein p53 by regulating its oligomerization. *J Biol Chem* (2014) 289:14782–95. doi: 10.1074/jbc.M113.527978
106. Elahian F, Sepehrizadeh Z, Moghimi B, Mirzaei SA. Human cytochrome b5 reductase: structure, function, and potential applications. *Crit Rev Biotechnol* (2014) 34:134–43. doi: 10.3109/07388551.2012.732031
107. McMillan BJ, Schnute B, Ohlenhard N, Zimmerman B, Miles L, Beglova N, et al. A tail of two sites: a bipartite mechanism for recognition of notch ligands by mind bomb E3 ligases. *Mol Cell* (2015) 57:912–24. doi: 10.1016/j.molcel.2015.01.019
108. Grossberger R, Gieffers C, Zachariae W, Podtelejnikov AV, Schleiffer A, Nasmyth K, et al. Characterization of the DOC1/APC10 subunit of the yeast and the human anaphase-promoting complex. *J Biol Chem* (1999) 274:14500–7. doi: 10.1074/jbc.274.20.14500
109. Alarcon R, Koumenis C, Geyer RK, Maki CG, Giaccia AJ. Hypoxia induces p53 accumulation through MDM2 down-regulation and inhibition of E6-mediated degradation. *Cancer Res* (1999) 59:6046–51.
110. Ansari T, Brimer N, Vande Pol SB. Peptide interactions stabilize and restructure human papillomavirus type 16 E6 to interact with p53. *J Virol* (2012) 86:11386–91. doi: 10.1128/JVI.01236-12
111. Gewin L, Galloway DA. E box-dependent activation of telomerase by human papillomavirus type 16 E6 does not require induction of c-myc. *J Virol* (2001) 75:7198–201. doi: 10.1128/JVI.75.15.7198-7201.2001
112. Beaudenon S, Dastur A, Huibregtse JM. Expression and assay of HECT domain ligases. *Methods Enzymol* (2005) 398:112–25. doi: 10.1016/S0076-6879(05)98011-7
113. Huibregtse JM, Scheffner M, Howley PM. Cloning and expression of the cDNA for E6-AP, a protein that mediates the interaction of the human papillomavirus E6 oncoprotein with p53. *Mol Cell Biol* (1993) 13:775–84. doi: 10.1128/MCB.13.2.775
114. Kao WH, Beaudenon SL, Talis AL, Huibregtse JM, Howley PM. Human papillomavirus type 16 E6 induces self-ubiquitination of the E6AP ubiquitin-protein ligase. *J Virol* (2000) 74:6408–17. doi: 10.1128/JVI.74.14.6408-6417.2000
115. Martinez-Noel G, Luck K, Kuhnle S, Desbuleux A, Szajner P, Galligan JT, et al. Network Analysis of UBE3A/E6AP-Associated Proteins Provides Connections to Several Distinct Cellular Processes. *J Mol Biol* (2018) 430:1024–50. doi: 10.1016/j.jmb.2018.01.021
116. Huibregtse JM, Scheffner M, Howley PM. A cellular protein mediates association of p53 with the E6 oncoprotein of human papillomavirus types 16 or 18. *EMBO J* (1991) 10:4129–35. doi: 10.1002/j.1460-2075.1991.tb04990.x
117. Martinez-Zapien D, Ruiz FX, Poirson J, Mitschler A, Ramirez J, Forster A, et al. Structure of the E6/E6AP/p53 complex required for HPV-mediated degradation of p53. *Nature* (2016) 529:541–5. doi: 10.1038/nature16481
118. Nuber U, Schwarz SE, Scheffner M. The ubiquitin-protein ligase E6-associated protein (E6-AP) serves as its own substrate. *Eur J Biochem* (1998) 254:643–9. doi: 10.1046/j.1432-1327.1998.2540643.x
119. Ro HS, Koh BH, Jung SO, Park HK, Shin YB, Kim MG, et al. Surface plasmon resonance imaging protein arrays for analysis of triple protein interactions of HPV, E6, E6AP, and p53. *Proteomics* (2006) 6:2108–11. doi: 10.1002/pmic.200500635
120. Sailer C, Offensperger F, Julier A, Kammer KM, Walker-Gray R, Gold MG, et al. Structural dynamics of the E6AP/UBE3A-E6-p53 enzyme-substrate complex. *Nat Commun* (2018) 9:4441. doi: 10.1038/s41467-018-06953-0
121. Scheffner M, Huibregtse JM, Howley PM. Identification of a human ubiquitin-conjugating enzyme that mediates the E6-AP-dependent ubiquitination of p53. *Proc Natl Acad Sci USA* (1994) 91:8797–801. doi: 10.1073/pnas.91.19.8797
122. Scheffner M, Huibregtse JM, Vierstra RD, Howley PM. The HPV-16 E6 and E6-AP complex functions as a ubiquitin-protein ligase in the ubiquitination of p53. *Cell* (1993) 75:495–505. doi: 10.1016/0092-8674(93)90384-3
123. Stutz C, Reinz E, Honegger A, Bulkescher J, Schweizer J, Zanier K, et al. Intracellular Analysis of the Interaction between the Human Papillomavirus Type 16 E6 Oncoprotein and Inhibitory Peptides. *PloS One* (2015) 10:e0132339. doi: 10.1371/journal.pone.0132339
124. Nakagawa S, Huibregtse JM. Human scribble (Vartul) is targeted for ubiquitin-mediated degradation by the high-risk papillomavirus E6 proteins and the E6AP ubiquitin-protein ligase. *Mol Cell Biol* (2000) 20:8244–53. doi: 10.1128/MCB.20.21.8244-8253.2000
125. Talis AL, Huibregtse JM, Howley PM. The role of E6AP in the regulation of p53 protein levels in human papillomavirus (HPV)-positive and HPV-negative cells. *J Biol Chem* (1998) 273:6439–45. doi: 10.1074/jbc.273.11.6439
126. Thatte J, Banks L. Human Papillomavirus 16 (HPV-16), HPV-18, and HPV-31 E6 Override the Normal Phosphoregulation of E6AP Enzymatic Activity. *J Virol* (2017) 91. doi: 10.1128/JVI.01390-17
127. White EA, Kramer RE, Tan MJ, Hayes SD, Harper JW, Howley PM. Comprehensive analysis of host cellular interactions with human papillomavirus E6 proteins identifies new E6 binding partners and reflects viral diversity. *J Virol* (2012) 86:13174–86. doi: 10.1128/JVI.02172-12
128. Huibregtse JM, Scheffner M, Howley PM. Localization of the E6-AP regions that direct human papillomavirus E6 binding, association with p53, and ubiquitination of associated proteins. *Mol Cell Biol* (1993) 13:4918–27. doi: 10.1128/MCB.13.8.4918
129. Kuhnle S, Martinez-Noel G, Leclere F, Hayes SD, Harper JW, Howley PM. Angelman syndrome-associated point mutations in the Zn(2+)-binding N-terminal (AZUL) domain of UBE3A ubiquitin ligase inhibit binding to the proteasome. *J Biol Chem* (2018) 293:18387–99. doi: 10.1074/jbc.RA118.004653
130. Cooper B, Schneider S, Bohl J, Jiang Y, Beaudet A, Vande Pol S. Requirement of E6AP and the features of human papillomavirus E6 necessary to support degradation of p53. *Virology* (2003) 306:87–99. doi: 10.1016/S0042-6822(02)00012-0
131. Peschiaroli A, Scialpi F, Bernassola F, El Sherbini el S, Melino G. The E3 ubiquitin ligase WWP1 regulates DeltaNp63-dependent transcription through Lys63 linkages. *Biochem Biophys Res Commun* (2010) 402:425–30. doi: 10.1016/j.bbrc.2010.10.050
132. Bellomaria A, Barbato G, Melino G, Paci M, Melino S. Recognition of p63 by the E3 ligase ITCH: Effect of an ectodermal dysplasia mutant. *Cell Cycle* (2010) 9:3730–9. doi: 10.4161/cc.9.18.12933
133. Bellomaria A, Barbato G, Melino G, Paci M, Melino S. Recognition mechanism of p63 by the E3 ligase Itch: novel strategy in the study and inhibition of this interaction. *Cell Cycle* (2012) 11:3638–48. doi: 10.4161/cc.21918
134. Melino S, Bellomaria A, Nepravishta R, Paci M, Melino G. p63 threonine phosphorylation signals the interaction with the WW domain of the E3 ligase Itch. *Cell Cycle* (2014) 13:3207–17. doi: 10.4161/15384101.2014.951285

135. Rossi M, Aqeilan RI, Neale M, Candi E, Salomoni P, Knight RA, et al. The E3 ubiquitin ligase Itch controls the protein stability of p63. *Proc Natl Acad Sci USA* (2006) 103:12753–8. doi: 10.1073/pnas.0603449103
136. Rossi M, De Simone M, Pollice A, Santoro R, La Mantia G, Guerrini L, et al. Itch/AIP4 associates with and promotes p63 protein degradation. *Cell Cycle* (2006) 5:1816–22. doi: 10.4161/cc.5.16.2861
137. Bakkers J, Camacho-Carvajal M, Nowak M, Kramer C, Danger B, Hammerschmidt M. Destabilization of DeltaNp63alpha by Nedd4-mediated ubiquitination and Ubc9-mediated sumoylation, and its implications on dorsoventral patterning of the zebrafish embryo. *Cell Cycle* (2005) 4:790–800. doi: 10.4161/cc.4.6.1694
138. Miyazaki K, Ozaki T, Kato C, Hanamoto T, Fujita T, Irino S, et al. A novel HECT-type E3 ubiquitin ligase, NEDL2, stabilizes p73 and enhances its transcriptional activity. *Biochem Biophys Res Commun* (2003) 308:106–13. doi: 10.1016/S0006-291X(03)01347-0
139. Rossi M, De Laurenzi V, Munarriz E, Green DR, Liu YC, Vousden KH, et al. The ubiquitin-protein ligase Itch regulates p73 stability. *EMBO J* (2005) 24:836–48. doi: 10.1038/sj.emboj.7600444
140. Gao K, An J, Zhang Y, Jin X, Ma J, Peng J, et al. The E3 ubiquitin ligase Itch and Yap1 have antagonistic roles in the regulation of ASPP2 protein stability. *FEBS Lett* (2015) 589:94–101. doi: 10.1016/j.febslet.2014.11.030
141. Gen Y, Yasui K, Kitaichi T, Iwai N, Terasaki K, Dohi O, et al. ASPP2 suppresses invasion and TGF-beta1-induced epithelial-mesenchymal transition by inhibiting Smad7 degradation mediated by E3 ubiquitin ligase ITCH in gastric cancer. *Cancer Lett* (2017) 398:52–61. doi: 10.1016/j.canlet.2017.04.002
142. Louria-Hayon I, Alsheich-Bartok O, Levav-Cohen Y, Silberman I, Berger M, Grossman T, et al. E6AP promotes the degradation of the PML tumor suppressor. *Cell Death Differ* (2009) 16:1156–66. doi: 10.1038/cdd.2009.31
143. Xu C, Fan CD, Wang X. Regulation of Mdm2 protein stability and the p53 response by NEDD4-1 E3 ligase. *Oncogene* (2015) 34:281–9. doi: 10.1038/onc.2013.557
144. Wu W, Sato K, Koike A, Nishikawa H, Koizumi H, Venkitaraman AR, et al. HERC2 is an E3 ligase that targets BRCA1 for degradation. *Cancer Res* (2010) 70:6384–92. doi: 10.1158/0008-5472.CAN-10-1304
145. Holloway A, Simmonds M, Azad A, Fox JL, Storey A. Resistance to UV-induced apoptosis by beta-HPV5 E6 involves targeting of activated BAK for proteolysis by recruitment of the HERC1 ubiquitin ligase. *Int J Cancer* (2015) 136:2831–43. doi: 10.1002/ijc.29350
146. Ho KC, Zhou Z, She YM, Chun A, Cyr TD, Yang X. Itch E3 ubiquitin ligase regulates large tumor suppressor 1 stability [corrected]. *Proc Natl Acad Sci USA* (2011) 108:4870–5. doi: 10.1073/pnas.1101273108
147. Salah Z, Melino G, Aqeilan RI. Negative regulation of the Hippo pathway by E3 ubiquitin ligase ITCH is sufficient to promote tumorigenicity. *Cancer Res* (2011) 71:2010–20. doi: 10.1158/0008-5472.CAN-10-3516
148. Chang L, Shen L, Zhou H, Gao J, Pan H, Zheng L, et al. ITCH nuclear translocation and H1.2 polyubiquitination negatively regulate the DNA damage response. *Nucleic Acids Res* (2019) 47:824–42. doi: 10.1093/nar/gky1199
149. Shinada K, Tsukiyama T, Sho T, Okumura F, Asaka M, Hatakeyama S. RNF43 interacts with NEDL1 and regulates p53-mediated transcription. *Biochem Biophys Res Commun* (2011) 404:143–7. doi: 10.1016/j.bbrc.2010.11.082
150. Garcia-Cano J, Sanchez-Tena S, Sala-Gaston J, Figueras A, Vinals F, Bartrons R, et al. Regulation of the MDM2-p53 pathway by the ubiquitin ligase HERC2. *Mol Oncol* (2020) 14:69–86. doi: 10.1002/1878-0261.12592
151. Bekker-Jensen S, Mailand N. Assembly and function of DNA double-strand break repair foci in mammalian cells. *DNA Repair (Amst)* (2010) 9:1219–28. doi: 10.1016/j.dnarep.2010.09.010
152. Nguyen Huu NS, Ryder WD, Zeps N, Flasza M, Chiu M, Hanby AM, et al. Tumour-promoting activity of altered WWP1 expression in breast cancer and its utility as a prognostic indicator. *J Pathol* (2008) 216:93–102. doi: 10.1002/path.2385
153. Jones DC, Wein MN, Oukka M, Hofstaetter JG, Glimcher MJ, Glimcher LH. Regulation of adult bone mass by the zinc finger adapter protein Schnurri-3. *Science* (2006) 312:1223–7. doi: 10.1126/science.1126313
154. Shu L, Zhang H, Boyce BF, Xing L. Ubiquitin E3 ligase Wwp1 negatively regulates osteoblast function by inhibiting osteoblast differentiation and migration. *J Bone mineral Res Off J Am Soc Bone Mineral Res* (2013) 28:1925–35. doi: 10.1002/jbmr.1938
155. Azmi P, Seth A. RNF11 is a multifunctional modulator of growth factor receptor signalling and transcriptional regulation. *Eur J Cancer* (2005) 41:2549–60. doi: 10.1016/j.ejca.2005.08.020
156. Chen C, Zhou Z, Liu R, Li Y, Azmi PB, Seth AK. The WW domain containing E3 ubiquitin protein ligase 1 upregulates ErbB2 and EGFR through RING finger protein 11. *Oncogene* (2008) 27:6845–55. doi: 10.1038/onc.2008.288
157. Yeung B, Ho KC, Yang X. WWP1 E3 ligase targets LATS1 for ubiquitin-mediated degradation in breast cancer cells. *PloS One* (2013) 8:e61027. doi: 10.1371/journal.pone.0061027
158. Marine JC, Lozano G. Mdm2-mediated ubiquitylation: p53 and beyond. *Cell Death Differ* (2010) 17:93–102. doi: 10.1038/cdd.2009.68
159. Wu Z, Zan P, Li S, Liu J, Wang J, Chen D, et al. Knockdown of WWP1 inhibits growth and invasion, but induces apoptosis of osteosarcoma cells. *Int J Clin Exp Pathol* (2015) 8:7869–77.
160. Zhou Z, Liu R, Chen C. The WWP1 ubiquitin E3 ligase increases TRAIL resistance in breast cancer. *Int J Cancer* (2012) 130:1504–10. doi: 10.1002/ijc.26122
161. Komuro A, Imamura T, Saitoh M, Yoshida Y, Yamori T, Miyazono K, et al. Negative regulation of transforming growth factor-beta (TGF-beta) signaling by WW domain-containing protein 1 (WWP1). *Oncogene* (2004) 23:6914–23. doi: 10.1038/sj.onc.1207885
162. Ebisawa T, Fukuchi M, Murakami G, Chiba T, Tanaka K, Imamura T, et al. Smurf1 interacts with transforming growth factor-beta type I receptor through Smad7 and induces receptor degradation. *J Biol Chem* (2001) 276:12477–80. doi: 10.1074/jbc.C100008200
163. Suzuki C, Murakami G, Fukuchi M, Shimanuki T, Shikauchi Y, Imamura T, et al. Smurf1 regulates the inhibitory activity of Smad7 by targeting Smad7 to the plasma membrane. *J Biol Chem* (2002) 277:39919–25. doi: 10.1074/jbc.M201901200
164. Tajima Y, Goto K, Yoshida M, Shinomiya K, Sekimoto T, Yoneda Y, et al. Chromosomal region maintenance 1 (CRM1)-dependent nuclear export of Smad ubiquitin regulatory factor 1 (Smurf1) is essential for negative regulation of transforming growth factor-beta signaling by Smad7. *J Biol Chem* (2003) 278:10716–21. doi: 10.1074/jbc.M212663200
165. Yamaguchi T, Kurisaki A, Yamakawa N, Minakuchi K, Sugino H. FKBP12 functions as an adaptor of the Smad7-Smurf1 complex on activin type I receptor. *J Mol Endocrinol* (2006) 36:569–79. doi: 10.1677/jme.1.01966
166. Xia Q, Zhang H, Zhang P, Li Y, Xu M, Li X, et al. Oncogenic Smurf1 promotes PTEN wild-type glioblastoma growth by mediating PTEN ubiquitylation. *Oncogene* (2020) 39:5902–15. doi: 10.1038/s41388-020-01400-1
167. Meulmeester E, Frenk R, Stad R, de Graaf P, Marine JC, Vousden KH, et al. Critical role for a central part of Mdm2 in the ubiquitylation of p53. *Mol Cell Biol* (2003) 23:4929–38. doi: 10.1128/MCB.23.14.4929-4938.2003
168. Saito A, Hayashi T, Okuno S, Nishi T, Chan PH. Modulation of p53 degradation via MDM2-mediated ubiquitylation and the ubiquitin-proteasome system during reperfusion after stroke: role of oxidative stress. *J Cereb Blood Flow Metab* (2005) 25:267–80. doi: 10.1038/sj.jcbfm.9600028
169. Boyer L, Turchi L, Desnues B, Doye A, Ponzio G, Mege JL, et al. CNF1-induced ubiquitylation and proteasome destruction of activated RhoA is impaired in Smurf1-/- cells. *Mol Biol Cell* (2006) 17:2489–97. doi: 10.1091/mbc.e05-09-0876
170. Guo R, Yamashita M, Zhang Q, Zhou Q, Chen D, Reynolds DG, et al. Ubiquitin ligase Smurf1 mediates tumor necrosis factor-induced systemic bone loss by promoting proteasomal degradation of bone morphogenetic signaling proteins. *J Biol Chem* (2008) 283:23084–92. doi: 10.1074/jbc.M709848200
171. Li S, Lu K, Wang J, An L, Yang G, Chen H, et al. Ubiquitin ligase Smurf1 targets TRAF family proteins for ubiquitination and degradation. *Mol Cell Biochem* (2010) 338:11–7. doi: 10.1007/s11010-009-0315-y
172. Gajjar M, Candeias MM, Malbert-Colas L, Mazars A, Fujita J, Olivares-Illana V, et al. The p53 mRNA-Mdm2 interaction controls Mdm2 nuclear trafficking and is required for p53 activation following DNA damage. *Cancer Cell* (2012) 21:25–35. doi: 10.1016/j.ccr.2011.11.016
173. Weber AM, Ryan AJ. ATM and ATR as therapeutic targets in cancer. *Pharmacol Ther* (2015) 149:124–38. doi: 10.1016/j.pharmthera.2014.12.001

174. Kang TH, Lindsey-Boltz LA, Reardon JT, Sancar A. Circadian control of XPA and excision repair of cisplatin-DNA damage by cryptochrome and HERC2 ubiquitin ligase. *Proc Natl Acad Sci USA* (2010) 107:4890–5. doi: 10.1073/pnas.0915085107
175. Izawa N, Wu W, Sato K, Nishikawa H, Kato A, Boku N, et al. HERC2 Interacts with Claspin and regulates DNA origin firing and replication fork progression. *Cancer Res* (2011) 71:5621–5. doi: 10.1158/0008-5472.CAN-11-0385
176. Bekker-Jensen S, Rendtlew Danielsen J, Fugger K, Gromova I, Nerstedt A, Lukas C, et al. HERC2 coordinates ubiquitin-dependent assembly of DNA repair factors on damaged chromosomes. *Nat Cell Biol* (2010) 12:80–6; sup pp 1-12. doi: 10.1038/ncb2008
177. Zhu M, Zhao H, Liao J, Xu X. HERC2/USP20 coordinates CHK1 activation by modulating CLASPIN stability. *Nucleic Acids Res* (2014) 42:13074–81. doi: 10.1093/nar/gku978
178. Yuan J, Luo K, Deng M, Li Y, Yin P, Gao B, et al. HERC2-USP20 axis regulates DNA damage checkpoint through Claspin. *Nucleic Acids Res* (2014) 42:13110–21. doi: 10.1093/nar/gku1034
179. Kuhnle S, Kogel U, Glockzin S, Marquardt A, Ciechanover A, Matentzoglu K, et al. Physical and functional interaction of the HECT ubiquitin-protein ligases E6AP and HERC2. *J Biol Chem* (2011) 286:19410–6. doi: 10.1074/jbc.M110.205211
180. Valnegri P, Huang J, Yamada T, Yang Y, Mejia LA, Cho HY, et al. RNF8/UBC13 ubiquitin signaling suppresses synapse formation in the mammalian brain. *Nat Commun* (2017) 8:1271. doi: 10.1038/s41467-017-01333-6
181. Oestergaard VH, Pentzold C, Pedersen RT, Iosif S, Alpi A, Bekker-Jensen S, et al. RNF8 and RNF168 but not HERC2 are required for DNA damage-induced ubiquitylation in chicken DT40 cells. *DNA Repair (Amst)* (2012) 11:892–905. doi: 10.1016/j.dnarep.2012.08.005
182. Wu W, Rokutanda N, Takeuchi J, Lai Y, Maruyama R, Togashi Y, et al. HERC2 Facilitates BLM and WRN Helicase Complex Interaction with RPA to Suppress G-Quadruplex DNA. *Cancer Res* (2018) 78:6371–85. doi: 10.1158/0008-5472.CAN-18-1877
183. Vissers JH, van Lohuizen M, Citterio E. The emerging role of Polycomb repressors in the response to DNA damage. *J Cell Sci* (2012) 125:3939–48. doi: 10.1242/jcs.107375
184. Wang Z, Wang J, Li X, Xing L, Ding Y, Shi P, et al. Bortezomib prevents oncogenesis and bone metastasis of prostate cancer by inhibiting WWP1, Smurf1 and Smurf2. *Int J Oncol* (2014) 45:1469–78. doi: 10.3892/ijo.2014.2545
185. Weber J, Polo S, Maspero E. HECT E3 Ligases: A Tale With Multiple Facets. *Front Physiol* (2019) 10:370. doi: 10.3389/fphys.2019.00370

Conflict of Interest: The authors declare that the research was conducted in the absence of any commercial or financial relationships that could be construed as a potential conflict of interest.

frontiers in Oncology

ORIGINAL RESEARCH
published: 16 April 2021
doi: 10.3389/fonc.2021.637040

Targeting ADT-Induced Activation of the E3 Ubiquitin Ligase Siah2 to Delay the Occurrence of Castration-Resistant Prostate Cancer

Tingmang Yan[1†‡], Dapeng Zhou[1‡], Youwei Shi[1], Di Cui[1], Juntao Jiang[1], Bangmin Han[1], Shujie Xia[1], Zhou Wang[2,3,4,5], Haitao Liu[1], Wenhuan Guo[6*] and Yifeng Jing[1*]*

[1] Department of Urology, Shanghai General Hospital, Shanghai Jiao Tong University School of Medicine, Shanghai, China, [2] Department of Urology, University of Pittsburgh School of Medicine, Pittsburgh, PA, United States, [3] Department of Pharmacology and Chemical Biology, University of Pittsburgh School of Medicine, Pittsburgh, PA, United States, [4] Department of Pathology, University of Pittsburgh School of Medicine, Pittsburgh, PA, United States, [5] UPMC Hillman Cancer Center, University of Pittsburgh School of Medicine, Pittsburgh, PA, United States, [6] Pathology Center, Shanghai General Hospital/Faculty of Basic Medicine, Shanghai Jiao Tong University School of Medicine, Shanghai, China

Siah2 is an E3 ubiquitin ligase that targets androgen receptor (AR) and plays an important role in the development of castration-resistant prostate cancer (CRPC). However, the regulation of Siah2 in prostate cancer (PCa) is largely unknown. In this study, we used AR-dependent and -independent cells lines to investigate the cellular roles of AR and androgen deprivation therapy (ADT) on Siah2 protein levels and E3 ligase activity using Western blotting and co-immunoprecipitation. We also validated our findings using patient samples taken before and after ADT. Finally, we used xenograft tumor models to test the effects of ADT combined with vitamin K3 (Vit K3) on tumor growth *in vivo*. Our results showed that AR stabilizes Siah2 protein by attenuating its self-ubiquitination and auto-degradation, likely by blocking its E3 ubiquitin ligase activity. Conversely, ADT decreased Siah2 protein expression but enhanced its E3 ligase activity in PCa cells. Notably, the findings that ADT decreasing Siah2 protein expression were verified in a series of paired PCa samples from the same patient. Additionally, we found that ADT-induced Siah2 activation could be abolished by Vit K3. Strikingly, ADT combined with Vit K3 treatment delayed the occurrence of CRPC and dramatically inhibited the growth of tumor xenografts compared with ADT treatment alone. AR is an inhibitor of Siah2 in PCa, and ADT leads to the continuous activation of Siah2, which may contribute to CRPC. Finally, ADT+Vit K3 may be a potential approach to delay the occurrence of CRPC.

Keywords: castration-resistant prostate cancer, androgen receptor, androgen deprivation therapy, Siah2, E3 ubiquitin ligase

OPEN ACCESS

Edited by:
Matthew K. Summers, The Ohio State University, United States

Reviewed by:
Marco A. Calzado, University of Cordoba, Spain
Feng Liu-Smith, University of Tennessee Health Science Center (UTHSC), United States

***Correspondence:**
Yifeng Jing
jyf_123@163.com
Wenhuan Guo
wenhuan1130@sina.com
Haitao Liu
doctorlht69@163.com

***Present address:**
Tingmang Yan, Department of Urology, Hua Shan Hospital, Fudan University School of Medicine, Shanghai, China

These authors have contributed equally to this work

Specialty section:
This article was submitted to Cancer Molecular Targets and Therapeutics, a section of the journal Frontiers in Oncology

Received: *02 December 2020*
Accepted: *26 March 2021*
Published: *16 April 2021*

Citation:
Yan T, Zhou D, Shi Y, Cui D, Jiang J, Han B, Xia S, Wang Z, Liu H, Guo W and Jing Y (2021) Targeting ADT-Induced Activation of the E3 Ubiquitin Ligase Siah2 to Delay the Occurrence of Castration-Resistant Prostate Cancer. Front. Oncol. 11:637040. doi: 10.3389/fonc.2021.637040

INTRODUCTION

Prostate cancer (PCa) is the most commonly diagnosed malignancy and the second leading cause of cancer-related mortality in American men, with an estimated 174,650 new cases and 31,620 deaths expected in 2020 (1). Notably, PCa has also become the most common male urogenital malignancy in China (2). Androgen deprivation therapy (ADT) remains the first-line therapy for men with metastatic

PCa; however, most patients ultimately relapse with castration-resistant prostate cancer (CRPC), which is currently incurable and accounts for most PCa-associated mortalities (3). Although the mechanisms of CRPC remain unclear, accumulating evidence has shown that androgen receptor (AR) signaling is central to CRPC progression (4, 5). Several mechanisms have been suggested to mediate androgen-independent AR signaling, including AR mutations, AR gene amplifications or overexpression, expression of specific AR splice variants, intratumoral androgen production, and abnormal post-translation modification of AR, such as phosphorylation, methylation, acetylation, ubiquitination, and SUMOylation (6).

Siah2 is a RING finger type ubiquitin ligase comprising a catalytic RING domain, two zinc fingers, and a C-terminal substrate-binding domain (SBD) (7). Many proteins have been identified as substrates of Siah2, including N-CoR, PHD, Sprouty2, β-catenin, and AR (8–12). Several studies have shown that Siah2 has important roles in tumorigenesis and metastasis in multiple cancers, including breast cancer, lung cancer, pancreatic cancer, melanoma, and PCa (13). Importantly, Siah2 has been identified as an E3 ubiquitin ligase of AR that specifically targets a selective pool of NCOR1-bound, repressed AR chromatin complexes for degradation. These complexes are typically involved in lipid metabolism, cell motility, and proliferation in PCa cells. Additionally, Siah2 is required for CRPC tumor growth in mice, whereas Siah2 deletion increases the castration sensitivity of TRAMP mice (12). Thus, Siah2 is a critical player in CRPC development.

Given its role in CRPC, it is important to know how Siah2 is regulated in PCa. We and others have previously reported that Siah2 is regulated by proteins, such as DHX15 and AKR1C3 in PCa (14, 15). However, the clinical relevance of these studies still needs further verification. In this study, we show that AR is a substrate of Siah2 that can inhibit Siah2 self-ubiquitination, stabilize Siah2 expression, and decrease its E3 ubiquitin ligase activity in PCa cells. Additionally, ADT significantly reduced Siah2 expression and enhanced its ligase activity. Notably, these findings are closely related to clinical PCa samples. Importantly, treatment with the specific Siah2 inhibitor, vitamin K3 (Vit K3), delayed LNCaP tumor progression to castration resistance in LNCaP tumors. Therefore, Vit K3 might be an adjuvant that can be combined with ADT to treat advanced PCa and delay CRPC.

MATERIALS AND METHODS

Plasmid Constructs

All plasmid constructs were created or obtained as previously described (14).

Cell Culture and Transfection

The human PCa cell lines LNCaP, 22Rv1, and PC3, and HEK293 cells were obtained from American Type Culture Collection (ATCC, Manassas, VA, USA). Cells were maintained in the appropriate medium (RPMI-1640 for LNCaP, PC3, and 22Rv1 and DMEM for HEK293) supplied with 10% fetal bovine serum, 5% antibiotics, and 1% L-glutamine at 37°C with 5% CO_2. Cells were verified as mycoplasma free using PCR. Cells were cultured in phenol red-free medium supplied with 5% dextran-coated charcoal-stripped fetal bovine serum (CS-FBS) for 24 h before treatment with dihydrotestosterone (Sigma-Aldrich, St Louis, MO, USA). In some experiments, cells were treated with the protein synthesis inhibitor cycloheximide (Sigma-Aldrich) at 50 μg/ml and/or the proteasome inhibitor MG132 (Sigma-Aldrich) at 5 μM for various times as described in the figure legends. Cell transfection was separately performed with Lipofectamine 2000 (Invitrogen, Carlsbad, CA, USA) for constructs or siRNAs according to the manufacturer's protocols. The siRNA targeting AR was purchased from Thermo Fisher Scientific (Waltham, MA, USA). The siRNAs targeting Siah2 were as follows: Siah2-1, 5′-UAUGACUUGCUUUCCUAGGCAAUCCAC-3′; Siah2-2, 5′-CCUCCCAUUCCUAACACACUGAUCUAU-3′.

Western Blot Analysis and Immunoprecipitation

Western blot and immunoprecipitation assays were performed as previously described (14). Primary antibodies against Siah2 (NBP1-19648, Novus Biologicals, Littleton, CO, USA, 1:1000), AR (sc-816, Santa Cruz Biotechnology, Dallas, TX, USA, 1:1000), Sprouty2 (sc-30049, Santa Cruz Biotechnology, 1:1000), Flag M2 (F1804, Sigma-Aldrich, 1:2000), Myc (MMS-150, Covance, Princeton, NJ, USA, 1:2000), HA (MMS-101P, Covance, 1:2000), and Tubulin (abs131993, Absin Bioscience, Shanghai, China, 1:5000) were used in the study.

In Vivo Ubiquitination Assay

HEK293 cells were transfected with Flag-AR, GFP-AR, and HA-ubiquitin as indicated for 24 h, and then were treated with 5 μM MG132 for 16 h before harvest. Cells were lysed in 100 μl RIPA buffer with 1% SDS to disrupt protein–protein interactions, and then boiled for 10 min at 95°C. The lysates were diluted 10-fold with RIPA buffer and immunoprecipitated with Flag M2 gel for 3 h followed by incubation with protein A/G Plus-Agarose for 3 h. After three washes, the immunoprecipitates were subjected to Western blot analysis.

RT-PCR and Real-Time PCR

RT-PCR and real-time PCR were performed as described previously (14). The primer sequences used were as follows: AR, 5′-TGGATGGATAGCTACTCCGG-3′ and 5′-CCCAGAAGCTTCATCTCCAC-3′; GAPDH, 5′-CGACCACTTTGTCAAGCTCA-3′ and 5′-AGGGGAGATTCAGTGTGGTG-3′; and Siah2, 5′-AGGTTGCCCTCTGCCGATA-3′ and 5′-ACATAGGTGAGTGGCCAAATCTC-3′.

Immunohistochemistry

Formalin-fixed paraffin-embedded (FFPE) PCa specimens were obtained from the surgical pathology archives of Shanghai General Hospital. Use of these prostate tissues was approved by the Shanghai General Hospital Review Board. Immunohistochemistry was performed as previously described (14) using an anti-Siah2 antibody (NB110-88113 [24E6H3], Novus Biologicals, 1:500).

Transwell Migration and BrdU Incorporation Assays

The transwell migration and BrdU incorporation assays were performed as previously described (14).

Animals and Xenograft Tumors

Male athymic BALB/c nude mice (5–6 weeks old) purchased from the Animal Center of the Chinese Academy of Sciences (Shanghai, China) were subcutaneously injected in one flank with 300 μl of LNCaP cells (1 × 106) mixed 1:1 (v:v) with Matrigel (Invitrogen). Tumors were measured with calipers twice per week. Tumor volumes were calculated using the formula length × width 2 × 0.52. Mice were randomized into three groups once the tumor volume reached 0.6 mm3: the sham-operated (n=5), castration (n=5), and castration+Vit K3(Sigma-Aldrich) injection groups (n=5). For the latter, a dose of 10 mg/kg Vit K3 (dissolved in DMSO at a final concentration of 0.1%) was administered *via* twice weekly intra-peritoneal injections. Tumor growth was monitored twice per week for 7 weeks, at which point the mice were sacrificed and tumors were harvested for Western blot analyses. All animal studies were conducted in accordance with the Shanghai Jiao Tong University Medical School's Animal Committee guidelines.

Statistical Analysis

Data are presented as mean ± standard error (SEM) or mean ± standard deviation (SD). Statistical analyses were performed with Student's t-test or one-way ANOVA. $P < 0.05$ was considered statistically significant.

RESULTS

Androgens Stabilized Siah2 Protein in PCa Cells

Due to the pivotal role of Siah2 in the development of CRPC, here we asked how Siah2 was regulated during ADT. Therefore, we first assessed whether Siah2 expression was altered following the treatment of PCa cells with androgens. Notably, treatment of LNCaP cells with 10 nM dihydrotestosterone (DHT) for 24 h led to a significant increase in Siah2 protein expression (**Figure 1A**). We next determined the expression of Siah2 in response to DHT in another AR-positive PCa cell line, 22Rv1. Treating 22Rv1 cells with DHT also dramatically increased Siah2 expression (**Figure 1A**). Furthermore, DHT effect on Siah2 showed a dose-dependent manner (**Figure S1A**). Nevertheless, DHT did not alter Siah2 mRNA levels in either LNCaP or 22Rv1 cells, which suggests that DHT regulates Siah2 expression at the post-transcriptional level (**Figure 1B**). To determine whether androgens altered Siah2 stability, we monitored the half-life of endogenous Siah2 in the presence of the protein synthesis inhibitor cycloheximide; 10 nM DHT prolonged the half-life of Siah2 from approximately 1.5 to 5 h in both LNCaP and 22Rv1 cells (**Figures 1C, D**). To further address the role of AR in DHT-mediated Siah2 stabilization in PCa cells, siRNAs specifically targeting AR or the antagonist flutamide were used to block AR. Both siRNAs and flutamide decreased Siah2 protein expression (**Figures 1E, F**). Consistently, DHT treatment increases Siah2 protein level in AR-positive LNCaP cells but not in AR-negative PC3 cells (**Figure S1B**). Additionally, co-transfection of HA-Siah2 with different amounts of Flag-AR into HEK293 cells showed that Siah2 protein levels increased with increasing amount of exogenous AR expression (**Figure 1G**). Finally, we found AR increased the expression of Wild-type Siah2 (Siah2-WT) but not RING mutant Siah2 (Siah2-RM, which lacks ubiquitin ligase activity), suggesting that AR stabilizes Siah2 by inhibiting its ubiquitin ligase activity (**Figure 1H**). Together, these findings demonstrate that AR stabilizes Siah2 protein in PCa cells.

AR Inhibits Siah2 Self-Ubiquitination and Decreases Its E3 Ligase Activity

Like other RING finger E3 ubiquitin ligases, Siah2 limits its own expression by self-ubiquitination and auto-degradation, which is a sign of its ubiquitin-ligase activity. To test the effect of AR stabilization on Siah2 E3 ligase activity, we monitored Siah2-mediated degradation of Sprouty2 (Spry2), one of the classic substrates of Siah2 and a marker for Siah2 ligase activity. Overexpressing wide-type Siah2 effectively reduced Spry2 half-life from approximately 5 to 3 h, while co-expression of AR prolonged Spry2 half-life to approximately 4 h (**Figures 2A, B**). RING mutant Siah2 alone or co-expression with AR did not change the half-life of Spry2 (**Figure S2A**), which indicated AR inhibits Siah2 E3 ligase activity. We next assessed the effect of DHT on endogenous Spy2 and PHD3, another classic substrate of Siah2. Treatment with 10 nM DHT for 24 h resulted in significantly increased Spry2 and Siah2 levels in both LNCaP and 22Rv1 cells (**Figure 2C**). As expected, DHT treatment increased PHD3 expression as well (**Figure 2D**). These observations suggest that Siah2 ligase activity was inhibited in the presence of AR.

We next determined whether AR stabilized Siah2 protein by inhibiting its self-ubiquitination. Therefore, we co-expressed Flag-Siah2-WT or Flag-Siah2-RM, HA-Ub, and GFP-AR in PC3 cells and treated the cells with the proteasome inhibitor MG132 for 6 h. We then immunoprecipitated Flag-Siah2 using anti-Flag M2 beads and performed Western blot analysis with an anti-HA antibody to detect Flag-Siah2 ubiquitination levels. As expected, Siah2-WT ubiquitination was decreased in the presence of AR, while ubiquitination of Siah2-RM was not changed (**Figure 2E**). Siah2 comprises three different domains: N-terminal domain, central RING domain/zinc finger domain, and C-terminal SBD. To map the Siah2 domains required for this AR interaction, we generated truncation mutants of Siah2 (14) and co-transfected them individually with AR into HEK293 cells. These co-immunoprecipitation assays revealed that both the SBD and the central RING domain/zinc finger domains were required for the interaction with AR (**Figure 2F**).

ADT Decreased Siah2 Expression and Increased Its Ligase Activity

Given that AR stabilized Siah2 protein and inhibited its E3 ligase activity, we hypothesized that ADT may increase Siah2 activity in

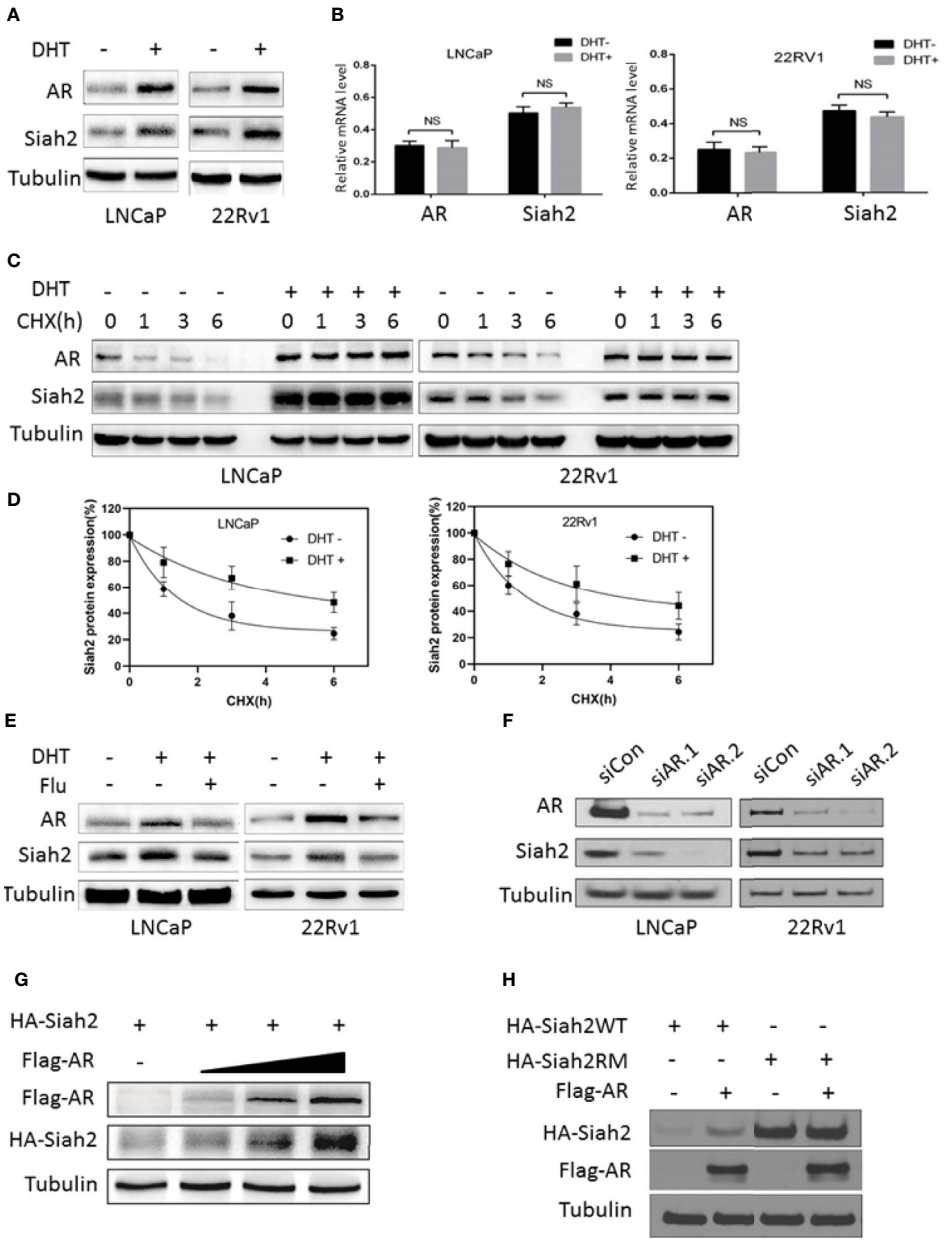

FIGURE 1 | Androgens stabilized Siah2 protein levels. **(A)** LNCaP and 22Rv1 cells were cultured in CS-FBS medium for 24 h, and then treated with 10 nM DHT or vehicle for 24 h. AR and Siah2 protein expression were detected using Western blotting. **(B)** LNCaP and 22Rv1 cells were treated as described in A, and then AR and Siah2 mRNA expression were detected by qPCR. **(C)** LNCaP and 22Rv1 cells were treated as described in A, and then treated with cycloheximide (CHX, 50 μg/ml) for 1, 3, and 6 h, after which cell lysates were subjected to Western blotting. **(D)** Degradation curves of Siah2 by cycloheximide chase experiments in the presence or absence of DHT. **(E)** LNCaP and 22Rv1 cells were treated as described in A, and then treated with flutamide (5 μM) for 24 h. AR and Siah2 protein expression were detected using Western blotting. **(F)** LNCaP and 22Rv1 cells were transfected with two different siRNAs targeting Siah2 or control for 72 h, and then subjected to Western blotting to detect Siah2 and AR expression. **(G)** HEK293 cells were transfected with HA-Siah2 and different doses of Flag-AR for 48 h. Cell lysates then were subjected to Western blotting and probed with anti-Flag and anti-HA antibodies. **(H)** 293 cells were transfected with Flag-AR and HA-Siah2WT or HA-Siah2RM for 48 h, cell lysates were subjected to Western blotting and probed with anti-Flag and anti-HA antibodies. NS, non-significant.

PCa. To test the effect of ADT on Siah2 in PCa cells, LNCaP or 22Rv1 cells were cultured in medium supplemented with 5% CS-FBS (to mimic ADT conditions) or in complete medium. As expected, both Siah2 and Spry2 expressions were significantly decreased when the cells were cultured in CS-FBS medium compared with those in complete medium, which was consistent with AR expression (**Figure 3A**). This result suggested that ADT treatment decreased Siah2 expression while enhancing its E3 ligase activity. To further confirm the effect of ADT on Siah2 activity, we monitored endogenous Spry2

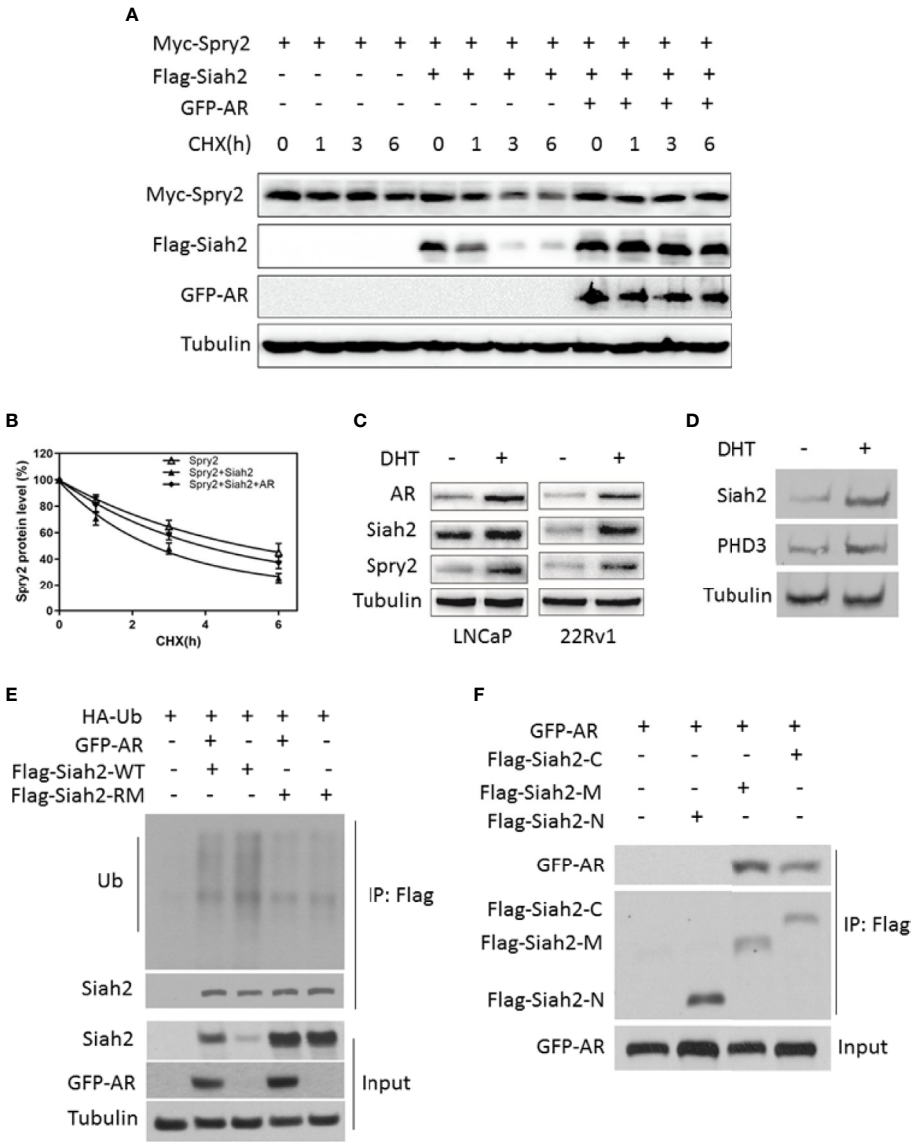

FIGURE 2 | AR inhibited Siah2 auto-ubiquitination and decreased its E3 ligase activity. **(A)** HEK293 cells were transfected with Flag-Siah2, GFP-AR, and Myc-Spry2 as indicated for 48 h, and then treated with cycloheximide (CHX, 50 μg/ml) for 1, 3, and 6 h. Cell lysates were then subjected to Western blotting. **(B)** Degradation curves of Spry2 by cycloheximide chase experiments in the presence or absence of Siah2 or AR. **(C)** LNCaP and 22Rv1 cells were cultured in CS-FBS medium for 24 h, and subsequently treated with 10 nM DHT or vehicle for 24 h. Spry2, Siah2, and AR protein expression were detected by Western blotting. **(D)** LNCaP cells were cultured in CS for 24 h, subsequently treated with 10 nM DHT or vehicle for 24 h. Siah2and PHD3 protein expression were detected by Western blotting. **(E)** PC3 cells were transfected with Flag-Siah2-WT or Flag-Siah2-RM, GFP-AR and HA-Ub as indicated for 24 h, and treated with 5 μM MG132 for 16 h. Cell lysates were immunoprecipitated with Flag antibody and subjected to Western blotting with HA and Flag antibody. **(F)** GFP-AR was co-transfected with Flag-Siah2 fragments (N, N-terminal region; M-middle region; C, C-terminal region) into HEK293 cells. Cell lysates were immunoprecipitated with Flag antibody and subjected to Western blotting with Flag and GFP antibodies.

and Siah2 expression in LNCaP cells using the cycloheximide chase assay. The Spry2 half-life was reduced from approximately 4.5 h in cells cultured in complete medium to 3 h when cells cultured in CS-FBS medium (**Figures 3B, C**), which suggests increased Siah2 activity.

To assess the relevance of our findings in human PCa, we evaluated Siah2 protein expression in 29 PCa patients who underwent radical prostatectomy after ADT treatment for 6–9 months. Siah2 was detected immunohistochemically both in biopsy samples (before ADT) and in radical prostatectomy samples (after ADT) from the same patient. Siah2 showed a nuclear expression pattern as described previously (14). Notably, Siah2 staining was significantly reduced in all patients after ADT (**Figures 3D, E**), which was consistent with our *in vitro* findings. These data suggest that ADT decreases Siah2 protein expression and enhances its E3 ligase activity in PCa.

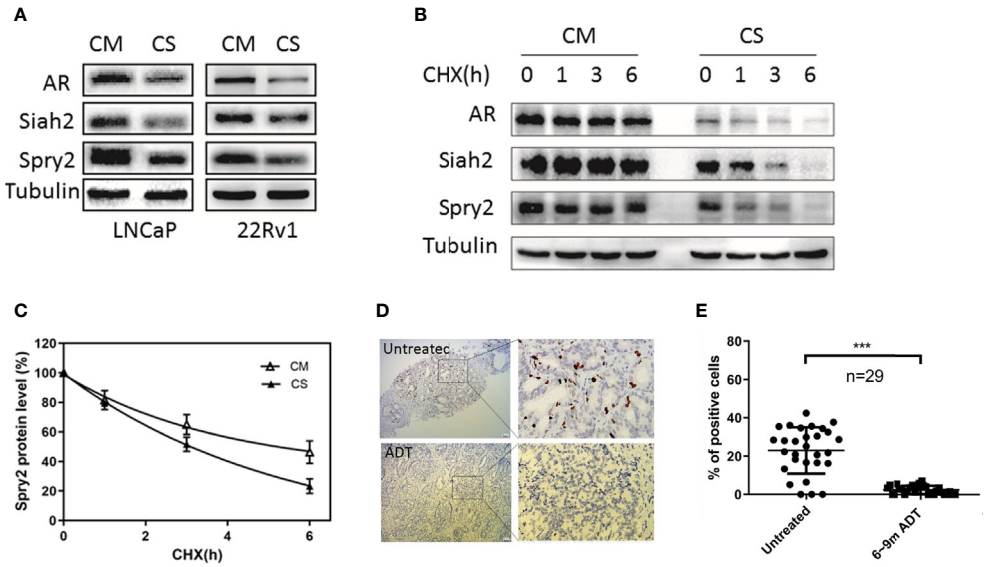

FIGURE 3 | ADT decreased Siah2 expression and increased its ligase activity. **(A)** LNCaP and 22Rv1 cells were cultured in complete medium for 24 h, and then maintained in CS-FBS medium for another 24 h. Spry2, Siah2, and AR protein expression were detected by Western blotting. **(B)** LNCaP cells were treated as described in **(A)**, and then treated with cycloheximide (CHX, 50μg/ml) for 1, 3, and 6 h, after which cell lysates were subjected to Western blotting. **(C)** Degradation curves of Siah2 by cycloheximide chase experiments. **(D)** Representative images of Siah2 immunohistochemistry staining in PCa specimens from the same patient. **(E)** Quantification of Siah2 immunohistochemistry staining in PCa samples from 29 patients who underwent radical prostatectomy after between 6 and 9 months of ADT treatment. ***P < 0.001.

Vit K3 Attenuated the Effects of ADT on Siah2 and Inhibited the Growth and Motility of PCa Cells

Given that Siah2 plays a key role in the development of CRPC (12) and that ADT triggers its ligase activation, we next asked whether Siah2 could be blocked when PCa cells were treated by ADT. The only Siah2-targeting drug described so far is Vit K3 (also known as menadione), which was identified as a specific inhibitor of Siah2 ubiquitin ligase activity in a screen of U.S. Food and Drug Administration-approved therapeutic drugs (16). We next verified whether Vit K3 could attenuate the effect of ADT on Siah2. As shown in **Figure 4A**, Siah2 and Spry2 expression were decreased in LNCaP and 22Rv1 cells cultured in CS-FBS medium compared with those in complete medium, as described previously. Significantly, Vit K3 treatment increased Siah2 and Spry2 expression in CS-FBS medium (**Figure 4A**), which indicates that Vit K3 inhibited Siah2 activity.

We next evaluated the physiologic significance of Vit K3 on PCa cells. Treatment with 20 μM Vit K3 for 24 h significantly reduced proliferation of AR-positive LNCaP and 22Rv1 cells, but not of AR-negative PC3 cells (**Figure 4B**). Given that the effect of Siah2 on PCa cell proliferation was AR-dependent, we argue that the inhibitory effect of Vit K3 on PCa cell growth is Siah2- and AR-dependent. To further verify the role of Siah2, siRNAs targeting Siah2 were transfected into LNCaP and 22Rv1 cells. Silencing Siah2 and Vit K3 treatment independently resulted in reduced PCa cell proliferation, but Vit K3 treatment in Siah2-knockdown cells did not further reduce cell proliferation (**Figures 4C, D**). Similarly, LNCaP cell motility was inhibited following Vit K3 treatment or Siah2 silencing, but no further changes were observed in Siah2-knockdown cells treated with Vit K3 (**Figures 4E, F**). Collectively, these data support a model in which Vit K3 inhibits the growth and motility of PCa cells through a mechanism that involves inhibition of Siah2 activity.

ADT Combined With Vit K3 Therapy Delayed the Formation of CRPC

Having established that Vit K3 abolished the Siah2 activation triggered by ADT in PCa cells *in vitro*, we next sought to determine whether this mechanism was active *in vivo*. Therefore, we subcutaneously injected LNCaP cells into nude mice and monitored tumor development. Both castration and castration+Vit K3 treatment significantly reduced tumor volumes compared with the sham-treatment group. However, in the castration alone group, tumor volumes started to increase 3 weeks after castration and grew extremely fast 4 weeks later, which suggests the formation of CRPC. Strikingly, tumors treated with castration+Vit K3 only grew very slowly 4 weeks after treatment and still did not show fast growth after 8 weeks (**Figures 5A, B**). Consistently, tumors derived from the Vit K3 treatment group were much smaller than those from the other two groups. Analysis of these tumors revealed significantly decreased Siah2 expression in response to castration, whereas Vit K3 treatment dramatically reversed expression Siah2, which was consistent with our *in vitro* findings (**Figure 5C**). These results strongly suggest that ADT+Vit K3 treatment may delay CRPC formation.

DISCUSSION

It is well established that the androgen-AR signaling axis plays a central role in CRPC. Most of the new drugs for CRPC approved by the FDA in recent years target AR signaling, including Abiraterone

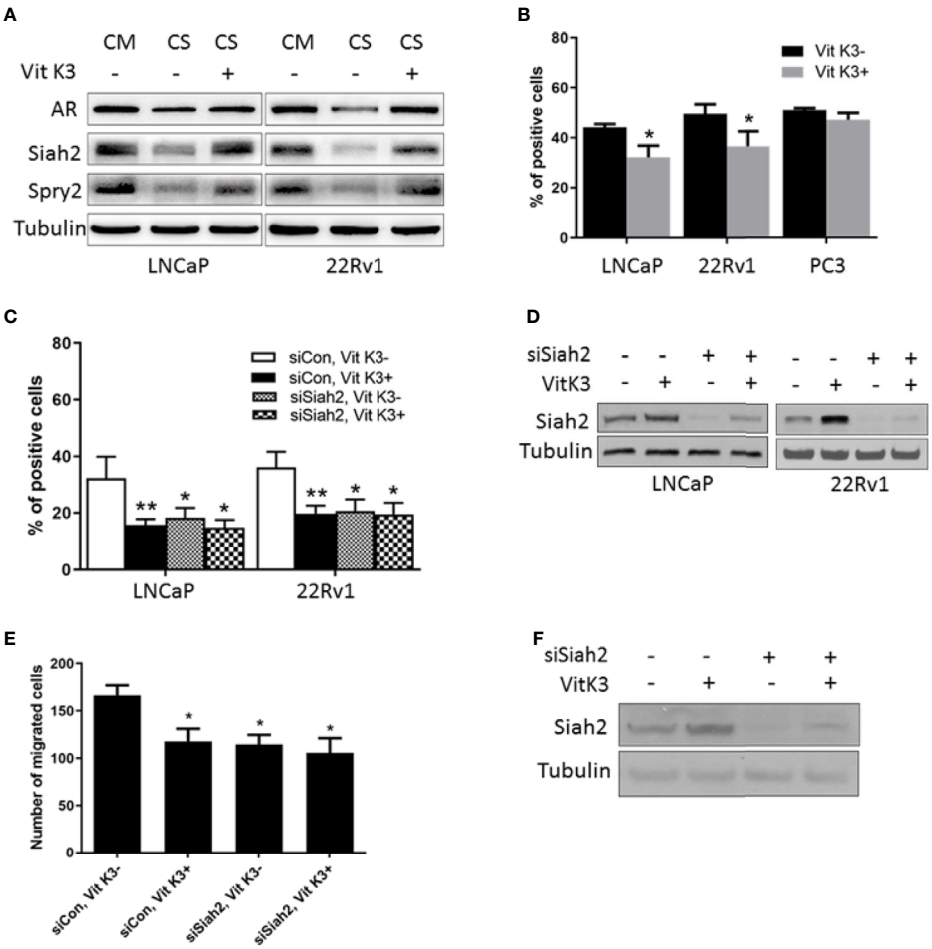

FIGURE 4 | Vit K3 attenuated the effects of ADT on Siah2. **(A)** LNCaP and 22Rv1 cells were cultured in CS-FBS medium for 24 h, and then treated with Vit K3 (20 μM) for 24 h. Spry2, Siah2, and AR protein expression were detected by Western blotting. **(B)** LNCaP, 22Rv1, and PC3 cells were treated with Vit K3 (20 μM) for 24 h, and then treated with 10 μM BrdU for 5 h (LNCaP) or 2 h (22Rv1, PC3, and DU145). The BrdU assay was performed as described in the Materials and Methods. **(C)** LNCaP and 22Rv1 cells were transfected with siRNAs targeting Siah2 or control as indicated for 72 h, and then treated with Vit K3 (20 μM) or vehicle as indicated for 24 h. BrdU assays were performed as described in **(B)**. **(D)** The expression of Siah2 protein from cells treated as described for C was detected by Western blotting. **(E)** LNCaP cells were transfected with si-Siah2 or si-control as indicated, and then cultured in transwell chambers, as described in the Materials and Methods. Cells were then treated with Vit K3 (20 μM) or vehicle for 24 h, and subsequently were stained with crystal violet, after which the number of cells per field was quantified. **(F)** The expression of Siah2 protein from cells treated as described for E was detected by Western blotting. *P < 0.05; **P < 0.01.

Acetate, an androgen synthesis inhibitor, and Enzalutamide and Apalutamide, second-generation AR antagonists. Although these second-generation antiandrogens show an overall survival benefit for advanced PCa, 20% to 40% of patients still do not respond to these therapies, and among the patients that do respond, resistance will eventually occur (17–19). Thus, the mechanisms of castration resistance need to be fully elucidated, as this will identify additional targets to treat and/or prevent CRPC.

Siah2 is an E3 ubiquitin ligase that targets AR and is thought to play an important role in the development of CRPC by targeting a select pool of chromatin-bound ARs that control the growth, survival, and tumorigenic capacity of PCa cells, especially under conditions of androgen deprivation (12). Interestingly, only small sets of metastatic PCa or CRPC showed a moderate 1.5- to 2-fold increase in Siah2 mRNA (12) These observations suggest that increased Siah2 transcription may not be the primary mechanism underlying the increased Siah2 activity observed in PCa tissues (15). Siah2 is very unstable because of self-ubiquitination and auto-degradation. Like other Ring finger E3 ubiquitin ligases, the ligase activity of Siah2 is reflected by its protein stability. Several factors, including the deubiquitinating enzymes USP13, AKR1C3, and DHX15 have been reported to stabilize Siah2 expression, by inhibiting its E3 ligase activity (14, 15, 20).

Here, we report that AR significantly stabilizes Siah2 protein expression and decreases its ligase activity in PCa cells. Notably, androgens extended the half-life of endogenous Siah2 to 5 h, which is much longer than the half-life in the presence of any of the other factors that have been reported to stabilize Siah2 (15, 20). These findings suggest that AR is a strong inhibitor of Siah2 ligase activity in PCa cells. As expected, ADT decreased Siah2 expression and

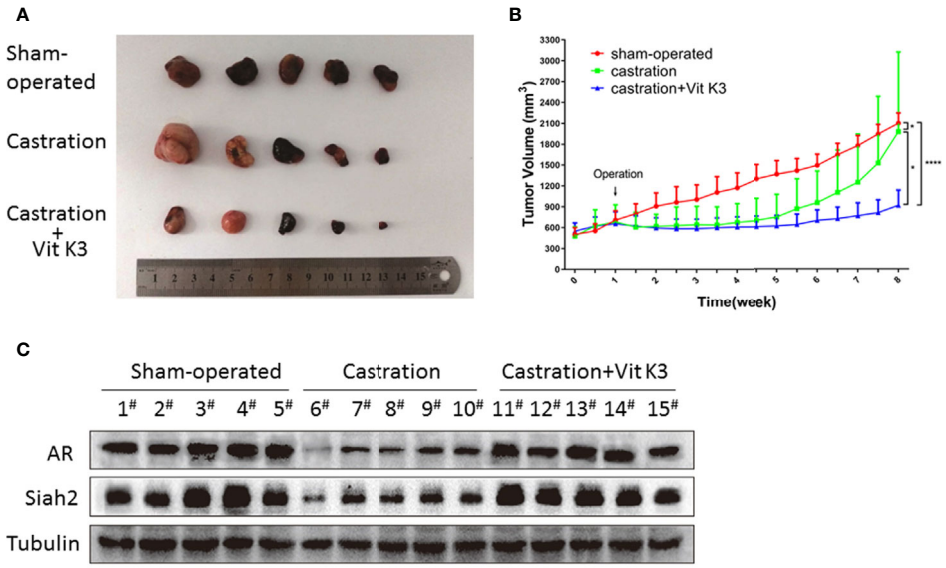

FIGURE 5 | ADT combined with Vit K3 therapy delayed the formation of CRPC. **(A)** LNCaP cells were subcutaneously injected into BALB/c nude mice, and the animals were treated as described in the Materials and Methods. The tumor xenografts with different treatments are shown as indicated. **(B)** The growth curve of tumor xenografts. **(C)** Xenograft tumor tissue lysates were analyzed by Western blotting to detect AR and Siah2 expression in the sham-operated, castration, and castration+Vit K3 groups. *P < 0.05, ****P < 0.0001.

enhanced its ligase activity. Importantly, we tested Siah2 expression in clinical PCa samples from the same patients before and after ADT, and found remarkably reduced Siah2 expression in response to ADT. These data indicate that during ADT, Siah2 is continuously activated in PCa. Based on these findings, we conclude that AR and Siah2 potentially form a positive regulatory loop in PCa, in which Siah2 mediates the ubiquitination-proteasomal degradation of a select pool of AR, whereas AR inhibits Siah2 ligase activity. ADT breaks the balance of these two proteins, which results in continuous Siah2 activation, which subsequently leads to CRPC.

Siah2 has three likely sites for intervention—interfering with its E3 ubiquitin ligase activity, the SBD domain, and the Siah–Siah dimerization domain (13). We demonstrated that AR reduced Siah2 auto-ubiquitination and increased Spry2 expression, a classic Siah2 substrate, which indicates that the mechanism through which AR stabilizes Siah2 is by blocking its E3 ligase activity. Co-immunoprecipitation studies revealed two domains of Siah2—the SBD and central RING domain/zinc finger domains—interacted with AR, consistent with the results of Qi et al. (12). We hypothesize that AR binding to the SBD is degraded as substrate, whereas AR binding to the central domain blocks the E3 ubiquitin ligase activity of Siah2. However, future structural studies will enable better assessment of the precise effects of AR on Siah2.

Vit K3 is a quinone used with cancer chemotherapeutics. Vit K3 and its analogs have been showed anticancer activities in several types of cancer including prostate cancer, breast cancer, melanoma and liver cancer *in vitro* and *in vivo* (16, 21, 22). Although the main biological effects on cancers are attributed to its role in the redox cycle and arylating nucleophilic substrates, Vit K3 has been identified as a specific inhibitor of Siah2 that inhibits both arms of the Siah2 downstream signaling network, the Ras/MAPK pathway and the hypoxic response pathway independent of reactive oxygen species. In this study, we showed that Vit K3 could abolish ADT-triggered Siah2 activation in PCa cells. Interestingly, we found that Vit K3 inhibited the growth of AR-positive LNCaP and 22Rv1 cells, but not AR-negative PC3 cells, which is consistent with its role of inhibiting Siah2 on PCa cells (12). Additionally, Vit K3 did not inhibit the growth or migration of Siah2-KD cells. Thus, we conclude that Vit K3 blocks PCa cell proliferation and motility at least partially by inhibiting Siah2.

Given that Siah2 plays a pivotal role in CRPC and that ADT triggers Siah2 activation in PCa cells, we hypothesized that ADT combined with a Siah2 inhibitor could block or delay the occurrence of CRPC. Strikingly, we demonstrated *in vivo* that ADT+Vit K3 treatment delayed the formation of CRPC and dramatically inhibited the growth of tumor xenografts compared with ADT alone. Importantly, analyses of these tumors suggested that Vit K3 delayed CRPC by inhibiting Siah2 activation.

In summary, this study provides new insights into the regulation of Siah2 in PCa. AR was identified as an inhibitor of Siah2. Because Siah2 is an E3 ubiquitin ligase for AR, we conclude that AR and Siah2 form a positive regulatory loop in PCa. ADT inhibits AR signaling, resulting in continuous Siah2 activation, which contributes to CRPC. Thus, ADT combined with Vit K3 may be a potential novel approach to delay the occurrence of CRPC.

DATA AVAILABILITY STATEMENT

The original contributions presented in the study are included in the article/**Supplementary Material**. Further inquiries can be directed to the corresponding authors.

AUTHOR CONTRIBUTIONS

YJ: conceptualization, investigation, supervision, writing the original draft, reviewing, and editing the manuscript. WG: methodology, investigation, reviewing, and editing the manuscript. TY: methodology, software, investigation, and writing the original draft. DZ: formal analysis, software, investigation, reviewing, and editing the manuscript. YS, DC, JJ, BH, HL, and SX: formal analysis, reviewing, and editing the manuscript. ZW: reviewing and editing the manuscript. All authors contributed to the article and approved the submitted version.

FUNDING

This work was supported by the National Natural Science Foundation of China (81872098), the National Natural Science Foundation of China (81502212), and the Science and Technology Commission of Shanghai Municipality, China (18ZR1430600).

ACKNOWLEDGMENTS

We thank James P. Mahaffey, PhD, from Liwen Bianji, Edanz Editing China (www.liwenbianji.cn/ac), for editing the English text of a draft of this manuscript.

SUPPLEMENTARY MATERIAL

The Supplementary Material for this article can be found online at: https://www.frontiersin.org/articles/10.3389/fonc.2021.637040/full#supplementary-material

Supplementary Figure 1 | Androgens stabilize Siah2 protein. **(A)** LNCaP cells were cultured in CS for 24 h, subsequently treated with different dose of DHT or flutamide (5μM) as indicated for another 24 h, and AR and Siah2 protein expression were detected by Western blotting. **(B)** LNCaP and PC3 cells were cultured in CS for 24 h, subsequently treated with 10 nM DHT or vehicle for 24 h. AR and Siah2 protein expression were detected by Western blotting.

Supplementary Figure 2 | AR inhibits Siah2 self-ubiquitination and decreases its E3 ligase activity. **(A)** 293 cells were transfected with Flag-Siah2, GFP-AR and Myc-Spry2 as indicated for 48 h and then treated with cycloheximide (CHX, 50 μg/ml) for 1, 3, 6 h and cell lysates were subjected to Western blotting.

REFERENCES

1. Siegel RL, Miller KD, Jemal A. Cancer statistics, 2020. *CA Cancer J Clin* (2020) 70:7–30. doi: 10.3322/caac.21590
2. Ye D, Zhu Y. Epidemiology of prostate cancer in China: an overview and clinical implication. *Chin J Surg* (2015) 53:249–52.
3. Hellerstedt BA, Pienta KJP. The cturrent state of hormonal therapy for prostate cancer. *CA Cancer J Clin* (2002) 52:154–79. doi: 10.3322/canjclin.52.3.154
4. Chan SC, Dehm SM. Constitutive activity of the androgen receptor. *Adv Pharmacol* (2014) 70:327–66. doi: 10.1016/B978-0-12-417197-8.00011-0
5. Kobayashi T, Inoue T, Kamba T, Ogawa O. Experimental evidence of persistent androgen-receptor-dependency in castration-resistant prostate cancer. *Int J Mol Sci* (2013) 14:15615–35. doi: 10.3390/ijms140815615
6. Tsao CK, Galsky MD, Small AC, Yee T, Oh WK. Targeting the androgen receptor signalling axis in castration-resistant prostate cancer (CRPC). *BJU Int* (2012) 110:1580–8. doi: 10.1111/j.1464-410X.2012.11445.x
7. Reed JC, Ely KR. Degrading liaisons: Siah structure revealed. *Nat Struct Biol* (2002) 9:8–10. doi: 10.1038/nsb0102-8
8. Zhang J, Guenther MG, Carthew RW, Lazar MA. Proteasomal regulation of nuclear receptor corepressor-mediated repression. *Genes Dev* (1998) 12:1775–80. doi: 10.1101/gad.12.12.1775
9. Nakayama K, Frew IJ, Hagensen M, Skals M, Habelhah H, Bhoumik A, et al. Siah2 regulates stability of prolyl-hydroxylases, controls HIF1alpha abundance, and modulates physiological responses to hypoxia. *Cell* (2004) 117:941–52. doi: 10.1016/j.cell.2004.06.001
10. Nadeau RJ, Toher JL, Yang X, Kovalenko D, Friesel R. Regulation of Sprouty2 stability by mammalian Seven-in-Absentia homolog 2. *J Cell Biochem* (2007) 100:151–60. doi: 10.1002/jcb.21040
11. Matsuzawa SI, Reed JC. Siah-1, SIP, and Ebi collaborate in a novel pathway for beta-catenin degradation linked to p53 responses. *Mol Cell* (2001) 7:915–26. doi: 10.1016/s1097-2765(01)00242-8
12. Qi J, Tripathi M, Mishra R, Sahgal N, Fazli L, Ettinger S, et al. The E3 ubiquitin ligase Siah2 contributes to castration-resistant prostate cancer by regulation of androgen receptor transcriptional activity. *Cancer Cell* (2013) 23:332–46. doi: 10.1016/j.ccr.2013.02.016
13. Wong CS, Möller A. Siah: a promising anticancer target. *Cancer Res* (2013) 73:2400–6. doi: 10.1158/0008-5472.CAN-12-4348
14. Jing Y, Nguyen MM, Wang D, Pascal LE, Guo W, Xu Y, et al. DHX15 promotes prostate cancer progression by stimulating Siah2-mediated ubiquitination of androgen receptor. *Oncogene* (2018) 37:638–50. doi: 10.1038/onc.2017.371
15. Fan L, Peng G, Hussain A, Fazli L, Guns E, Gleave M, et al. The Steroidogenic Enzyme AKR1C3 Regulates Stability of the Ubiquitin Ligase Siah2 in Prostate Cancer Cells. *J Biol Chem* (2015) 290:20865–79. doi: 10.1074/jbc.M115.662155
16. Shah M, Stebbins JL, Dewing A, Qi J, Pellecchia M, Ronai ZA. Inhibition of Siah2 ubiquitin ligase by vitamin K3 (menadione) attenuates hypoxia and MAPK signaling and blocks melanoma tumorigenesis. *Pigment Cell Melanoma Res* (2009) 22:799–808. doi: 10.1111/j.1755-148X.2009.00628.x
17. Ryan CJ, Smith MR, de Bono JS, Molina A, Logothetis CJ, de Souza P, et al. Abiraterone in metastatic prostate cancer without previous chemotherapy. *N Engl J Med* (2013) 368:138–48. doi: 10.1056/NEJMoa1209096
18. Scher HI, Fizazi K, Saad F, Taplin M-E, Sternberg CN, Miller K, et al. Increased survival with enzalutamide in prostate cancer after chemotherapy. *N Engl J Med* (2012) 367:1187–97. doi: 10.1056/NEJMoa1207506
19. Fizazi K, Shore N, Tammela TL, Ulys A, Vjaters E, Polyakov S, et al. Darolutamide in Nonmetastatic, Castration-Resistant Prostate Cancer. *N Engl J Med* (2019) 380:1235–46. doi: 10.1056/NEJMoa1815671
20. Scortegagna M, Subtil T, Qi J, Kim H, Zhao W, Gu W, et al. USP13 enzyme regulates Siah2 ligase stability and activity via noncatalytic ubiquitin-binding domains. *J Biol Chem* (2011) 286:27333–41. doi: 10.1074/jbc.M111.218214
21. Wellington KW, Hlatshwayo V, Kolesnikova NI, Saha ST, Kaur M, Motadi LR. Anticancer activities of vitamin K3 analogues. *Invest New Drugs* (2020) 38:378–91. doi: 10.1007/s10637-019-00855-8
22. Jamison JM, Gilloteaux J, Taper HS, Summers JL. Evaluation of the in vitro and in vivo antitumor activities of vitamin C and K-3 combinations against human prostate cancer. *J Nutr* (2001) 131:158–60. doi: 10.1093/jn/131.1.158S

Conflict of Interest: The authors declare that the research was conducted in the absence of any commercial or financial relationships that could be construed as a potential conflict of interest.

frontiers in Oncology

MINI REVIEW
published: 11 June 2021
doi: 10.3389/fonc.2021.679445

Targeting the MYC Ubiquitination-Proteasome Degradation Pathway for Cancer Therapy

Xiao-Xin Sun, Yanping Li, Rosalie C. Sears and Mu-Shui Dai**

Department of Molecular & Medical Genetics, School of Medicine and the OHSU Knight Cancer Institute, Oregon Health & Science University, Portland, OR, United States

Deregulated MYC overexpression and activation contributes to tumor growth and progression. Given the short half-life and unstable nature of the MYC protein, it is not surprising that the oncoprotein is highly regulated *via* diverse posttranslational mechanisms. Among them, ubiquitination dynamically controls the levels and activity of MYC during normal cell growth and homeostasis, whereas the disturbance of the ubiquitination/deubiquitination balance enables unwanted MYC stabilization and activation. In addition, MYC is also regulated by SUMOylation which crosstalks with the ubiquitination pathway and controls MYC protein stability and activity. In this mini-review, we will summarize current updates regarding MYC ubiquitination and provide perspectives about these MYC regulators as potential therapeutic targets in cancer.

Keywords: MYC, protein stability, ubiquitination, deubiquitination, ubiquitin ligase, deubiquitinating enzyme, SUMOylation, SUMO-specific protease

OPEN ACCESS

Edited by:
Alena Malyukova, Karolinska Institutet (KI), Sweden

Reviewed by:
Paul B. Fisher, Virginia Commonwealth University, United States
Pádraig D'Arcy, Linköping University, Sweden
Markus E. Diefenbacher, University of Wuerzburg, Germany

****Correspondence:***
Mu-Shui Dai
daim@ohsu.edu
Rosalie C. Sears
searsr@ohsu.edu

Specialty section:
This article was submitted to Cancer Molecular Targets and Therapeutics, a section of the journal Frontiers in Oncology

Received: *11 March 2021*
Accepted: *24 May 2021*
Published: *11 June 2021*

Citation:
Sun X-X, Li Y, Sears RC and Dai M-S (2021) Targeting the MYC Ubiquitination-Proteasome Degradation Pathway for Cancer Therapy. Front. Oncol. 11:679445. doi: 10.3389/fonc.2021.679445

INTRODUCTION

The c-Myc oncoprotein (MYC thereafter) is a basic helix-loop-helix and leucine zipper (bHLH-LZ) transcription factor that regulates almost all aspects of cell biology by regulating gene transcription, including cell growth and proliferation, apoptosis and senescence, angiogenesis, metabolism, ribosome biogenesis, and stem cell homeostasis (1–4). MYC heterodimerizes with its partner protein MAX *via* its C-terminal bHLH-LZ domain and binds to the E-box element (CACGTG) at target gene promoters (5–7). The N-terminal transcription activation domain (TAD) recruits key transcription co-activators, chromatin modifiers, and mediators to promote the transcription-initiating complex formation and initiate transcription initiation (8, 9). MYC also promotes RNA polymerase II (RNAPII) pause-release upon recruiting the pTEF phosphorylation complex to phosphorylate Serine 2 of the C-terminal domain (CTD) of RNAPII (10). Early individual gene and profiling studies have identified a large number of MYC target genes (4, 11). Recent genome wide studies suggest that MYC might also be a global gene amplifier, promoting the transcription of most, if not all, actively transcribed genes (12–15). Currently, there are several models demonstrating the different modes of MYC transactivation function, including specific-gene regulation, global gene activation, and gene-specific affinity models (1, 3). New studies also suggest that MYC supports genome integrity by clearing stalled RNAPII and resolving transcription-replication conflicts (1, 16).

Since deregulated MYC overexpression contributes significantly to human cancers by regulating the expression of genes involved in almost all aspects of the cancer hallmarks (4, 17, 18), MYC levels and activity must be tightly controlled during normal homeostasis. Under normal physiological

condition, MYC is an unstable protein with a half-life less than 15–30 min whereas in growth stimulated cells, MYC is transiently stabilized by shutting down proteasome degradation of MYC. This is controlled by a phosphorylation cascade involving two residues at the TAD: Thr (T) 58 and Ser (S) 62 (19–21). Upon growth stimulation, MYC is phosphorylated by RAS-induced kinases and cyclin-dependent kinases such as CDK2 at S62. Upon reduction in the growth signals, GSK3 is activated to phosphorylate T58, which requires prior S62 phosphorylation. Then, T58 phosphorylation promotes the recruitment of the proline isomerase PIN1 to catalyze the *cis*-to-*trans* isomerization of MYC at Pro (P) 63, followed by the recruitment of the phosphatase PP2A to dephosphorylate MYC at S62. T58 phosphorylated MYC is then targeted by the Fbw7 ubiquitin (Ub) E3 ligase for proteasome degradation (22–25). During the past two decades, more than a dozen ubiquitin ligases have been reported to regulate MYC stability and/or activity. In this mini-review, we briefly describe recent progress in understanding MYC control by the ubiquitin proteasome system including novel ubiquitin ligases and deubiquitinating enzymes and then focus on the perspectives of targeting these molecules for cancer therapy.

MYC UBIQUITIN LIGASES

To date, at least 18 Ub ligases have been discovered to mediate MYC ubiquitination, which regulates MYC protein stability and/or activity (**Figure 1**). While most of the Ub ligases, such as SCF^{Fbw7}, target MYC protein for degradation resulting in the inhibition of MYC activity, several other Ub ligases stabilize MYC. This can be done by antagonizing SCF^{Fbw7}-mediated MYC degradation, as in the case for $SCF^{\beta\text{-}TRCP}$, which ubiquitinates MYC *via* K33/K63/K48 mixed linkage, counteracting SCF^{Fbw7}-mediated K48-linked MYC ubiquitination and degradation (26). In another example, RNF4, a SUMO-targeted ubiquitin ligase (StubL), mediates K11- and K33-linked ubiquitination of MYC independently of SUMOylation, resulting in MYC stabilization (27). Also, HUWE1 mediates MYC ubiquitination by enhancing the recruitment of p300 and promoting MYC activity without targeting MYC for degradation (28). Yet, HUWE1 ubiquitinates and degrades Miz1, a protein that binds to MYC and accumulates at MYC-bound chromatin associated with repressed transcription (29). Thus, depletion of HUWE1 switches MYC from activating to repressive and suppresses MYC activity (29). On the other hand, SCF^{Skp2}-mediated ubiquitination promotes MYC activity, but in this case it is coupled with targeting MYC for proteasome degradation (30, 31). We have reviewed most of the MYC Ub ligases, and the reader can refer to our previous publications (32, 33). Here, we describe newly identified MYC regulators and briefly discuss the role for the MYC ubiquitin ligases in the context of cell cycle and chromatin association.

Recently, the Westermarck group (34) showed that UBR5 ubiquitinates MYC and prevents cells from accumulating excess MYC protein. Interestingly, UBR5 suppresses MYC-dependent priming to therapy-induced apoptosis in cancer cells as it resets MYC to levels that are not enough to induce apoptosis, whereas in normal cells accumulated MYC triggers apoptosis. Indeed, MYC and UBR5 are often co-amplified in MYC-driven human cancers. Yet, UBR5 high expression (UBR5-high) cells dominate MYC-high cells at the single cell level in basal type breast cancers. This study suggests that UBR5-mediated MYC ubiquitination and degradation prevents the accumulation of too much MYC and thus benefits cancer cell survival (34). Therefore, UBR5 may promote tumor cell resistance to cancer therapy. It would be interesting to consider how UBR5 and other regulators of MYC that control MYC ubiquitination levels can tune MYC oncogenic potential.

The leucine-rich repeats (LRR) containing F-box protein FBXL16 has recently been shown to regulate MYC stability by antagonizing SCF^{Fbw7}. Interestingly, FBXL16 binds to Skp1 and PP2A but not Cul1, indicating that it may not form a SCF E3 ligase complex (35). FBXL16 binds to wild-type MYC and the T58A or S62A mutant with equal efficiency and does not compete with FBW7 for binding to MYC, but inhibits FBW7-mediated MYC ubiquitination in cells and *in vitro*. As both F-box and the LRR domains are required for FBXL16's activity to counteract FBW7, it is possible that FBXL16 may form a complex with FBW7 and MYC where it directly suppresses FBW7 ligase activity. On another note, as FBXL16 also binds to PP2A and negatively affects its phosphatase activity (36), it would be interesting to test whether FBXL16 stabilizes MYC partially *via* inhibiting PP2A, thus suppressing MYC S62 dephosphorylation. Nevertheless, this less studied F-box protein functions to promote cancer cell growth and potentiates MYC oncogenic activity.

MYC UBIQUITINATION DYNAMICS

The identification of increasing numbers of Ub ligases targeting MYC suggests that these Ub ligases may control MYC levels and activity dynamically and coordinately and act in a cell context-dependent fashion. For example, FBXO32 is uniquely reported to function under starvation conditions and cell cycle exit, where it catalyzes K48-linked polyubiquitination of MYC at K326 leading to MYC degradation (37, 38). Several other MYC Ub ligases have been reported to function at specific cell cycle phases. TRUSS targets MYC for proteasomal degradation in G1 phase (39, 40). SKP2 expression is high at the G1/S transition and peaks at S phase, and SKP2 promotes S phase entry of MYC containing rat-1 cells, but not MYC null cells (30). In addition, overexpression of SKP2 correlates with the reduction of TRUSS in human cancers (40), suggesting an interplay of MYC Ub ligases in tightly controlling MYC stability during the cell cycle. Also, acting later in the cell cycle, FBXO28 is subjected to regulation by S- and G2/M-phase kinases, cyclin A-CDK2, and cyclin B-CDK1 that mediate phosphorylation of FBXO28 at S344 (41). This activates the Ub ligase activity of FBXO28 to ubiquitinate MYC at C-terminal lysines and recruit p300 co-activator for transactivation of a subset of target genes important for S- and G2/M-phases.

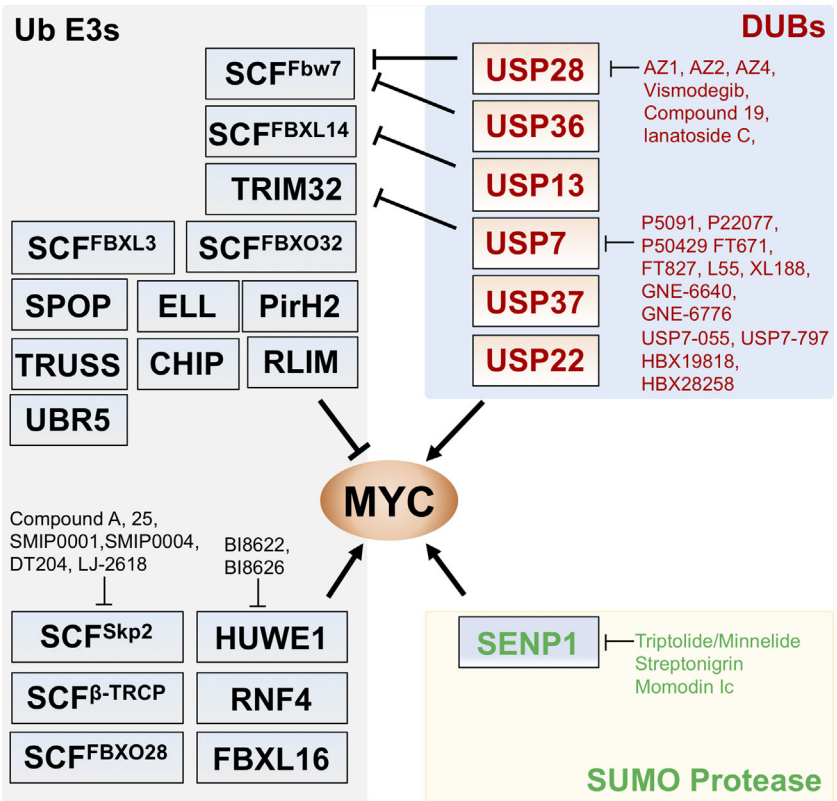

FIGURE 1 | Regulation of MYC by Ub ligases, deubiquitinating enzymes (DUBs), and SUMO protease. Shown are the known Ub ligases (left) mediating MYC ubiquitination, DUBs (upper right) for MYC deubiquitination and SENP1 (lower right) that deSUMOylates and stabilizes MYC. The arrows indicate positive regulation of MYC activity whereas the bars indicate the inhibition. Small molecule inhibitors targeting the indicated Ub ligases, DUBs, and SENP1 are indicated.

Genome-wide studies revealed wide-spread chromatin binding of MYC, including at high-affinity sites (E-box and CG island regions in the promoter and enhancer regions) bound by endogenous low levels of MYC and at low-affinity sites that are bound by overexpressed and deregulated levels of MYC through a mechanism called "invasion" (13–15, 42). In some experimental conditions, MYC is considered as a transcription amplifier to upregulate most, if not all, active transcribed genes. However, the DNA binding of MYC often does not match its transcription activity (3, 43). Also, MYC binding in certain binding sites with high-affinity promoters, such as ribosome biogenesis genes, can be saturated, and not increase with increasing MYC levels (44). These observations suggest additional control mechanisms between MYC DNA binding and transcriptional regulation.

Emerging evidences suggest that proper chromatin turnover of MYC is critical for its transactivation activity. This is initially observed by two studies showing that SKP2-mediated MYC ubiquitination and proteasome degradation increase MYC activity (30, 31). SKP2 binds to the MYC Box (MB) II which is also the binding motif for the TRAPP co-activator and is essential for MYC transactivation activity. The proteasome can be recruited by MYC and SKP2 to MYC target gene promoters such as the cyclin D2 promoter (31, 45). FBXO28 also binds to MB II and increases MYC activity by non-proteolytic ubiquitination of MYC (41). The role for MYC turnover in target gene transcription activation is further highlighted by a recent study (46) showing that MYC associates with the elongation factor complex PAF1 at promoters and ubiquitination and degradation releases this association. Upon MYC ubiquitination and degradation, the PAF1 complex can then be transferred to and bound to RNA Pol II to promote transcription elongation. Interestingly, PAF1C, a component of the PAF1 complex, interacts with the MBI and phosphorylation at T58 and S62 in MBI promotes PAF1C binding to MYC. Therefore, it would be interesting to examine whether and how MBI phosphorylation coordinates the recruitment of the PAF1 complex with Fbw7-mediated ubiquitination and degradation of MYC, and the role of other E3 ligases such as SKP2 that activate MYC transactivation in this dynamic process controlling transcription. The study also agrees with a recent work by Chen et al. (47) showing that depletion of PAF1 results in an increased release of paused Pol II and transcription elongation of many genes by recruiting the super elongation complex (SEC). Adding to the complexity is that ELL, a component of SEC that promotes transcription elongation, has recently been identified as a MYC Ub ligase. ELL ubiquitinates MYC and targets it for degradation and suppresses MYC-driven tumorigenesis (48).

Whether this occurs at the chromatin and how ELL suppresses MYC activity remains to be addressed. Together, these observations are consistent with our studies indicating that MYC DNA binding and turnover are cyclic at promoters together with the cyclic binding of general transcription factors, mediators, and chromatin modifying enzymes as in the case of ERα turnover at promoters (49, 50).

MYC DEUBIQUITINATING ENZYMES (DUBS)

MYC ubiquitination can be removed by deubiquitination. Several deubiquitinating enzymes have been shown to deubiquitinate MYC and regulate its levels and activity. For example, USP28 deubiquitinates MYC *via* counteracting Fbw7α (51, 52), whereas USP36 deubiquitinates MYC in the nucleolus by counteracting Fbw7γ (33, 53). The role of USP36 in regulating MYC ubiquitination and stabilization was also reported in *Drosophila*, showing that the nucleolar isoform of *Drosophila* USP36 (dUSP36) deubiquitinates dMYC and regulates dMYC-dependent cell growth (54). USP22 and USP37 have been shown to deubiquitinate and stabilize MYC (55, 56). USP7 has been shown to deubiquitinate N-Myc (57) and antagonize TRIM32-mediated MYC ubiquitination (58). USP13 can antagonize FBXL14 by removing FBXL14-mediated MYC ubiquitination (59). The Otub6B isoform can regulate MYC levels but not its transcription, although it is unclear whether the isoform can directly mediate MYC deubiquitination (60). While USP36 regulates MYC deubiquitination in the nucleolus, many of the DUBs act on MYC in the nucleoplasm. It is interesting to know whether these DUBs counteract MYC ubiquitin ligases on chromatin to control MYC turnover during transcription and whether they crosstalk with other chromatin modifications, given that USP36 also deubiquitinates H2B (61).

CROSSTALK OF MYC SUMOYLATION WITH UBIQUITINATION

Recent studies have shown that MYC is also subject to SUMOylation (62–65). A unique feature about MYC SUMOylation is that it acts promiscuously with respect to the accepting lysines as mutating up to 10 lysines identified by mass spectrometry analysis still failed to abolish MYC SUMOylation (62). This might explain the early observations documenting MYC SUMOylation without a clear effect on MYC stability and activity (63, 65). We recently showed that the SUMO-specific protease SENP1 deSUMOylates MYC (66). Interestingly, SENP1-mediated deSUMOylation stabilizes and activates MYC, likely due to the indirect deubiquitination of MYC as MYC can be co-modified by both Ub and SUMO (66). This is also strongly supported by multiple recent proteomic studies showing ubiquitination of SUMO as well as SUMO-conjugation to multiple lysines of ubiquitin (67, 68). Similar regulation has been observed for HIF1α SUMOylation in that SENP1 deSUMOylation of HIF1α results in HIF1α stabilization as well (69). It is likely that SUMOylation actually regulates the stability of a large number of proteins *via* crosstalk with the Ub system. Nevertheless, the SUMO regulation of MYC adds another layer of complexity to the regulation of MYC protein stability and activity and provides another target in MYC-driven cancer cell growth. Given that SUMOylation plays a key role in transcription regulation (70, 71), it is interesting to understand how MYC SUMOylation/deSUMOylation plays a role in MYC turnover at the chromatin.

TARGETING MYC UBIQUITINATION PATHWAY

MYC is commonly considered "undruggable" and direct targeting of MYC is very challenging because of its nucleus localization and the absence of active sites amendable to conventional small molecule ligand-binding (72–74), although this concept has evolved (75, 76). Recently, Omomyc, a peptide that competitively binds to E-box elements as a heterodimer with MAX or as a homodimer and suppresses the binding of MYC to E-boxes (77–79), has been shown to have therapeutic potential *in vivo* in various cancer models (77, 79, 80). Targeting MYC regulatory pathways, such as MYC ubiquitination and deubiquitination whose deregulation contributes to MYC stabilization in cancer, is another highly desirable approach. Several MYC Ub ligases, such as SKP2, HUWE1, and β-TRCP, promote MYC function and thus are promising therapeutic targets (**Figure 1**, **Table 1**). In particular, therapeutically targeting SKP2, which is overexpressed in a variety of cancers, has exciting potential to capitalize on MYC's pro-apoptotic function. N-terminal ubiquitination of MYC by SKP2 increases MYC's transactivation of pro-proliferative target genes while loss of SKP2 can not only lead to increased MYC levels but also increased apoptotic activity (30, 31, 107, 108). Inhibitors of SKP2 with anti-tumor properties include several natural products and recently identified small molecule compounds (83, 109). Small molecule compound A was found to inhibit SKP2 incorporation into the SCF complex, thus suppressing its ubiquitin ligase activity (81). SMIP0001 and SMIP0004 (82) have been shown to reduce SKP2 levels and thus induce p27 accumulation. Compound 25 and its analogs (83) disrupt the SKP2-SKP1 interaction in the SCF complex and inhibit the ligase activity and have been shown to suppress cancer cell growth. Chemical library screens identified a novel compound, designated as DT204, that reduces SKP2 binding to Cullin-1 and Commd1, and synergistically enhances BTZ-induced apoptosis (84). NSC689857 and NSC681152 disrupt the SKP2-Cks1 interaction (85), thus inhibiting p27 ubiquitination. It is interesting to examine whether these compounds that specifically inhibit p27 degradation also suppress MYC activity. A selenonucleoside called LJ-2618 downregulates the expression of SKP2 by promoting its degradation and induces G2/M cell cycle arrest in prostate cancer cells and xenograft tumor *in vivo* (86). Likewise, all-*trans* retinoic acid (ATRA) stimulates the ubiquitin-mediated degradation of SKP2 (87). This finding is intriguing because of the known effects

TABLE 1 | Inhibitors targeting the MYC degradation pathway.

Name	Mode of action	Clinical trial	References
Compound A	Inhibits SKP2 incorporation into the SCF complex	No	81
SMIP0001, SMIP0004	Reduce SKP2 levels	No	82
Compound 25	disrupts the SKP2-SKP1 interaction	No	83
DT204	Reduces SKP2 binding to Cullin-1 and Commd1	No	84
NSC689857 NSC681152	Disrupt the SKP2-Cks1 interaction	No	85
LJ-2618	Promotes SKP2 degradation	No	86
ATRA	Promotes SKP2 degradation	FDA approved	87
BI8622, BI8626	Inhibit HUWE1	No	29
P5091, P22077, P50429	Covalent USP7 inhibitor	No	88, 89, 115
HBX19818, HBX28258	Covalent USP7 inhibitors	No	90
GNE-6640, GNE-6776	Non-covalent USP7 inhibitors	No	91
FT671	Non-covalent USP7 inhibitor	No	92
FT827, L55	Covalent USP7 inhibitors		93
XL188	Non-covalent USP7 inhibitor	No	94
USP7-055, USP7-797	Non-covalent USP7 inhibitors	No	95
Compound 4	Non-competitive USP7 inhibitor	No	96
Compound 46	USP7 inhibitor	No	97
AZ1, AZ2, AZ4	USP28 inhibitors	No	117
Compound 19	USP28 inhibitor	No	118
Vismodegib	Binds to and inhibits USP28	FDA approved	100
lanatoside C	Inhibits USP28-MYC binding	No	101
Streptonigrin	SENP1 inhibitor	No	102
Triptolide (Minnelide)	SENP1 inhibitor	Phase I and II clinical trials	103, 104
Momordin Ic	SENP1 inhibitor	No	119

of ATRA in stimulating cell differentiation, a consequence of MYC inhibition in some settings (110).

Targeting positive ubiquitination mediated by HUWE1 could also suppress MYC's oncogenic activity. A recent high-throughput screening (HTS) has identified small molecule inhibitors of HUWE1, BI8622 and BI8626, that suppress transactivation of MYC target genes while increasing transrepression and the induction of apoptosis in colorectal cancer cells (29). Treatment of these compounds inhibits MYC-dependent transactivation in colorectal cancer cells but not in stem cells or normal colon epithelial cells, and this effect is associated with the role of HUWE1 inhibition in stabilizing Miz1 and Miz1-mediated suppression of MYC target genes (29). Also, HUWE1 is frequently deregulated in multiple myeloma (MM) and targeting HUWE1 with the small molecule inhibitors in combination with lenalidomide results in synergistic growth inhibition in MM cells *in vitro* and *in vivo* (111).

Many of the MYC DUBs positively regulate MYC stability and activity and could emerge as important cancer therapeutic targets as well. Studies have clearly indicated that different thresholds of MYC elicit different activities and that specific levels of MYC are required to maintain tumorigenesis (112, 113), supporting the idea of dropping MYC levels below these thresholds by strategies like inhibiting DUBs, such as USP28 or USP36 that antagonize FBW7-mediated MYC ubiquitination (52, 53) and USP7 that deubiquitinates N-MYC (57). Indeed, emerging studies have discovered a number of small molecule inhibitors for USP7 (114, 115) (**Table 1**). These USP7 inhibitors include trisubstituted thiophene P5091 (88) and its analogs P22077 (89) and P50429 (90), the acridine derivatives HBX19818 and HBX28258 (91), 2-Amino-4-ethylpyridine derivatives GNE-6640 and GNE-6776 (92), pyrazolo[3,4-d]pyrimidin-4-one-piperidine compounds FT671 and FT827 (93) and the derivative compound L55 (94), a Quinazolin-4-one derivative XL 188 (95), and recently reported novel chemical series including compounds USP7-055 and USP7-797 (96), compound 4 (97), and compound 46 (98). These USP7 inhibitors showed anti-proliferative effect in cancer cell lines and mouse xenograft models. For example, P5091 treatment induced multiple myeloma (MM) cell death, overcomes the resistance to Bortezomib, and inhibits MM xenograft tumor growth (88). Both P22077 and P50429 showed anti-proliferative effect in HCT116 cancer cells and mouse xenograft models (88, 116, 117). Treatment with GNE-6640 and GNE-6776 induced cancer cell death and increases cytotoxicity with chemotherapeutic agents (92). Most of these above studies focused on the role of USP7 in degrading MDM2 to induce p53 and p53-dependent anti-proliferative effects. Yet, effects on p53 mutant cancers are also evident (96). It would be beneficial to understand whether such a role also involves USP7 activity to deubiquitinate N-MYC especially in neuroblastoma with N-MYC amplification or antagonize TRIM32-mediated MYC ubiquitination (58) and whether USP7 deubiquitinates c-MYC as well.

Recently, a high throughput screening (HTS) identified the first set of benzylaminoethanol compounds AZ1, AZ2, and AZ4 that specifically inhibit USP28 (99). By inhibiting USP28, these compounds indeed reduce cellular MYC levels, induce apoptosis, and inhibit cell proliferation in a dose-dependent manner (99). AZ1 was also recently shown to markedly inhibit tumor cell growth and reduce tumor burden in an orthotopically transplanted lung tumor model in mice with well tolerance at doses up to 375 mg/kg (118). Liu et al. (100) reported a new compound 19, a [1,2,3]triazolo[4,5-d] pyrimidine derivative, that specifically inhibits USP28 and reduces gastric cancer cell proliferation and EMT with a better IC_{50} than that of AZ1. These effects are likely due to binding to USP28 and inducing USP28 degradation through ubiquitin-proteasome system (100).

Vismodegib, a sonic hedgehog inhibitor used for the treatment of basal cell carcinoma, was recently shown to bind to USP28 and inhibit its DUB activity (101). Vismodegib exhibits selectivity towards USP28 and its evolutionally related USP25. Treatment of cancer cells with Vismodegib reduces the levels of c-Myc and Notch1 and suppresses cell growth (101). In addition, lanatoside C, a cardiac glycoside, has been shown to reduce MYC levels and suppress gastric cancer cell proliferation by inhibiting USP28 binding to MYC, thereby destabilizing MYC, although it remains to be determined whether lanatoside C directly targets USP28 (102).

Given that SENP1 positively regulates MYC levels and activity, SENP1 is an interesting cancer therapeutic target. Several SENP1 inhibitors have been reported (103–105). Streptonigrin (SN), a natural product isolated from Streptomyces flocculus, has been shown to inhibit SENP1 activity (IC_{50} = 0.518 μM towards SENP1, IC_{50} = 6.919 μM towards SENP2) (103). Triptolide, a small natural compound extracted from a Chinese herb Tripterygium wilfordii, has been shown to inhibit SENP1 expression (with IC_{50} = 0.0203 μM in PC-3 cells) (105) and destabilize MYC (104), yet the underlying mechanism is unknown. A water-soluble prodrug of Triptolide called Minnelide has been shown to exhibit promising anti-tumor effects in pancreatic and liver cancers (119). A phase II trial of Minnelide in patients with refractory pancreatic cancer (NCT03117920) was just completed with results pending. Also, a phase I clinical trial of Minnelide (NCT03129139) is ongoing in patients with advanced solid tumors. Also, Momordin Ic (Mc), a natural pentacyclic triterpenic compound, was shown to inhibit SENP1 activity with an IC_{50} of 15.37 μM *in vitro* (106). It is conceivable that by inhibiting MYC deSUMOylation, these SENP1 inhibitors could indirectly suppress MYC deubiquitination, thereby destabilizing MYC and exhibiting anti-proliferative effect in cancer cells.

CONCLUSION AND PERSPECTIVES

Emerging evidence supports the dynamic MYC turnover by proteasome-mediated degradation and the complex crosstalk among different posttranslational modifications (PTMs) of MYC (ubiquitination, phosphorylation, acetylation, SUMOylation, and their reverse processes), resulting in the tight control of MYC transactivation activity, thus emphasizing the importance of MYC in the multi-step regulation of gene transcription and its deregulation in cancer. While several MYC Ub ligases such as the above mentioned SKP2 and HUWE1 have been actively explored as therapeutic targets, small molecule inhibitors suppressing other MYC ligases remain to be identified. This therapeutic strategy holds promise as, for example, knockdown of FBW7 is synthetically lethal to MYC-overexpressing cancer cells (120). Conversely, targeting UBR5 to accumulate MYC beyond the threshold levels that trigger cancer cell apoptosis in MYC-high cancers (34) is another example of inducing MYC synthetic lethality. Together, targeting these MYC posttranslational modifiers could yield potential cancer therapeutics, and additional research understanding the dynamic control processes and the effects of perturbing MYC levels in cancer will be important for their application. Future work would also be needed to further understand the crosstalk between MYC PTMs and the combined intervention of targeting multiple MYC PTMs. Further structure-biology studies and medicinal chemistry optimization could aid in improving target specificity and developing novel compounds. It is hopeful that certain compounds targeting the MYC ubiquitination-proteasome degradation pathways could ultimately move to clinic trials for treating MYC-dependent cancers. If successful, combinational therapies with other targeted therapies could also be desirable to treat advanced cancers, given that MYC crosstalk with many other oncogenic pathways such as RAS, mTOR, HIF signaling, and others.

AUTHOR CONTRIBUTIONS

X-XS, YL, RS, M-SD wrote and edited the manuscript. All authors contributed to the article and approved the submitted version.

FUNDING

This work was supported by NIH grants R01 CA186241 to M-SD and RS, R01 GM130604 to M-SD, U54 CA209988 to RS, U01 CA224012 to RS, and R01 CA196228 to RS.

REFERENCES

1. Baluapuri A, Wolf E, Eilers M. Target Gene-Independent Functions of MYC Oncoproteins. *Nat Rev Mol Cell Biol* (2020) 21:255–67. doi: 10.1038/s41580-020-0215-2
2. Bretones G, Delgado MD, Leon J. Myc and Cell Cycle Control. *Biochim Biophys Acta* (2015) 1849:506–16. doi: 10.1016/j.bbagrm.2014.03.013
3. Kress TR, Sabo A, Amati B. MYC: Connecting Selective Transcriptional Control to Global RNA Production. *Nat Rev Cancer* (2015) 15:593–607. doi: 10.1038/nrc3984
4. Meyer N, Penn LZ. Reflecting on 25 Years With MYC. *Nat Rev Cancer* (2008) 8:976–90. doi: 10.1038/nrc2231
5. Bieda M, Xu X, Singer MA, Green R, Farnham PJ. Unbiased Location Analysis of E2F1-Binding Sites Suggests a Widespread Role for E2F1 in the Human Genome. *Genome Res* (2006) 16:595–605. doi: 10.1101/gr.4887606
6. Fernandez PC, Frank SR, Wang L, Schroeder M, Liu S, Greene J, et al. Genomic Targets of the Human c-Myc Protein. *Genes Dev* (2003) 17:1115–29. doi: 10.1101/gad.1067003
7. Mao DY, Watson JD, Yan PS, Barsyte-Lovejoy D, Khosravi F, Wong WW, et al. Analysis of Myc Bound Loci Identified by CpG Island Arrays Shows That Max Is Essential for Myc-Dependent Repression. *Curr Biol* (2003) 13:882–6. doi: 10.1016/S0960-9822(03)00297-5
8. Adhikary S, Eilers M. Transcriptional Regulation and Transformation by Myc Proteins. *Nat Rev Mol Cell Biol* (2005) 6:635–45. doi: 10.1038/nrm1703
9. Tu WB, Helander S, Pilstal R, Hickman KA, Lourenco C, Jurisica I, et al. Myc and its Interactors Take Shape. *Biochim Biophys Acta* (2015) 1849:469–83. doi: 10.1016/j.bbagrm.2014.06.002
10. Rahl PB, Lin CY, Seila AC, Flynn RA, McCuine S, Burge CB, et al. c-Myc Regulates Transcriptional Pause Release. *Cell* (2010) 141:432–45. doi: 10.1016/j.cell.2010.03.030

11. Patel JH, Loboda AP, Showe MK, Showe LC, McMahon SB. Analysis of Genomic Targets Reveals Complex Functions of MYC. *Nat Rev Cancer* (2004) 4:562–8. doi: 10.1038/nrc1393
12. Lin CJ, Nasr Z, Premsrirut PK, Porco JA Jr, Hippo Y, Lowe SW, et al. Targeting Synthetic Lethal Interactions Between Myc and the eIF4F Complex Impedes Tumorigenesis. *Cell Rep* (2012) 1:325–33. doi: 10.1016/j.celrep.2012.02.010
13. Nie Z, Hu G, Wei G, Cui K, Yamane A, Resch W, et al. c-Myc is a Universal Amplifier of Expressed Genes in Lymphocytes and Embryonic Stem Cells. *Cell* (2012) 151:68–79. doi: 10.1016/j.cell.2012.08.033
14. Sabo A, Kress TR, Pelizzola M, de Pretis S, Gorski MM, Tesi A, et al. Selective Transcriptional Regulation by Myc in Cellular Growth Control and Lymphomagenesis. *Nature* (2014) 511:488–92. doi: 10.1038/nature13537
15. Walz S, Lorenzin F, Morton J, Wiese KE, von Eyss B, Herold S, et al. Activation and Repression by Oncogenic MYC Shape Tumour-Specific Gene Expression Profiles. *Nature* (2014) 511:483–7. doi: 10.1038/nature13473
16. Endres T, Solvie D, Heidelberger JB, Andrioletti V, Baluapuri A, Ade CP, et al. Ubiquitylation of MYC Couples Transcription Elongation With Double-Strand Break Repair at Active Promoters. *Mol Cell* (2021) 81:830–44.e813. doi: 10.1016/j.molcel.2020.12.035
17. Dang CV. MYC on the Path to Cancer. *Cell* (2012) 149:22–35. doi: 10.1016/j.cell.2012.03.003
18. Gabay M, Li Y, Felsher DW. MYC Activation Is a Hallmark of Cancer Initiation and Maintenance. *Cold Spring Harbor Perspect Med* (2014) 4:a014241. doi: 10.1101/cshperspect.a014241
19. Lutterbach B, Hann SR. Hierarchical Phosphorylation at N-terminal Transformation-Sensitive Sites in c-Myc Protein Is Regulated by Mitogens and in Mitosis. *Mol Cell Biol* (1994) 14:5510–22. doi: 10.1128/MCB.14.8.5510
20. Sears R, Nuckolls F, Haura E, Taya Y, Tamai K, Nevins JR. Multiple Ras-Dependent Phosphorylation Pathways Regulate Myc Protein Stability. *Genes Dev* (2000) 14:2501–14. doi: 10.1101/gad.836800
21. Hann SR. Role of Post-Translational Modifications in Regulating c-Myc Proteolysis, Transcriptional Activity and Biological Function. *Semin Cancer Biol* (2006) 16:288–302. doi: 10.1016/j.semcancer.2006.08.004
22. Moberg KH, Mukherjee A, Veraksa A, Artavanis-Tsakonas S, Hariharan IK. The Drosophila F Box Protein Archipelago Regulates dMyc Protein Levels In Vivo. *Curr Biol* (2004) 14:965–74. doi: 10.1016/j.cub.2004.04.040
23. Yada M, Hatakeyama S, Kamura T, Nishiyama M, Tsunematsu R, Imaki H, et al. Phosphorylation-Dependent Degradation of c-Myc Is Mediated by the F-Box Protein Fbw7. *EMBO J* (2004) 23:2116–25. doi: 10.1038/sj.emboj.7600217
24. Welcker M, Orian A, Jin J, Grim JE, Harper JW, Eisenman RN, et al. The Fbw7 Tumor Suppressor Regulates Glycogen Synthase Kinase 3 Phosphorylation-Dependent c-Myc Protein Degradation. *Proc Natl Acad Sci USA* (2004) 101:9085–90. doi: 10.1073/pnas.0402770101
25. Welcker M, Orian A, Grim JE, Eisenman RN, Clurman BE. A Nucleolar Isoform of the Fbw7 Ubiquitin Ligase Regulates c-Myc and Cell Size. *Curr Biol* (2004) 14:1852–7. doi: 10.1016/j.cub.2004.09.083
26. Popov N, Schulein C, Jaenicke LA, Eilers M. Ubiquitylation of the Amino Terminus of Myc by SCF(beta-TrCP) Antagonizes SCF(Fbw7)-mediated Turnover. *Nat Cell Biol* (2010) 12:973–81. doi: 10.1038/ncb2104
27. Thomas JJ, Abed M, Heuberger J, Novak R, Zohar Y, Beltran Lopez AP, et al. Rnf4-Dependent Oncogene Activation by Protein Stabilization. *Cell Rep* (2016) 16:3388–400. doi: 10.1016/j.celrep.2016.08.024
28. Adhikary S, Marinoni F, Hock A, Hulleman E, Popov N, Beier R, et al. The Ubiquitin Ligase HectH9 Regulates Transcriptional Activation by Myc and Is Essential for Tumor Cell Proliferation. *Cell* (2005) 123:409–21. doi: 10.1016/j.cell.2005.08.016
29. Peter S, Bultinck J, Myant K, Jaenicke LA, Walz S, Muller J, et al. Tumor Cell-Specific Inhibition of MYC Function Using Small Molecule Inhibitors of the HUWE1 Ubiquitin Ligase. *EMBO Mol Med* (2014) 6:1525–41. doi: 10.15252/emmm.201403927
30. Kim SY, Herbst A, Tworkowski KA, Salghetti SE, Tansey WP. Skp2 Regulates Myc Protein Stability and Activity. *Mol Cell* (2003) 11:1177–88. doi: 10.1016/S1097-2765(03)00173-4
31. von der Lehr N, Johansson S, Wu S, Bahram F, Castell A, Cetinkaya C, et al. The F-Box Protein Skp2 Participates in c-Myc Proteosomal Degradation and Acts as a Cofactor for c-Myc-Regulated Transcription. *Mol Cell* (2003) 11:1189–200. doi: 10.1016/S1097-2765(03)00193-X
32. Chen Y, Sun XX, Sears RC, Dai MS. Writing and Erasing MYC Ubiquitination and Sumoylation. *Genes Dis* (2019) 6:359–71. doi: 10.1016/j.gendis.2019.05.006
33. Sun XX, Sears RC, Dai MS. Deubiquitinating C-Myc: USP36 Steps Up in the Nucleolus. *Cell Cycle* (2015) 14:3786–93. doi: 10.1080/15384101.2015.1093713
34. Qiao X, Liu Y, Prada ML, Mohan AK, Gupta A, Jaiswal A, et al. Ubr5 Is Coamplified With MYC in Breast Tumors and Encodes an Ubiquitin Ligase That Limits MYC-Dependent Apoptosis. *Cancer Res* (2020) 80:1414–27. doi: 10.1158/0008-5472.CAN-19-1647
35. Morel M, Shah KN, Long W. The F-box Protein FBXL16 Up-Regulates the Stability of C-MYC Oncoprotein by Antagonizing the Activity of the F-Box Protein FBW7. *J Biol Chem* (2020) 295:7970–80. doi: 10.1074/jbc.RA120.012658
36. Honarpour N, Rose CM, Brumbaugh J, Anderson J, Graham RL, Sweredoski MJ, et al. F-Box Protein FBXL16 Binds PP2A-B55alpha and Regulates Differentiation of Embryonic Stem Cells Along the FLK1+ Lineage. *Mol Cell Proteomics* (2014) 13:780–91. doi: 10.1074/mcp.M113.031765
37. Mei Z, Zhang D, Hu B, Wang J, Shen X, Xiao W. Fbxo32 Targets c-Myc for Proteasomal Degradation and Inhibits c-Myc Activity. *J Biol Chem* (2015) 290:16202–14. doi: 10.1074/jbc.M115.645978
38. Chou JL, Su HY, Chen LY, Liao YP, Hartman-Frey C, Lai YH, et al. Promoter Hypermethylation of FBXO32, a Novel TGF-beta/SMAD4 Target Gene and Tumor Suppressor, Is Associated With Poor Prognosis in Human Ovarian Cancer. *Lab Invest* (2010) 90:414–25. doi: 10.1038/labinvest.2009.138
39. Choi SH, Wright JB, Gerber SA, Cole MD. Myc Protein is Stabilized by Suppression of a Novel E3 Ligase Complex in Cancer Cells. *Genes Dev* (2010) 24:1236–41. doi: 10.1101/gad.1920310
40. Jamal A, Swarnalatha M, Sultana S, Joshi P, Panda SK, Kumar V. The G1 Phase E3 Ubiquitin Ligase TRUSS That Gets Deregulated in Human Cancers Is a Novel Substrate of the S-Phase E3 Ubiquitin Ligase Skp2. *Cell Cycle* (2015) 14:2688–700. doi: 10.1080/15384101.2015.1056946
41. Cepeda D, Ng HF, Sharifi HR, Mahmoudi S, Cerrato VS, Fredlund E, et al. CDK-Mediated Activation of the SCF(FBXO) (28) Ubiquitin Ligase Promotes MYC-Driven Transcription and Tumourigenesis and Predicts Poor Survival in Breast Cancer. *EMBO Mol Med* (2013) 5:999–1018. doi: 10.1002/emmm.201202341
42. Lin CY, Loven J, Rahl PB, Paranal RM, Burge CB, Bradner JE, et al. Transcriptional Amplification in Tumor Cells With Elevated C-Myc. *Cell* (2012) 151:56–67. doi: 10.1016/j.cell.2012.08.026
43. Perna D, Faga G, Verrecchia A, Gorski MM, Barozzi I, Narang V, et al. Genome-Wide Mapping of Myc Binding and Gene Regulation in Serum-Stimulated Fibroblasts. *Oncogene* (2012) 31:1695–709. doi: 10.1038/onc.2011.359
44. Lorenzin F, Benary U, Baluapuri A, Walz S, Jung LA, von Eyss B, et al. Different Promoter Affinities Account for Specificity in MYC-dependent Gene Regulation. *Elife* (2016) 5:e15161. doi: 10.7554/eLife.15161
45. von der Lehr N, Johansson S, Larsson LG. Implication of the Ubiquitin/Proteasome System in Myc-Regulated Transcription. *Cell Cycle* (2003) 2:403–7. doi: 10.4161/cc.2.5.484
46. Jaenicke LA, von Eyss B, Carstensen A, Wolf E, Xu W, Greifenberg AK, et al. Ubiquitin-Dependent Turnover of MYC Antagonizes MYC/PAF1C Complex Accumulation to Drive Transcriptional Elongation. *Mol Cell* (2016) 61:54–67. doi: 10.1016/j.molcel.2015.11.007
47. Chen FX, Woodfin AR, Gardini A, Rickels RA, Marshall SA, Smith ER, et al. PAF1, a Molecular Regulator of Promoter-Proximal Pausing by RNA Polymerase Ii. *Cell* (2015) 162:1003–15. doi: 10.1016/j.cell.2015.07.042
48. Chen Y, Zhou C, Ji W, Mei Z, Hu B, Zhang W, et al. ELL Targets c-Myc for Proteasomal Degradation and Suppresses Tumour Growth. *Nat Commun* (2016) 7:11057. doi: 10.1038/ncomms11057
49. Metivier R, Penot G, Hubner MR, Reid G, Brand H, Kos M, et al. Estrogen Receptor-Alpha Directs Ordered, Cyclical, and Combinatorial Recruitment of Cofactors on a Natural Target Promoter. *Cell* (2003) 115:751–63. doi: 10.1016/S0092-8674(03)00934-6
50. Reid G, Hubner MR, Metivier R, Brand H, Denger S, Manu D, et al. Cyclic, Proteasome-Mediated Turnover of Unliganded and Liganded ERalpha on

Responsive Promoters Is an Integral Feature of Estrogen Signaling. *Mol Cell* (2003) 11:695–707. doi: 10.1016/S1097-2765(03)00090-X
51. Diefenbacher ME, Chakraborty A, Blake SM, Mitter R, Popov N, Eilers M, et al. Usp28 Counteracts Fbw7 in Intestinal Homeostasis and Cancer. *Cancer Res* (2015) 75:1181–6. doi: 10.1158/0008-5472.CAN-14-1726
52. Popov N, Wanzel M, Madiredjo M, Zhang D, Beijersbergen R, Bernards R, et al. The Ubiquitin-Specific Protease USP28 is Required for MYC Stability. *Nat Cell Biol* (2007) 9:765–74. doi: 10.1038/ncb1601
53. Sun XX, He X, Yin L, Komada M, Sears RC, Dai MS. The Nucleolar Ubiquitin-Specific Protease USP36 Deubiquitinates and Stabilizes C-Myc. *Proc Natl Acad Sci USA* (2015) 112:3734–9. doi: 10.1073/pnas.1411713112
54. Thevenon D, Seffouh I, Pillet C, Crespo-Yanez X, Fauvarque MO, Taillebourg E. A Nucleolar Isoform of the Drosophila Ubiquitin Specific Protease Dusp36 Regulates Myc-Dependent Cell Growth. *Front Cell Dev Biol* (2020) 8:506. doi: 10.3389/fcell.2020.00506
55. Kim D, Hong A, Park HI, Shin WH, Yoo L, Jeon SJ, et al. Deubiquitinating Enzyme USP22 Positively Regulates c-Myc Stability and Tumorigenic Activity in Mammalian and Breast Cancer Cells. *J Cell Physiol* (2017) 232:3664–76. doi: 10.1002/jcp.25841
56. Pan J, Deng Q, Jiang C, Wang X, Niu T, Li H, et al. USP37 Directly Deubiquitinates and Stabilizes c-Myc in Lung Cancer. *Oncogene* (2015) 34:3957–67. doi: 10.1038/onc.2014.327
57. Tavana O, Li D, Dai C, Lopez G, Banerjee D, Kon N, et al. HAUSP Deubiquitinates and Stabilizes N-Myc in Neuroblastoma. *Nat Med* (2016) 22:1180–6. doi: 10.1038/nm.4180
58. Nicklas S, Hillje AL, Okawa S, Rudolph IM, Collmann FM, van Wuellen T, et al. A Complex of the Ubiquitin Ligase TRIM32 and the Deubiquitinase USP7 Balances the Level of c-Myc Ubiquitination and Thereby Determines Neural Stem Cell Fate Specification. *Cell Death Differ* (2019) 26:728–40. doi: 10.1038/s41418-018-0144-1
59. Fang X, Zhou W, Wu Q, Huang Z, Shi Y, Yang K, et al. Deubiquitinase USP13 Maintains Glioblastoma Stem Cells by Antagonizing FBXL14-Mediated Myc Ubiquitination. *J Exp Med* (2017) 214:245–67. doi: 10.1084/jem.20151673
60. Sobol A, Askonas C, Alani S, Weber MJ, Ananthanarayanan V, Osipo C, et al. Deubiquitinase OTUD6B Isoforms Are Important Regulators of Growth and Proliferation. *Mol Cancer Res* (2017) 15:117–27. doi: 10.1158/1541-7786.MCR-16-0281-T
61. DeVine T, Sears RC, Dai MS. The Ubiquitin-Specific Protease USP36 Is a Conserved Histone H2B Deubiquitinase. *Biochem Biophys Res Commun* (2018) 495:2363–8. doi: 10.1016/j.bbrc.2017.12.107
62. Gonzalez-Prieto R, Cuijpers SA, Kumar R, Hendriks IA, Vertegaal AC. c-Myc Is Targeted to the Proteasome for Degradation in a SUMOylation-Dependent Manner, Regulated by PIAS1, SENP7 and RNF4. *Cell Cycle* (2015) 14:1859–72. doi: 10.1080/15384101.2015.1040965
63. Kalkat M, Chan PK, Wasylishen AR, Srikumar T, Kim SS, Ponzielli R, et al. Identification of C-MYC SUMOylation by Mass Spectrometry. *PloS One* (2014) 9:e115337. doi: 10.1371/journal.pone.0115337
64. Rabellino A, Melegari M, Tompkins VS, Chen W, Van Ness BG, Teruya-Feldstein J, et al. Pias1 Promotes Lymphomagenesis Through MYC Upregulation. *Cell Rep* (2016) 15:2266–78. doi: 10.1016/j.celrep.2016.05.015
65. Sabo A, Doni M, Amati B. Sumoylation of Myc-family Proteins. *PloS One* (2014) 9:e91072. doi: 10.1371/journal.pone.0091072
66. Sun XX, Chen Y, Su Y, Wang X, Chauhan KM, Liang J, et al. SUMO Protease SENP1 deSUMOylates and Stabilizes C-Myc. *Proc Natl Acad Sci USA* (2018) 115:10983–8. doi: 10.1073/pnas.1802932115
67. Hendriks IA, Vertegaal AC. A Comprehensive Compilation of SUMO Proteomics. *Nat Rev Mol Cell Biol* (2016) 17:581–95. doi: 10.1038/nrm.2016.81
68. Lamoliatte F, McManus FP, Maarifi G, Chelbi-Alix MK, Thibault P. Uncovering the SUMOylation and Ubiquitylation Crosstalk in Human Cells Using Sequential Peptide Immunopurification. *Nat Commun* (2017) 8:14109. doi: 10.1038/ncomms14109
69. Cheng J, Kang X, Zhang S, Yeh ET. SUMO-Specific Protease 1 Is Essential for Stabilization of HIF1alpha During Hypoxia. *Cell* (2007) 131:584–95. doi: 10.1016/j.cell.2007.08.045
70. Chymkowitch P, Nguea PA, Enserink JM. SUMO-Regulated Transcription: Challenging the Dogma. *Bioessays* (2015) 37:1095–105. doi: 10.1002/bies.201500065
71. Cubenas-Potts C, Matunis MJ. SUMO: A Multifaceted Modifier of Chromatin Structure and Function. *Dev Cell* (2013) 24:1–12. doi: 10.1016/j.devcel.2012.11.020
72. Cermelli S, Jang IS, Bernard B, Grandori C. Synthetic Lethal Screens as a Means to Understand and Treat MYC-Driven Cancers. *Cold Spring Harbor Perspect Med* (2014) 4:a014209. doi: 10.1101/cshperspect.a014209
73. Delmore JE, Issa GC, Lemieux ME, Rahl PB, Shi J, Jacobs HM, et al. BET Bromodomain Inhibition as a Therapeutic Strategy to Target C-Myc. *Cell* (2011) 146:904–17. doi: 10.1016/j.cell.2011.08.017
74. Li B, Simon MC. Molecular Pathways: Targeting MYC-Induced Metabolic Reprogramming and Oncogenic Stress in Cancer. *Clin Cancer Res* (2013) 19:5835–41. doi: 10.1158/1078-0432.CCR-12-3629
75. Dang CV, Reddy EP, Shokat KM, Soucek L. Drugging the 'Undruggable' Cancer Targets. *Nat Rev Cancer* (2017) 17:502–8. doi: 10.1038/nrc.2017.36
76. Duffy MJ, Crown J. Drugging "Undruggable" Genes for Cancer Treatment: Are We Making Progress? *Int J Cancer* (2021) 148:8–17. doi: 10.1002/ijc.33197
77. Beaulieu ME, Jauset T, Masso-Valles D, Martinez-Martin S, Rahl P, Maltais L, et al. Intrinsic Cell-Penetrating Activity Propels Omomyc From Proof of Concept to Viable anti-MYC Therapy. *Sci Transl Med* (2019) 11:eaar5012. doi: 10.1126/scitranslmed.aar5012
78. Demma MJ, Mapelli C, Sun A, Bodea S, Ruprecht B, Javaid S, et al. Omomyc Reveals New Mechanisms to Inhibit the MYC Oncogene. *Mol Cell Biol* (2019) 39:e00248–19. doi: 10.1128/MCB.00248-19
79. Masso-Valles D, Soucek L. Blocking Myc to Treat Cancer: Reflecting on Two Decades of Omomyc. *Cells* (2020) 9:883. doi: 10.3390/cells9040883
80. Wang E, Sorolla A, Cunningham PT, Bogdawa HM, Beck S, Golden E, et al. Tumor Penetrating Peptides Inhibiting MYC as a Potent Targeted Therapeutic Strategy for Triple-Negative Breast Cancers. *Oncogene* (2019) 38:140–50. doi: 10.1038/s41388-018-0421-y
81. Chen Q, Xie W, Kuhn DJ, Voorhees PM, Lopez-Girona A, Mendy D, et al. Targeting the P27 E3 Ligase SCF(Skp2) Results in p27- and Skp2-Mediated Cell-Cycle Arrest and Activation of Autophagy. *Blood* (2008) 111:4690–9. doi: 10.1182/blood-2007-09-112904
82. Rico-Bautista E, Yang CC, Lu L, Roth GP, Wolf DA. Chemical Genetics Approach to Restoring p27Kip1 Reveals Novel Compounds With Antiproliferative Activity in Prostate Cancer Cells. *BMC Biol* (2010) 8:153. doi: 10.1186/1741-7007-8-153
83. Chan CH, Morrow JK, Li CF, Gao Y, Jin G, Moten A, et al. Pharmacological Inactivation of Skp2 SCF Ubiquitin Ligase Restricts Cancer Stem Cell Traits and Cancer Progression. *Cell* (2013) 154:556–68. doi: 10.1016/j.cell.2013.06.048
84. Malek E, Abdel-Malek MA, Jagannathan S, Vad N, Karns R, Jegga AG, et al. Pharmacogenomics and Chemical Library Screens Reveal a Novel SCF (SKP2) Inhibitor That Overcomes Bortezomib Resistance in Multiple Myeloma. *Leukemia* (2017) 31:645–53. doi: 10.1038/leu.2016.258
85. Ungermannova D, Lee J, Zhang G, Dallmann HG, McHenry CS, Liu X. High-Throughput Screening AlphaScreen Assay for Identification of Small-Molecule Inhibitors of Ubiquitin E3 Ligase Scfskp2-Cks1. *J Biomol Screen* (2013) 18:910–20. doi: 10.1177/1087057113485789
86. Byun WS, Jin M, Yu J, Kim WK, Song J, Chung HJ, et al. A Novel Selenonucleoside Suppresses Tumor Growth by Targeting Skp2 Degradation in Paclitaxel-Resistant Prostate Cancer. *Biochem Pharmacol* (2018) 158:84–94. doi: 10.1016/j.bcp.2018.10.002
87. Dow R, Hendley J, Pirkmaier A, Musgrove EA, Germain D. Retinoic Acid-Mediated Growth Arrest Requires Ubiquitylation and Degradation of the F-Box Protein Skp2. *J Biol Chem* (2001) 276:45945–51. doi: 10.1074/jbc.M103593200
88. Chauhan D, Tian Z, Nicholson B, Kumar KG, Zhou B, Carrasco R, et al. A Small Molecule Inhibitor of Ubiquitin-Specific Protease-7 Induces Apoptosis in Multiple Myeloma Cells and Overcomes Bortezomib Resistance. *Cancer Cell* (2012) 22:345–58. doi: 10.1016/j.ccr.2012.08.007
89. Altun M, Kramer HB, Willems LI, McDermott JL, Leach CA, Goldenberg SJ, et al. Activity-Based Chemical Proteomics Accelerates Inhibitor Development for Deubiquitylating Enzymes. *Chem Biol* (2011) 18:1401–12. doi: 10.1016/j.chembiol.2011.08.018
90. Pozhidaeva A, Valles G, Wang F, Wu J, Sterner DE, Nguyen P, et al. Usp7-Specific Inhibitors Target and Modify the Enzyme's Active Site Via Distinct

Chemical Mechanisms. *Cell Chem Biol* (2017) 24:1501–12.e1505. doi: 10.1016/j.chembiol.2017.09.004
91. Reverdy C, Conrath S, Lopez R, Planquette C, Atmanene C, Collura V, et al. Discovery of Specific Inhibitors of Human USP7/HAUSP Deubiquitinating Enzyme. *Chem Biol* (2012) 19:467–77. doi: 10.1016/j.chembiol.2012.02.007
92. Kategaya L, Di Lello P, Rouge L, Pastor R, Clark KR, Drummond J, et al. USP7 Small-Molecule Inhibitors Interfere With Ubiquitin Binding. *Nature* (2017) 550:534–8. doi: 10.1038/nature24006
93. Turnbull AP, Ioannidis S, Krajewski WW, Pinto-Fernandez A, Heride C, Martin ACL, et al. Molecular Basis of USP7 Inhibition by Selective Small-Molecule Inhibitors. *Nature* (2017) 550:481–6. doi: 10.1038/nature24451
94. Li M, Liu S, Chen H, Zhou X, Zhou J, Zhou S, et al. N-Benzylpiperidinol Derivatives as Novel USP7 Inhibitors: Structure-Activity Relationships and X-Ray Crystallographic Studies. *Eur J Med Chem* (2020) 199:112279. doi: 10.1016/j.ejmech.2020.112279
95. Lamberto I, Liu X, Seo HS, Schauer NJ, Iacob RE, Hu W, et al. Structure-Guided Development of a Potent and Selective Non-Covalent Active-Site Inhibitor of USP7. *Cell Chem Biol* (2017) 24:1490–500.e1411. doi: 10.1016/j.chembiol.2017.09.003
96. Ohol YM, Sun MT, Cutler G, Leger PR, Hu DX, Biannic B, et al. Novel, Selective Inhibitors of USP7 Uncover Multiple Mechanisms of Antitumor Activity In Vitro and In Vivo. *Mol Cancer Ther* (2020) 19:1970–80. doi: 10.1158/1535-7163.MCT-20-0184
97. Gavory G, O'Dowd CR, Helm MD, Flasz J, Arkoudis E, Dossang A, et al. Discovery and Characterization of Highly Potent and Selective Allosteric USP7 Inhibitors. *Nat Chem Biol* (2018) 14:118–25. doi: 10.1038/nchembio.2528
98. O'Dowd CR, Helm MD, Rountree JSS, Flasz JT, Arkoudis E, Miel H, et al. Identification and Structure-Guided Development of Pyrimidinone Based USP7 Inhibitors. *ACS Med Chem Lett* (2018) 9:238–43. doi: 10.1021/acsmedchemlett.7b00512
99. Wrigley JD, Gavory G, Simpson I, Preston M, Plant H, Bradley J, et al. Identification and Characterization of Dual Inhibitors of the USP25/28 Deubiquitinating Enzyme Subfamily. *ACS Chem Biol* (2017) 12:3113–25. doi: 10.1021/acschembio.7b00334
100. Liu Z, Zhao T, Li Z, Sun K, Fu Y, Cheng T, et al. Discovery of [1,2,3]Triazolo [4,5-D]Pyrimidine Derivatives as Highly Potent, Selective, and Cellularly Active USP28 Inhibitors. *Acta Pharm Sin B* (2020) 10:1476–91. doi: 10.1016/j.apsb.2019.12.008
101. Wang H, Meng Q, Ding Y, Xiong M, Zhu M, Yang Y, et al. USP28 and USP25 Are Downregulated by Vismodegib In Vitro and in Colorectal Cancer Cell Lines. *FEBS J* (2021) 288:1325–42. doi: 10.1111/febs.15461
102. Hu Y, Yu K, Wang G, Zhang D, Shi C, Ding Y, et al. Lanatoside C Inhibits Cell Proliferation and Induces Apoptosis Through Attenuating Wnt/beta-Catenin/c-Myc Signaling Pathway in Human Gastric Cancer Cell. *Biochem Pharmacol* (2018) 150:280–92. doi: 10.1016/j.bcp.2018.02.023
103. Ambaye N, Chen CH, Khanna S, Li YJ, Chen Y. Streptonigrin Inhibits SENP1 and Reduces the Protein Level of Hypoxia-Inducible Factor 1alpha (HIF1alpha) in Cells. *Biochemistry* (2018) 57:1807–13. doi: 10.1021/acs.biochem.7b00947
104. Han Y, Huang W, Liu J, Liu D, Cui Y, Huang R, et al. Triptolide Inhibits the AR Signaling Pathway to Suppress the Proliferation of Enzalutamide Resistant Prostate Cancer Cells. *Theranostics* (2017) 7:1914–27. doi: 10.7150/thno.17852
105. Huang W, He T, Chai C, Yang Y, Zheng Y, Zhou P, et al. Triptolide Inhibits the Proliferation of Prostate Cancer Cells and Down-Regulates SUMO-Specific Protease 1 Expression. *PloS One* (2012) 7:e37693. doi: 10.1371/journal.pone.0037693
106. Wu J, Lei H, Zhang J, Chen X, Tang C, Wang W, et al. Momordin Ic, a New Natural SENP1 Inhibitor, Inhibits Prostate Cancer Cell Proliferation. *Oncotarget* (2016) 7:58995–9005. doi: 10.18632/oncotarget.10636
107. Zhang Q, Spears E, Boone DN, Li Z, Gregory MA, Hann SR. Domain-Specific c-Myc Ubiquitylation Controls c-Myc Transcriptional and Apoptotic Activity. *Proc Natl Acad Sci USA* (2013) 110:978–83. doi: 10.1073/pnas.1208334110
108. Gstaiger M, Jordan R, Lim M, Catzavelos C, Mestan J, Slingerland J, et al. Skp2 is Oncogenic and Overexpressed in Human Cancers. *Proc Natl Acad Sci USA* (2001) 98:5043–8. doi: 10.1073/pnas.081474898
109. Huang HC, Lin CL, Lin JK. 1,2,3,4,6-Penta-O-Galloyl-Beta-D-Glucose, Quercetin, Curcumin and Lycopene Induce Cell-Cycle Arrest in MDA-MB-231 and BT474 Cells Through Downregulation of Skp2 Protein. *J Agric Food Chem* (2011) 59:6765–75. doi: 10.1021/jf201096v
110. Shachaf CM, Kopelman AM, Arvanitis C, Karlsson A, Beer S, Mandl S, et al. MYC Inactivation Uncovers Pluripotent Differentiation and Tumour Dormancy in Hepatocellular Cancer. *Nature* (2004) 431:1112–7. doi: 10.1038/nature03043
111. Crawford LJ, Campbell DC, Morgan JJ, Lawson MA, Down JM, Chauhan D, et al. The E3 Ligase HUWE1 Inhibition as a Therapeutic Strategy to Target MYC in Multiple Myeloma. *Oncogene* (2020) 39:5001–14. doi: 10.1038/s41388-020-1345-x
112. Shachaf CM, Gentles AJ, Elchuri S, Sahoo D, Soen Y, Sharpe O, et al. Genomic and Proteomic Analysis Reveals a Threshold Level of MYC Required for Tumor Maintenance. *Cancer Res* (2008) 68:5132–42. doi: 10.1158/0008-5472.CAN-07-6192
113. Murphy DJ, Junttila MR, Pouyet L, Karnezis A, Shchors K, Bui DA, et al. Distinct Thresholds Govern Myc's Biological Output In Vivo. *Cancer Cell* (2008) 14:447–57. doi: 10.1016/j.ccr.2008.10.018
114. Pozhidaeva A, Bezsonova I. Usp7: Structure, Substrate Specificity, and Inhibition. *DNA Repair (Amst)* (2019) 76:30–9. doi: 10.1016/j.dnarep.2019.02.005
115. Li P, Liu HM. Recent Advances in the Development of Ubiquitin-Specific-Processing Protease 7 (USP7) Inhibitors. *Eur J Med Chem* (2020) 191:112107. doi: 10.1016/j.ejmech.2020.112107
116. Fan YH, Cheng J, Vasudevan SA, Dou J, Zhang H, Patel RH, et al. USP7 Inhibitor P22077 Inhibits Neuroblastoma Growth Via Inducing p53-Mediated Apoptosis. *Cell Death Dis* (2013) 4:e867. doi: 10.1038/cddis.2013.400
117. Weinstock J, Wu J, Cao P, Kingsbury WD, McDermott JL, Kodrasov MP, et al. Selective Dual Inhibitors of the Cancer-Related Deubiquitylating Proteases USP7 and USP47. *ACS Med Chem Lett* (2012) 3:789–92. doi: 10.1021/ml200276j
118. Prieto-Garcia C, Hartmann O, Reissland M, Braun F, Fischer T, Walz S, et al. Maintaining Protein Stability of Np63 Via USP28 Is Required by Squamous Cancer Cells. *EMBO Mol Med* (2020) 12:e11101. doi: 10.15252/emmm.201911101
119. Banerjee S, Saluja A. Minnelide, a Novel Drug for Pancreatic and Liver Cancer. *Pancreatology* (2015) 15:S39–43. doi: 10.1016/j.pan.2015.05.472
120. Rottmann S, Wang Y, Nasoff M, Deveraux QL, Quon KC. A TRAIL Receptor-Dependent Synthetic Lethal Relationship Between MYC Activation and GSK3beta/FBW7 Loss of Function. *Proc Natl Acad Sci USA* (2005) 102:15195–200. doi: 10.1073/pnas.0505114102

Conflict of Interest: The authors declare that the research was conducted in the absence of any commercial or financial relationships that could be construed as a potential conflict of interest.

frontiers in Oncology

ORIGINAL RESEARCH
published: 30 July 2021
doi: 10.3389/fonc.2021.624837

Upregulation of KLK8 Predicts Poor Prognosis in Pancreatic Cancer

Qing Hua[1,2,3], *Tianjiao Li*[2,4,5,6], *Yixuan Liu*[2,7], *Xuefang Shen*[1,2], *Xiaoyan Zhu*[8]* and *Pingbo Xu*[1,2]*

[1] Department of Anesthesiology, Shanghai Cancer Centre, Fudan University, Shanghai, China, [2] Department of Oncology, Shanghai Medical College, Fudan University, Shanghai, China, [3] Department of Anesthesiology, Zhongshan Hospital, Fudan University, Shanghai, China, [4] Department of Pancreatic Surgery, Shanghai Cancer Centre, Fudan University, Shanghai, China, [5] Shanghai Pancreatic Cancer Institute, Fudan University Shanghai, Shanghai, China, [6] Pancreatic Cancer Institute, Fudan University, Shanghai, China, [7] Department of Clinical Laboratory, Shanghai Cancer Centre, Fudan University, Shanghai, China, [8] Department of Physiology, Navy Medical University, Shanghai, China

Pancreatic ductal adenocarcinoma (PDAC) is a growing cause of cancer-related mortality worldwide. Kallikrein-related peptidase 8 (KLK8) has potential clinical values in many cancers. However, the clinicopathological significances of KLK8 in PDAC remain unknown. We explored the relationship of KLK8 to clinicopathological features of PDAC based on public databases. KLK8 expression was examined in human PDAC tissues. Cell proliferation and apoptosis were evaluated in KLK8-overexpressed human pancreatic cancer cell lines Mia-paca-2 and Panc-1. The related signaling pathways of KLK8 involved in pancreatic cancer progression were analyzed by gene set enrichment analysis (GSEA) and further verified in *in vitro* studies. We found that KLK8 was up-regulated in tumor tissues in the TCGA-PAAD cohort, and was an independent prognostic factor for both overall survival and disease-free survival of PDAC. KLK8 mRNA and protein expressions were increased in PDAC tissues compared with para-cancerous pancreas. KLK8 overexpression exerted pro-proliferation and anti-apoptotic functions in Mia-paca-2 and Panc-1 cells. GSEA analysis showed that KLK8 was positively associated with PI3K-Akt-mTOR and Notch pathways. KLK8-induced pro-proliferation and anti-apoptotic effects in Mia-paca-2 and Panc-1 cells were attenuated by inhibitors for PI3K, Akt, and mTOR, but not by inhibitor for Notch. Furthermore, overexpression of KLK8 in Mia-paca-2 and Panc-1 cells significantly increased epidermal growth factor (EGF) levels in the culture media. EGF receptor (EGFR) inhibitor could block KLK8-induced activation of PI3K/Akt/mTOR pathway and attenuate pro-proliferation and anti-apoptotic of KLK8 in Mia-paca-2 and Panc-1 cells. In conclusion, KLK8 overexpression exerts pro-proliferation and anti-apoptotic functions in pancreatic cancer cells *via* EGF signaling-dependent activation of PI3K/Akt/mTOR pathway. Upregulated KLK8 in PDAC predicts poor prognosis and may be a potential therapeutic target for PDAC.

Keywords: apoptosis, kallikrein-related peptidase 8, pancreatic ductal adenocarcinoma, PI3K-Akt-mTOR pathway, proliferation

OPEN ACCESS

Edited by:
Alena Malyukova, Karolinska Institutet (KI), Sweden

Reviewed by:
Giulio Innamorati, University of Verona, Italy
Yoshio Bando, Akita University, Japan

***Correspondence:**
Pingbo Xu
xupingboshanghai@163.com
Xiaoyan Zhu
xiaoyanzhu@smmu.edu.cn

Specialty section:
This article was submitted to Cancer Molecular Targets and Therapeutics, a section of the journal Frontiers in Oncology

Received: *01 November 2020*
Accepted: *08 June 2021*
Published: *30 July 2021*

Citation:
Hua Q, Li T, Liu Y, Shen X, Zhu X and Xu P (2021) Upregulation of KLK8 Predicts Poor Prognosis in Pancreatic Cancer. Front. Oncol. 11:624837. doi: 10.3389/fonc.2021.624837

BACKGROUND

Pancreatic cancer is one of the most leading causes of cancer death in both males and females because of its poor prognosis, with almost as many deaths (n = 432,000) as cases (n = 459,000) (1). According to 2020 cancer statistics, approximately 57,600 new cases of pancreatic cancer will be diagnosed, killing almost 47,050 people in the United States in 2020, making it the fourth leading cause of cancer-associated death (2). Despite the advanced therapeutic approaches, the 5-year relative survival rate of pancreatic cancer remains poor, estimated at 9% (3–5). To further improve the survival rates, it is critical to identify a more sensitive and effective biomarker associated with the tumorigenesis and progression for early detection, which will improve the prognosis for pancreatic cancer.

Tissue kallikrein-related peptidases (KLKs) are a group of serine proteases encoded by 15 highly conserved genes (*KLK1-KLK15*) arranged in a tandem cluster (~300 kb) on chromosome 19q13.3–13.4 (6–9). KLK8, an important member of the KLKs family, is a synaptic, plasticity-modulating extracellular serine protease and has been found in many tissues and biological fluids, involved in a variety of biological activities, for instance, epidermal proliferation and differentiation, terminal differentiation of keratinocytes and so on (10, 11). Abnormal KLK8 expression has been found in several malignancies, including ovarian, cervical, gland and lung cancers (12–15). Meanwhile, accumulating evidence support the clinical utility of KLK8 as a biomarker for cancer survival and prognosis. However, the expression pattern and role of KLK8 in pancreatic cancer remains unknown.

In this study, we explored the expression of KLK8 in the pancreatic cancer at both the mRNA and protein levels and investigated the correlation between KLK8 expression and prognosis of pancreatic cancer patients. We also investigated whether and how KLK8 affected the proliferation and apoptosis of pancreatic cancer cells. Our findings demonstrated that upregulation of KLK8 was related to a poor prognosis in pancreatic cancer. Overexpression of KLK8 might promote proliferation and inhibit apoptosis *via* epidermal growth factor (EGF) signaling-dependent activation of PI3K/Akt/mTOR pathway in pancreatic cancer cells.

METHODS

Patients and Specimens

Thirty pancreatic cancer tissue samples and their matched para-cancerous pancreas from pancreatic cancer patients who underwent surgery in Fudan University Shanghai Cancer Center (Fudan Center) between June 2016 and April 2018 were obtained during operations. All diagnoses were confirmed by two pathologists. All specimens were acquired after written informed consent following procedures approved by the Ethics Committee of Fudan University Shanghai Cancer Center.

The Cancer Genome Atlas Analysis and GSEA

The GEPIA database provided differential gene expression analysis of 31 kinds of cancers based on integrated analysis of the TCGA and GTEx databases. TCGA Pancreatic Cancer (PAAD) cohort consisted of 178 primary pancreatic cancer and 4 normal samples. And gene expression of 167 normal pancreatic tissue was also downloaded from GTEx (http://commonfund.nih.gov/GTEx/) to explore the differential expressed genes between tumors and normal tissues. All data on expression and clinical features were obtained from the USUC Xena Cancer Genomics Browser (https://xenabrowser.net/datapages/?dataset=TCGA). The differentially expressed genes with $|\log2foldchange| \geq 1$ and $P < 0.05$ were selected based on 178 pancreatic cancer samples and 171 normal pancreas samples. X-tile program (www.tissuearray.org/rimmlab/) was used to determine the optimum cutoff value of KLK8 with minimum p value defined by Kaplan–Meier survival analysis and log-rank test. To elucidate the mechanisms behind KLK8 in pancreatic cancer, Gene set enrichment analysis (GSEA) was performed on the Broad Institute Platform, and statistical significance (false discovery rate, FDR) was set at 0.25. Hallmark gene set collection was used to find relative signaling pathways of KLK8 from control and KLK8 overexpression group according to the genes presenting the strongest enrichment scores.

RNA Extraction and Real-Time Quantitative Polymerase Chain Reaction (RT-qPCR)

Total RNA from 30 random pairs of fresh pancreatic cancer tissue and adjacent normal mucosa were isolated using the Trizol reagent (TaKaRa, Japan) according to the manufacturer's instruction. Primers for RT-qPCR were designed using Primer Express v2.0 software (Applied BioSystems). The primer sequences for KLK8 were as follows: forward 5'- AAG TGCACC GTC TCA GGC-3' and reverse 5'- TCC TCA CAC TTC TTC TGG GG-3'. β-actin was used as an internal control, and the primer sequences were as follows: forward 5'-CTA CGT CGC CCT GGA CTT CGA GC -3' and reverse 5'- GAT GGA GCC GCC GAT CCA CAC GG -3'. Real-time PCR was carried out using SYBR Green I (Applied BioSystems) and the relative expression was calculated using the $2^{-\Delta\Delta CT}$ method and normalized to β-actin (human) as the internal control gene.

Immunohistochemical (IHC) Staining

The immunohistochemistry (IHC) was performed on formalin fixation and paraffin embedding (FFPE) samples to study the protein expression in the clinical specimens. Immunohistochemistry staining of KLK8 was performed using a primary antibody against KLK8 (1:100 dilution; ab150395; Abcam, Cambridge, UK) according to the manufacturer's instructions. Briefly, FFPE pancreatic cancer tissues and paired adjacent noncancerous

Abbreviations: PDAC, Pancreatic ductaladenocarcinoma; KLK8, Kallikrein-related peptidase 8; GSEA, gene set enrichment analysis; PI3K, Phosphatidylinositide 3 kinases; mTOR, mammalian target of rapamycin; KLKs, kallikrein-related peptidases; PAAD, Pancreatic Cancer; OSCC, Oral squamous cell carcinoma; CRC, Colorectal cancer; H/R, Hypoxia/Reoxygenation; EMT, epithelial-mesenchymal transition; EGF, epidermal growth factor; EGFR, epidermal growth factor Receptor.

tissues were sectioned to a thickness of 4 μm. After routine deparaffinization, rehydration, antigen retrieval, and blocking with 3% hydrogen peroxide, the sections were then incubated with primary antibody which is specific for KLK8 (1:100 dilution; ab150395; Abcam, Cambridge, UK) overnight at 4°C and then with HRP-labeled secondary antibody. Finally, the sections were stained with diaminobenzidine and counterstained with hematoxylin. Staining was independently examined by two experienced investigators blinded to the clinical characteristics of the patients. The score for KLK8 staining was based on the integrated staining intensity and the percentage of positive cells. Staining intensity was scored as follows (16): 0 = no color; 1 = yellow; 2 = light brown; and 3 = dark brown. The proportion of immune-positive tumor cells (number of positively labeled tumor cells/number of total tumor cells) was scored as follows (17): 0, positive cells <5%; 1, 6%- 25% positive cells;2, 26%- 50% positive cells; 3, positive cells 51%- 75%; and 4>76%.). The comprehensive score was the product of staining intensity and average proportion of positive cells and expressed as follows (18): negative staining (0-2); weak expression (3-5); moderate expression (6-9); and strong expression (10-12).

Cell Culture and Stable Transfection

The human pancreatic cancer cell line Mia-paca-2, Panc-1 and human embryonic kidney cell line 293T (293T) were obtained from Type Culture Collection of the Chinese Academy of Sciences (Shanghai, China). Mia-paca-2 and Panc-1 cells were cultured in DMEM (Invitrogen). All medium was supplemented with 10% fetal bovine serum (Gibco, USA) and 1% penicillin/streptomycin (Invitrogen). KLK8 overexpression was performed using a lentiviral packaging system. To construct overexpressing exogenous KLK8 cell lines, full-length KLK8 (NM_144505) was cloned into the expression vector Ubi-MCS-3FLAG-CBh-gcGFP-IRES-puromycin (Shanghai Genechem Co. Shanghai, China) and transfected into Mia-paca-2 and Panc-1 cell lines according to the manufacturer's instructions. Briefly, Mia-paca-2 and Panc-1 cells were placed in 6-well plates at a density of 1 × 10^5cells/well the day before infection. The next day lentivirus were added in cell culture medium. Viruses were removed 24 h after infection and fresh cell culture medium was added. 72h after transfection, puromycin (2 μg/ml; Roche, USA) was added into the cell culture medium to generate stable KLK8-overexpression cell line four weeks later. Antibiotic-resistant cells were pooled for subsequent analysis.

Western Blot Analysis

The cells were lysed, and proteins were extracted through standard protocols. The proteins were separated by SDS-polyacrylamide gel electrophoresis and subjected to western blot analyses. Protein bands were detected by the chemiluminescence method. Specific primary antibodies against KLK8(1:1000 dilution; ab150395; Abcam, Cambridge, UK),PI3K (1:1000 dilution; #4257; Cell Signaling Technology, Danvers, MA, USA), Akt (1:1000 dilution; ab8805; Abcam, Cambridge, UK), mTOR (1:1000 dilution; ab32028; Abcam, Cambridge, UK), p-PI3K(1:1000 dilution,P85 Tyr458; #17366; Cell Signaling Technology, Danvers, MA, USA), p-Akt(1:5000 dilution, Ser473; ab81283; Abcam, Cambridge, UK), p-mTOR (1:1000 dilution, Ser2448; ab109268; Abcam, Cambridge, UK), p-4EBP1 (1:1000 dilution, Ser65; #9451; Cell Signaling Technology, Danvers, MA, USA), p-S6P-p70S6K (1:1000 dilution, Thr389; #9234; Cell Signaling Technology, Danvers, MA, USA), Notch1 (1:1000 dilution; ab52627; Abcam, Cambridge, UK), *c-myc* (1:1000 dilution; ab32072; Abcam, Cambridge, UK), cyclin D1 (1:1000 dilution; #2922; Cell Signaling Technology, Danvers, MA, USA), cleaved caspase-3 (1:500 dilution; #9664; Cell Signaling Technology, Danvers, MA, USA), cleaved caspase-9 (1:1000 dilution; #52873; Cell Signaling Technology, Danvers, MA, USA), Bax (1:1000 dilution; ab32503; Abcam, Cambridge, UK) were used. β-Actin (1:5000 dilution; sc-47778; Santa, Cruz, CA, USA) was used as a loading control. The chemiluminescent signals were detected with the chemiluminescence imaging system and quantified by Image J software (v1.37).

Cell Counting Kit-8 (CCK8) Assay

The density of 1000 pretreated cells/well were seeded into a 96-well plate. The cells were incubated with CCK8 reagent (DOJINDO, Japan) at 37°C for 1 h and absorbance at 450 nm were measured using a microplate reader (BioTek, Vermont, USA) for the appropriate time.

Colony Formation

Log phase Mia-paca-2 and Panc-1 cells were collected. The 500 cells were planted in each well of the 6-well plate and incubated at 37°C exposed to 5% CO_2. After 14 days, the cells were fixed by 4% paraformaldehyde and stained by 0.1% crystal violet and the colonies were counted visually, with >100 cells/colony considered a clone.

Apoptosis Assessment

Following transfected with KLK8 and vector plasmid, cells were washed with PBS 3 times and then stained using the Annexin V-FITC Apoptosis Detection Kit (BD Biosciences) according to the instruction. Then cells were analyzed with a FACS flow cytometer (BD Biosciences).

Enzyme-Linked Immunosorbent Assay

Mia-paca-2 and Panc-1 cells were plated in 12-well plates and Enzyme-linked immunosorbent assay (ELISA) was performed to detected the EGF levels in the supernatants after cultured for 48 hours using the Human EGF Quantikine ELISA Kit (#DEG00, R&D Systems, Minneapolis, MN, USA) according to manufacturer's instructions

Statistical Analysis

Data were expressed as means ± standard error of the mean (SEM) from at least three experiments. All statistical analyses were performed using SPSS 13.0 (SPSS Inc.). Independent samples t-test was used to compare control and treatment groups and one-way ANOVA was performed to compare the data of multiple groups. The Kaplan Meier estimation method was used for overall survival analysis, and a log-rank test was used to compare differences. $P < 0.05$ was considered to be statistically significant.

RESULTS

KLK8 Was Associated With Pancreatic Cancer Progression and Patients' Outcome

Based on the indicated role of KLK8 in malignant disease found in GEPIA (http://gepia.cancer-pku.cn/detail.php?gene=KLK8) (**Figure 1A**), we analyzed the expression of KLK8 in the independent public dataset from Oncomine (https://www.oncomine.org/resource/main.html) and found that KLK8 expression was elevated in the pancreatic cancer tissue samples in comparison to the normal pancreas (**Figure 1B**, P<0.0001). To further examine the potential relationship between KLK8 and PAAD, we analyzed data from the TCGA-PAAD cohort which was replenished by GTEX database, and found that KLK8 was significantly upregulated in tumor tissues compared to normal tissues (**Figure 1C**, P<0.0001). Then we evaluated the relationship between KLK8 expression and patients' outcomes. The Kaplan–Meier curve analysis of the TCGA-PAAD database indicated that higher KLK8 expression in PAAD was correlated with shorter OS and DFS rates (P<0.01, **Figure 1D**). Notably, there are 8 pancreatic neuroendocrine tumor (NET) samples in the TCGA-PAAD database, which exhibit low KLK8 expression. NET is known to have a very different prognosis as compared to PDAC (19). Therefore, we deleted these 8 NETs, and the remaining cohort consisted of 170 primary PDACs samples were used for performing the survival analysis. As shown in **Figure 1E**, we found that higher KLK8 expression in PDAC was correlated with shorter OS ($P < 0.05$) and DFS ($P < 0.01$) rates. These results suggest that KLK8 is highly expressed in pancreatic cancer and is correlated with the prognosis of patients with pancreatic cancer.

KLK8 Was Elevated in Pancreatic Cancer Tissues at Both the mRNA and Protein Levels

To further investigate the expression of KLK8 in pancreatic cancers, KLK8 protein expression was assessed in 20 pancreatic cancer tissues and para-cancerous pancreas by IHC staining. Compared with normal tissues, the level of KLK8 were significantly increased in pancreatic cancer tissues (**Figures 2A–C**, P<0.01). We also performed H&E staining of sequential sections of those used for IHC staining. As shown in **Supplemental Figures S1A, B**, it was found that the tumor tissues exhibited typical pancreatic ductal adenocarcinoma. There were full of exocrine portions, plenty of infiltrating lymphocytes and some epithelioid cells in the para-cancerous tissues. Then, KLK8 mRNA expression was determined in 30 paired PDAC tissues and matched para-cancerous pancreas. It was found that KLK8 mRNA levels were significantly increased in pancreatic cancer tissue samples as comparison to the adjacent non-tumor tissues (**Figure 2D**, $p < 0.01$). These findings were consistent with the data obtained from the public datasets (**Figure 1**).

KLK8 Exerted Pro-Proliferation and Anti-Apoptotic Functions in Pancreatic Cancer Cells

Abnormal cell proliferation and apoptosis are characteristics of human malignant tumor (20). We then determined whether elevated KLK8 expression could influence the proliferation and apoptosis of pancreatic cancer cells by using KLK8-overexpressed Mia-paca-2 and Panc-1 cell lines. The efficacy of KLK8 overexpression in two cell lines was confirmed by western blot analysis (**Figure 3A**). We performed CCK-8 and colony formation assay to assess the effects of KLK8 in pancreatic cell proliferation. As shown in **Figures 3B, C**, a significant promotion of cell proliferation was observed in the KLK8-overexpression group in comparison to the control group. In addition, the number of cell colonies were significantly increased in both Mia-paca-2 and Panc-1 pancreatic cancer cells overexpressed with KLK8 (**Figures 3D, E**).

We then clarified the effect of KLK8 overexpression on pancreatic cancer apoptosis. As shown in **Figures 4A–D**, compared with control group, the percentage of apoptosis cells was significantly reduced in KLK8 overexpressed pancreatic cancer cells. In addition, western blot assay showed that compared with control group, pro-apoptotic markers cleaved caspase-3, cleaved caspase-9 and Bax significantly declined in KLK8-overexpression Mia-paca-2 and Panc-1 cells (**Figure 4E**).

KLK8 Accelerated Cell Growth and Inhibited Apoptosis *via* PI3K-Akt-mTOR Signaling Pathway in Pancreatic Cancer Cells

To gain an insight into the mechanisms by which KLK8 promoted PDAC progression, the gene expression in PDAC tissues with high expression of KLK8 and those with low expression of KLK8 was analyzed by gene set enrichment analysis (GSEA) based on the TCGA database. GSEA results showed that 14 enriched pathways were differentially expressed according to diverse KLK8 expression levels (**Figure 5A**, p<0.05). Notably, KLK8 was positively associated with PI3K-AKT-mTOR and Notch signaling pathways, both of which are known to play critical roles in cell proliferation and apoptosis (**Figures 5B, C**). We observed significantly enhanced phosphorylated PI3K, phosphorylated Akt and phosphorylated mTOR expression in Mia-paca-2 and Panc-1 cells overexpressed with KLK8. KLK8 overexpression also led to significant increases in phosphorylated 4EBP1 and phosphorylated S6P-p70S6K, two of the most distinctive downstream targets of mTOR, in pancreatic cancer cell lines (**Figure 5D**). In addition, KLK8 overexpression also led to significant increases in Notch-1 protein expression. C-myc and Cyclin D1, two downstream targets of Notch signaling, were increased in pancreatic cancer cells overexpressed with KLK8 (**Figure 5D**). These findings suggest that KLK8 overexpression activates PI3K-Akt-mTOR and Notch pathways (**Figure 5D**).

Next, we explored whether activation of PI3K-Akt-mTOR and Notch signaling pathways contributed to the pro-proliferation and anti-apoptotic functions of KLK8 in pancreatic cancer cells. Both CCK8 assay and colony formation assay showed that the pro-proliferation effects of KLK8 on pancreatic cells were counteracted by PI3K inhibitor LY294002 (75 μM), Akt inhibitor Deguelin (500 nM), and mTOR inhibitor Rapamycin (100 nM) (**Figure 6**). However, Notch inhibitor RO4929097 (10 μM) had no significant effect on KLK8-induced pro-proliferation in pancreatic

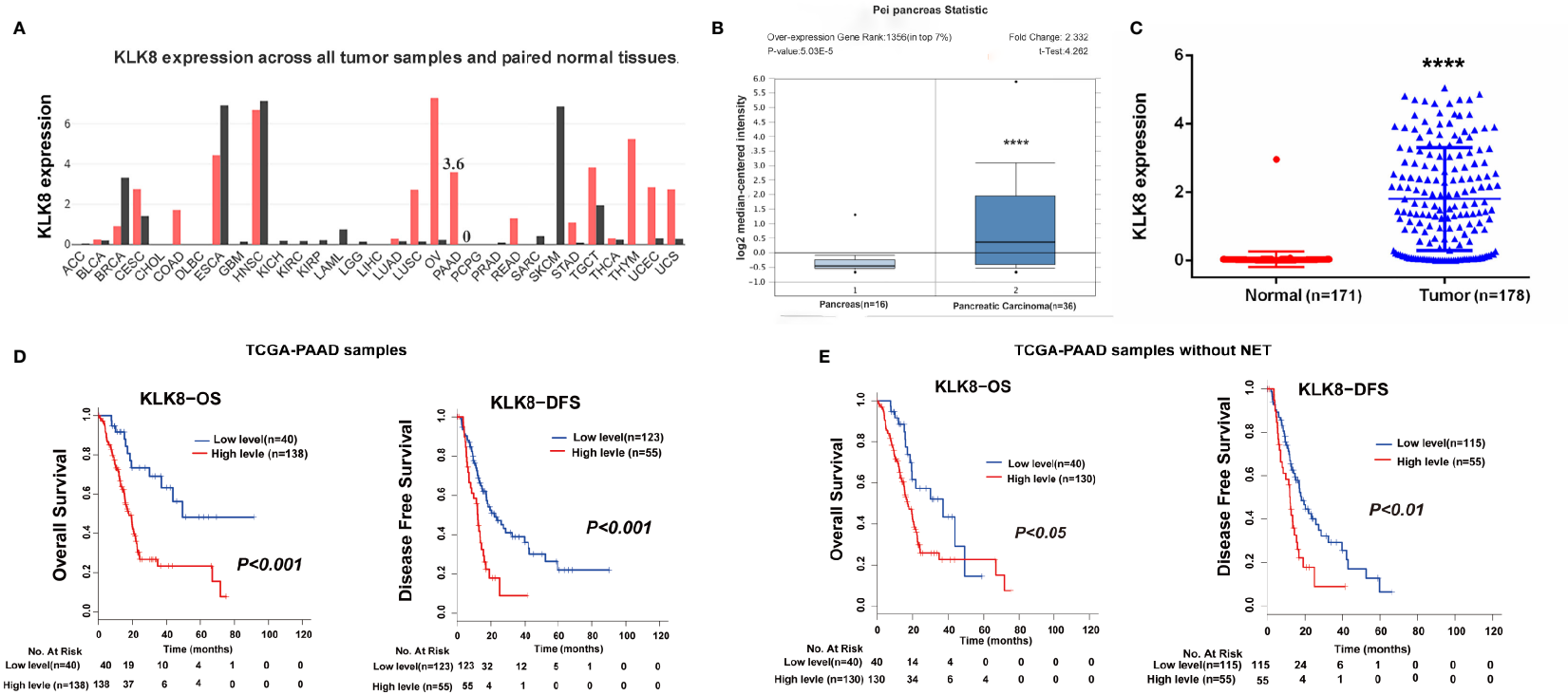

FIGURE 1 | KLK8 was associated with PDAC tumorigenesis and prognosis in the TCGA-PAAD cohort. **(A)** KLK8 expression in different cancers and their paired normal tissues in the GEPIA. The height of bar represents the median expression of certain tumor type or normal tissue. **(B)** KLK8 expression of normal specimens and pancreatic carcinoma from an independent pancreatic dataset in the Oncomine database. The expression fold-change was 2.332. **(C)** In the TCGA-PAAD cohort, KLK8 was more significantly expressed in cancer patients (n=178) than in normal controls (n =171). **(D)** The TCGA-PAAD database has 178 pancreatic cancer samples, including 8 pancreatic neuroendocrine tumor (NET) samples. Overall survival (OS, left panel) and Disease-free survival (DFS, right panel) were compared between patients with low and high KLK8 expression in the TCGA-PAAD cohort (n=178). **(E)** We deleted these 8 NETs, and the remaining cohort consisted of 170 primary PDACs samples (TCGA-PAAD cohort without NETs, n=170) were used for performing the survival analysis. OS (left panel) and DFS (right panel) was compared between patients with low and high KLK8 expression. ****p < 0.0001 *vs* normal.

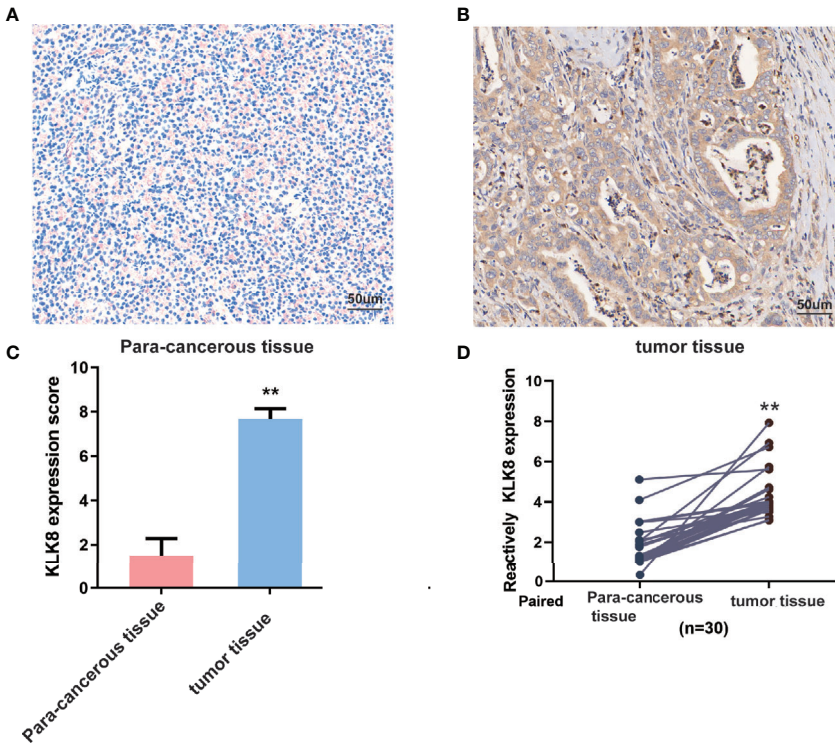

FIGURE 2 | KLK8 expression in pancreatic cancer tissues and para-cancerous pancreas. **(A, B)** Representative immunohistochemistry staining of KLK8 in pancreatic cancer tissues and para-cancerous pancreas (n=20). **(A)** showed negative KLK8 staining in para-cancerous pancreas. **(B)** showed strong positive KLK8 staining in PDAC tissues. **(C)** Quantified data of the score for KLK8 staining. **(D)** Quantitative real-time PCR detection of KLK8 mRNA expression in paired human PDAC tissue samples and para-cancerous pancreas (n=30). Data were presented as the mean ± SEM. **p < 0.01 *vs* Non-tumor tissue.

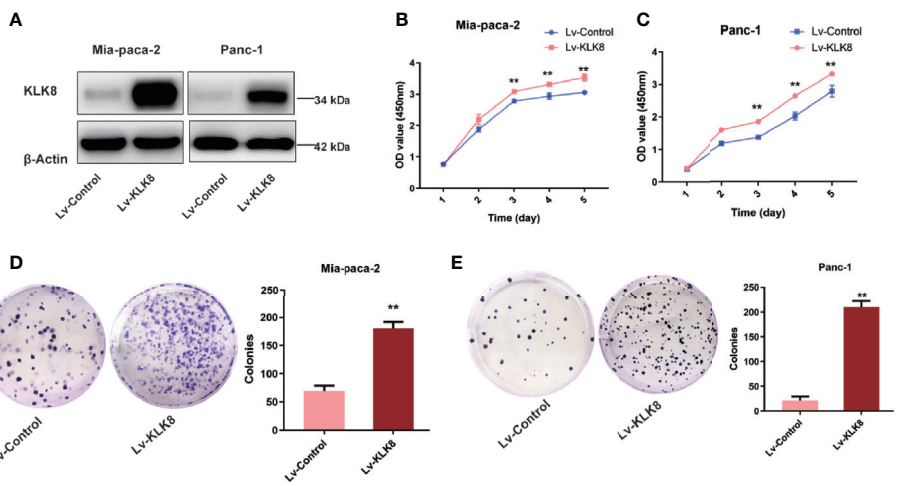

FIGURE 3 | KLK8 overexpression promoted the proliferation of PDAC cells. KLK8 overexpression was induced with recombinant Lentivirus infection (Lv-KLK8) in human pancreatic cancer cell lines Mia-paca-2 and Panc-1, and an empty adenovirus served as control (Lv-Control). **(A)** Mia-paca-2 and Panc-1 cells transfected with KLK8 overexpression vectors were validated at protein level by western blot analysis. **(B, C)** Cell proliferation was detected by CCK8 Assay in Mia-paca-2 **(B)** and Panc-1 **(C)** cells. **(D, E)** Colony formation was detected in Mia-paca-2 **(D)** and Panc-1 **(E)** cells. Data were presented as the mean ± SEM (n=3). **p < 0.01 *vs* Lv-control.

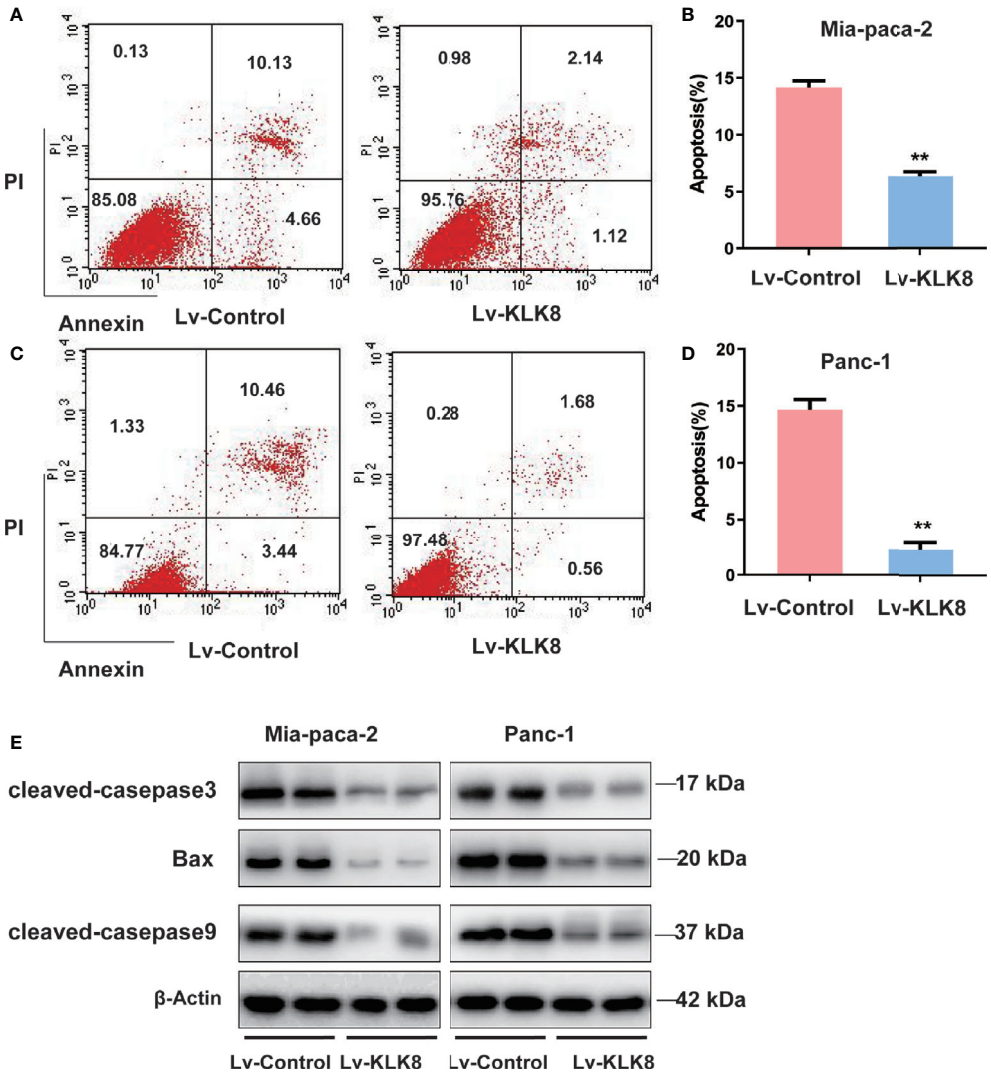

FIGURE 4 | KLK8 overexpression inhibited apoptosis of PDAC cells. KLK8 overexpression was induced with recombinant Lentivirus infection (Lv-KLK8) in human pancreatic cancer cell lines Mia-paca-2 **(A, B)** and Panc-1 **(C, D)**, and an empty adenovirus served as control (Lv-Control). Cell apoptosis was determined by Annexin V-FITC and PI double staining analysis performed by flow cytometry. Representative flow cytometry images were shown **(A, C)**. **(B, D)** demonstrated the quantified data of cell apoptosis. **(E)** pro-apoptotic markers cleaved caspase-3, cleaved caspase-9 and Bax assessed by western blot. Data are expressed as the mean ± SEM (n=3). **$p < 0.01$ *vs* Lv-control.

cells (**Figure 6**). We also measured the effects of the specific inhibitors on cell proliferation in Lv-control treated cells. As shown in **Supplemental Figures S2A, B**, it was found that only PI3K inhibitor LY294002 at the dose of 75 μM significantly inhibited cell proliferation in both Mia-paca-2 and Panc-1 cells treated with Lv-control. However, Akt inhibitor Deguelin (500 nM), mTOR inhibitor Rapamycin (100 nM), and Notch inhibitor RO4929097 (10 μM) had no significant effect on cell proliferation in Lv-control treated pancreatic cancer cells.

We then examined the effects of the specific inhibitors on cell apoptosis. As shown in **Figures 7**, **8**, PI3K inhibitor LY294002 at the dose of 75 μM significantly promoted cell apoptosis in both Mia-paca-2 and Panc-1 cells treated with Lv-control. In Lv-KLK8 treated pancreatic cancer cells, we found that LY294002 reversed the anti-apoptotic effect of KLK8 overexpression. Moreover, KLK8-overexpressed pancreatic cancer cells treated by LY294002 showed higher levels of apoptosis than Lv-control treated cells (**Figures 7A, B**, **8A**).

Both Deguelin (500 nM) and Rapamycin (100 nM) had no significant effect on cell apoptosis in Lv-control treated pancreatic cancer cells (**Figures 7C, D**, **8B**). In Lv-KLK8 treated pancreatic cancer cells, we found that Deguelin and Rapamycin reversed the anti-apoptotic effect of KLK8 overexpression (**Figures 7A, B**, **8A**). Moreover, KLK8-overexpressed pancreatic cancer cells treated by Deguelin showed higher levels of apoptosis than Lv-control treated Mia-paca-2 and Panc-1 cells (**Figures 7A, B**).

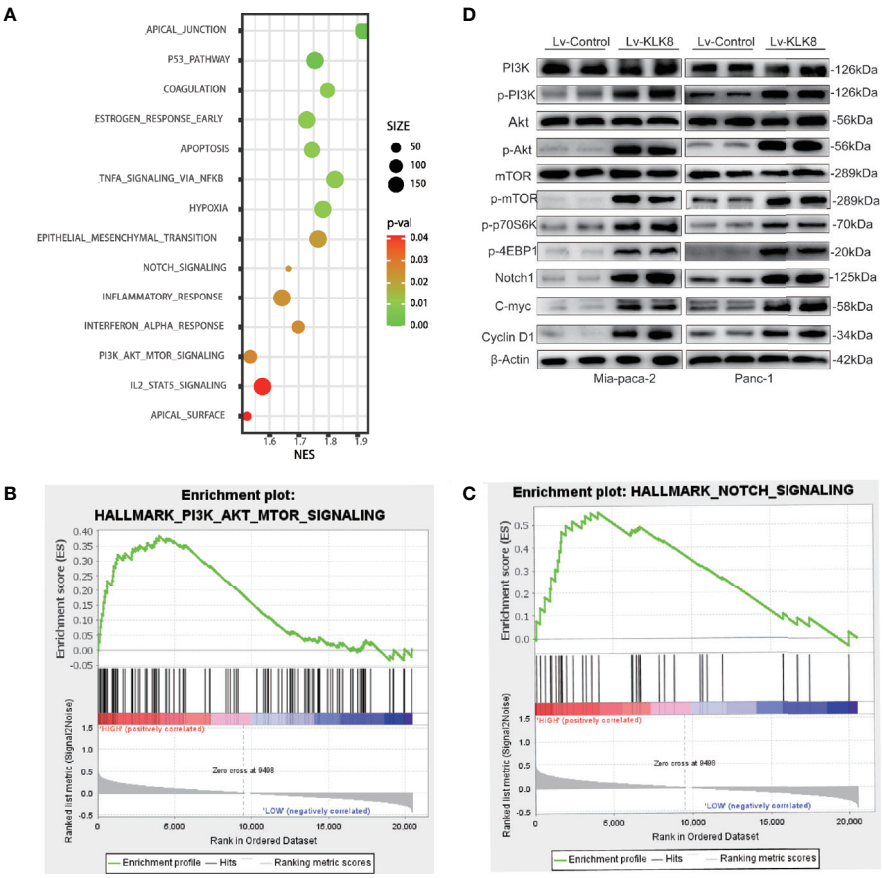

FIGURE 5 | Significantly-altered pathways were predicted in PDAC and verified in KLK8-overexpressed pancreatic cancer cells. **(A)** Gene sets enriched in the transcriptional profiles of tumors belonging to the top KLK8 high-expression group, compared with the bottom-expression group in the TCGA dataset. Shown are the NES (normalized enrichment score) values for each pathway using the Hallmark gene sets. The functional annotations of KLK8 positive and negative expression in PDAC was predicted. A nominal p value of <0.05 is considered statistically significant. **(B, C)** GSEA highlighted positive association of increased KLK8 expression levels with PI3K-Akt-mTOR **(B)** and Notch **(C)** signal pathways. **(D)** levels of key proteins in PI3K-AKT-mTOR and Notch signaling pathways were examined in KLK8-overexpressed Mia-paca-2 and Panc-1 cells using western blot. NES = normalized enrichment score. (n=3).

KLK8-overexpressed Panc-1 cells treated by Rapamycin also showed higher levels of apoptosis than Lv-control treated cells (**Figures 7A, B**).

However, Notch inhibitor RO4929097 (10 μM) had no significant effect on cell apoptosis in Lv-control treated pancreatic cancer cells (**Figures 7C, D**). In addition, RO4929097 had no significant effect on KLK8-induced anti-apoptotic function in pancreatic cells (**Figures 7A, B**, **8A**).

EGF Signaling Contributes to KLK8-Induced Activation of PI3K-Akt-mTOR Signaling Pathway and KLK8-Induced Pro-Proliferation and Anti-Apoptotic Effects in Pancreatic Cancer Cells

As a secreted serine protease, KLK8 is known to mediate the proteolytic process of pro-EGF into mature EGF (21).EGF is known to activate PI3K/Akt/mTOR pathway in a variety of cancers (22–25). Thus, we further investigated whether EGF signaling pathway contributes to KLK8-induced proliferation and anti-apoptotic effects in pancreatic cancer cells. As shown in **Figure 9A**, it was found that overexpression of KLK8 in Mia-paca-2 and Panc-1 cells significantly increased EGF levels in the culture media. Western blot results demonstrated that KLK8-induced activation of PI3K/Akt/mTOR pathway was profoundly blocked by AG1478, the specific EGF receptor (EGFR) antagonist (**Figure 9B**). In addition, it was found that EGFR antagonist AG1478 significantly attenuated the pro-proliferation and anti-apoptotic effects of KLK8 overexpression in both Mia-paca-2 and Panc-1 cells (**Figures 9C–H**). These findings indicate that EGF signaling contributes to KLK8-induced activation of PI3K-Akt-mTOR signaling pathway and KLK8-induced pro-proliferation and anti-apoptotic effects in pancreatic cancer cells (**Figure 10**).

DISCUSSION

Pancreatic cancer continues to have a poor 5-year survival rate despite its rising incidence (26, 27). By 2030, it is estimated to

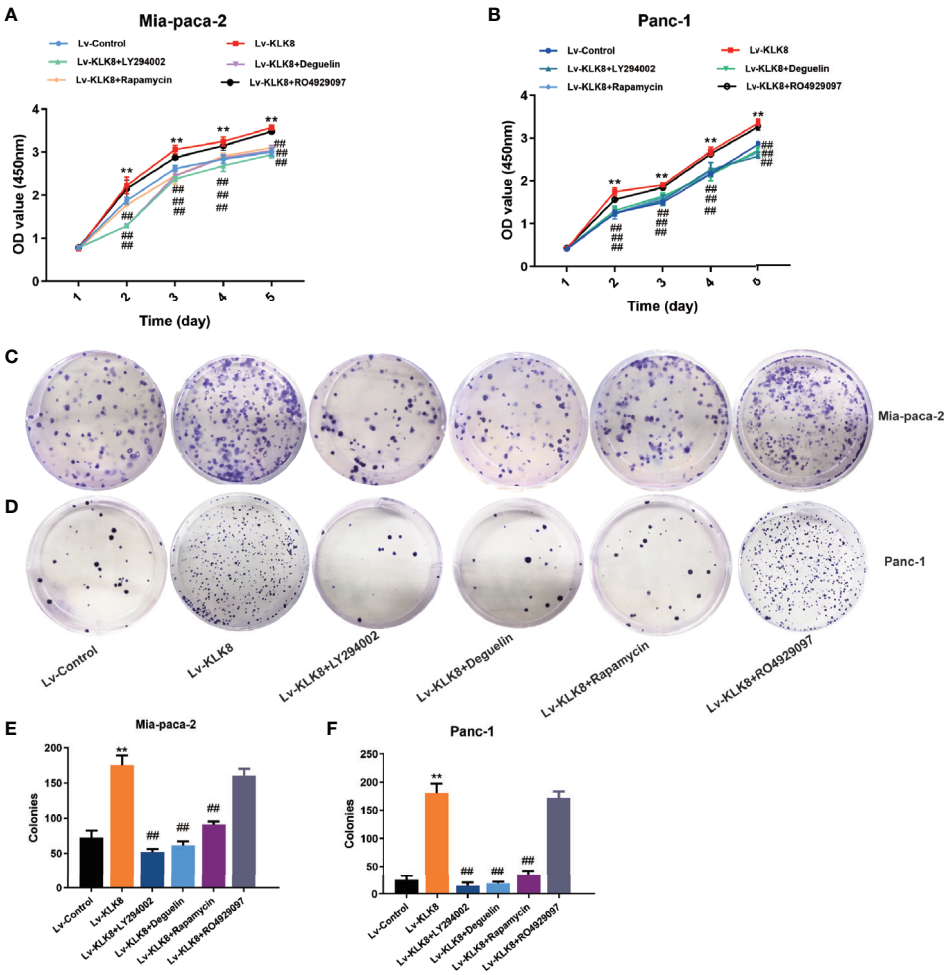

FIGURE 6 | KLK8 promoted pancreatic cancer cells proliferation *via the* activation of the PI3K-Akt-mTOR pathway. Mia-paca-2 and Panc-1 cells in Lv-KLK8 group were treated with PI3K inhibitor LY294002(75 μM), Akt inhibitor Deguelin (500 nM), mTOR inhibitor Rapamycin (100 nM) or Notch inhibitor RO4929097 (10 μM) in Mia-paca-2 and Panc-1 cells. **(A, B)** Cell proliferation was detected by CCK8 Assay in Mia-paca-2 **(A)** and Panc-1 **(B)** cells. **(C, D)** Colony formation was detected in Mia-paca-2 **(C)** and Panc-1 **(D)** cells. **(E, F)** demonstrated the quantified data of cell colonies. Data were presented as the mean ± SEM (n=3). $^{**}p < 0.01$ *vs* Lv-control; $p < 0.05$, $^{\#\#}p < 0.01$ *vs* Lv-KLK8.

become the second leading cause of cancer related deaths (5). Pancreatic resection is still the only curative intent therapy for PDAC patients. However, pancreatic resection is complex and carries with it the risk of major morbidity and mortality (28). Thus, there is a desperate need for investigating the pathogenesis and identifying molecular biomarkers of PDAC to facilitate early diagnosis, prognosis prediction, and the development of effective therapeutic strategies for PDAC patients.

KLK8, also known as neuropsin, is a member of human kallikrein-related peptidase (KLKs) family which has been related to malignant behavior at multiple stages of tumor progression, including proliferation, migration and angiogenesis (29, 30). Previous studies have found that abnormal expression of KLK8 was associated with several malignancies, including ovarian, cervical, gland and lung cancers (12, 31–34).However, the expression level and prognostic significance of KLK8 in PDAC are still unknown. In this study, we identified up-regulated KLK8 expression in pancreatic cancer compared with adjacent tissues through TCGA database, which was further confirmed by using clinical samples. Furthermore, we found that high KLK8 expression predicts poorer OS and DFS in pancreatic cancer patients. These results indicated that KLK8 could be a prognostic marker for PDAC. Similar to our findings, several studies have confirmed that the upregulation of KLK8 was related to poorer cancer prognosis. For example, KLK8 has been recognized as a poor prognostic marker for lung and breast cancer (15, 31). But in other tumors, such as ovarian cancer, the elevated expression of KLK8 is a favorable prognostic marker (35). These results suggest that KLK8 may play different roles in different cancers, and the aberrant expression of KLK8 may serve as a potential clinical biomarker for cancer diagnosis or prognosis.

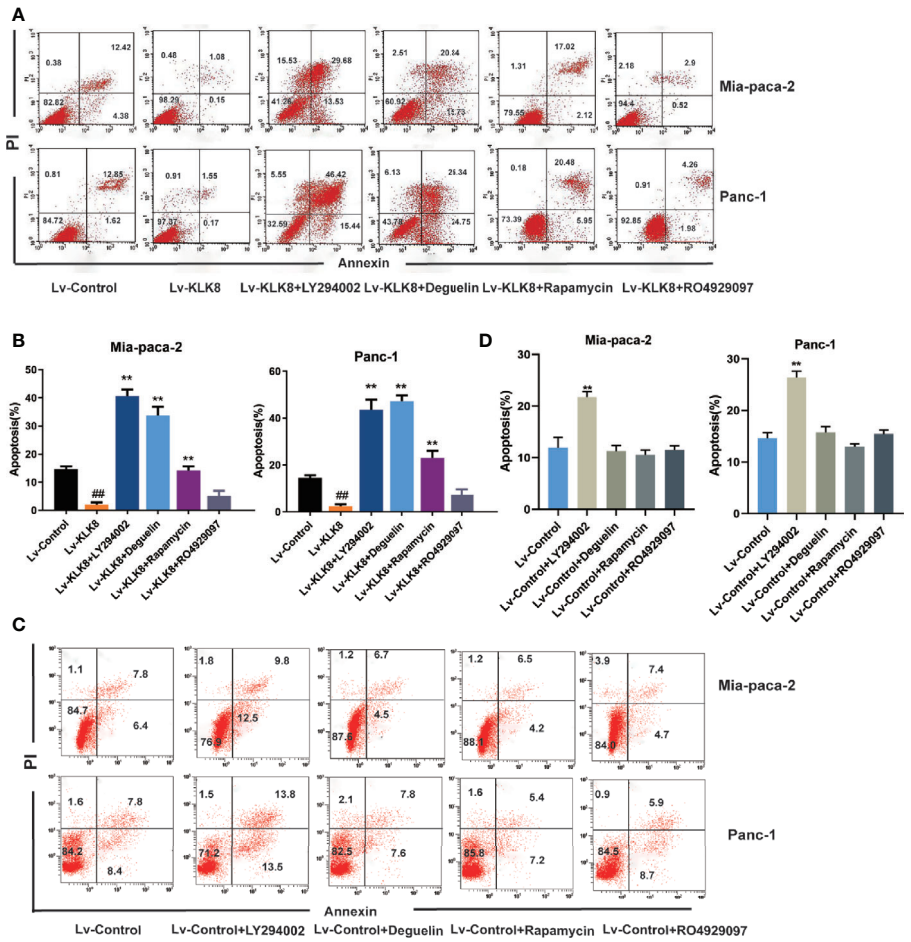

FIGURE 7 | KLK8 suppressed pancreatic cancer cells apoptosis through the activation of PI3K-Akt-mTOR pathway. Mia-paca-2 and Panc-1 cells in Lv-Control and Lv-KLK8 were treated with PI3K inhibitor LY294002 (75 μM), Akt inhibitor Deguelin(500 nM), mTOR inhibitor Rapamycin (100 nM) or Notch inhibitor RO4929097 (10 μM). Cell apoptosis was determined by Annexin V-FITC and PI double staining analysis performed by flow cytometry. Representative flow cytometry images were shown **(A, C)**. **(B, D)** demonstrated the quantified data of cell apoptosis. Data are presented as means ± SEM (n = 3). $^{**}p < 0.01$ *vs* Lv-control; $p < 0.05$, $^{\#\#}p < 0.01$ *vs* Lv-KLK8.

KLK family members have been implicated in the pathogenesis and progression of malignant tumor (36, 37). For example, overexpression of KLK7 is found to stimulate colon cancer cell proliferation both *in vivo* and *in vitro* (38). KLK13 enhances the invasiveness and motility of lung cancer *via* increasing laminin degradation and N-cadherin expression (39). KLK5 promotes metastatic dissemination of Oral squamous cell carcinoma(OSCC) by promoting loss of junctional integrity through cleavage of desmoglein 1 (40). KLK14 acts at the cleavage site of PAR-2 to induce ERK1/2 activation, thus promoting colon cancer proliferation (41). As for KLK8, it can facilitate colorectal cancer (CRC) cell proliferation, migration and invasion *in vitro* (9). In this study, by using two pancreatic cancer cell lines, we demonstrated for the first time that overexpression of KLK8 significantly inhibited PDAC cell apoptosis, meanwhile profoundly promoted PDAC cell proliferation. These data suggest that KLK8 may promote tumor growth and suppress tumor apoptosis, and may be a potential molecular target in therapy for pancreatic cancer.

Notably, our recent study has shown that KLK8 overexpression in coronary artery endothelial cells cleaves VE-cadherin, thus leading to endothelial cell damage and endothelial hyperpermeability (42). In contrast, the present study showed that KLK8 overexpression significantly increased cell viability of pancreatic cancer cells. Previous studies also demonstrate that KLK8 overexpression significantly increases cell viabilities in neonatal cardiomyocytes and cardiac fibroblasts (21, 42). Taken together, these findings suggest that KLK8 might modulate cell functions in a cell type-dependent manner.

The activity of KLK family members is typically controlled by itself or other proteases in the proteolytic activation cascade (43, 44). For example, KLK5 is thought to initiate the cascade reaction through auto-activation, and is activated by other proteases including the transmembrane serine protease matriptase and

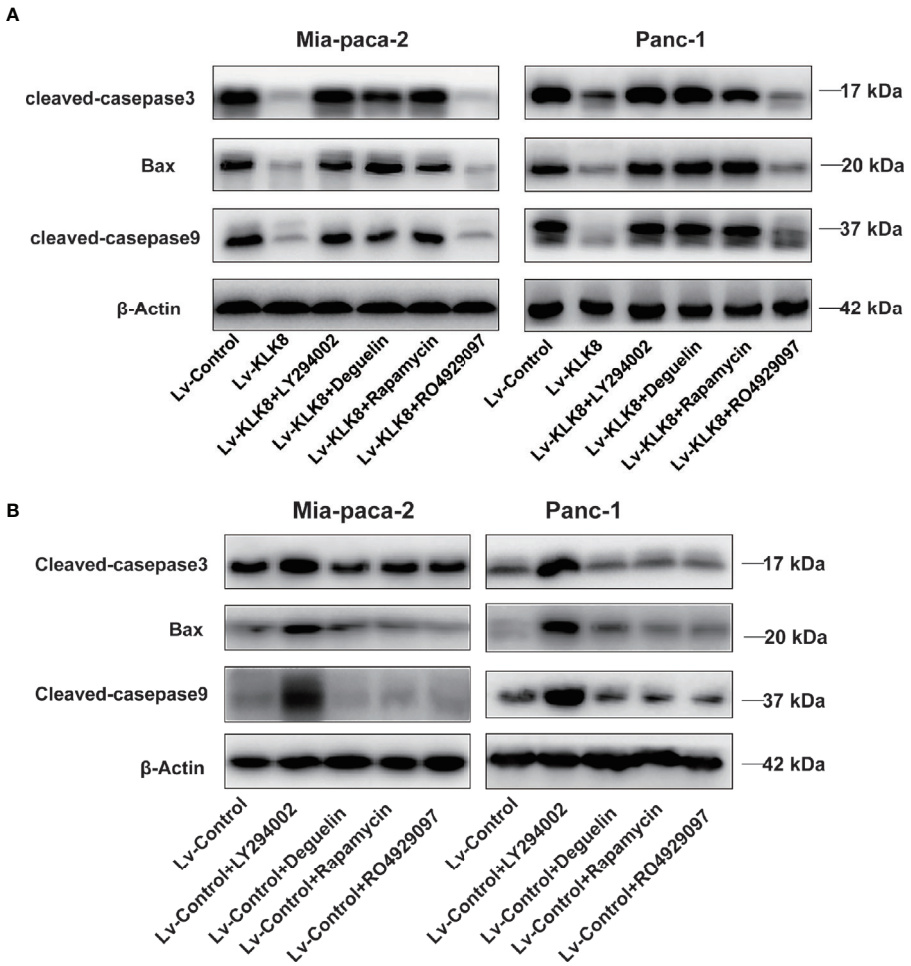

FIGURE 8 | KLK8 decreased protein levels of pro-apoptotic proteins through the activation of PI3K-Akt-mTOR pathway. Mia-paca-2 and Panc-1 cells in Lv-KLK8 **(A)** and Lv-Control **(B)** were treated with PI3K inhibitor LY294002(75 μM), Akt inhibitor Deguelin (500 nM), mTOR inhibitor Rapamycin (100 nM) or Notch inhibitor RO4929097 (10 μM). **(A, B)** protein levels of pro-apoptotic markers cleaved caspase-3, cleaved caspase-9 and Bax were assessed by western blot.

matrix metalloproteases (MMPs) (45). KLK5 activates other KLKs, such as KLK7 and KLK14 (46).Pro-KLK8 has been found to be activated by KLK5 and other proteases such as lysyl endopeptidase and MMP9 (47). The present study found that lentivirus-mediated KLK8 overexpression exhibited significant pro-proliferation and anti-apoptotic effects in pancreatic cancer cells, suggesting that the active form of KLK8 is increased after KLK8 overexpression. Whether KLK8 is activated through auto-activation or by other proteases merits further investigation.

Phosphatidylinositide 3 kinases (PI3Ks) and their downstream mediators Akt and mammalian target of rapamycin (mTOR) are well-known to regulate cell proliferation, apoptosis, homeostasis and metabolism (48). Previous studies have demonstrated that activation of PI3K/AKT/mTOR signaling pathway facilitates pancreatic cancer cell proliferation. In contrast, blockade of PI3K/AKT/mTOR signaling pathway promotes pancreatic cancer cell death (49–51). Overexpression of KLK8 has been found to induce Akt activation under Hypoxia/Reoxygenation (H/R) stimulation in neonatal rat cardiomyocytes (8). In the present study, GSEA analysis and western blot assay revealed that KLK8 overexpression resulted in the activation of PI3K/AKT/mTOR signaling pathway in pancreatic cancer cells. In addition, the pro-proliferation and anti-apoptotic functions of KLK8 were reversed by inhibitors targeting PI3K, Akt and mTOR. These findings suggest that elevated KLK8 may exert the pro-proliferation and anti-apoptotic effects in pancreatic cancer cells through activating PI3K-Akt-mTOR signaling pathway.

In addition, we noticed that PI3K inhibitor LY294002 at the dose of 75 μM significantly promoted cell apoptosis in both Mia-paca-2 and Panc-1 cells treated with Lv-control. KLK8-overexpressed pancreatic cancer cells treated by LY294002 showed higher levels of apoptosis than Lv-control treated cells. These findings suggest that PI3K inhibitor LY294002 may promote apoptosis independently from the signaling mediated by KLK8. As for Akt inhibitor Deguelin and mTOR inhibitor

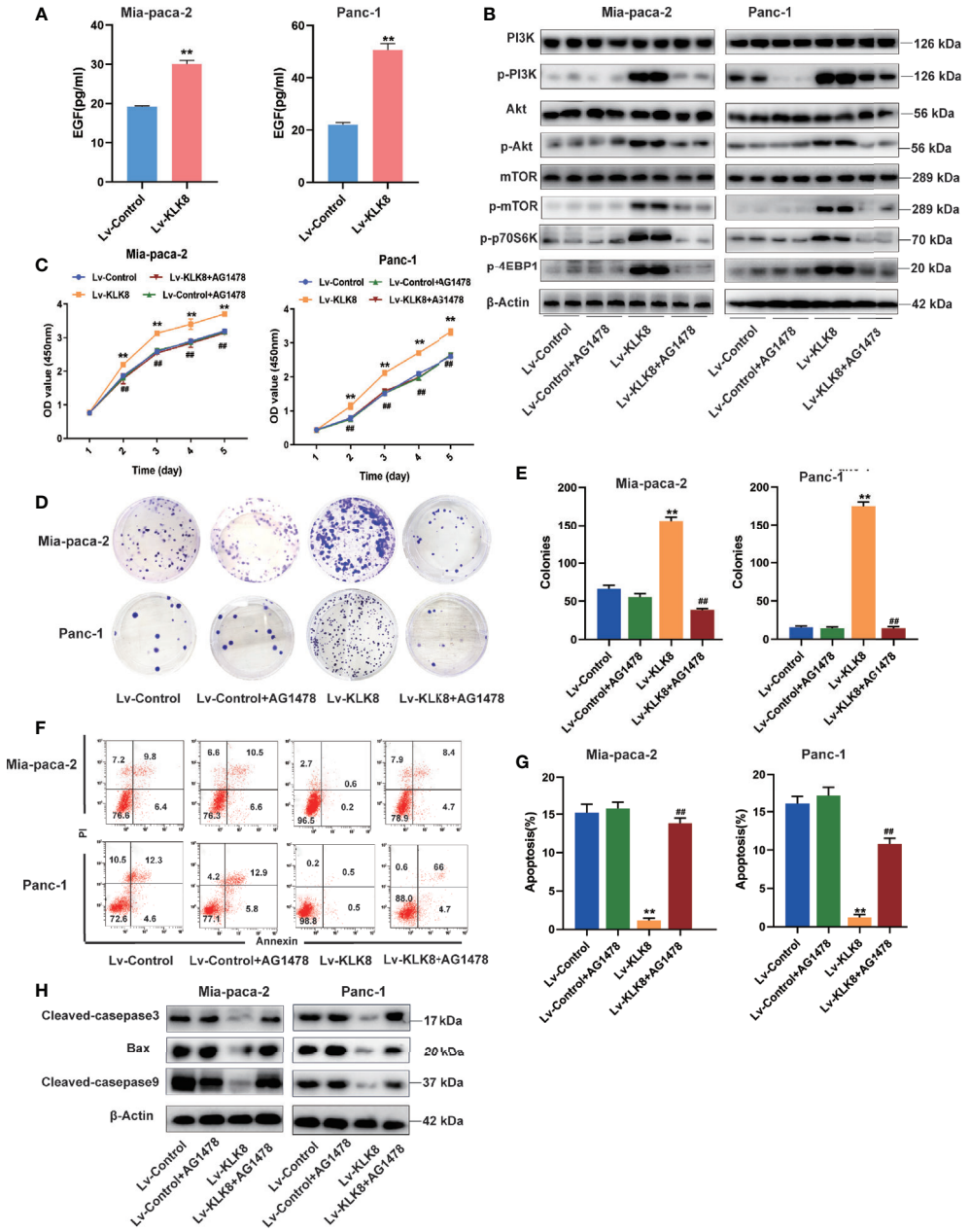

FIGURE 9 | EGF signaling contributes to KLK8-induced activation of PI3K-Akt-mTOR signaling pathway and KLK8-induced pro-proliferation and anti-apoptotic effects in pancreatic cancer cells. Mia-paca-2 and Panc-1 cells were treated with EGFR antagonist AG1478 (100 nM). Twenty-four hours later, cells were harvested for measuring cell protein level, proliferation and apoptosis. **(A)** Expression level of EGF in Mia-paca-2 and Panc-1 cells were evaluated by ELISA assay. **(B)** Levels of key proteins in PI3K-AKT-mTOR signaling pathways were examined in Mia-paca-2 and Panc-1 cells using western blot **(C)** Cell proliferation was detected by CCK8 assay in Mia-paca-2 and Panc-1 cells. **(D)** Colony formation was detected in Mia-paca-2 and Panc-1 cells. **(E)** Demonstrated the quantified data of cell colonies. **(F)** Cell apoptosis was determined by Annexin V-FITC and PI double staining analysis performed by flow cytometry. Representative flow cytometry images were shown. **(G)** Demonstrated the quantified data of cell apoptosis. **(H)** Pro-apoptotic markers cleaved caspase-3, cleaved caspase-9 and Bax assessed by western blot. Data were presented as the mean ± SEM (n=3). $^{**}p < 0.01$ *vs* Lv-control; $p < 0.05$, $^{\#\#}p < 0.01$ vs Lv-KLK8.

Rapamycin, both inhibitors had no significant effect on cell apoptosis in Lv-control treated pancreatic cancer cells. However, KLK8-overexpressed pancreatic cancer cells treated by Deguelin showed higher levels of apoptosis than Lv-control treated Mia-paca-2 and Panc-1 cells. KLK8-overexpressed Panc-1 cells treated by Rapamycin also showed higher levels of apoptosis than Lv-control treated cells. These findings suggest that Deguelin and Rapamycin may cause KLK8 to functionally

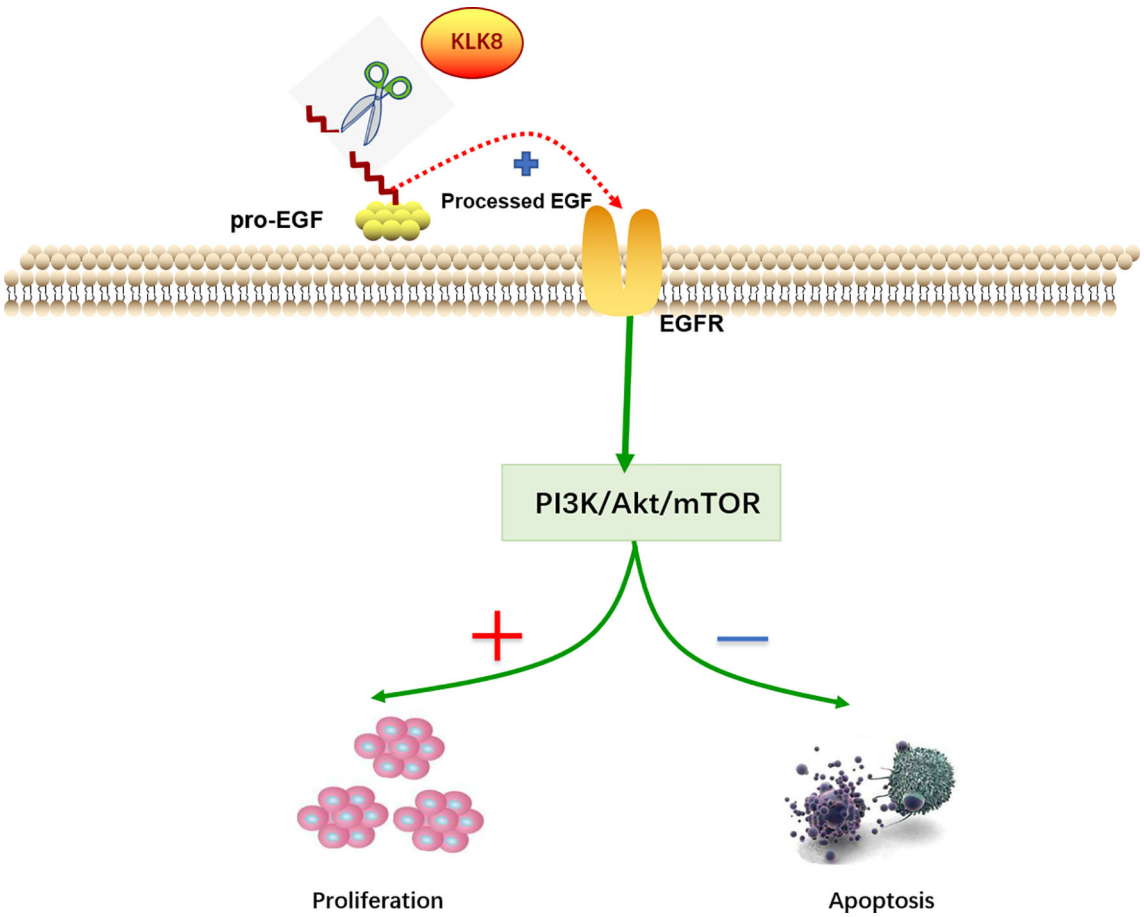

FIGURE 10 | Molecular mechanisms of KLK8-induced pro-proliferation and anti-apoptotic effects in pancreatic cancer cells. KLK8-mediated release of mature EGF contributes to the activation of PI3K-Akt-mTOR signaling pathway, thereby promoting the proliferation and inhibiting the apoptosis of pancreatic cancer cells.

switch from being anti-apoptotic to pro-apoptotic in pancreatic cancer cells, a possibility that merits further investigation.

As a secreted serine protease, KLK8 is known to cleave several membrane proteins including protease-activated receptors (PARs), neuregulin-1, synaptic adhesion molecule L1, Ephrin type-B receptor 2, and VE-cadherin (10, 21, 42, 44). In addition, the proteolytic process of pro-EGF into mature EGF can also be mediated by KLK8. EGF/EGFR signaling pathway has been known to promote the proliferation of pancreatic cancers *via* activating PI3K/AKT pathway. In this study, we found that EGF levels significantly increased in KLK8-overexpression Mia-paca-2 and Panc-1 cells. Inhibition of EGFR could block KLK8-induced activation of PI3K/Akt/mTOR pathway and attenuated the pro-proliferation and anti-apoptotic effects of KLK8 overexpression in both Mia-paca-2 and Panc-1 cells. Taken together, these results indicate that the effects of KLK8 on PI3K/Akt/mTOR activation, pancreatic cell proliferation and apoptosis might be, at least partly, due to KLK8-mediated release of mature EGF.

Notch signaling pathway also plays an important role in the occurrence and progression of pancreatic cancer (52–54). In the present study, GSEA analysis and western blot assay revealed that KLK8 overexpression resulted in the activation of Notch signaling pathway. However, Notch inhibitor didn't influence the KLK8-induced effects in pancreatic cancer cells. These results suggest that the pro-proliferation and anti-apoptotic functions of KLK8 may not be dependent on activation of Notch signaling pathway. Notably, our GSEA analysis data showed that KLK8 overexpression might also lead to the activation of EMT (epithelial-mesenchymal transition), glycolysis and KRAS signaling pathway, which have been implicated in the pathogenesis and progression of pancreatic cancers (17, 55–57). Whether these processes and the related signaling pathways contribute to the KLK8-induced pro-proliferation and anti-apoptotic effects in pancreatic cancers merits further investigation.

CONCLUSIONS

In summary, our findings indicate that KLK8 overexpression exerts pro-proliferation and anti-apoptotic functions in pancreatic cancer cells *via* EGF signaling-dependent activation of PI3K/Akt/mTOR pathway. Positive KLK8 staining is

associated with PDAC progression and predict poorer survival in patients, thus providing additional evidence for patient-tailored therapeutic strategies.

DATA AVAILABILITY STATEMENT

The original contributions presented in the study are included in the article/**Supplementary Material**. Further inquiries can be directed to the corresponding authors.

ETHICS STATEMENT

This study was approved by the Ethics Committee of Fudan University Shanghai Cancer Center. The patients/participants provided their written informed consent to participate in this study. Written informed consent was obtained from the individual(s) for the publication of any potentially identifiable images or data included in this article.

AUTHOR CONTRIBUTIONS

QH was responsible for conducting the study, under the supervision of XZ and PX and contributed to the experimental design. QH, TL and YL did the experiments and analyzed the data. QH and XS wrote the paper. All authors contributed to the article and approved the submitted version.

FUNDING

This work was supported by grants from National Natural Science Foundation of China (No. 81471852, No.31671213, No.31871156) and Shanghai Natural Science Foundation Program (20ZR1412900).

ACKNOWLEDGMENTS

We appreciated two expert pancreatic pathologists, Dr Cong Tan and Yupeng Zeng for data interpretation of the H&E and IHC staining images of clinical samples.

SUPPLEMENTARY MATERIAL

The Supplementary Material for this article can be found online at: https://www.frontiersin.org/articles/10.3389/fonc.2021.624837/full#supplementary-material

REFERENCES

1. Bray F, Ferlay J, Soerjomataram I, Siegel RL, Torre LA, Jemal A. Global Cancer Statistics 2018: GLOBOCAN Estimates of Incidence and Mortality Worldwide for 36 Cancers in 185 Countries. *CA Cancer J Clin* (2018) 68(6):394–424. doi: 10.3322/caac.21492
2. Siegel RL, Miller KD, Jemal A. Cancer Statistics, 2020. *CA Cancer J Clin* (2020) 70(1):7–30. doi: 10.3322/caac.21590
3. Sohal DPS, Willingham FF, Falconi M, Raphael KL, Crippa S. Pancreatic Adenocarcinoma: Improving Prevention and Survivorship. *Am Soc Clin Oncol Educ Book* (2017) 37:301–10. doi: 10.1200/EDBK_175222
4. Ilic M, Ilic I. Epidemiology of Pancreatic Cancer. *World J Gastroenterol* (2016) 22(44):9694–705. doi: 10.3748/wjg.v22.i44.9694
5. Rahib L, Smith BD, Aizenberg R, Rosenzweig AB, Fleshman JM, Matrisian LM. Projecting Cancer Incidence and Deaths to 2030: The Unexpected Burden of Thyroid, Liver, and Pancreas Cancers in the United States. *Cancer Res* (2014) 74(11):2913–21. doi: 10.1158/0008-5472.CAN-14-0155
6. Filippou PS, Karagiannis GS, Musrap N, Diamandis EP. Kallikrein-Related Peptidases (KLKs) and the Hallmarks of Cancer. *Crit Rev Clin Lab Sci* (2016) 53(4):277–91. doi: 10.3109/10408363.2016.1154643
7. Goldhardt O, Warnhoff I, Yakushev I, Begcevic I, Forstl H, Magdolen V, et al. Kallikrein-Related Peptidases 6 and 10 are Elevated in Cerebrospinal Fluid of Patients With Alzheimer's Disease and Associated With CSF-TAU and FDG-PET. *Transl Neurodegener* (2019) 8:25. doi: 10.1186/s40035-019-0168-6
8. Huang M, Du J, Wang Y, Ma S, Hu T, Shang J, et al. Tissue Kallikrein-Related Peptidase8 Protects Rat Heart Against Acute Ischemia Reperfusion Injury. *Int J Biol Macromol* (2019) 140:1126–33. doi: 10.1016/j.ijbiomac.2019.08.195
9. Liu X, Quan B, Tian Z, Xi H, Jia G, Wang H, et al. Elevated Expression of KLK8 Predicts Poor Prognosis in Colorectal Cancer. *BioMed Pharmacother* (2017) 88:595–602. doi: 10.1016/j.biopha.2017.01.112
10. Eissa A, Amodeo V, Smith CR, Diamandis EP. Kallikrein-Related Peptidase-8 (KLK8) Is an Active Serine Protease in Human Epidermis and Sweat and Is Involved in a Skin Barrier Proteolytic Cascade. *J Biol Chem* (2011) 286(1):687–706. doi: 10.1074/jbc.M110.125310
11. Shingaki K, Matsuzaki S, Taniguchi M, Kubo T, Fujiwara T, Kanazawa S, et al. Molecular Mechanism of Kallikrein-Related Peptidase 8/Neuropsin-Induced Hyperkeratosis in Inflamed Skin. *Br J Dermatol* (2010) 163(3):466–75. doi: 10.1111/j.1365-2133.2010.09864.x
12. Cane S, Bignotti E, Bellone S, Palmieri M, De las Casas L, Roman JJ, et al. The Novel Serine Protease Tumor-Associated Differentially Expressed Gene-14 (KLK8/Neuropsin/Ovasin) Is Highly Overexpressed in Cervical Cancer. *Am J Obstet Gynecol* (2004) 190(1):60–6. doi: 10.1016/j.ajog.2003.07.020
13. Darling MR, Tsai S, Jackson-Boeters L, Daley TD, Diamandis EP. Human Kallikrein 8 Expression in Salivary Gland Tumors. *Head Neck Pathol* (2008) 2:169–74. doi: 10.1007/s12105-008-0068-z
14. Magklara A, Scorilas A, Katsaros D, Massobrio M, Yousef GM, Fracchioli S, et al. The Human KLK8 (Neuropsin/Ovasin) Gene: Identification of Two Novel Splice Variants and its Prognostic Value in Ovarian Cancer. *Clin Cancer Res* (2001) 7:806–11 doi: 10.1016/j.ajog.2003.07.020
15. Planque C, Choi YH, Guyetant S, Heuze-Vourc'h N, Briollais L, Courty Y. Alternative Splicing Variant of Kallikrein-Related Peptidase 8 as an Independent Predictor of Unfavorable Prognosis in Lung Cancer. *Clin Chem* (2010) 56(6):987–97. doi: 10.1373/clinchem.2009.138917
16. Cheng Y, Zhu Y, Xu J, Yang M, Chen P, Xu W, et al. PKN2 in Colon Cancer Cells Inhibits M2 Phenotype Polarization of Tumor-Associated Macrophages *via* Regulating DUSP6-Erk1/2 Pathway. *Mol Cancer* (2018) 17(1):13. doi: 10.1186/s12943-017-0747-z
17. Nie S, Qian X, Shi M, Li H, Peng C, Ding X, et al. ALDH1A3 Accelerates Pancreatic Cancer Metastasis by Promoting Glucose Metabolism. *Front Oncol* (2020) 10:915. doi: 10.3389/fonc.2020.00915
18. Xie P, Zhang M, He S, Lu K, Chen Y, Xing G, et al. The Covalent Modifier Nedd8 Is Critical for the Activation of Smurf1 Ubiquitin Ligase in Tumorigenesis. *Nat Commun* (2014) 5(1):1–16. doi: 10.1038/ncomms4733
19. Strosberg JR, Cheema A, Weber JM, Ghayouri M, Han G, Hodul PJ, et al. Relapse-Free Survival in Patients With Nonmetastatic, Surgically Resected Pancreatic Neuroendocrine Tumors: An Analysis of the AJCC and ENETS Staging Classifications. *Ann Surg* (2012) 256(2):321–5. doi: 10.1097/SLA.0b013e31824e6108

20. Adamopoulos PG. Kallikrein-Related Peptidases and Associated microRNAs as Promising Prognostic Biomarkers in Gastrointestinal Malignancies. *Biol Chem* (2017) 399(8):821–36. doi: 10.1515/hsz-2017-0342
21. Cao B, Yu Q, Zhao W, Tang Z, Cong B, Du J, et al. Kallikrein-Related Peptidase 8 Is Expressed in Myocardium and Induces Cardiac Hypertrophy. *Sci Rep* (2016) 7:20024. doi: 10.1038/srep20024
22. Daveri E, Adamo AM, Alfine E, Zhu W, Oteiza PI. Hexameric Procyanidins Inhibit Colorectal Cancer Cell Growth Through Both Redox and non-Redox Regulation of the Epidermal Growth Factor Signaling Pathway. *Redox Biol* (2021) 38:101830. doi: 10.1016/j.redox.2020.101830
23. Zhang Y, Wang L, Zhang M, Jin M, Bai C, Wang X. Potential Mechanism of Interleukin-8 Production From Lung Cancer Cells: An Involvement of EGF-EGFR-PI3K-Akt-Erk Pathway. *J Cell Physiol* (2012) 227(1):35–43. doi: 10.1002/jcp.22722
24. Zhang C, Huang L, Xiong J, Xie L, Ying S, Jia Y, et al. Isoalantolactone Inhibits Pancreatic Cancer Proliferation by Regulation of PI3K and Wnt Signal Pathway. *PloS One* (2021) 16(3):e0247752. doi: 10.1371/journal.pone.0247752
25. Wang P, Zhao L, Gong S, Xiong S, Wang J, Zou D, et al. HIF1alpha/HIF2alpha-Sox2/Klf4 Promotes the Malignant Progression of Glioblastoma *via* the EGFR-PI3K/AKT Signalling Pathway With Positive Feedback Under Hypoxia. *Cell Death Dis* (2021) 12(4):312. doi: 10.1038/s41419-021-03598-8
26. Pereira SP, Oldfield L, Ney A, Hart PA, Keane MG, Pandol SJ, et al. Early Detection of Pancreatic Cancer. *Lancet Gastroenterol Hepatol* (2020) 5 (7):698–710. doi: 10.1016/S2468-1253(19)30416-9
27. Pishvaian MJ, Blais EM, Brody JR, Lyons E, DeArbeloa P, Hendifar A, et al. Overall Survival in Patients With Pancreatic Cancer Receiving Matched Therapies Following Molecular Profiling: A Retrospective Analysis of the Know Your Tumor Registry Trial. *Lancet Oncol* (2020) 21(4):508–18. doi: 10.1016/S1470-2045(20)30074-7
28. Sahni S, Krisp C, Molloy MP, Nahm C, Maloney S, Gillson J, et al. PSMD11, PTPRM and PTPRB as Novel Biomarkers of Pancreatic Cancer Progression. *Biochim Biophys Acta Gen Subj* (2020) 1864(11):129682. doi: 10.1016/j.bbagen.2020.129682
29. Adamopoulos PG, Tsiakanikas P, Scorilas A. Kallikrein-Related Peptidases and Associated microRNAs as Promising Prognostic Biomarkers in Gastrointestinal Malignancies. *Biol Chem* (2018) 399(8):821–36. doi: 10.1515/hsz-2017-0342
30. Schmitt M, Magdolen V, Yang F, Kiechle M, Bayani J, Yousef GM, et al. Emerging Clinical Importance of the Cancer Biomarkers Kallikrein-Related Peptidases (KLK) in Female and Male Reproductive Organ Malignancies. *Radiol Oncol* (2013) 47(4):319–29. doi: 10.2478/raon-2013-0053
31. Michaelidou K, Ardavanis A, Scorilas A. Clinical Relevance of the Deregulated Kallikrein-Related Peptidase 8 mRNA Expression in Breast Cancer: A Novel Independent Indicator of Disease-Free Survival. *Breast Cancer Res Treat* (2015) 152(2):323–36. doi: 10.1007/s10549-015-3470-8
32. Dimopoulos MA, Diamandis EP, Camp RL, Kowalski D, Markakis S, Scorilas A, et al. Expression and Prognostic Significance of Kallikrein-Related Peptidase 8 Protein Levels in Advanced Ovarian Cancer by Using Automated Quantitative Analysis. *Thromb Haemostasis* (2017) 101 (03):541–6. doi: 10.1160/TH08-01-0052
33. Ahmed N, Dorn J, Napieralski R, Drecoll E, Kotzsch M, Goettig P, et al. Clinical Relevance of Kallikrein-Related Peptidase 6 (KLK6) and 8(KLK8) mRNA Expression in Advanced Serous Ovarian Cancer. *Biol Chem* (2016) 397(12):1265–76. doi: 10.1515/hsz-2016-0177
34. Prezas P, Scorilas A, Yfanti C, Viktorov P, Agnanti N, Diamandis E, et al. The Role of Human Tissue Kallikreins 7 and 8 in Intracranial Malignancies. *Biol Chem* (2006) 387(12):1607–12. doi: 10.1515/BC.2006.200
35. Borgono CA. Human Kallikrein 8 Protein Is a Favorable Prognostic Marker in Ovarian Cancer. *Clin Cancer Res* (2006) 12(5):1487–93. doi: 10.1158/1078-0432.CCR-05-2106
36. Matin F, Jeet V, Srinivasan S, Cristino AS, Panchadsaram J, Clements JA, et al. MicroRNA-3162-5p-Mediated Crosstalk Between Kallikrein Family Members Including Prostate-Specific Antigen in Prostate Cancer. *Clin Chem* (2019) 65 (6):771–80. doi: 10.1373/clinchem.2018.295824
37. Kryza T, Bock N, Lovell S, Rockstroh A, Lehman ML, Lesner A, et al. The Molecular Function of Kallikrein-Related Peptidase 14 Demonstrates a Key Modulatory Role in Advanced Prostate Cancer. *Mol Oncol* (2020) 14(1):105–28. doi: 10.1002/1878-0261.12587
38. Walker F, Nicole P, Jallane A, Soosaipillai A, Mosbach V, Oikonomopoulou K, et al. Kallikrein-Related Peptidase 7 (KLK7) Is a Proliferative Factor That Is Aberrantly Expressed in Human Colon Cancer. *Biol Chem* (2014) 395 (9):1075–86. doi: 10.1515/hsz-2014-0142
39. Chou RH, Lin SC, Wen HC, Wu CW, Chang WS. Epigenetic Activation of Human Kallikrein 13 Enhances Malignancy of Lung Adenocarcinoma by Promoting N-Cadherin Expression and Laminin Degradation. *Biochem Biophys Res Commun* (2011) 409(3):442–7. doi: 10.1016/j.bbrc.2011.05.022
40. Jiang R, Shi Z, Johnson JJ, Liu Y, Stack MS. Kallikrein-5 Promotes Cleavage of Desmoglein-1 and Loss of Cell-Cell Cohesion in Oral Squamous Cell Carcinoma. *J Biol Chem* (2011) 286(11):9127–35. doi: 10.1074/jbc.M110.191361
41. Gratio V, Loriot C, Virca GD, Oikonomopoulou K, Walker F, Diamandis EP, et al. Kallikrein-Related Peptidase 14 Acts on Proteinase-Activated Receptor 2 to Induce Signaling Pathway in Colon Cancer Cells. *Am J Pathol* (2011) 179 (5):2625–36. doi: 10.1016/j.ajpath.2011.07.016
42. Du J-K, Yu Q, Liu Y-J, Du S-F, Huang L-Y, Xu D-H, et al. A Novel Role of Kallikrein-Related Peptidase 8 in the Pathogenesis of Diabetic Cardiac Fibrosis. *Theranostics* (2021) 11(9):4207–31. doi: 10.7150/thno.48530
43. Yu Y. Putative Kallikrein Substrates and Their (Patho) Biological Functions. *Biol Chem* (2014) 395(9):931–43. doi: 10.1515/hsz-2014-0129
44. Kishibe M. Physiological and Pathological Roles of Kallikrein-Related Peptidases in the Epidermis. *J Dermatol Sci* (2019) 95(2):50–5. doi: 10.1016/j.jdermsci.2019.06.007
45. Eissa A, Diamandis EP. Human Tissue Kallikreins as Promiscuous Modulators of Homeostatic Skin Barrier Functions. *Biol Chem* (2008) 389 (6):669–80. doi: 10.1515/BC.2008.079
46. Egelrud T, Brattsand M. Purification, Molecular Cloning, and Expression of a Human Stratum Corneum Trypsin-Like Serine Protease With Possible Function in Desquamation. *J Biol Chem* (1999) 274(42):30033–40. doi: 10.1074/jbc.274.42.30033
47. Shiosaka S, Ishikawa Y. Neuropsin—A Possible Modulator of Synaptic Plasticity. *J Chem Neuroanat* (2011) 42:24–9. doi: 10.1016/j.jchemneu.2011.05.014
48. Tsuji-Tamura K, Sato M, Fujita M, Tamura M. The Role of PI3K/Akt/mTOR Signaling in Dose-Dependent Biphasic Effects of Glycine on Vascular Development. *Biochem Biophys Res Commun* (2020) 529:596–602. doi: 10.1016/j.bbrc.2020.06.085
49. Zhuang H, Zhang C, Hou B. FAM83H Overexpression Predicts Worse Prognosis and Correlates With Less CD8(+) T Cells Infiltration and Ras-PI3K-Akt-mTOR Signaling Pathway in Pancreatic Cancer. *Clin Transl Oncol* (2020) 22(12):2244–52. doi: 10.1007/s12094-020-02365-z
50. Lan CY, Chen SY, Kuo CW, Lu CC, Yen GC. Quercetin Facilitates Cell Death and Chemosensitivity Through RAGE/PI3K/AKT/mTOR Axis in Human Pancreatic Cancer Cells. *J Food Drug Anal* (2019) 27(4):887–96. doi: 10.1016/j.jfda.2019.07.001
51. Yu JS, Cui W. Proliferation, Survival and Metabolism: The Role of PI3K/AKT/mTOR Signalling in Pluripotency and Cell Fate Determination. *Development* (2016) 143(17):3050–60. doi: 10.1242/dev.137075
52. Rice MA, Hsu EC, Aslan M, Ghoochani A, Su A, Stoyanova T. Loss of Notch1 Activity Inhibits Prostate Cancer Growth and Metastasis and Sensitizes Prostate Cancer Cells to Antiandrogen Therapies. *Mol Cancer Ther* (2019) 18(7):1230–42. doi: 10.1158/1535-7163.MCT-18-0804
53. Kong L, Liu P, Zheng M, Wang Z, Gao Y, Liang K, et al. The miR-1224-5p/ELF3 Axis Regulates Malignant Behaviors of Pancreatic Cancer *via* PI3K/AKT/Notch Signaling Pathways. *Onco Targets Ther* (2020) 13:3449–66. doi: 10.2147/OTT.S248507
54. Bao B, Wang Z, Ali S, Kong D, Li Y, Ahmad A, et al. Notch-1 Induces Epithelial-Mesenchymal Transition Consistent With Cancer Stem Cell Phenotype in Pancreatic Cancer Cells. *Cancer Lett* (2011) 307(1):26–36. doi: 10.1016/j.canlet.2011.03.012
55. Hou P, Kapoor A, Zhang Q, Li J, Wu CJ, Li J, et al. Tumor Microenvironment Remodeling Enables Bypass of Oncogenic KRAS Dependency in Pancreatic Cancer. *Cancer Discov* (2020) 10(7):1058–77. doi: 10.1158/2159-8290.CD-19-0597

56. Wang W, Chen H, Gao W, Wang S, Wu K, Lu C, et al. Girdin Interaction With Vimentin Induces EMT and Promotes the Growth and Metastasis of Pancreatic Ductal Adenocarcinoma. *Oncol Rep* (2020) 44(2):637–49. doi: 10.3892/or.2020.7615
57. Recouvreux MV, Moldenhauer MR, Galenkamp KMO, Jung M, James B, Zhang Y, et al. Glutamine Depletion Regulates Slug to Promote EMT and Metastasis in Pancreatic Cancer. *J Exp Med* (2020) 217(9):e20200388. doi: 10.1084/jem.20200388

Conflict of Interest: The authors declare that the research was conducted in the absence of any commercial or financial relationships that could be construed as a potential conflict of interest.

Publisher's Note: All claims expressed in this article are solely those of the authors and do not necessarily represent those of their affiliated organizations, or those of the publisher, the editors and the reviewers. Any product that may be evaluated in this article, or claim that may be made by its manufacturer, is not guaranteed or endorsed by the publisher.

frontiers in Oncology

ORIGINAL RESEARCH
published: 16 August 2021
doi: 10.3389/fonc.2021.657723

CISD2 Promotes Resistance to Sorafenib-Induced Ferroptosis by Regulating Autophagy in Hepatocellular Carcinoma

Bowen Li, Shibo Wei, Liang Yang, Xueqiang Peng, Yingbo Ma, Bo Wu, Qing Fan, Shuo Yang, Xinyu Li, Hongyuan Jin, Shilei Tang, Mingyao Huang, Hangyu Li and Jingang Liu**

Department of General Surgery, The Fourth Affiliated Hospital of China Medical University, Shenyang, China

OPEN ACCESS

Edited by:
Alena Malyukova, Karolinska Institutet (KI), Sweden

Reviewed by:
Sonam Dhamija, Council of Scientific and Industrial Research (CSIR), India
Alessandro Granito, University of Bologna, Italy

***Correspondence:**
Jingang Liu
liujg1347@126.com
Hangyu Li
sj_li_hangyu@sina.com

Specialty section:
This article was submitted to Cancer Molecular Targets and Therapeutics, a section of the journal Frontiers in Oncology

Received: *23 January 2021*
Accepted: *15 July 2021*
Published: *16 August 2021*

Citation:
Li B, Wei S, Yang L, Peng X, Ma Y, Wu B, Fan Q, Yang S, Li X, Jin H, Tang S, Huang M, Li H and Liu J (2021) CISD2 Promotes Resistance to Sorafenib-Induced Ferroptosis by Regulating Autophagy in Hepatocellular Carcinoma. Front. Oncol. 11:657723. doi: 10.3389/fonc.2021.657723

Purpose: Sorafenib is a multi-kinase inhibitor that is used as a standard treatment for advanced hepatocellular carcinoma (HCC). However, the mechanism of sorafenib resistance in HCC is still unclear. It has been shown that CISD2 expression is related to the progression and poor prognosis of HCC. Here, we show a new role for CISD2 in sorafenib resistance in HCC.

Methods: Bioinformatic analysis was used to detect the expression of negative regulatory genes of ferroptosis in sorafenib-resistant samples. The concentration gradient method was used to establish sorafenib-resistant HCC cells. Western blot was used to detect the protein expression of CISD2, LC3, ERK, PI3K, AKT, mTOR, and Beclin1 in HCC samples. Quantitative real-time PCR (qPCR) was used to detect gene expression. CISD2 shRNA and Beclin1 shRNA were transfected to knock down the expression of the corresponding genes. Cell viability was detected by a CCK-8 assay. ROS were detected by DCFH-DA staining, and MDA and GSH were detected with a Lipid Peroxidation MDA Assay Kit and Micro Reduced Glutathione (GSH) Assay Kit, respectively. Flow cytometry was used to detect apoptosis and the levels of ROS and iron ions.

Results: CISD2 was highly expressed in HCC cells compared with normal cells and was associated with poor prognosis in patients. Knockdown of CISD2 promoted a decrease in the viability of drug-resistant HCC cells. CISD2 knockdown promoted sorafenib-induced ferroptosis in resistant HCC cells. The levels of ROS, MDA, and iron ions increased, but the change in GSH was not obvious. Knockdown of CISD2 promoted uncontrolled autophagy in resistant HCC cells. Inhibition of autophagy attenuated CISD2 knockdown-induced ferroptosis. The autophagy promoted by CISD2 knockdown was related to Beclin1. When CISD2 and Beclin1 were inhibited, the effect on ferroptosis was correspondingly weakened.

Conclusion: Inhibition of CISD2 promoted sorafenib-induced ferroptosis in resistant cells, and this process promoted excessive iron ion accumulation through autophagy,

leading to ferroptosis. The combination of CISD2 inhibition and sorafenib treatment is an effective therapeutic strategy for resistant HCC.

Keywords: hepatocellular carcinoma, sorafenib resistance, ferroptosis, CISD2, autophagy, Beclin1

INTRODUCTION

Hepatocellular carcinoma (HCC) is the second leading cause of cancer death worldwide (1). Due to the late presentation of symptoms, fewer than 20% of patients presenting with HCC are candidates for potentially curative treatment, such as surgical resection, ablation, or radioactive embolization (2). Once HCC becomes advanced, there are few systemic therapeutic options for its management.

Sorafenib is the only targeted drug for the treatment of advanced HCC approved by the US Food and Drug Administration, but its efficacy as a monotherapy remains unsatisfactory, with a median overall prolonged survival benefit of only 3 months compared to placebo (3). Furthermore, primary and acquired drug resistance makes the number of HCC patients with complete response to sorafenib very low (4). In view of the emerging crisis of sorafenib resistance in HCC, further research to develop a new therapeutic strategy is urgently needed.

The redox status of cancer cells usually differs from that of normal cells (5), and the increases in antioxidant factors induce the initiation and progression of HCC (6). Ferroptosis, defined as a new programmed oxidative cell death discovered in recent years, is characterized increased ROS production *via* the Fenton reaction and the accumulation of lipid peroxidation products (7). Sorafenib can induce HCC cell ferroptosis resulting from inhibition of system X_C^- followed by cellular GSH depletion (8, 9), and the induction of ferroptosis is a promising strategy to combat apoptosis-resistant HCC (10). It was previously reported that capecitabine (an anti-metabolic fluorouracil deoxynucleoside carbamate drug) can induce ferroptosis in metastatic breast cancer (11), and relatedly, capecitabine was reported to be safe and effective in HCC patients experiencing sorafenib failure (12–14).

NEET proteins are conserved proteins that retain the CDGSH iron sulfur domain (CISD) and are encoded by three genes: CISD1 encodes mitoNEET (mNT), CISD2 encodes nutrient-deprivation autophagy factor-1 (NAF-1), and CISD3 encodes MiNT (Miner2) (15). These recently discovered proteins play key roles in many processes involved in iron, iron-sulfur, and reactive oxygen homoeostasis and autophagy regulation in cells (16). The Fe-S cluster is redox active, and its biochemical properties are regulated by its redox state (17, 18). Moreover, CISD2 was shown to mediate longevity (19, 20) and to promote the development of breast cancer, cervical cancer, lung adenocarcinoma, pancreatic cancer, and prostate cancer (21–25). However, CISD2 is infrequently reported in research of liver cancer. CISD2 is a regulator of autophagy initiation under conditions of nutrient deprivation (26). Nevertheless, it is not clear whether CISD2 regulates autophagy in drug-resistant cells. More biochemical studies are needed to describe precisely how CISD2 can regulate autophagy pathways and what effects it produces in cancers.

In this study, we aimed to explore the role of CISD2 in ferroptosis in sorafenib-resistant HCC and to investigate how it affects ferroptosis by regulating autophagy. Our research provides a new strategy for targeted therapy of sorafenib-resistant HCC.

MATERIALS AND METHODS

Cell Culture and Reagents

A normal hepatocyte line (L02) and HCC cell lines (Hep3B, HepG2, Huh7, and PLC) were purchased from Shanghai Institute of Cell Bank (Shanghai, China). Huh7 cells were cultured in Dulbecco's modified Eagle's medium (Gibco, Grand Island, USA) supplemented with $NaHCO_3$ (1.5 g/L). HepG2 and PLC cells were grown in minimum essential medium (Gibco, Grand Island, USA) with $NaHCO_3$ (1.5 g/L) and sodium pyruvate. Cells were cultured with 10% fetal bovine serum (Pansera ES, Pan biotech GmbH, Germany), penicillin (U/ml), and streptomycin (0.1 mg/ml) at 37°C in a humidified atmosphere containing 5% CO_2. Cells were exposed to sorafenib (Solarbio, Beijing, China) for the indicated time and at the indicated concentration. Drug-resistant cell lines were established by stepwise selection of cells cultured in growth media with increasing concentrations of the drug over a period of 6 months. Erastin, staurosporine (STS), ferrostatin-1 (Fer-1), deferoxamine (DFO), ZVAD-FMK, and necrosulfonamide (NSA) were purchased from MedChemExpress (New Jersey, USA). Sorafenib and pioglitazone (Pg) were purchased from Solarbio Biotechnology Company (Beijing, China).

HCC Patients

Human HCC tissues and adjacent normal tissues (ANTs) were collected from patients with hepatocellular carcinoma at the Fourth Affiliated Hospital of China Medical University and Liaoning Cancer Hospital, and all patients were diagnosed by pathological examination. Sample collection was approved by the research ethics committee of the Fourth Affiliated Hospital of China Medical University. Each patient provided informed consent to participate in the study. The patients had not undergone preoperative chemotherapy or radiotherapy. All collected samples were immediately frozen in liquid nitrogen and stored until subsequent analysis.

Bioinformatics Technology

The expression levels of genes in sorafenib-resistant HCC samples from the Gene Expression Omnibus (GEO) database were obtained. Differential gene expression analysis was

performed with R-based open-source software. Kaplan–Meier survival analysis was performed on patients stratified by CISD2 expression (high expression *vs* low expression) with the R "ggplot2" package. For Gene set enrichment analysis (GSEA), the RNA sequencing data for 374 samples of HCC and 50 samples of normal tissues were extracted from the Cancer Genome Atlas (TCGA) program database. In brief, the 374 patients were divided into the CISD2 high expression group and the CISD2 low expression group. We used GSEA v2.0 software for GSEA (http://software.broadinstitute.org/gsea/index.jsp). Statistical significance was evaluated by comparing the enrichment fractions from the enrichment results to obtain P values.

Cell Viability Assays

Cell viability was assessed using a cell counting kit-8 (CCK-8) (Yeasen, Shanghai, China). Cells were seeded in 96-well plates at 5×10^3 cells/well and transfected with CISD2 shRNA, Beclin1 shRNA, or the corresponding negative control shRNA (Ctrl shRNA) for 48 h. Then added with different concentrations of sorafenib or indicated concentration of erastin, STS, Fer-1, DFO, ZVAD-FMK, NSA cultured for 24 h at 37°C. After that, CCK-8 reagent was added and incubated for 2 h at 37°C. Thereafter, the absorbance was measured at 490 nm using a SpectraMax M2 microplate reader (Molecular Devices, Sunnyvale, CA, USA).

Apoptosis Analysis

Apoptosis was detected using an FITC Annexin V/Dead Cell Apoptosis Kit (Thermo Fisher Scientific, Waltham, MA, USA). After transfected with CISD2 shRNA or Ctrl shRNA for 48 h, cells were treated with sorafenib (10 μmol) for 24 h and washed with PBS three times. Determine the cell density and dilute in 1× annexin-binding buffer to 1×10^6 cells/ml, and 5 μl of FITC annexin V, 1 μl of 1× propidium iodide (PI, 100 μg/ml) were added to the suspension for 15 min in the dark. Finally, 400 μl of 1× binding buffer was added to each tube. Flow cytometry (BD LSRFortessa, Becton Dickinson, USA) was used to detect apoptosis in each group.

Cell Proliferation Assay

Cell proliferation was evaluated by 5-ethynyl-2'-deoxyuridine (EdU) incorporation or colony formation assays. The EdU incorporation assay was performed with a Cell-Light™ EdU Apollo567 *In Vitro* Kit (RIBOBIO, Guangzhou, China). Cells in the logarithmic growth phase were seeded into 96-well plates with 1×10^5 cells/well and cultured for 24 h. After 48 h of transfection with CISD2 shRNA and the corresponding Ctrl shRNA, cells were treated with sorafenib and cultured for 24 h. After that, 50 μmol/L EdU-containing medium was prepared, and the cells were incubated for 2 h. Then, the cells were fixed with 4% paraformaldehyde for 30 min room temperature and added 100 μl 0.5% TritonX-100. After that, cells were stained with 1×Apollo® solution for 30 min room temperature and kept in the dark. Finally, DNA was stained with 1× Hoechst33342 and incubated at room temperature for 30 min. Images were acquired under an inverted fluorescence microscope. For the colony formation assay, 1×10^3 cells were seeded per well. After 24 h, the HCC cells were treated with different concentrations. After another 2 weeks, the cells were washed with PBS and stained with 0.1% Crystal Violet Stain Solution (Yeasen, Shanghai, China).

Quantitative Real-Time Polymerase Chain Reaction (qPCR)

After transfection with CISD2 shRNA, Beclin1 shRNA, or the corresponding Ctrl shRNA for 48 h, total RNA was extracted with TRIzol (Invitrogen, Thermo Fisher Scientific, USA). Then, a 1/5 volume of chloroform was added for extraction and centrifugation to obtain the upper clear liquid phase, and the same volume of isopropanol was then added and stored at −20°C overnight. cDNA was obtained by reverse transcription with a PrimeScript™ RT Reagent Kit (Promega, USA) in the Promega GoScript reverse transcription system (A5000). Real-time PCR analysis was performed using Promega GoTaq® qPCR Master Mix in an ABI 7500 Fast Real-Time PCR System (Applied Biosystems, USA). With 18S rRNA as the internal reference, qPCR was carried out in a 20 μl reaction system. The $2^{-\Delta\Delta Ct}$ method was used to analyze the data. Three complex wells were set up for all reactions, and the experiment was repeated three times.

Western Blot Assay

Cells were transfected with CISD2 shRNA, Beclin1 shRNA, or the corresponding Ctrl shRNA for 48 h. Then, cells were treated with sorafenib (10 μmol) for 24 h. RIPA buffer was used to extract the lysate from hepatocellular carcinoma cells, and the protein concentration was determined with a BCA protein assay kit (Beyotime, Shanghai). Then, buffer was added for denaturation of the proteins in the lysate. Total protein was separated by 7–15% SDS-PAGE. Electrophoresis was carried out at 80 V for 20 min and 100 V for 1 h and 30 min. Then, proteins were transferred to a polyvinylidene difluoride (PVDF) membrane at 50 V for 2 h. Then, 5% bovine serum albumin (BSA; Biosharp, Beijing, China) was used to block the membrane for 2 h. The membrane was incubated with antibodies specific for CISD2 (Proteintech, 1:2,000 dilution), LC3, ERK, p-ERK, PI3K, p-PI3K, AKT, p-AKT, mTOR, p-mTOR, Beclin1, and β-actin (all from Cell Signaling Technology, 1:1,000 dilution) overnight at 4°C. The next day, the membrane was washed three times with PBS for 10 min each. A horseradish peroxidase (HRP)-labeled goat anti-mouse antibody (Cell Signaling Technology, 1:5,000 dilution) was added and incubated at room temperature for 1 h. Then, the membrane was washed with PBS for 10 min each. Finally, immunoreactions were detected with an ECL Substrate Kit (Tanon 5200, Shanghai, China), and the experiment was repeated three times.

RNA Interference and Gene Transfection

All plasmids were purchased from GeneChem (Shanghai, China). Cells were seeded in six-well plates at a density of 5×10^5 cells/well. Cells were seeded, and after 24 h, when the cell density reached 50–70%, they were transfected with CISD2 shRNA, Beclin1 shRNA, or the corresponding Ctrl shRNA with Lipofectamine 3000 (Thermo Fisher Scientific, Waltham, MA, USA). The medium was changed after 6 h.

ROS Level Assay

Reactive oxygen species (ROS) generation in HCC cells was assessed with 2',7'-dichlorofluorescein diacetate (DCFH-DA) (Beyotime, Shanghai, China). Cells were seeded into six-well plates with 5×10^5 cells/well, and CISD2 shRNA or Ctrl shRNA was transfected for 48 h. Then cells were treated with sorafenib or erastin for 24 h. DCFH-DA was diluted with serum-free medium at a ratio of 1:1,000, and the final concentration was 10 μmol/L. The cell culture medium was removed, and DCFH-DA was added. The cells were incubated at 37°C for 20 min. The cells were washed three times with serum-free medium. ROS levels were analyzed by flow cytometry (BD LSRFortessa, Becton Dickinson, USA) or immunofluorescence assays.

Lipid Peroxidation Assay

Intracellular lipid peroxidation was evaluated by measuring the concentration of malondialdehyde (MDA) with a Lipid Peroxidation MDA Assay Kit (Beyotime, Shanghai, China). After transfection with CISD2 shRNA, Beclin1 shRNA, or the corresponding Ctrl shRNA for 48 h, cells were treated with sorafenib or erastin for 24 h. Then, a certain number of cells was collected, and the lysate was incubated at 4°C for 2 h and centrifuged at 12,000 × r for 10 min to obtain the supernatant for subsequent analysis. Then, 0.2 ml of MDA detection working solution was added. After mixing, the mixture was heated to 100°C or boiled in a water bath for 15 min. The absorbance was measured at 532 nm with a microplate reader. After the MDA content in the sample solution was calculated, it was normalized to the MDA content in the parental cell sample as the protein content per unit weight.

Measurement of Iron Content

The intracellular iron content was measured by using calcein-acetoxymethyl ester (Ca-AM; AnaSpec, Campus Drive Fremont, USA). Cells were seeded into six-well plates with 5×10^5 cells/well and cultured for 24 h. Then cells were transfected with CISD2 shRNA or the corresponding Ctrl shRNA for 48 h. After that, the cells were treated with sorafenib or erastin for 24 h. The cells were collected and cultured at 37°C at a density of 1×10^6 cells/ml in 0.05 μmol Ca-AM for 15 min. After that, the cells were washed twice with 0.5 ml of PBS and used for flow cytometric analysis or immunofluorescence assays. Calcein was excited at 488 nm, and fluorescence was measured at 525 nm. The difference in the average fluorescence intensity reflected the iron content. A Prussian Blue Iron Stain Kit (Solarbio, Beijing, China) was used to detect trivalent iron.

GSH Assay

Cellular GSH in HCC cell lysates was evaluated with a Micro Reduced Glutathione (GSH) Assay Kit (Solarbio, Beijing, China). Cells were seeded into six-well plates and cultured for 24 h. Then cells were transfected with CISD2 shRNA, Beclin1 shRNA, or the corresponding Ctrl shRNA for 48 h. After that, the cells were treated with sorafenib or erastin for 24 h. Approximately 1×10^6 cells/ml of each sample was collected. First, the cells were washed twice with PBS (cells were resuspended in PBS and centrifuged at 600 × r for 10 min). A three-fold volume of the cell precipitation reagent was added to resuspend the cells, and the cells were subjected to two to three freeze-thaw cycles and centrifuged at 8,000 × r for 10 min. The supernatant was collected at 4°C for testing. Then, 20 μl of the sample, 140 μl of Reagent II, and 40 μl of Reagent III were added sequentially. After mixing, the mixture was allowed to stand for 2 min, and the absorbance (A2) was measured at 412 nm: ΔA= A2 - A1.

Immunofluorescence Staining

Cells were seeded on the prepared cover glasses in six-well plates for 24 h and were reached to 30%. Then, Ctrl shRNA or CISD2 shRNA plasmid was transfected and cultured for 48 h. After that, cells were treated with sorafenib for 24 h. After cells were washed three times with PBS for 5 min each, cells were fixed with 4% polyoxymethylene for 15 min at room temperature and washed with PBS three times again. The cells were incubated with 1% Triton X-100 for 20 min at room temperature and washed three times with PBS for 5 min each. Then, the cells were incubated with bovine serum albumin (BSA) for 1 h in 37°C and washed with PBS three times, after which LC3-labeled goat anti-mouse antibody was added and incubated at 37°C for 2 h. Finally, DAPI was used to stain nuclei, and the cells were incubated in the dark for 5 min. PBS was used to wash the cells three times for 5 min each. The number and distribution of LC3 were observed under a fluorescence microscope.

Transmission Electron Microscopy

By transfected CISD2 shRNA or the corresponding Ctrl shRNA for 48 h, and cells were treated with sorafenib for 24 h. The collected cells were treated with 5% glutaraldehyde and stored at 4°C overnight. Then samples went through ultracryomicrotomy to generate slices of 70 nm in thickness and staining with 20 μ 2% phosphotungstic acid for 10 min. All samples were analyzed by a H-7650 electron microscope at 100KV.

Co-immunoprecipitation

Drug-resistant HCC cells were collected and incubated on ice for 40 min in 300 μl of lysis buffer containing a protease inhibitor. Then, the supernatant was collected, and 2 μg of the anti-CISD2 antibody, anti-Beclin1 antibody, or immunoglobulin G (Proteintech) was added and incubated overnight at 4°C. Then, 20 μl of protein A/G-agarose beads (Santa Cruz Biotechnology, Shanghai, China) was added and incubated at 4°C for 3 h with shaking. The beads were collected and washed with lysis buffer three times. Finally, 40 μl of loading buffer was added and boiled for 5 min, and western blot analysis was performed.

Immunohistochemistry

The expression of CISD2 in human HCC tissues was observed in paraffin sections. Antigen was retrieved with citrate, and the sections were dehydrated and cleared through an alcohol gradient. The sections were stained with an immunohistochemical kit (Invitrogen, Thermo Fisher Scientific, USA) according to the manufacturer's instructions. The sections were incubated with an anti-CISD2 primary antibody (Proteintech, 1:100) and were then restained with hematoxylin. Each slide was observed under a microscope.

Statistical Analysis

Data are presented as the mean ± standard deviation (SD) or standard error of the mean values. The statistical significance of differences between treatment groups was assessed by using the Mann–Whitney U-test or analysis of variance (ANOVA) with the Bonferroni *post hoc* test. The statistical software IBM® SPSS® Statistics version 24.0 for Windows (IBM, Armonk, NY, USA) was used. Statistical significance was defined as a two-sided P value <0.05.

RESULTS

CISD2 Is Upregulated in HCC Cell Lines and Related to Poor Prognosis

To explore the relationship between ferroptosis and drug resistance, we identified 49 negative regulators of ferroptosis in the ferroptosis database (http://www.zhounan.org/ferrdb/). Then, we analyzed the expression levels of genes in samples of sorafenib-resistant HCC tissue in the Gene Expression Omnibus (GEO) database (GSE73571, GSE93595, GSE94550). CISD2 was more highly expressed than the other investigated genes (**Figure 1A**). By comparing the HCC RNA-seq data of 371 tumor tissues with that of 50 adjacent normal tissues from TCGA, we found that CISD2 was upregulated in HCC (**Figure 1B**). In addition, Kaplan-Meier survival analysis indicated that the survival rate of patients with relatively high CISD2 expression was lower than that of patients with low CISD2 expression (**Figure 1C**). Next, we aimed to study the potential function of CISD2 in HCC cell lines by qPCR (**Figure 1D**). The expression of CISD2 in HCC cells (Huh7, HepG2, Hep3B, and PLC) was higher than that in normal liver cells. Western blot analysis showed that the expression level in PLC cells was relatively low and that the expression level in Huh7 cells was relatively high (**Figure 1E**). We selected these two cell

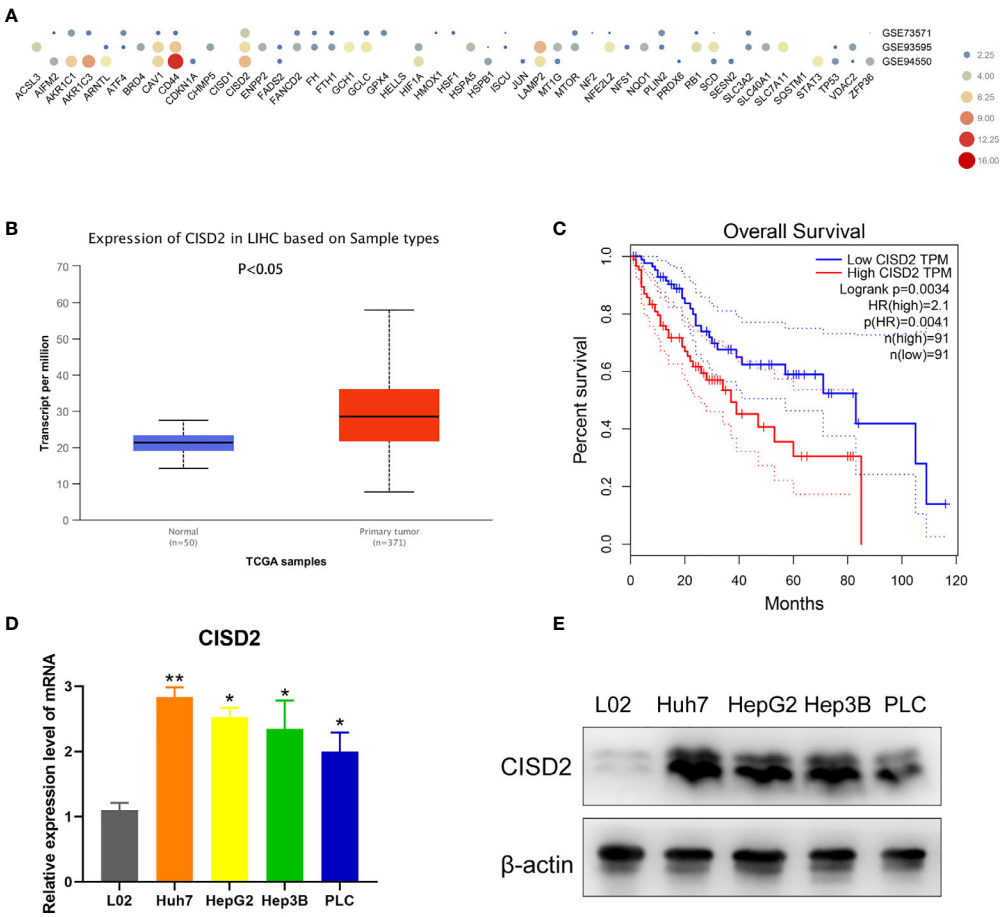

FIGURE 1 | CISD2 is upregulated in HCC cell lines and related to poor prognosis. **(A)** Bioinformatics was used to detect the expression level of ferroptosis genes in gene expression omnibus (GEO) database from GSE73571, GSE93595, GSE94550. **(B)** TCGA database was used to analyze the HCC RNA-seq data of 371 tumor tissues against 50 adjacent normal tissues. **(C)** GEPIA database was used to detect the Kaplan-Meier survival analysis. **(D, E)** qPCR and western blot were used to detect the expression level of normal hepatic epithelial cell (L02) and HCC cell lines (Huh7, HepG2, Hep3B, PLC) (n=3, $^{*}P < 0.05$, $^{**}P < 0.01$ *versus* L02).

lines for subsequent research. These data suggested that CISD2 was highly expressed in HCC and correlated with the poor prognosis of HCC patients.

Knockdown of CISD2 Reverses Sorafenib Resistance

We used Huh7 and PLC cells to establish sorafenib-resistant cell lines using the concentration gradient method (from 1 to 5 μmol) over a 6-month period **(Figure 2A)**. A CCK-8 assay was used to detect the changes in cell viability under sorafenib treatment **(Figure 2B)**. The IC_{50} in Huh7 cells was 5.31 ± 0.428 μmol, while that in resistant Huh7 cells was 11.71 ± 1.775 μmol; the IC_{50} in PLC cells was 7.449 ± 0.336 μmol, while that in resistant PLC cells was 13.532 ± 1.009 μmol **(Supplemental Figure S1A)**. After sorafenib treatment at 10 μmol, the level of p-ERK in drug-resistant cells was not reduced, while the level of p-ERK in non-drug-resistant cells was reduced **(Figure 2C)**, indicating that the drug-resistant cell lines we cultured were clearly resistant. To detect the effect of CISD2 on drug-resistant cells, we transfected CISD2 shRNA to knockdown CISD2, and qPCR was used to detect the transfection efficiency **(Supplemental Figure S1B).** After that, we selected the cells exhibiting the highest transfection efficiency for western blot analysis **(Figure 2D)**. CISD2 knockdown resulted in some loss of cell viability without sorafenib treatment, but there was no significant difference compared with Ctrl shRNA (Huh7-R, P=0.0686; PLC-R, P=0.0547), and CISD2 knockdown aggravated the toxicity of sorafenib treatment at different concentrations **(Figure 2E)**. We further detected the effect of CISD2 on the proliferation of resistant HCC cells. We used an EdU incorporation assay and found that CISD2 knockdown inhibited cell division **(Figures 2F, G)**. The colony formation assay showed that CISD2 knockdown inhibited cell proliferation **(Supplemental Figure S1C)**.

Knockdown of CISD2 Promotes Ferroptosis in Sorafenib-Resistant Cells

Inducing ferroptosis is one of the best ways to prevent cancer drug resistance, and this method is used to treat refractory high-risk neuroblastoma (27). Current studies suggest that sorafenib can induce ferroptosis in hepatocellular carcinoma cells (8). We also found that the effect of sorafenib on apoptosis was not obvious; however, the apoptosis rate was increased after STS (an apoptosis inducer) treatment **(Supplemental Figure S2A)**, and sorafenib-induced cell death was restored by co-treatment with Fer-1 or DFO (ferroptosis inhibitors) **(Supplemental Figure S2B)**. In the above study, we confirmed that CISD2 knockdown reversed sorafenib resistance. We then explored whether CISD2 knockdown can reverse sorafenib resistance by inducing ferroptosis. We used sorafenib at a higher concentration (10 μmol) to treat resistant cells. A CCK-8 assay was used to detect cell viability. The results showed that Fer-1 and DFO weakened the effects of both sorafenib and erastin in both Ctrl shRNA- and CISD2 shRNA-transfected cells. However, ZVAD-FMK (an apoptosis inhibitor) and NSA (a necroptosis inhibitor) exerted no influence on sorafenib- or erastin-induced growth inhibition **(Figures 3A, B)**. Flow cytometric analysis showed that the apoptosis induced by CISD2 knockdown was not obvious under sorafenib treatment **(Figures 3C, D)**. This finding suggests that CISD2 knockdown promotes sorafenib-induced ferroptosis in resistant HCC cells.

Iron accumulation and lipid peroxidation are related to the process of ferroptosis. Thus, we detected ferrous ions, ROS, and malondialdehyde (MDA, a lipid peroxidation product). The level of ROS in the CISD2 shRNA group was higher than that in the Ctrl shRNA group under sorafenib treatment as determined by flow cytometry in Huh7-R cell (**P=0.0028) and PLC-R cell (**P=0.0019) **(Figure 4A)**, and the fluorescence detection also showed that knockdown of CISD2 enhanced ROS fluorescence expression **(Figures 4C, D)**. The level of MDA was increased in CISD2 shRNA group under treatment with sorafenib in Huh7-R cell (**P=0.0069) and PLC-R cell (**P=0.0016) **(Figure 4B)**. In addition, the content of iron ions was increased in CISD2 shRNA group under treatment with sorafenib, as shown by flow cytometry in Huh7-R cell (**P=0.0035) and PLC-R cell (**P=0.0026) **(Figure 4E)**, and fluorescence detection was also consistent with it **(Figures 4G, H)**. CISD2 shRNA group was highly enriched in iron ions compared with Ctrl shRNA group, as determined by high magnification fluorescence detection and Perls staining **(Supplemental Figure S3)**. However, the decrease in the GSH level induced by sorafenib appeared to not be affected by inhibition of CISD2 **(Figure 4F)**. This finding implies that inhibition of GSH itself might be less effective in the context of ferroptosis induction without iron accumulation. These results suggest that CISD2 knockdown can promote the sensitivity of drug-resistant cells to sorafenib and lead to ferroptosis.

Knockdown of CISD2 Promotes Autophagy in Sorafenib-Resistant Cells

To understand the possible mechanism of CISD2, we conducted GSEA on database data for liver cancer samples. The results showed that the correlation between CISD2 and autophagy was the second highest and that there was a negative regulatory relationship between CISD2 and autophagy **(Figure 5A)**. After that, we found that the autophagy level was increased when CISD2 was knocked down. Western blot analysis showed that the LC3 I converted to LC3 II and the expression level of p62 decreased gradually **(Figures 5B, C)**. Immunofluorescence staining showed that the number of LC3 spots was increased after CISD2 knockdown **(Figures 5D, E)**. And transmission electron microscopy showed that CISD2 knockdown promoted the increase of autophagosomes **(Figure 5F)**. Studies have shown that the mTOR pathway plays an important role in the formation of autophagosomes and that the mTOR pathway is the convergence point of upstream AMPK and PI3K/Akt signal transduction (28). When the mTOR pathway is inhibited, autophagy can be activated. We used western blot to evaluate the expression of key proteins in the classic autophagy mTOR pathway. However, the levels of p-PI3K, p-AKT, and p-mTOR did not change after CISD2 knockdown **(Figures 5G–I)**. The results showed that CISD2 knockdown had no effect on the mTOR pathway.

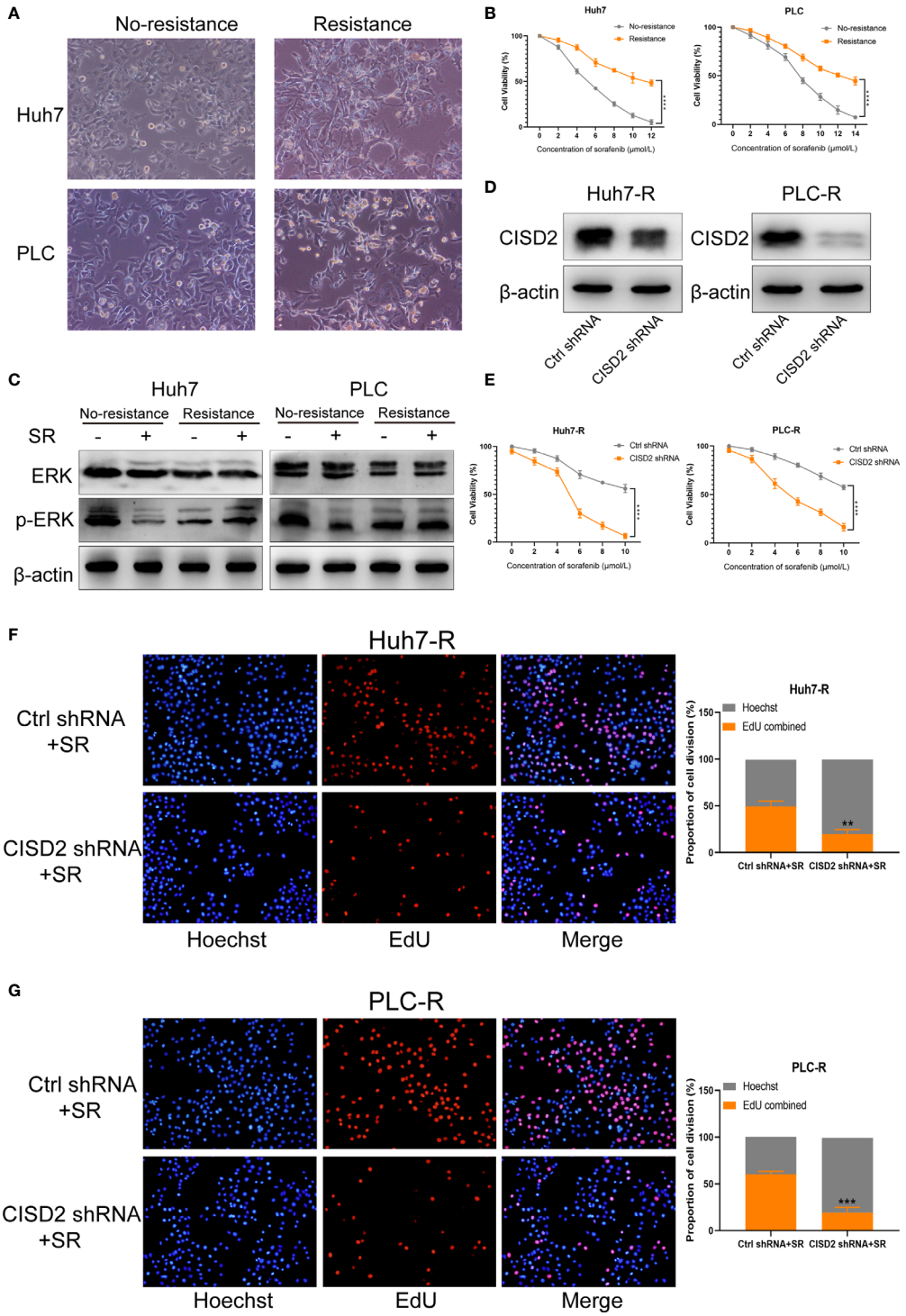

FIGURE 2 | Knockdown of CISD2 reverses sorafenib resistance. **(A)** Sorafenib-resistant cells were cultured for 6 months by the concentration gradient increasing method, and the morphology of resistant cancer cells was detected. **(B)** CCK-8 method was used to detect the cell viability under treatment with different concentrations of sorafenib (n = 3, $^{****}P < 0.0001$ *versus* No resistance). **(C)** Western blot was used to detect the expression level of ERK and p-ERK protein on treatment with sorafenib (SR, 10 μmol). **(D)** Western blot was used to detect the expression level of CISD2 under transfected CISD2 shRNA or Ctrl shRNA in Huh7-resistant cell (Huh7-R) and PLC-resistant cell (PLC-R). **(E)** CCK-8 method was used to detect the cell viability with different concentrations of sorafenib under transfected CISD2 shRNA or Ctrl shRNA (n = 3, $^{****}P < 0.0001$ *versus* Ctrl shRNA). **(F, G)** EdU method was used to detect cell proliferation under treatment with sorafenib (10 μmol) or transfected CISD2 shRNA in resistant cells (n = 3, $^{**}P < 0.01$, $^{***}P < 0.001$ *versus* Ctrl shRNA+SR).

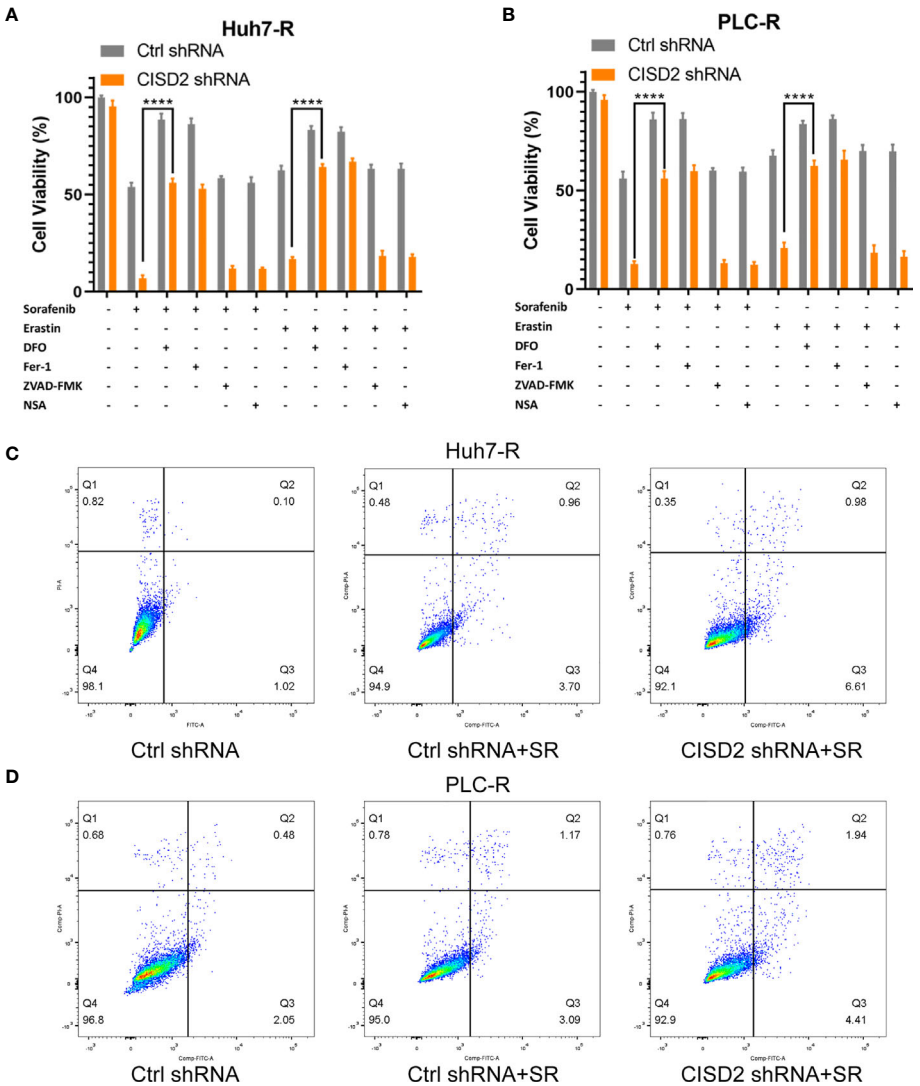

FIGURE 3 | Knockdown of CISD2 mainly promotes ferroptosis and not apoptosis in sorafenib-resistant cells. **(A, B)** CCK-8 method was used to detect the cell viability under different treatment with sorafenib (10 μmol) or transfected CISD2 shRNA, and erastin (10 μmol) as positive control, with or without cell death inhibitors (Fer-1, 1 μmol; DFO, 200 μmol; ZVAD-FMK, 10 μmol) (n = 3, ****$P < 0.0001$ *versus* sorafenib/erastin group). **(C, D)** Cell apoptosis was detected by flow cytometry under treatment with sorafenib (10 μmol) or transfected CISD2 shRNA (horizontal axis label FITC Annexin V and vertical axis label PI).

Inhibiting Autophagy Alleviates Ferroptosis in Sorafenib-Resistant Cells With CISD2 Knockdown

Studies have shown that autophagy plays an important role in the occurrence of ferroptosis (29–31). We thus sought to further verify whether autophagy is involved in the ferroptosis induced by CISD2 knockdown. We used the autophagy inhibitors bafilomycin A1 (BafA1) and 3-methyladenine (3-MA) separately as an autophagy initiation inhibitor and a lysosomal inhibitor, respectively, to detect autophagy. We then used CCK-8 to evaluate cell viability after 12 or 24 h of treatment. The results showed that both 3-MA and BafA1 inhibited cell death. In addition, 3-MA played a stronger role in the setting of CISD2 knockdown, and we chose it for the next experiment (**Figure 6A**). Western blot analysis showed that after treatment with 3-MA, the change from LC3 I to LC3 II was partially decreased (**Figure 6B**), and the number of fluorescent LC3 puncta was reduced (**Figure 6C**). The expression levels of MDA and ROS in drug-resistant cells in the 3-MA treatment group were decreased (**Figures 6D, E**) and that iron ions were also decreased under co-treatment with 3-MA (**Figure 6F**). The GSH level in sorafenib-resistant cells was not affected by treatment with 3-MA (**Figure 6G**). These results suggest that inhibiting autophagy alleviates ferroptosis partially in the setting of CISD2 knockdown. In summary, CISD2 mediates cellular resistance to sorafenib-induced ferroptosis by regulating autophagy.

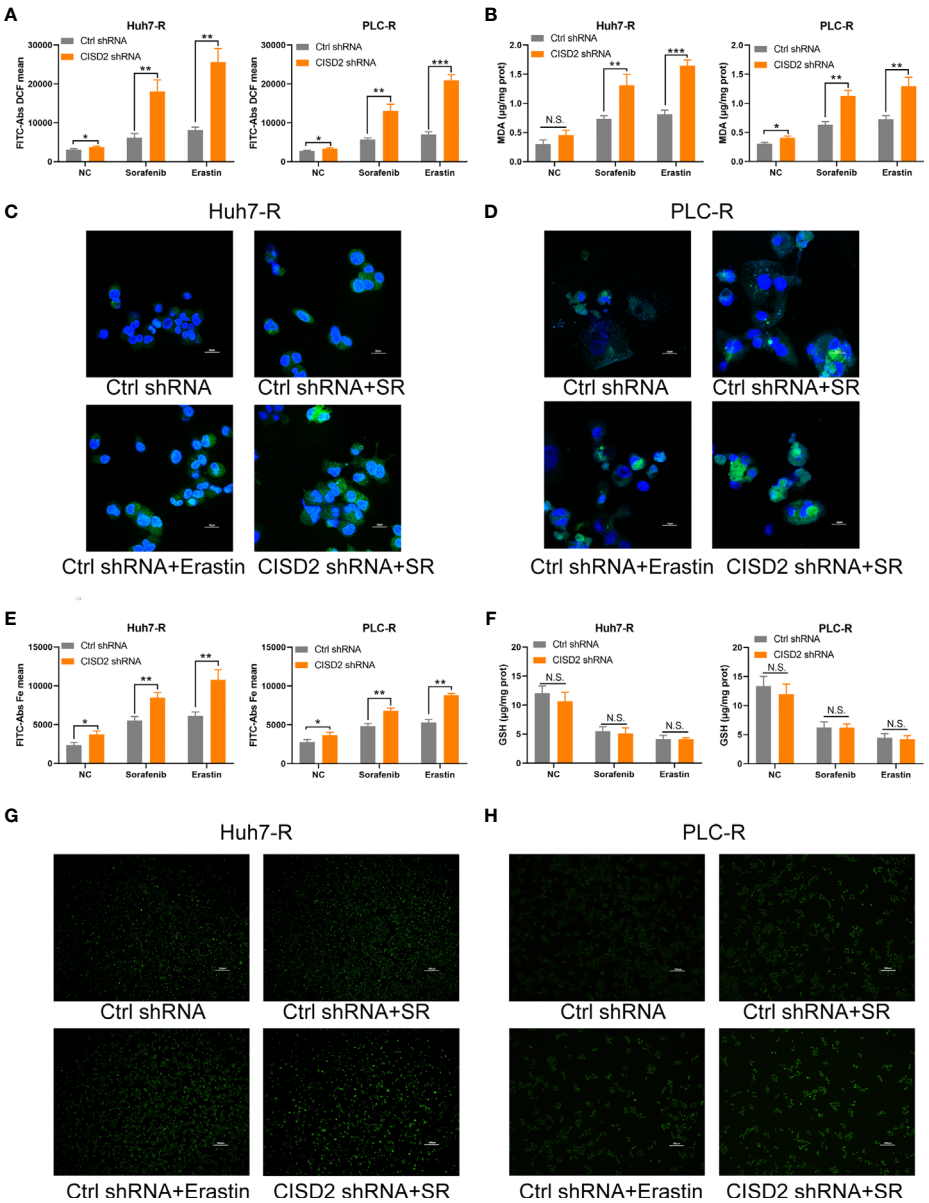

FIGURE 4 | Knockdown of CISD2 promotes ferroptosis in sorafenib-resistant cells. **(A)** Flow cytometry was used to detect the expression level of ROS under treatment with sorafenib (10 μmol) or transfected CISD2 shRNA, and erastin (10 μmol) as positive control. **(B)** MDA kit was used to detect the expression level of MDA under treatment with sorafenib (10 μmol) or transfected CISD2 shRNA, and erastin (10 μmol) as positive control. **(C, D)** Immunofluorescence was used to detect the expression of ROS by adding DCFH-DA under treatment with sorafenib (10 μmol) or transfected CISD2 shRNA. **(E)** Flow cytometry was used to detect the expression level of iron ions under treatment with sorafenib (10 μmol) or transfected CISD2 shRNA, and erastin (10 μmol) as positive control. **(F)** GSH kit was used to detect the expression level of GSH under treatment with sorafenib (10 μmol) or transfected CISD2 shRNA, and erastin (10 μmol) as positive control. **(G, H)** Immunofluorescence was used to detect the expression level of iron ions under treatment with sorafenib (10 μmol) or transfected CISD2 shRNA. (n = 3, *P < 0.05, **P < 0.01, ***P < 0.001 *versus* Ctrl shRNA, N.S. means no significance).

Inhibition of CISD2 Promotes Ferroptosis Regulated by Beclin1 in Sorafenib-Resistant Cells

To explore the regulatory target of CISD2 in autophagy, we evaluated the expression of the autophagy-related genes Beclin1, ATG3, ATG4, ATG5, ATG7, ATG9, ATG10, and ATG12 after knockdown of CISD2. The results showed that among these genes, Beclin1 was the most upregulated (**Figure 7A**). After that, we used western blot to confirm that CISD2 knockdown promoted Beclin1 expression (**Figure 7B**). Therefore, we explored whether CISD2 affects ferroptosis by regulating Beclin1. We transfected resistant cells with Beclin1 shRNA to

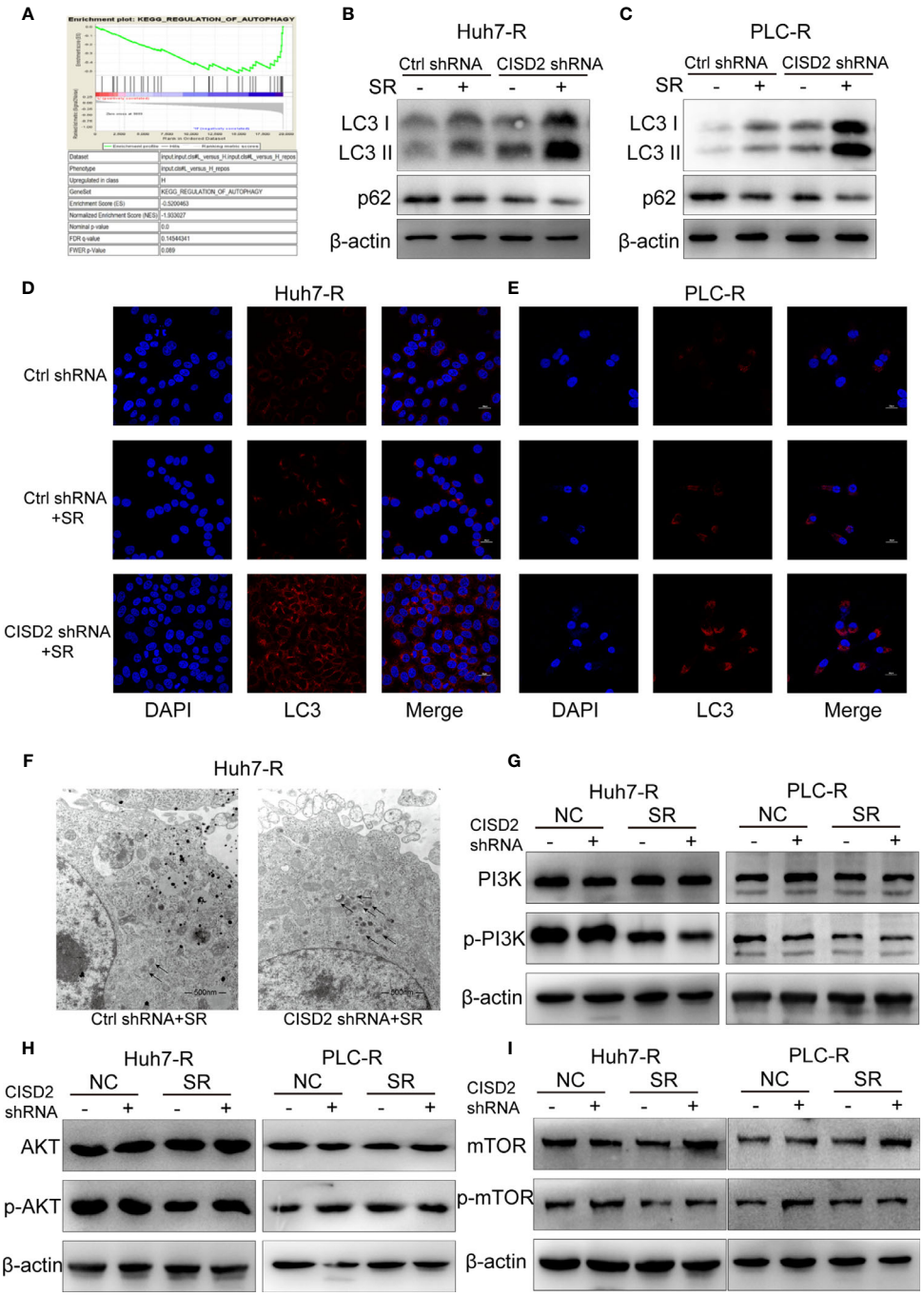

FIGURE 5 | Knockdown of CISD2 promotes autophagy in sorafenib-resistant cells. **(A)** GSEA was used to detect the function of CISD2. **(B, C)** Western blot was used to detect the expression level of LC3 and p62 under treatment with sorafenib (10 μmol) or transfected CISD2 shRNA in resistant cells. **(D, E)** Immunofluorescence was used to detect the expression of LC3 under treatment with sorafenib (10 μmol) or transfected CISD2 shRNA. **(F)** Transmission electron microscopy was used to detect the number of autophagosomes under treatment with sorafenib (10 μmol) or transfected CISD2 shRNA. **(G–I)** Western blot was used to detect the expression level of PI3K, p-PI3K, AKT, p-AKT, mTOR, p-mTOR under treatment with sorafenib (10 μmol) or transfected CISD2 shRNA.

knockdown Beclin1, and the knockdown efficiency was determined by qPCR and western blot analysis (**Figures 7C, D**). In order to further explore, we used Pg as a CISD2 inhibitor to treat resistant HCC cells. After co-treatment with sorafenib and Pg, the level of LC3 was increased but was decreased by co-treatment with Beclin1 shRNA (**Figure 7E**). The immunofluorescence results showed that LC3 spots increased after sorafenib and Pg co-treatment but decreased after Beclin1

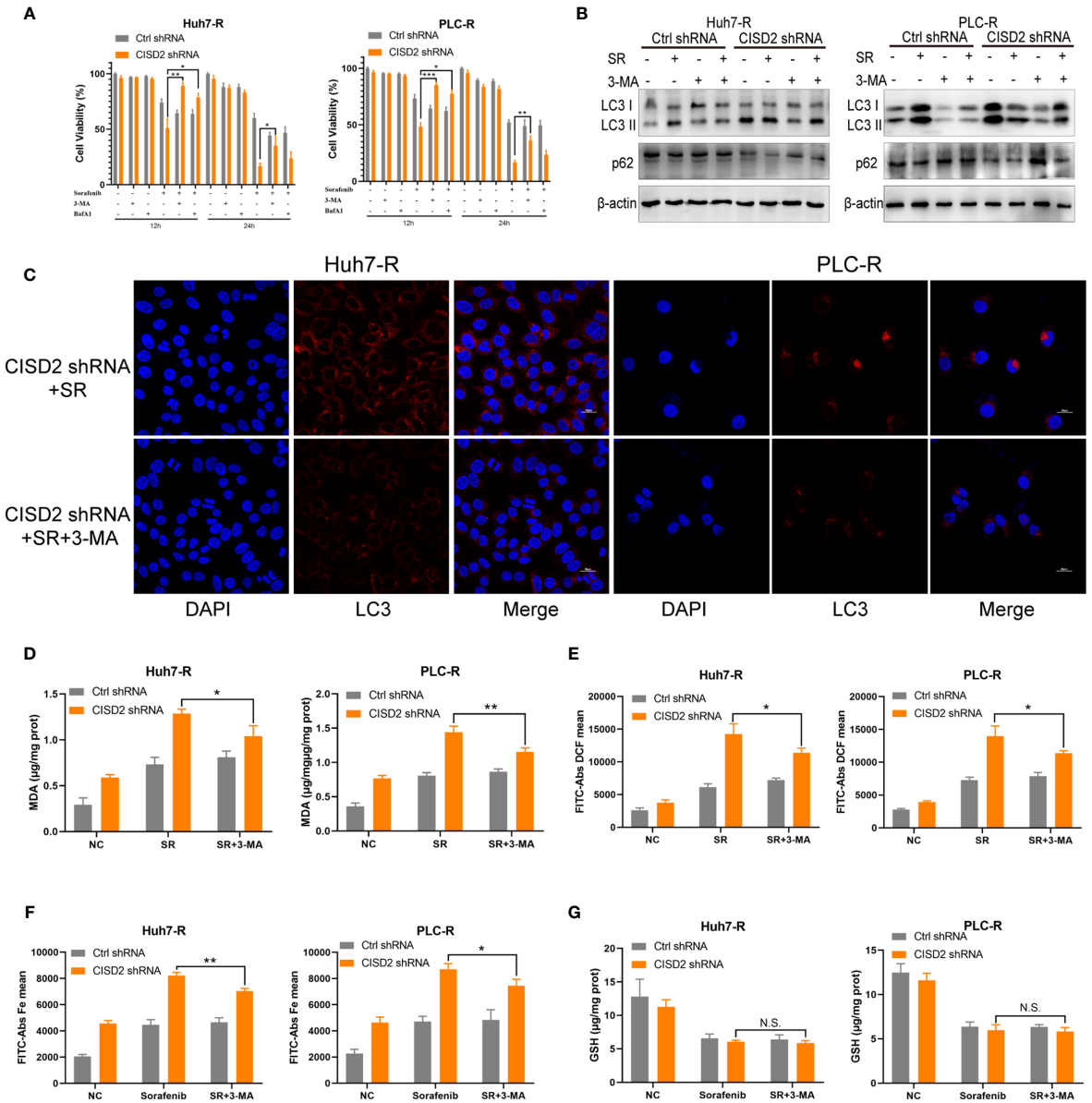

FIGURE 6 | Inhibiting autophagy alleviates ferroptosis in sorafenib-resistant cells with CISD2 knockdown. **(A)** CCK-8 was used to detect the cell viability under treatment with sorafenib (10 μmol), 3-MA (1 mmol), BafA1 (20 nmol), or transfected CISD2 shRNA (n = 3, $^{*}P < 0.05$, $^{**}P < 0.01$, $^{***}P < 0.001$ *versus* 3-MA treatment or BafA1). **(B)** Western blot was used to detect the expression level of LC3, p62 under treatment with sorafenib (10 μmol), 3-MA (1 mmol), or transfected CISD2 shRNA in resistant cells. **(C)** Immunofluorescence was used to detect the expression level of LC3 under treatment with sorafenib (10 μmol), 3-MA (1 mmol), or transfected CISD2 shRNA. **(D)** MDA kit was used to detect the expression level of MDA under treatment with sorafenib (10 μmol), 3-MA (1 mmol), or transfected CISD2 shRNA (n = 3, $^{*}P < 0.05$, $^{**}P < 0.01$ *versus* 3-MA treatment). **(E)** Flow cytometry was used to detect the expression level of ROS under treatment with sorafenib (10 μmol), 3-MA (1 mmol), or transfected CISD2 shRNA (n = 3, $^{*}P < 0.05$ *versus* 3-MA treatment). **(F)** Flow cytometry was used to detect the expression level of iron ions under treatment with sorafenib (10 μmol), 3-MA (1 mmol), or transfected CISD2 shRNA (n = 3, $^{*}P < 0.05$, $^{**}P < 0.01$ *versus* 3-MA treatment). **(G)** GSH kit was used to detect the expression level of GSH under treatment with sorafenib (10 μmol), 3-MA (1 mmol), or transfected CISD2 shRNA (n=3, N.S. means no significance).

knockdown (**Figure 7F**). These results showed that Beclin1 knockdown partially inhibited autophagy. After that, we evaluated cell viability by CCK-8. The results showed that Beclin1 knockdown increased cell viability in sorafenib and Pg co-treatment group (**Figure 7G**). We further examined the changes in MDA, the key indicator of ferroptosis. The results showed that knockdown of Beclin1 decreased the MDA level in sorafenib and Pg co-treatment group (**Figure 7H**). After that, we found by co-immunoprecipitation experiments that CISD2 can bind Beclin1 (**Figure 8A**). In conclusion, CISD2 promotes

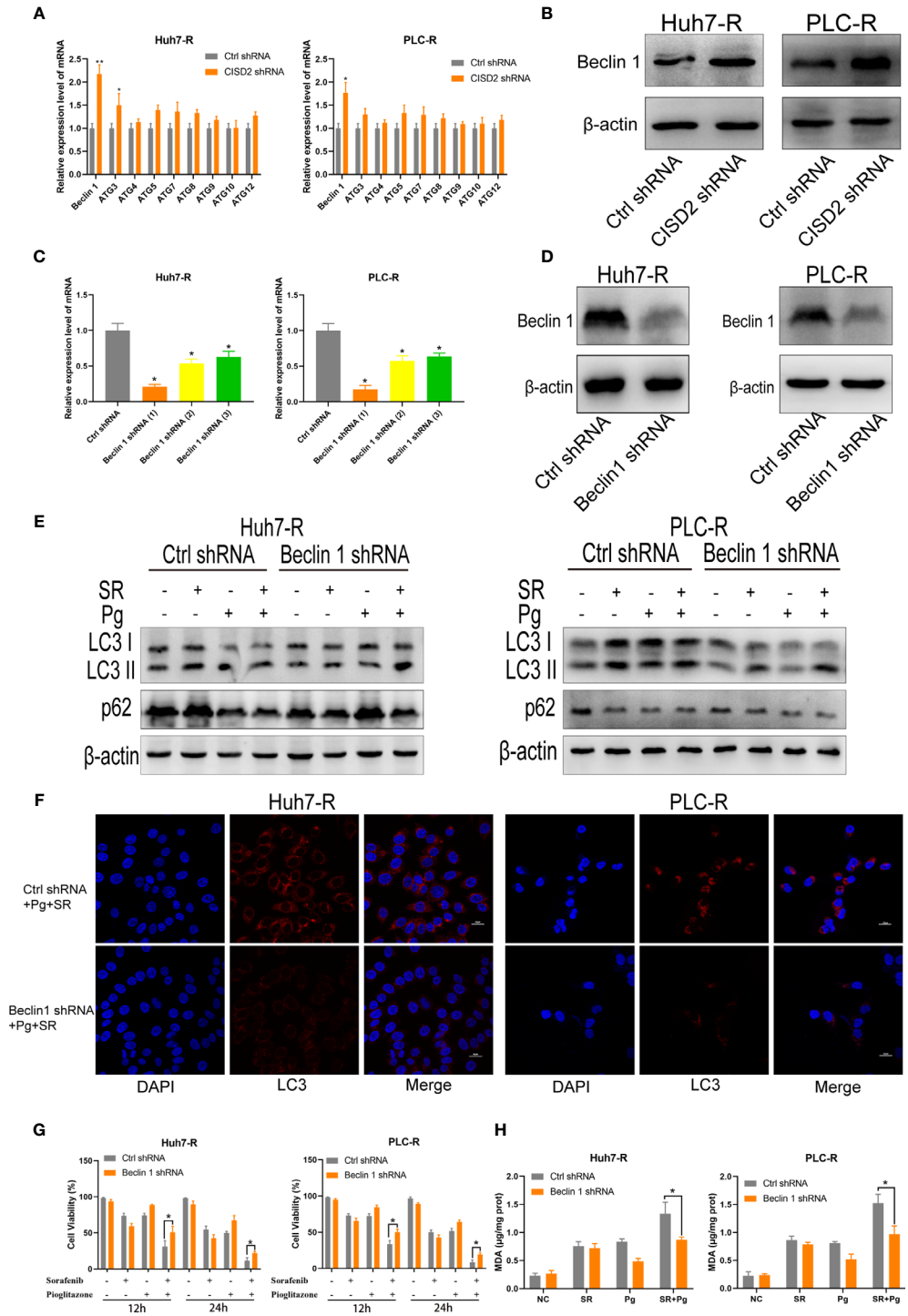

FIGURE 7 | Inhibition of CISD2 promotes ferroptosis regulated by Beclin1 in sorafenib-resistant cells. **(A)** qPCR was used to detect the autophagy-related gene expression under transfected CISD2 shRNA (n = 3, $^{*}P < 0.05$, $^{**}P < 0.01$ *versus* Ctrl shRNA). **(B)** Western blot was used to detect the expression level of Beclin1 under transfected CISD2 shRNA. **(C, D)** qPCR and western blot were used to detect the Beclin1 expression under transfected Beclin1 shRNA (n = 3, $^{*}P < 0.05$ *versus* Ctrl shRNA). **(E)** Western blot was used to detect the expression level of LC3, p62 under treatment with sorafenib (10 μmol), Pg (10 μmol), or transfected Beclin1 shRNA. **(F)** Immunofluorescence was used to detect the expression of LC3 under different treatment with sorafenib (10 μmol), Pg (10 μmol), or transfected Beclin1 shRNA. **(G)** CCK-8 was used to detect the cell viability under treatment with sorafenib (10 μmol), Pg (10 μmol), or transfected Beclin1 shRNA (n = 3, $^{*}P < 0.05$ *versus* Ctrl shRNA). **(H)** MDA kit was used to detect the expression of MDA under treatment with sorafenib (10 μmol), Pg (10 μmol), or transfected Beclin1 shRNA (n = 3, $^{*}P < 0.05$ *versus* Ctrl shRNA).

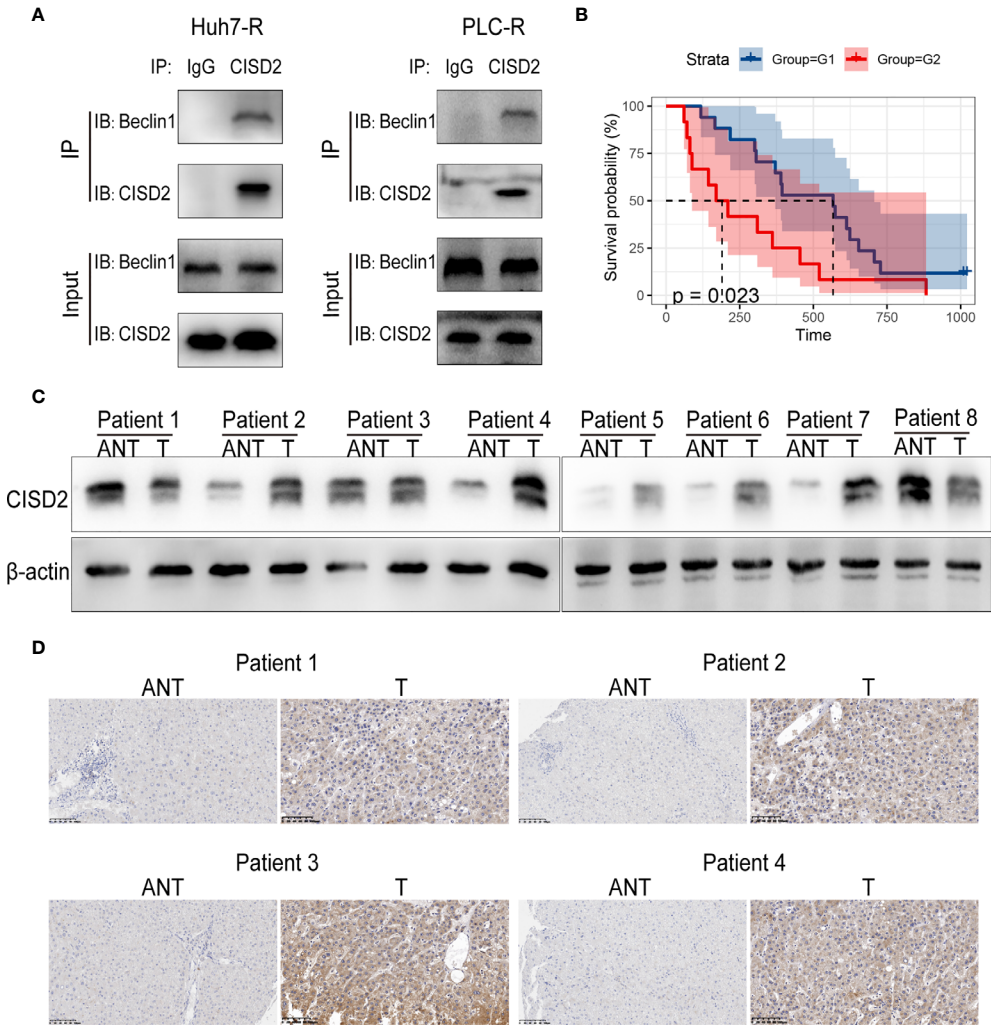

FIGURE 8 | Correlation between CISD2 expression and the survival of HCC patients. **(A)** Co-immunoprecipitation of endogenous CISD2 and Beclin1 in HCC resistant cells. **(B)** Correlation between CISD2 expression and survival analysis of HCC patients (G1=CISD2 low expression group, G2=CISD2 high expression group). **(C)** Western blot was used to detect the expression level of CISD2 in HCC tissues (T) and adjacent normal tissues (ANT). **(D)** Immunohistochemistry was used to detect the expression level of CISD2 in HCC tissues and adjacent normal tissues.

resistance to sorafenib-induced ferroptosis by regulating Beclin1 in HCC cells.

Correlation Between CISD2 Expression and the Survival of HCC Patients

We then sought to evaluate the correlation between CISD2 expression and the survival prognosis of HCC patients. We divided patients into high and low CISD2 expression groups and found that the survival time of patients with high CISD2 expression was lower than that of patients with low CISD2 expression (P=0.023) (**Figure 8B**). Western blot analysis showed that CISD2 expression in HCC tissue was higher than that in adjacent normal tissue (**Figure 8C**). The immunohistochemical results showed that CISD2 was more highly expressed in HCC tissues than in adjacent normal tissues and was mainly localized in the cytoplasm (**Figure 8D**). In summary, CISD2 is highly expressed in HCC patients and is associated with poor prognosis.

DISCUSSION

In the past few decades, although a large number of studies have been carried out to improve the efficacy of anticancer drugs by overcoming chemotherapeutic resistance, it is still a major clinical challenge in the treatment of HCC (32). Sorafenib, as the first-line drug for the treatment of advanced liver cancer, is often due to the drug resistance of liver cancer, with low response rate and poor survival and prognosis effect of patients (33). It is

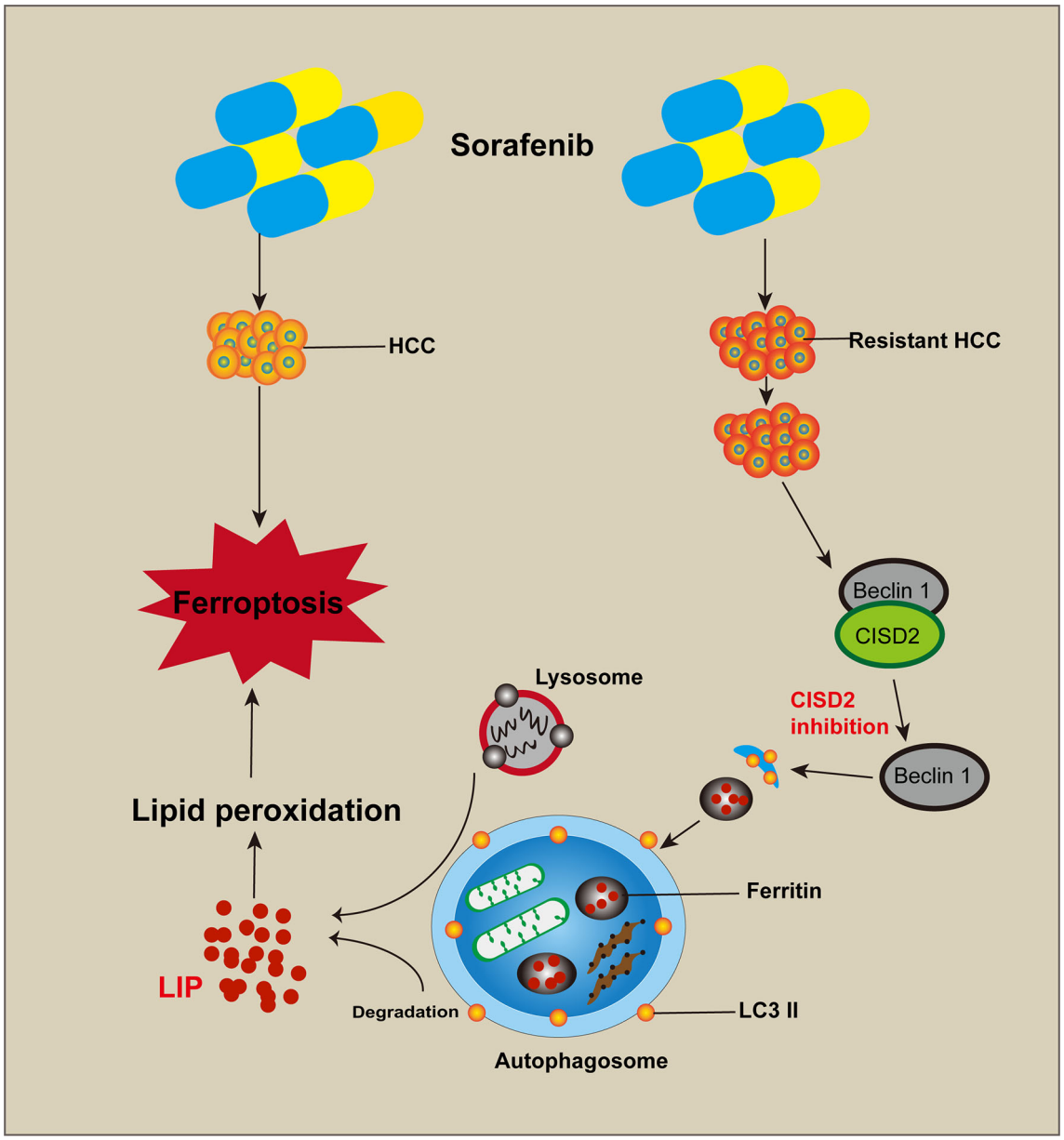

FIGURE 9 | Cartoon diagram of CISD2 promotes resistance to sorafenib-induced ferroptosis by regulating autophagy in hepatocellular carcinoma. Inhibition of CISD2 restored sorafenib-induced ferroptosis and reversed drug resistance, and these effects were related to the inhibition of CISD2-promoted autophagy. Through this process, the excessive activation of autophagy promoted the release of iron ions and induced lipid peroxidation to promote ferroptosis.

necessary to study the mechanism of resistance and further therapy.

The main mechanism of drug therapy is induction of apoptosis. However, cancer cells can usually develop mechanisms to prevent apoptosis by acquiring a drug resistance phenotype and upregulating pro-survival signals (34). It is necessary to explore other forms of cell death to solve the problem of drug resistance. In recent years, studies have shown that the induction of ferroptosis in cancer cells has become a new treatment strategy, and its clinical application in cancer treatment is anticipated to be promoted (35).

Currently, some clinical drugs, such as sorafenib, sulfasalazine, lanperisone, acetaminophen, and cisplatin, can induce ferroptosis in several types of cancer cells, supporting the feasibility of exploiting ferroptosis for the treatment of drug-resistant cancers (36, 37). Genetic silencing of cystine/glutamate-induced ferroptosis in resistant head and neck cancer (HNC) cells enhanced sensitivity to cisplatin (38). Furthermore, ferroptosis

inducers (FINs) were able to sensitize zero-valent iron nanoparticle (ZVI NP)-resistant cancer cells to become treatable without damaging non-malignant cells (39). However, tumor cells can also resist ferroptosis through the regulation of internal antioxidant factors, thus promoting drug resistance (40). Activation of the nuclear factor erythroid-2-related factor 2 (NRF2)-antioxidant response element (ARE) pathway contributes to artesunate (a ferroptosis inducer) resistance in cisplatin-resistant head and neck cancer cells, but genetic silencing of NRF2 or trigonelline reverses artesunate resistance in cisplatin-resistant HNC cells *in vitro* and *in vivo* (41). Metallothionein (MT)-1G, a protein transcribed from NRF2, can also inhibit ferroptosis and promote sorafenib resistance in HCC (42). Therefore, understanding homoeostasis and utilizing the iron dependence of ROS may be a new anticancer treatment strategy for drug resistance in human liver cancer. Our study confirmed that sorafenib induced the HCC cell ferroptosis, further supporting the research of sorafenib-induced ferroptosis in other studies (8, 9). Therefore, it may be an effective strategy for the treatment of HCC by inducing ferroptosis.

NEET proteins are involved in regulating iron and reactive oxygen species in cancer cells (15, 43) and promote the proliferation of breast cancer cells (21). CISD2, a member of the NEET family, can promote the invasion and migration of pancreatic cancer cells and promote the tumorigenesis and poor prognosis of lung cancer (23, 24). Regarding drug resistance, CISD2 has been identified as a novel biomarker of sulfasalazine resistance, and its inhibition promotes the sensitivity of head and neck cancer cells to sulfasalazine-induced ferroptosis by increasing the accumulation of iron oxide and lipid ROS in mitochondria (44). However, the specific mechanism of CISD2 in drug resistance of HCC has not been reported. Our study revealed the mechanism of resistance to sorafenib-induced ferroptosis related to CISD2 expression. Silencing CISD2 sensitized resistant HCC cells to sorafenib-induced ferroptosis. Therefore, CISD2 was identified as a new biomarker for resistance to sorafenib-induced ferroptosis for the first time. Our results highlight CISD2 as a candidate target for modulating ferroptosis in HCC cells.

At present, the researches on ferroptosis-antagonizing tumor resistance mainly focus on the inhibition of ferroptosis defense system, such as GPX4. However, it has been reported that the core negative regulatory genes of ferroptosis include not only GPX4 but also ferroptosis suppressor protein 1 (FSP1), dihydroorotate dehydrogenase (DHODH), and others (45–47). It is a challenge to antagonize tumor resistance. However, regulating iron ions to promote ferroptosis can avoid this problem. Its purpose is more unified, that is, to promote the increase of iron ion expression in tumor cells. And to explore the regulation of iron ions to promote ferroptosis is expected to become an effective strategy for the treatment of tumor resistance (48). Autophagy, as a metabolic process invoked to cope with environmental stress and maintain homoeostasis, is of great importance for the development of tumor cells. However, there are different views on the role of autophagy in tumor cells. Currently, it is generally believed that autophagy has dual effects in the early stage of tumor occurrence and after tumor formation. On the one hand, autophagy can control the proliferation of tumor cells and inhibit angiogenesis to exert an anticancer effect (49); on the other hand, autophagy can improve the stress resistance ability of tumor cells to facilitate their survival and therapeutic resistance (50, 51). With the improved understanding of autophagy in tumor research, clinical adjuvant therapies targeting autophagy have been evaluated (52). However, the therapeutic effect and the selection of the target are still controversial.

In addition, autophagy plays an important role in the induction of ferroptosis by ferritin degradation and leads to an increase in the cellular labile iron pool, which induces oxidative stress during the occurrence of ferroptosis (29, 30). In this process, inhibition of system X_C^- by ferroptotic agents (e.g., erastin and sorafenib) induces the endoplasmic reticulum (ER) stress response (9). A sustained ER stress-activated unfolded protein response (UPR) can ultimately promote cytotoxic autophagy in cancer cells (53). However, only when autophagy reaches a certain intensity does it trigger ferroptosis. Disruption of intracellular redox homoeostasis during the ferroptosis process causes mitochondrial damage and may promote the subsequent initiation of autophagy, and these events may act as a feedback loop to further induce ferroptosis until cell death occurs. Formosanin C (FC) has chemotherapeutic potential against apoptosis-resistant HCC with higher NCOA4 expression *via* ferritinophagy (10). Inhibition of autophagy and ferritinophagy reduces HCC sensitivity to sorafenib or erastin by inactivating ferroptosis (54). Carbonic anhydrase 9 (CA9) confers resistance to ferroptosis/apoptosis in malignant mesothelioma cells, and inhibition of CA9 promotes mitochondrial fission and autophagy with increased levels of catalytic Fe^{2+}, peroxides, mitochondrial O_2^-, and lipid peroxidation (55). Since many studies have shown that autophagy can induce ferroptosis, the level of autophagic activity may play an important role in determining the target of anticancer drugs in tumor cells. In our study, we found that CISD2 inhibition promoted autophagy in sorafenib-resistant HCC cells and increased the iron content. However, ferroptosis was reduced obviously after early inhibition of autophagy. Therefore, our study showed that ferroptosis promoted by CISD2 inhibition is mainly regulated by autophagy.

In further exploration of autophagy, we found that the expression of Beclin1 was increased after autophagy was promoted by inhibiting CISD2. Studies have shown that CISD2 can bind Beclin1 in the endoplasmic reticulum and play a regulatory role in autophagy initiation (26). CISD2 interacts with BCL-2 at the ER and affects its interaction with the tumor suppressor Beclin1 (56). Beclin1 plays an important role in the regulation of autophagy and apoptosis. For example, Beclin1 interacts with class III PI3Ks to promote the induction of autophagy (57). In addition, Beclin1 directly blocks the activity of system X_C^- by binding with its core component solute carrier family 7 member 11 (SLC7A11) and plays an unprecedented role in promoting ferroptosis (58). While autophagy inhibition by 3-MA or Beclin1 knockdown was partially protective against CISD2

loss of function mediated cell death, these treatments did not completely inhibit autophagy. Interestingly, sorafenib seems to override the effect of autophagy inhibition by 3-MA or Beclin1 knockdown in the absence of CISD2 function. In our study, we found that inhibition of CISD2 induces ferroptosis, which can be suppressed by silencing Beclin1, and further experiments verified that CISD2 can bind Beclin1 (**Figure 9**). Our study revealed for the first time that autophagy promotes ferroptosis in drug-resistant cells and reverses the phenomenon of drug resistance. Our findings can provide a reference for targeted therapy of drug-resistant cancers. However, autophagy also exerts its antitumor effect through a previously unknown mechanism, and we suggest that controlling the intensity of autophagy to induce ferroptosis may be a potential treatment strategy for resistant cancers.

CONCLUSIONS

In conclusion, the results of this study showed that CISD2 was highly expressed and related to sorafenib resistance. Inhibition of CISD2 restored sorafenib-induced ferroptosis and reversed drug resistance, and these effects were related to the inhibition of CISD2-promoted autophagy. Through this process, the excessive activation of autophagy promoted the release of iron ions and induced lipid peroxidation to promote ferroptosis. Our study provides a reference for targeted therapy of drug-resistant tumors with ferroptosis.

DATA AVAILABILITY STATEMENT

Publicly available datasets were analyzed in this study. This data can be found here: http://software.broadinstitute.org/gsea/index.jsp.

ETHICS STATEMENT

The studies involving human participants were reviewed and approved by Ethics Committee of the Fourth Affiliated Hospital of China Medical University. The patients/participants provided their written informed consent to participate in this study.

AUTHOR CONTRIBUTIONS

BL performed the experiment and wrote the manuscript. BW contributed to the analysis of bioinformatics. LY, XP, YM, QF, SW, HJ, SY, XL, MH, and ST performed reagent preparation. HL and JL conceived the study and reviewed this article. All authors contributed to the article and approved the submitted version.

FUNDING

This research was supported by the National Natural Science Foundation of China (No. 81472302, No. 81871983, No. 82003040), Natural Science Foundation of Liaoning Province (LQNK201719), and Natural Science Foundation of Liaoning Province (2020-BS-103).

SUPPLEMENTARY MATERIAL

The Supplementary Material for this article can be found online at: https://www.frontiersin.org/articles/10.3389/fonc.2021.657723/full#supplementary-material

Supplementary Figure 1 | (A) The IC_{50} of sorafenib resistant HCC. **(B)** qPCR was used to detected the expression level of CISD2 under transfected CISD2 shRNA. **(C)** Clone formation assay was used to detect the proliferation of resistant cells under treatment with sorafenib (10 μmol) or transfected CISD2 shRNA.

Supplementary Figure 2 | (A) Flow cytometry was used to detect the apoptosis level of HCC cells under treatment with sorafenib (5 μmol) or STS (0.5 μmol). **(B)** CCK-8 method was used to detect the cell viability under treatment with sorafenib (5 μmol), erastin (5 μmol) with or without cell death inhibitors (Fer-1, 1 μmol; DFO, 200 μmol; ZVAD-FMK, 10 μmol) for 24 h (n=3, $^{*}P<0.05$ *versus* NC group).

Supplementary Figure 3 | Inverted fluorescence and Perls stain were used to detect the expression level of iron ions under treatment with sorafenib (10 μmol), erastin (10 μmol), or transfected CISD2 shRNA.

REFERENCES

1. Torre LA, Bray F, Siegel RL, Ferlay J, Lortet-Tieulent J, Jemal A. Global Cancer Statistics, 2012. *CA Cancer J Clin* (2015) 65(2):87–108. doi: 10.3322/caac.21262
2. Lin S, Hoffmann K, Schemmer P. Treatment of Hepatocellular Carcinoma: A Systematic Review. *Liver Cancer* (2012) 1(3-4):144–58. doi: 10.1159/000343828
3. Llovet JM, Ricci S, Mazzaferro V, Hilgard P, Gane E, Blanc JF, et al. Sorafenib in Advanced Hepatocellular Carcinoma. *N Engl J Med* (2008) 359(4):378–90. doi: 10.1056/NEJMoa0708857
4. Gao L, Wang X, Tang Y, Huang S, Hu CA, Teng Y. FGF19/FGFR4 Signaling Contributes to the Resistance of Hepatocellular Carcinoma to Sorafenib. *J Exp Clin Cancer Res* (2017) 36(1):8. doi: 10.1186/s13046-016-0478-9
5. Gorrini C, Harris IS, Mak TW. Modulation of Oxidative Stress as an Anticancer Strategy. *Nat Rev Drug Discov* (2013) 12(12):931–47. doi: 10.1038/nrd4002
6. Kudo Y, Sugimoto M, Arias E, Kasashima H, Cordes T, Linares JF, et al. PKClambda/iota Loss Induces Autophagy, Oxidative Phosphorylation, and NRF2 to Promote Liver Cancer Progression. *Cancer Cell* (2020) 38(2):247–262 e11. doi: 10.1016/j.ccell.2020.05.018
7. Dixon SJ, Lemberg KM, Lamprecht MR, Skouta R, Zaitsev EM, Gleason CE, et al. Ferroptosis: An Iron-Dependent Form of Nonapoptotic Cell Death. *Cell* (2012) 149(5):1060–72. doi: 10.1016/j.cell.2012.03.042
8. Louandre C, Ezzoukhry Z, Godin C, Barbare JC, Maziere JC, Chauffert B, et al. Iron-Dependent Cell Death of Hepatocellular Carcinoma Cells Exposed to Sorafenib. *Int J Cancer* (2013) 133(7):1732–42. doi: 10.1002/ijc.28159
9. Dixon SJ, Patel DN, Welsch M, Skouta R, Lee ED, Hayano M, et al. Pharmacological Inhibition of Cystine-Glutamate Exchange Induces Endoplasmic Reticulum Stress and Ferroptosis. *Elife* (2014) 3:e02523. doi: 10.7554/eLife.02523
10. Lin PL, Tang HH, Wu SY, Shaw NS, Su CL. Saponin Formosanin C-Induced Ferritinophagy and Ferroptosis in Human Hepatocellular Carcinoma Cells. *Antioxidants (Basel)* (2020) 9(8):682. doi: 10.3390/antiox9080682

11. Qiu Y, Cao Y, Cao W, Jia Y, Lu N. The Application of Ferroptosis in Diseases. *Pharmacol Res* (2020) 159:104919. doi: 10.1016/j.phrs.2020.104919
12. Marinelli S, Granito A, Piscaglia F, Renzulli M, Stagni A, Bolondi L. Metronomic Capecitabine in Patients With Hepatocellular Carcinoma Unresponsive to or Ineligible for Sorafenib Treatment: Report of Two Cases. *Hepat Mon* (2013) 13(9):e11721. doi: 10.5812/hepatmon.11721
13. Granito A, Marinelli S, Terzi E, Piscaglia F, Renzulli M, Venerandi L, et al. Metronomic Capecitabine as Second-Line Treatment in Hepatocellular Carcinoma After Sorafenib Failure. *Dig Liver Dis* (2015) 47(6):518–22. doi: 10.1016/j.dld.2015.03.010
14. Trevisani F, Brandi G, Garuti F, Barbera MA, Tortora R, Casadei Gardini A, et al. Metronomic Capecitabine as Second-Line Treatment for Hepatocellular Carcinoma After Sorafenib Discontinuation. *J Cancer Res Clin Oncol* (2018) 144(2):403–14. doi: 10.1007/s00432-017-2556-6
15. Mittler R, Darash-Yahana M, Sohn YS, Bai F, Song L, Cabantchik IZ, et al. NEET Proteins: A New Link Between Iron Metabolism, Reactive Oxygen Species, and Cancer. *Antioxid Redox Signal* (2019) 30(8):1083–95. doi: 10.1089/ars.2018.7502
16. Nechushtai R, Karmi O, Zuo K, Marjault HB, Darash-Yahana M, Sohn YS, et al. The Balancing Act of NEET Proteins: Iron, ROS, Calcium and Metabolism. *Biochim Biophys Acta Mol Cell Res* (2020) 1867(11):118805. doi: 10.1016/j.bbamcr.2020.118805
17. Tamir S, Paddock ML, Darash-Yahana-Baram M, Holt SH, Sohn YS, Agranat L, et al. Structure-Function Analysis of NEET Proteins Uncovers Their Role as Key Regulators of Iron and ROS Homeostasis in Health and Disease. *Biochim Biophys Acta* (2015) 1853(6):1294–315. doi: 10.1016/j.bbamcr.2014.10.014
18. Golinelli-Cohen MP, Lescop E, Mons C, Goncalves S, Clemancey M, Santolini J, et al. Redox Control of the Human Iron-Sulfur Repair Protein MitoNEET Activity *Via* Its Iron-Sulfur Cluster. *J Biol Chem* (2016) 291(14):7583–93. doi: 10.1074/jbc.M115.711218
19. Chen YF, Kao CH, Chen YT, Wang CH, Wu CY, Tsai CY, et al. Cisd2 Deficiency Drives Premature Aging and Causes Mitochondria-Mediated Defects in Mice. *Genes Dev* (2009) 23(10):1183–94. doi: 10.1101/gad.1779509
20. Wu CY, Chen YF, Wang CH, Kao CH, Zhuang HW, Chen CC, et al. A Persistent Level of Cisd2 Extends Healthy Lifespan and Delays Aging in Mice. *Hum Mol Genet* (2012) 21(18):3956–68. doi: 10.1093/hmg/dds210
21. Sohn YS, Tamir S, Song L, Michaeli D, Matouk I, Conlan AR, et al. NAF-1 and mitoNEET Are Central to Human Breast Cancer Proliferation by Maintaining Mitochondrial Homeostasis and Promoting Tumor Growth. *Proc Natl Acad Sci U S A* (2013) 110(36):14676–81. doi: 10.1073/pnas.1313198110
22. Liu L, Xia M, Wang J, Zhang W, Zhang Y, He M. CISD2 Expression Is a Novel Marker Correlating With Pelvic Lymph Node Metastasis and Prognosis in Patients With Early-Stage Cervical Cancer. *Med Oncol* (2014) 31(9):183. doi: 10.1007/s12032-014-0183-5
23. Yang Y, Bai YS, Wang Q. CDGSH Iron Sulfur Domain 2 Activates Proliferation and EMT of Pancreatic Cancer Cells *Via* Wnt/beta-Catenin Pathway and Has Prognostic Value in Human Pancreatic Cancer. *Oncol Res* (2017) 25(4):605–15. doi: 10.3727/096504016X14767450526417
24. Li SM, Chen CH, Chen YW, Yen YC, Fang WT, Tsai FY, et al. Upregulation of CISD2 Augments ROS Homeostasis and Contributes to Tumorigenesis and Poor Prognosis of Lung Adenocarcinoma. *Sci Rep* (2017) 7(1):11893. doi: 10.1038/s41598-017-12131-x
25. Zhu QQ, Tian L, Li DL, Wu ZH, He YY, Zhang HK. Elevated CISD2 Expression Predicts Poor Diagnosis and Promotes Invasion and Migration of Prostate Cancer Cells. *Eur Rev Med Pharmacol Sci* (2020) 24(12):6597–604. doi: 10.26355/eurrev_202006_21645
26. Chang NC, Nguyen M, Germain M, Shore GC. Antagonism of Beclin 1-Dependent Autophagy by BCL-2 at the Endoplasmic Reticulum Requires NAF-1. *EMBO J* (2010) 29(3):606–18. doi: 10.1038/emboj.2009.369
27. Hassannia B, Wiernicki B, Ingold I, Qu F, Van Herck S, Tyurina YY, et al. Nano-Targeted Induction of Dual Ferroptotic Mechanisms Eradicates High-Risk Neuroblastoma. *J Clin Invest* (2018) 128(8):3341–55. doi: 10.1172/JCI99032
28. Paquette M, El-Houjeiri L, Pause A. mTOR Pathways in Cancer and Autophagy. *Cancers (Basel)* (2018) 10(1):18. doi: 10.3390/cancers10010018
29. Hou W, Xie Y, Song X, Sun X, Lotze MT, Zeh HJ3rd, et al. Autophagy Promotes Ferroptosis by Degradation of Ferritin. *Autophagy* (2016) 12 (8):1425–8. doi: 10.1080/15548627.2016.1187366
30. Gao M, Monian P, Pan Q, Zhang W, Xiang J, Jiang X. Ferroptosis Is an Autophagic Cell Death Process. *Cell Res* (2016) 26(9):1021–32. doi: 10.1038/cr.2016.95
31. Zhou B, Liu J, Kang R, Klionsky DJ, Kroemer G, Tang D. Ferroptosis Is a Type of Autophagy-Dependent Cell Death. *Semin Cancer Biol* (2020) 66:89–100. doi: 10.1016/j.semcancer.2019.03.002
32. Bangaru S, Marrero JA, Singal AG. Review Article: New Therapeutic Interventions for Advanced Hepatocellular Carcinoma. *Aliment Pharmacol Ther* (2020) 51(1):78–89. doi: 10.1111/apt.15573
33. Tang W, Chen Z, Zhang W, Cheng Y, Zhang B, Wu F, et al. The Mechanisms of Sorafenib Resistance in Hepatocellular Carcinoma: Theoretical Basis and Therapeutic Aspects. *Signal Transduct Target Ther* (2020) 5(1):87. doi: 10.1038/s41392-020-0187-x
34. Su Z, Yang Z, Xie L, DeWitt JP, Chen Y. Cancer Therapy in the Necroptosis Era. *Cell Death Differ* (2016) 23(5):748–56. doi: 10.1038/cdd.2016.8
35. Mou Y, Wang J, Wu J, He D, Zhang C, Duan C, et al. Ferroptosis, a New Form of Cell Death: Opportunities and Challenges in Cancer. *J Hematol Oncol* (2019) 12(1):34. doi: 10.1186/s13045-019-0720-y
36. Su Y, Zhao B, Zhou L, Zhang Z, Shen Y, Lv H, et al. Ferroptosis, a Novel Pharmacological Mechanism of Anti-Cancer Drugs. *Cancer Lett* (2020) 483:127–36. doi: 10.1016/j.canlet.2020.02.015
37. Li B, Yang L, Peng X, Fan Q, Wei S, Yang S, et al. Emerging Mechanisms and Applications of Ferroptosis in the Treatment of Resistant Cancers. *BioMed Pharmacother* (2020) 130:110710. doi: 10.1016/j.biopha.2020.110710
38. Roh JL, Kim EH, Jang HJ, Park JY, Shin D. Induction of Ferroptotic Cell Death for Overcoming Cisplatin Resistance of Head and Neck Cancer. *Cancer Lett* (2016) 381(1):96–103. doi: 10.1016/j.canlet.2016.07.035
39. Huang KJ, Wei YH, Chiu YC, Wu SR, Shieh DB. Assessment of Zero-Valent Iron-Based Nanotherapeutics for Ferroptosis Induction and Resensitization Strategy in Cancer Cells. *Biomater Sci* (2019) 7(4):1311–22. doi: 10.1039/c8bm01525b
40. Toyokuni S, Ito F, Yamashita K, Okazaki Y, Akatsuka S. Iron and Thiol Redox Signaling in Cancer: An Exquisite Balance to Escape Ferroptosis. *Free Radic Biol Med* (2017) 108:610–26. doi: 10.1016/j.freeradbiomed.2017.04.024
41. Roh JL, Kim EH, Jang H, Shin D. Nrf2 Inhibition Reverses the Resistance of Cisplatin-Resistant Head and Neck Cancer Cells to Artesunate-Induced Ferroptosis. *Redox Biol* (2017) 11:254–62. doi: 10.1016/j.redox.2016.12.010
42. Sun X, Niu X, Chen R, He W, Chen D, Kang R, et al. Metallothionein-1G Facilitates Sorafenib Resistance Through Inhibition of Ferroptosis. *Hepatology* (2016) 64(2):488–500. doi: 10.1002/hep.28574
43. Lipper CH, Karmi O, Sohn YS, Darash-Yahana M, Lammert H, Song L, et al. Structure of the Human Monomeric NEET Protein MiNT and its Role in Regulating Iron and Reactive Oxygen Species in Cancer Cells. *Proc Natl Acad Sci U S A* (2018) 115(2):272–7. doi: 10.1073/pnas.1715842115
44. Kim EH, Shin D, Lee J, Jung AR, Roh JL. CISD2 Inhibition Overcomes Resistance to Sulfasalazine-Induced Ferroptotic Cell Death in Head and Neck Cancer. *Cancer Lett* (2018) 432:180–90. doi: 10.1016/j.canlet.2018.06.018
45. Doll S, Freitas FP, Shah R, Aldrovandi M, da Silva MC, Ingold I, et al. FSP1 Is a Glutathione-Independent Ferroptosis Suppressor. *Nature* (2019) 575 (7784):693–8. doi: 10.1038/s41586-019-1707-0
46. Bersuker K, Hendricks JM, Li Z, Magtanong L, Ford B, Tang PH, et al. The CoQ Oxidoreductase FSP1 Acts Parallel to GPX4 to Inhibit Ferroptosis. *Nature* (2019) 575(7784):688–92. doi: 10.1038/s41586-019-1705-2
47. Mao C, Liu X, Zhang Y, Lei G, Yan Y, Lee H, et al. DHODH-Mediated Ferroptosis Defence Is a Targetable Vulnerability in Cancer. *Nature* (2021) 593(7860):586–90. doi: 10.1038/s41586-021-03539-7
48. Ploetz E, Zimpel A, Cauda V, Bauer D, Lamb DC, Haisch C, et al. Metal-Organic Framework Nanoparticles Induce Pyroptosis in Cells Controlled by the Extracellular Ph. *Adv Mater* (2020) 32(19):e1907267. doi: 10.1002/adma.201907267
49. Nassour J, Radford R, Correia A, Fuste JM, Schoell B, Jauch A, et al. Autophagic Cell Death Restricts Chromosomal Instability During Replicative Crisis. *Nature* (2019) 565(7741):659–63. doi: 10.1038/s41586-019-0885-0
50. Poillet-Perez L, Xie X, Zhan L, Yang Y, Sharp DW, Hu ZS, et al. Autophagy Maintains Tumour Growth Through Circulating Arginine. *Nature* (2018) 563 (7732):569–73. doi: 10.1038/s41586-018-0697-7
51. Yu T, Guo F, Yu Y, Sun T, Ma D, Han J, et al. Fusobacterium Nucleatum Promotes Chemoresistance to Colorectal Cancer by Modulating Autophagy. *Cell* (2017) 170(3):548–563 e16. doi: 10.1016/j.cell.2017.07.008

52. Dikic I, Elazar Z. Mechanism and Medical Implications of Mammalian Autophagy. *Nat Rev Mol Cell Biol* (2018) 19(6):349–64. doi: 10.1038/s41580-018-0003-4
53. Munoz-Guardiola P, Casas J, Megias-Roda E, Sole S, Perez-Montoyo H, Yeste-Velasco M, et al. The Anti-Cancer Drug ABTL0812 Induces ER Stress-Mediated Cytotoxic Autophagy by Increasing Dihydroceramide Levels in Cancer Cells. *Autophagy* (2020) 17(6):1349–66. doi: 10.1080/15548627.2020.1761651
54. Liu Z, Wang Q, Wang X, Xu Z, Wei X, Li J. Circular RNA cIARS Regulates Ferroptosis in HCC Cells Through Interacting With RNA Binding Protein ALKBH5. *Cell Death Discov* (2020) 6:72. doi: 10.1038/s41420-020-00306-x
55. Li Z, Jiang L, Chew SH, Hirayama T, Sekido Y, Toyokuni S. Carbonic Anhydrase 9 Confers Resistance to Ferroptosis/Apoptosis in Malignant Mesothelioma Under Hypoxia. *Redox Biol* (2019) 26:101297. doi: 10.1016/j.redox.2019.101297
56. Tamir S, Rotem-Bamberger S, Katz C, Morcos F, Hailey KL, Zuris JA, et al. Integrated Strategy Reveals the Protein Interface Between Cancer Targets Bcl-2 and NAF-1. *Proc Natl Acad Sci U S A* (2014) 111(14):5177–82. doi: 10.1073/pnas.1403770111
57. Kang R, Zeh HJ, Lotze MT, Tang D. The Beclin 1 Network Regulates Autophagy and Apoptosis. *Cell Death Differ* (2011) 18(4):571–80. doi: 10.1038/cdd.2010.191
58. Song X, Zhu S, Chen P, Hou W, Wen Q, Liu J, et al. AMPK-Mediated BECN1 Phosphorylation Promotes Ferroptosis by Directly Blocking System Xc(-) Activity. *Curr Biol* (2018) 28(15):2388–99.e5. doi: 10.1016/j.cub.2018.05.094

Conflict of Interest: The authors declare that the research was conducted in the absence of any commercial or financial relationships that could be construed as a potential conflict of interest.

Publisher's Note: All claims expressed in this article are solely those of the authors and do not necessarily represent those of their affiliated organizations, or those of the publisher, the editors and the reviewers. Any product that may be evaluated in this article, or claim that may be made by its manufacturer, is not guaranteed or endorsed by the publisher.

Advantages of publishing in Frontiers

OPEN ACCESS
Articles are free to read for greatest visibility and readership

FAST PUBLICATION
Around 90 days from submission to decision

HIGH QUALITY PEER-REVIEW
Rigorous, collaborative, and constructive peer-review

TRANSPARENT PEER-REVIEW
Editors and reviewers acknowledged by name on published articles

Frontiers
Avenue du Tribunal-Fédéral 34
1005 Lausanne | Switzerland

Visit us: www.frontiersin.org
Contact us: frontiersin.org/about/contact

REPRODUCIBILITY OF RESEARCH
Support open data and methods to enhance research reproducibility

DIGITAL PUBLISHING
Articles designed for optimal readership across devices

FOLLOW US
@frontiersin

IMPACT METRICS
Advanced article metrics track visibility across digital media

EXTENSIVE PROMOTION
Marketing and promotion of impactful research

LOOP RESEARCH NETWORK
Our network increases your article's readership